Biopolymers for Bioartificial Pancreas

Odugbemi, M.

BIOPOLYMERS FOR BIOARTIFICIAL PANCREAS

MoyinOluwa Oluwakiite Odugbemi

A thesis submitted in partial fulfilment of the requirements of the University of Westminster for the degree of Doctor of Philosophy

October 2018

AUTHOR'S DECLARATION

I declare that this present work was carried out in accordance with the guidelines and regulations of the University of Westminster. The work is original except where indicated by reference in text.

This submission or part of it is not substantially the same as any I previously or am currently making, whether in published or unpublished form, for a degree, diploma or similar qualification at another university or similar institution.

Until the outcome of the current application to the University of Westminster is known, the work will not be submitted for any such publication at another university or similar institution.

Any views expressed in this work are those of the author and in no way represent those of the University of Westminster.

Signed: MoyinOluwa Odugbemi Date: October 2018

ACKNOWLEDGEMENTS

I would especially like to thank Professor Ipsita Roy, my supervisor, for all of her support throughout my PhD. Her patience, advice and direction during this project have been invaluable and it has been a privilege working with her. This project would not have been possible without her. I would also like to extend my gratitude to Dr. Jochenn Salber at Ruhr University, Bochum for all his help and advice during the project. Many thanks to Professor Victor Gault and Dr. Varun Pathak at University of Ulster for their help with BRIN BD11 cell work. Thanks to Professor Atul Bhaskar and Faezeh Shatchy at the University of Southampton for their help with the 3D modelling. I would also like to thank Evita Ning and Hector Martinez at Cellink for their help with the 3D printing. Thank you to Dr. Nicola Mordan at UCL for her help with SEM imaging.

I am grateful to Dr. Robin Lawrence whose support and medical advice was invaluable throughout the duration of the PhD. Thanks to Dr. Godfrey Kyazze, Dr. Amara Anyogu, Dr. Saki Raheem and Prof Taj Keshavarz for their additional support. Massive thanks to all the technical staff at University of Westminster especially Neville Antonio for his help with fermentation.

My gratitude goes to Dr. Pooja Basnett who offered me hands-on training in the lab and whose friendship and support I have relied on. I would like to thank my colleagues in lab C7.01 and C4.03 especially Louise, Hima, Barbara, Elena, Faye and Emma for their friendship and support.

To my massive wall of friends- Jack, Megan, Tim, Colleen, Essie, Nick, Jonny, Anthony, Claudia, Jen, Jess, Sarah, Pemi, Kovie, Tokunbo, Femi, Wole, Sabirah and internet friend Justin: thank you, we did it!

I am thankful for Lydia and Janelle for being the best flatmates ever. My gratitude goes to The Cokers, Abioduns and Obires for housing me and feeding me. Thank you to Tobi, Mikey, Rimike and Reni for the cuddles. Thanks to my sisters Damiloju and Daara for supporting and understanding me.

I would most especially like to thank my parents, Mr and Mrs Lekan and Tinu Odugbemi, for being my number one fans and encouraging me to follow my dreams, however wild. Thank you for your support: physically, financially and emotionally. *Ẹṣe, ẹ jere ọmọ.*

And finally, Abba, the ground of being. It was always, always only you. Thank you.

ABSTRACT

The concept of the bioartificial pancreas has developed substantially in the last decade, after the first successful islet transplantation in 2000. Islets are clusters of endocrine cells found in the pancreas. Amongst these cells, the insulin secreting beta cells are targeted by the immune system in Type 1 Diabetes. One of the major challenges islet transplantation has faced is the rapid loss of islets, post-transplantation. To mitigate this, a bioartificial pancreas that provides support and immuno-isolation for islets before transplantation has been investigated.

Polyhydroxyalkanoates (PHAs) are intracellular energy storage polymers synthesized by Gram-positive and Gram-negative bacteria. Because of their high degree of biocompatibility and structural properties, PHAs have been chosen as the scaffold material for the bioartificial pancreas. Alginate is a naturally occurring polysaccharide made up of mannuoronate and guluronate units. Because of its ability to mimic the extracellular matrix, it has been widely investigated for its use as a hydrogel and is being investigated for its use in islet transplantation.

This project aimed to produce a bioartificial pancreas that contains pancreatic cells encapsulated in an alginate hydrogel environment (mimicking islets) and a PHA scaffold providing support and an additional layer of immuno-isolation.

To identify a scaffold material, two PHAs were produced- P(3HB), a stiff, brittle polymer by *Bacillus subtilis* OK2 fermentation and a novel

elastomeric P(3HO-co-HD) by *Pseudomonas mendocina* CH50. Several studies were performed on these produced polymers. Initially, they were characterised chemically, structurally, mechanically and thermally and compared to PLLA, a FDA approved polymer. It was observed that when these polymers were compared in terms of viability and insulin release, cells seeded in P(3HO-co-HD) performed best. Porosity was introduced into the P(3HO-co-HD) scaffold to mimic the mechanical properties of the native pancreas and facilitate exchange of nutrients and waste. The effect of the type of porogen, porogen size and concentration was also investigated. It was observed that the scaffold obtained using 100µm NaCl, at a concentration of 15% w/v was the best scaffold for the BRIN BD11cells. Next, the polymers were fabricated into 2D & 3D structures and evaluated for function. No statistical difference was observed when the mechanical properties of both 2D & 3D structures were compared. The same trend was observed for the viabilities and insulin release of BRIN BD11 cells seeded in these structures.

In addition, three P(3HO-co-HD) dominated P(3HO-co-HD)/P(3HB) blends: 95:5, 90:10 & 80:20 were made in order to improve the handling of P(3HO-co-HD). When the handling of the scaffolds, the viability and insulin release of BRIN BD11 cells seeded in these blends were considered, the 95:5 P(3HO-co-HD)/P(3HB) blend was selected as the best combination. Further, the 95:5 P(3HO-co-HD)/P(3HB) blend was processed into 2D & 3D structures, evaluated and compared to 2D & 3D P(3HO-co-HD) structures. No significant difference was observed when the

95:5 P(3HO-co-HD)/P(3HB) blend and P(3HO-co-HD) structures were compared based on cell viability and insulin release.

Finally, two kinds of alginate hydrogel structures were made- alginate microbeads and 3D printed block hydrogels. The effect of cell densities ($1X10^5$cells/ml & $5X10^5$cells/ml) and alginate concentration (2%, 4% & 5% w/v) on cell viability was evaluated. The two structures were then compared based on cell viability and insulin release. Of all the conditions, 5% w/v alginate 3D printed block hydrogels containing $5x10^5$cells/ml performed best based on cell viability and insulin release of BRIN BD11 cells seeded.

In conclusion, in this work, two PHAs including a novel PHA have been successfully produced. In addition, the best blend structure for scaffold creation has been identified and evaluated. Further, alginate hydrogels with optimum cell densities and structures have been selected and used for the creation of the inner hydrogel environment. These represent the framework for the successful development of bioartificial pancreas in the future.

TABLE OF CONTENTS

LIST OF FIGURES

LIST OF TABLES

LIST OF ABBREVIATIONS

%WA	% Water absorption
%WL	% Weight loss
β-cell	Beta cells
γ-PGA	Poly-(γ-glutamic acid)
ΔH_f	Enthalpy of formation
2D	Two-dimensional
3D	Three-dimensional
ADP	Adenosine diphosphate
ANOVA	Analysis of variance
ASTM	American Society for Testing and Materials
ATP	Adenosine triphosphate
ATR-FTIR	Attenuated Total Reflectance Fourier-Transform Infrared Spectroscopy
AutoCAD	Autodesk Computer Aided Design
C/N	Carbon: nitrogen ratio
CGM	Continuous glucose monitoring
CSII	Continuous subcutaneous insulin infusion
Dcw	Dry cell weight

DMSO	Dimethyl sulphoxide
DNA	Deoxyribonucleic acid
DOT	Dissolved oxygen tension
DSC	Differential scanning calorimetry
ECACC	European collection of authenticated cell cultures
ECM	Extracellular matrix
EDTA	Ethylenediaminetetraacetic acid
EGTA	Ethylene glycol-bis(β-aminoethyl ether)-*N*,*N*,*N′*,*N′*-tetraacetic acid
FTIR	Fourier-Transform Infrared Spectroscopy
GC	Gas Chromatography
GC-MS	Gas Chromatography Mass Spectrometry
GIP	Gastric inhibitory peptide
GLP-1	Glucagon-like peptide-1
GLUT2	Glucose transporter 2
HA	Hydroxyapatite
HB	Hydroxybutyrate
HD	Hydroxydecanoate
HEPA	High efficiency particulate air
HEPES	4-(2-hydroxyethyl)-1-piperazineethanesulfonic acid

HNF-4α	Hepatocyte nuclear factor 4α
HO	Hydroxyoctanoate
HV	Hydroxyvalerate
IBMIR	Instant blood mediated immune response
JDRF	Juvenile Diabetes Research Foundation
KRB	Krebs-Ringer modified buffer
mcl-PHA	Medium chain length polyhydroxyalkanaotes
mRNA	Messenger Ribonucleic acid
MTT	3-(4,5-dimethylthiazol-2-yl)-2,5-diphenyltetrazolium bromide
NMR	Nuclear Magnetic Resonance
NOD	Non-obese diabetic mice
OD	Optical density
P(3HB)	Poly(3-hydroxybutyrate)
P(3HB-co-4HB)	Poly(3-hydroxybutyrate-co-4- hydroxybutyrate)
P(3HB-co-3HHx)	Poly(3-hydroxybutyrate-co-hydroxyhexanoate)
P(3HB-co-3HV-co-3HHx)	Poly(3-hydroxybutyrate-co-hydroxyvalerate-co-hydroxyhexanoate)
P(3HHx-co-3HO)	Poly(3-hydroxyhexanoate-co-hydroxyoctanoate)
P(3HO)	Poly(3-hydroxyoctanoate)

P(3HO-co-3HD)	Poly(3-hydroxyoctanoate-co-hydroxydecanoate)
P(3HO-co-3HHx)	Poly(3-hydroxyoctanoate-co-hydroxyhexanoate)
P(3HV)	Poly(3-hydroxyvalerate)
P(4HB)	Poly(4-hydroxybutyrate)
PCL	Polycaprolactone
PDMS	Polydimethylsiloxane
PEG	Polyethylene glycol
PEG-MAL	Polyethylene glycol-maleimide
PGA	Poly(glycolic acid)
PHA	Polyhydroxyalkanoate
PhaA	Acetyl-CoA acetyltransferase
PhaB	Acetoacetyl-CoA reductase
PhaC	PHA synthase subunit PhaC
PhaG	(R)-3-hydroxydecanoyl-ACP:CoA transacylase
PhaJ	(R)-specific enoyl-CoA hydratase
PLA	Poly(lactic acid)
PLGA	Poly(lactic-co-glycolic acid)
PLLA	Poly(lactic acid)
PP	Pancreatic polypeptide

PTFE	Polytetrafluoroethylene
PVA	Poly(vinyl alcohol)
RGD peptide	Arginylglycylaspartic acid
R_T	Retention time
RPMI	Roswell Park Memorial Institute medium
scl-PHA	Short chain length polyhydroxyalkanoates
SEM	Scanning Electron Microscopy
T1DM	Type 1 Diabetes Mellitus
TCA	Tricarboxylic acid cycle
TCP	Tissue culture plastic
TE	Tissue Engineering
T_g	Glass transition temperature
T_m	Melting temperature
UV	Ultraviolet
VDCC	Voltage dependent calcium channels
VEGF	Vascular endothelial growth factor

CHAPTER ONE:

INTRODUCTION

1. INTRODUCTION

1.1 INCIDENCE OF DIABETES

Globally, diabetes has become a major concern, hence the World Health Organisation commissioned a special global report on Diabetes in 2016. The last three decades have seen a dramatic rise in the amount of people living with diabetes. In 1980, the number of people living with diabetes was estimated to be 108 million; by 2014, this number had risen to 422 million. This number represents approximately 9% of the world population. Currently, diabetes and its complications is one of the leading causes of death in people aged 20-79 (World Health Organisation, 2016).

Projections show that there will be a marked increase in the percentage of the population living with diabetes between 2018 and 2045. The total population of diabetes sufferers is expected to increase from 422 million to 628.6 million (approximately 8.8% to 9.9% of total adults). The total expenditure on management and care of patients with diabetes will increase from $727 billion to $776 billion (World Health Organisation, 2016).

1,106,500 of young people between the ages of 0-19 were living with Type 1 diabetes as at 2017 with 132,600 new cases being diagnosed every year (Ogurtsova *et al.*, 2017). In 2016, about 4.5 million people in the United Kingdom suffered from diabetes and that number is predicted to rise to about 5 million by 2025. In 2013, the treatment and maintenance of people with diabetes cost the UK about £10-13.75 billion (Diabetes UK, 2017). Type 1 Diabetes Mellitus (T1DM) is the most common chronic disease in children (Atkinson, Eisenbarth and Michels, 2014). About 500,000 children have been

diagnosed with the disease worldwide with about 32,000 of them in the UK (Diabetes UK 2015).

1.2 DIABETES MELLITUS

Diabetes refers to a group of metabolic disorders in which there is an inability to maintain blood glucose levels, resulting in hyperglycaemia. They significantly affect the quality of life of sufferers and if left untreated, can lead to retinopathy, neuropathy and nephropathy (Nathan, 1993; Zimmet, Alberti and Shaw, 2001; Bluestone, Herold and Eisenbarth, 2010; Lukic, Pejnovic and Lukic, 2014). There are two well-known types of diabetes, Type 1 - T1DM (insulin dependent) and Type 2.

Diagnosis of diabetes has been described as fasting plasma glucose value greater than 7mmol/L and random blood glucose level value greater than 11mmol/L. Diagnosis criteria also includes glycated haemoglobin (HbA1C) greater than 6.5% and 2-hour postprandial glucose level greater than 11mmol/L (American Diabetes Association, 2012). In addition to hyperglycaemia, diabetes is also associated with three main symptoms- polyuria (excessive urination), polyphagia (excessive appetite) and polydipsia (increased thirst) (Atkinson, Eisenbarth and Michels, 2014). These usually present as primary symptoms. Diabetes also leads to weight loss and in long term has effects such as vision loss, kidney failure and neuropathy leading to foot ulcers. In severe cases, ketoacidosis can occur leading to coma and eventually death. It has also shown comorbidity with cardiovascular diseases, obesity, declined cognitive function and hypertension (Alberti and Zimmet, 1998; Hassing *et al.*, 2004).

1.2.1 Type 1 Diabetes (T1DM)

T1DM is a genetically inherited irreparable autoimmune disease in which the insulin producing β-cells of the pancreas are destroyed, leading to serious insulin dependence. Individuals with T1DM resort to supplementary insulin and dietary regulation to prevent further complications of the disease like retinopathy, neuropathy and nephropathy (Nathan, 1993; Alberti and Zimmet, 1998; Daneman, 2006; Clery *et al.*, 2017).

1.2.2 Type 2 Diabetes

Type 2 diabetes on the other hand, results from irregularities in insulin action and secretion. It is caused by a mix of genetics and lifestyle choices and can be managed through changes in diet, physical activity and medication (Vijan, 2010; Chatterjee, Khunti and Davies, 2017). It is the more common and better studied of the two types.

1.3 THE PANCREAS

The pancreas is an organ measuring about 14-18 cm long, 2-9cm wide, 2-3cm thick and weighing- about 70-150g. (Slack, 1995; Dolenšek, Rupnik and Stožer, 2015; Tortora and Derrickson, 2017). The pancreas is viscoelastic, more viscous than the spleen, kidney and liver, with a Young's modulus between 1.4-2.1KPa and a dynamic modulus of 120-180Pa (Sugimoto *et al.*, 2014).

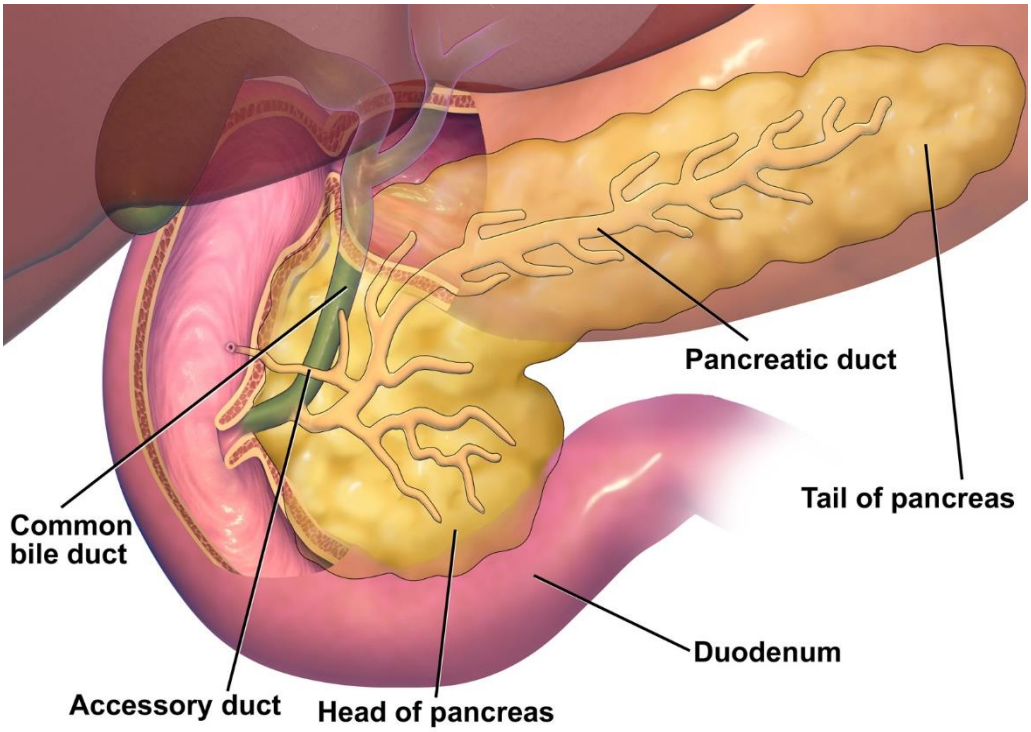

Figure 1.1: The anatomy of the pancreas (taken from Staff, 2014).

The pancreas has four parts as shown in Figure 1.1. The head is found in the concave groove of the duodenum, surrounding the mesenteric artery and vein. The neck is found between the head and the body of the pancreas covering the blood vessels. The body is the largest part containing the bulk of the cells and the tail acts as the boundary between the pancreas and the spleen (Ionescu-Tirgoviste *et al.*, 2015).

The pancreas has two types of cells that perform two different actions: the exocrine cells responsible for enzyme secretion and the endocrine cells in charge of hormone secretion. The enzyme secreting exocrine cells form most of the cells in the pancreas. These cells are easily visualised and are arranged in clusters called acini found around interconnected lobes which drain the secretory products into the pancreatic duct from where it proceeds to the duodenum (Dolenšek, Rupnik and Stožer, 2015; Ionescu-Tirgoviste *et al.*, 2015).

1.3.1 Islets of Langerhans

The endocrine cells of the pancreas are found in spherical clusters called islets of Langerhans, named after Paul Langerhans who identified them in the late 19th century. There are about 3million islets in the average pancreas arranged in density routes (Kulkarni, 2004). There are four kinds of endocrine cells– α, β, δ and Pancreatic Polypeptide producing (PP) cells that secrete glucagon, insulin, somatostatin and pancreatic polypeptides respectively (Figure 1.2). Of these cells, the β cells are the most abundant making up about 70-80% of islets, α-cells account for 17%, δ for 7% and PP for 6-7%. Islets also include ghrelin-secreting cells that are part of the appetite regulation system of the body. Insulin and glucagon are particularly involved in the essential glucose regulation system of the body (Wills, Thomas and Gillham, 2006; Naish *et al.*, 2009; Ahmed, 2011).

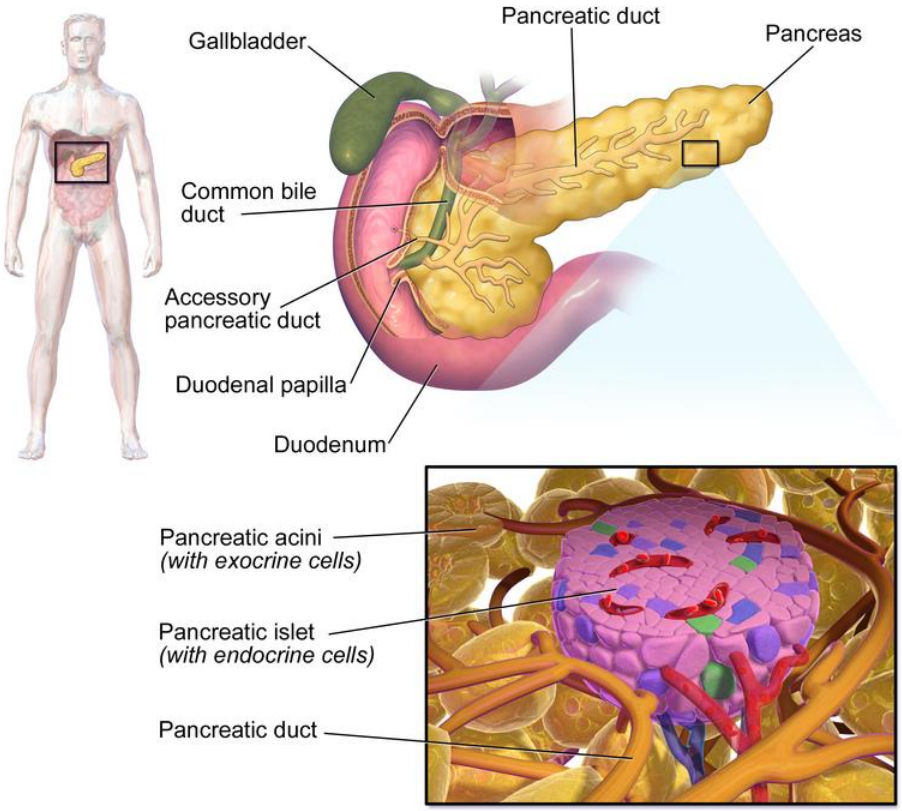

Figure 1.2: The anatomy of the pancreas showing the exocrine and endocrine cells (taken from Staff, 2014).

1.3.2 Insulin

Insulin is a protein made of polypeptides linked by three covalent disulphide bonds with a molecular weight of 6,000 Daltons. It is derived by the cleavage of proinsulin a prohormone. Insulin is dimer of two chains, the A chain with 21 amino acids residues and the B chain with 30 amino acid residues (Humbel, 1965; Wills, Thomas and Gillham, 2006).

1.3.3 Insulin Synthesis

The synthesis of insulin begins with the translation of insulin mRNA to produce preproinsulin, a single chain peptide. It is then transported into the endoplasmic reticulum in which the signal peptide is cleaved and proinsulin is formed. Proinsulin as a peptide has three chains- the B chain (carboxy terminal), C-chain (central chain) and the A chain- (the amino terminal) (Steiner and Oyer, 1967; Wills, Thomas and Gillham, 2006).

The endoplasmic reticulum contains many enzymes, including the endopeptidases (prohormone convertases) and carboxypeptidases. These enzymes cleave the C-peptide chain leaving the A and B chains which form insulin. Insulin is then stored in granules of the Golgi apparatus (Steiner and Oyer, 1967; Wills, Thomas and Gillham, 2006).

1.3.4 Insulin Secretion

1.3.4.1 Glucose stimulated insulin secretion (GSIS)

Primarily, insulin secretion in the islets of Langerhans occurs in a biphasic manner. Initially, increase in blood glucose triggers an insulin secretion within 5-10 minutes. The second is a glucose independent secretion over 2-3 hours. (Gerich, 2002; Lorenzo *et al.*, 2010)

Figure 1.3 shows the insulin secretion process in the β-cell.

1. Initially, glucose is transported into the cells through the glucose transporter (GLUT2). It ensures that the rate of entry is proportional to the blood glucose levels.
2. After transporting, the glucose in the cell is phosphorylated to glucose-6-phosphate through the action of glucokinase.
3. Glucose-6-phosphate enters the glycolytic pathway and the Kreb's cycle.
4. Acetyl-coA oxidation produces ATP molecules leading to a rise in the ATP:ADP ratio in the cell.
5. This increased ATP:ADP ratio closes the ATP sensitive potassium channel leading to a build-up of potassium ions intracellularly. This leads to a depolarisation of the cell membrane.

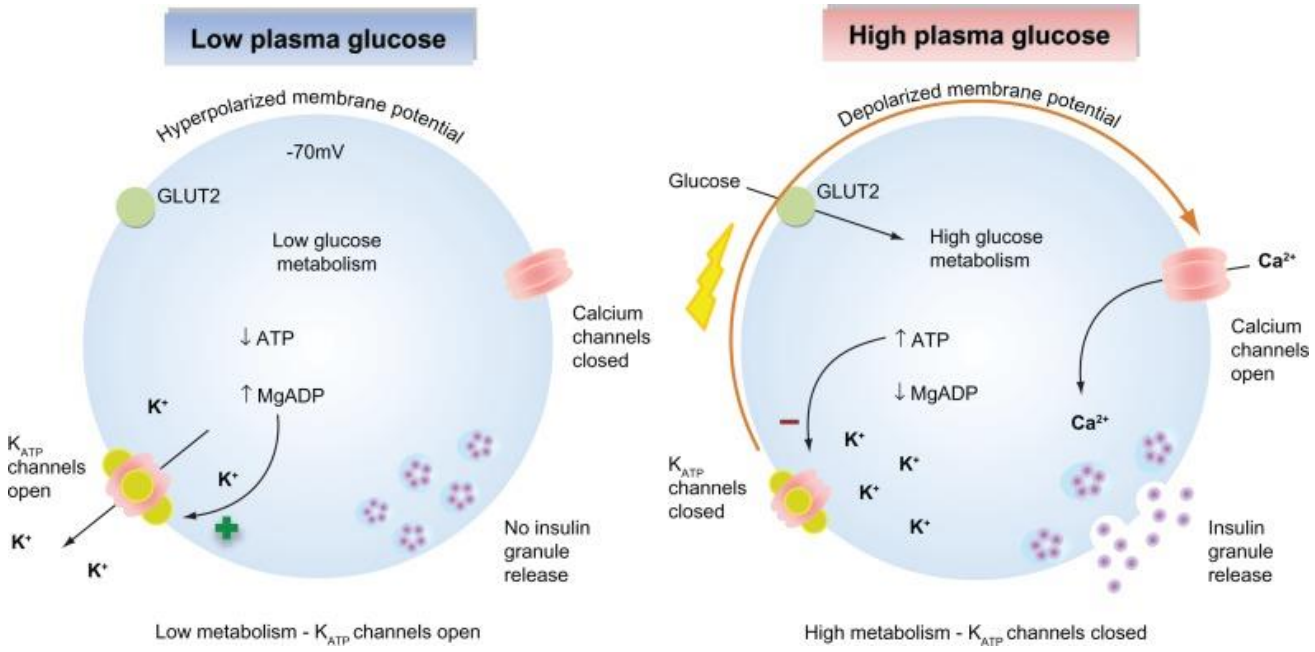

Figure 1.3: Insulin secretion in pancreatic β-cells. When plasma glucose is low, the decreased ratio of ATP/ADP will increase K^+ channel opening. Consequently, the cell membrane is hyperpolarized, preventing voltage-gated calcium channel opening, Ca^{2+} influx and insulin secretion. At high blood glucose levels, glucose is transported into the cell through GLUT2. Glucose metabolism leads to an increased ATP/ADP ratio resulting in closing of the K^+ channel and depolarisation of the membrane. This leads to an opening of the calcium channel, influx of Ca^{2+} and insulin secretion (Lang and Light, 2010).

6. Depolarisation triggers the opening of the voltage dependent calcium channels (VDCC) and an influx of calcium ions.
7. The increase in intracellular calcium ions leads to the release of insulin from intracellular secretory vesicles (Schuit *et al.*, 1997, 1999; Gerich, 2002; Lang and Light, 2010; Lorenzo *et al.*, 2010; Santulli *et al.*, 2015).

1.3.4.2 Other factors involved in insulin secretion

Elevated levels of amino acids like L-glutamine, L-arginine, alanine and leucine lead to an increase in insulin secretion in β-cells. This effect can be observed individually as in the case of arginine and also in combination like leucine and glutamine (Van Loon *et al.*, 2003; Newsholme *et al.*, 2007; Henquin and Nenquin, 2016).

Glucagon triggers insulin secretion through lipolysis. In insulin deficiency, lipolysis induction through glucagon action leads to the creation of glucose and induction of insulin secretion (Liljenquist *et al.*, 1974).

Incretins like glucagon like peptide (GLP-1) and glucose dependent insulinotropic peptide (GIP) lead to the rapid secretion of insulin. They also induce insulin gene transcription and islet generation (Macdonald *et al.*, 2002; Pederson and McIntosh, 2016).

1.4 TREATMENT OF TYPE 1 DIABETES

1.4.1 Insulin Supplementation

Traditional treatment for T1DM is insulin replacement. This usually takes the form of daily injections of insulin to prevent hyperglycaemia. Apart from the obvious

problem of daily insulin injections, this method still faces the challenge of the insulin being exogenous and not being as sensitive as endogenous insulin produced by the body (Godfrey *et al.*, 2012; Klein and Klein, 2015). Continuous subcutaneous insulin infusion (CSII) via the insulin pump has been shown to be safer and more effective at reducing blood glucose levels without increasing the risk of hypo- or hyperglycaemia (Misso *et al.*, 2010). Combining continuous glucose monitoring (CGM) with CSII leads to stabilisation of blood glucose levels (Bergenstal *et al.*, 2010; Varanasi *et al.*, 2011).

1.4.2 Whole Pancreas Transplantation

Whole pancreas transplants represent the holy grail of type 1 diabetes treatment. Between 1966, when the first successful pancreas transplant was performed, and 2014, over 40,000 pancreases have been transplanted with treatments showing insulin independence up to 2 years after the transplant (Godfrey *et al.*, 2012; Ramesh, Chhabra and Brayman, 2013; Gruessner and Gruessner, 2014). Because of some of the complications associated with this method including morbidity, a 1-3% rate of morbidity has been reported, immune rejection, lifelong immunosuppression for organ recipients and a shortage of suitable donors, transplantation is only recommended to patients who do not respond to insulin replacement therapies and are at a high risk of nephropathy (White, Shaw and Sutherland, 2009; Godfrey *et al.*, 2012).

1.4.3 Islet Transplantation

The Edmonton procedure has led to the recognition of islet transplantation as an emerging treatment option for patients with recurrent and refractory hypoglycaemia. This procedure led to the successful transplantation of the islet cells, leading to insulin independence in seven patients as described in 2000 and then repeated in 36 subjects in 2006 (Shapiro *et al.*, 2000, 2006). In 2012, the Shapiro group observed that 79% of the patients that received islet transplants regained glucose regulation function. 96% survival rates and insulin independence rates of 50-60% were observed after 4 years (Barton *et al.*, 2012). Globally, over 750 patients have received islet transplants with similar success rates (Barton *et al.*, 2012; McCall and Shapiro, 2012).

Several factors have been identified which determine to a large extent, the success of an islet transplant procedure. Some of these include donor age, cause of death and plasma glucose levels of donor, recipient age, success of islet isolation procedure, co-morbidities, cold ischemia time and the kind of immunosuppressors/vasopressors used (Zeng *et al.*, 1994; Robertson, 2000; Matsumoto *et al.*, 2004; Nano *et al.*, 2005).

Table 1.1 is a summary of the treatment options for type 1 diabetes with their limitations.

Table 1.1: Treatment options for type 1 diabetes

	Treatment	**Limitations**	**Reference**
1.	Insulin supplementation	Long term effects- renal failure, nephropathy, frequent episodes of hypoglycaemia	Stevens *et al.* 2001

2.	Pancreas transplantation	Lack of donors, Immuno-suppression	Robertson 2000
3.	Islet transplantation	Lack of donors, Low survival of Islets	Shapiro *et al.* 2006
4.	Islet encapsulation/ seeding and transplantation	Lack of donors, Biocompatibility/ biodegradability of encapsulating/ seeding materials Low survival of Islets	Bromberg & LeRoith 2006 Robertson 2000

1.4.4 Challenges of Islet Transplantation

Even though islet transplantation has been found to be successful experimentally, it has not yet gained wide clinical acceptance and usage. This is due to different factors including loss of islet cells upon transplantation (up to 60% are lost in the first few days), reduced function of the transplanted islet cells with time, risks associated with extended exposure to immunosuppression, increased risks of developing T1DM in donors and a resultant distinct dearth of donor islet cells (McCall & Shapiro 2012, Martin *et al.*, 2015). Of all sixty-five patients who underwent an islet transplantation in 2004 under the Edmonton protocol, sixty- three of the patients received multiple transplants indicating that one transplantation was not sufficient (Ryan *et al.* 2005).

One of the major factors preventing islet transplantation from being converted into mainstream clinical practice is the poor graft function in the long term. This is due to a lower number of islet cells surviving than the number that were transplanted. Islets also have a high specificity (high oxygen demand and vascularisation needs) and are susceptible to the immune response.

To circumnavigate some of the issues associated with transplanting islets, different strategies have been suggested. These include the immunoisolation of islet cells

through the design of multifunctional scaffolds, encapsulating islet cells (mimicking their natural environment) and better immunosuppression strategies (Hatziavramidis *et al.*, 2013).

Encapsulation of islets before transplantation is a field that has been developed in response to the Edmonton protocol in which there was a loss of islets post transplantation and the potential for the elimination of immune suppressive drugs in transplantation. Encapsulating systems can be divided into two types, hydrogel systems and macroencapsulation systems (An *et al.*, 2018). Encapsulating islets is an area that has been researched and discussed extensively. Encapsulation provides a means for immunoisolation and protection of the islets. The ideal material for islet encapsulation should be biocompatible, inert, porous, allowing for exchange of oxygen, nutrients, glucose and insulin but also protective of the islet cells, protecting them from response molecules of the immune system (Lim and Sun, 1980; Weir, 2013; Kepsutlu *et al.*, 2014). Due to their highly hydrophilic nature and their ability to mimic the extracellular matrix, hydrogels are favoured in the field of Tissue Engineering as encapsulation materials. More recently, these hydrogels are being investigated with addition of varying factors like vascular endothelial growth factor (VEGF), a promoter of angiogenesis to further mimic the extracellular matrix -ECM (Phelps *et al.* 2009).

Different polymeric materials have been suggested and tested as scaffolds for islet transplantation. These materials range from synthetic to natural polymers with varying physical, mechanical and thermal properties (described later). These

scaffolds offer support and protection for the islets; potentially shielding them from the instant blood mediated inflammatory response (IBMIR).

1.5 THE BIOARTIFICIAL PANCREAS

A bioartificial pancreas is a biomimetic device that substitutes for the endocrine portion of the pancreas while also avoiding the need for immunosuppressive drugs. The bioartificial pancreas combines encapsulation and the concept of a scaffold to create 3D macro and micro environments that mimic the native pancreas. It provides immunoisolation for the cells while also providing a semipermeable membrane for exchange of oxygen and nutrients (Kizilel, Garfinkel and Opara, 2005; Hwang *et al.*, 2016).

1.5.1 Biomaterial for Bioartificial Pancreas

Biomaterials for bioartificial pancreas have the typical material requirements for Tissue Engineering (TE). Typical materials for tissue engineering must:

- Support growth, attachment and proliferation of cells
- Mimic native environment of the tissue
- Provide mechanical support for the cells
- Be non-immunogenic, non-toxic, biodegradable and biocompatible
- Support blood supply to the cells (vascularisation)
- Promote rapidity in response to stimulus (Gunatillake and Adhikari, 2003; Kim *et al.*, 2008; Iacovacci *et al.*, 2016).

A variety of different materials have and can be considered for the development of Bioartificial Pancreas. These are described below:

1.5.1.1 Poly (ethylene) glycol

Poly(ethylene) glycol (PEG) has been widely investigated for use in islet encapsulation in the form of hydrogels because of its highly adjustable material characteristics. PEG has been shown to trigger a minimal immune response and promote cell adhesion, making it a good candidate for islet transplantation. Reported ways in which it's been used in islet transplantation include cell encapsulation in the form of hydrogels and in the modification of islet surfaces to reduce the instant blood mediated inflammatory reaction (IBMIR) pre-transplant (Lim and Sun, 1980; Kizilel *et al.*, 2010; Lin and Anseth, 2011).

Cruise *et al.* observed 90% encapsulation efficiency and islet viability after encapsulation of islets in photopolymerised PEG. This could be attributed to the fact that photopolymerised PEG forms an immune barrier on the surface of porcine islets. These findings are corroborated by studies showing that encapsulating islets cells in photopolymerised PEG is more efficient; with no loss of functionality to the cells (Cruise *et al.*, 1998; Teramura and Iwata, 2011). Polyethylene glycol conjugated with maleimide (PEG-MAL) is a derivative of PEG that has been used for encapsulation of β-cells. These encapsulated structures did not impair insulin release and showed physical stability up to 30 days, post-transplantation. Since vascularisation is an important factor for survival of islets, vascular endothelial growth factor was bound to the PEG-MAL structures which led to vascularisation

within 4 weeks of transplantation in diabetic rats (Phelps *et al.*, 2013; Teramura *et al.*, 2013).

Binding islets to PEG and its derivatives is a viable method of protecting islets post-transplantation. Treating islets with isocyanate, monosuccinimide and disuccinimide derivatives of PEG provided significant cyto-protective functions to the cells (Panza *et al.*, 2000; Xie *et al.*, 2005). When PEG was used as an immobiliser for microencapsulation of islets, increased encapsulation efficiency and insulin response were observed (Teramura and Iwata, 2011).

Further, PEG has also been used to coat microspheres of other materials used for islet transplantation. For example, coating the surface of alginate-polylysine islet microspheres with charged derivatives of PEG has been shown to further increase their biocompatibility (Chen *et al.*, 1998).

Using PEG hydrogels requires increased cell densities of up to 10^7 cells/ml. This is not always viable in situations where islets are limited. Cell adhesion rates vary with molecular weights of PEG structures. Because of this, other strategies like functionalisation of the surface of the PEG with proteins and ligands responsible for cell adhesion or insulin secretion in cells must be applied to make them more cytocompatible. PEG hydrogels have been functionalised with proteins like glucagon-like peptide-1 (GLP-1) and ligands like thiolated ephrin A5-Fc to foster the cell-cell interactions that are important for the survival and function of islets post transplantation (Kizilel *et al.*, 2010; Lin and Anseth, 2011).

1.5.1.2 Polyvinyl alcohol (PVA)

Polyvinyl alcohol (PVA) has been explored as a hydrogel material for many different biomedical applications. Due to its highly hydrophilic nature, it forms hydrogels easily and can be easily manipulated. It has also been shown to have selective permeabilities to different substances (Inoue *et al.*, 1992). Several studies have been performed in which islets encapsulated in PVA hydrogels have been transplanted into rats and they have all reported success in decreasing non-fasting blood glucose levels (Qi *et al.*, 2004, 2012). Although it possesses high hydrophilicity, it has a low mechanical strength. This can be circumnavigated through addition of substances like glutaraldehyde or by using specific methods for preparation of the hydrogel such as the addition of structural support like a mesh. (Young *et al.*, 2002).

1.5.1.3 Gamma Polyglutamic acid (γ-PGA)

Gamma Polyglutamic acid (γ-PGA) is a natural, hydrophilic, biodegradable and biocompatible homopolymer of D- and L-glutamic acid. Because of its high biocompatibility, hydrophilicity and low mechanical strength, it has been investigated widely as a carrier system in drug delivery, cell therapy and for the encapsulation of cells for soft tissue engineering (Shih and Van, 2001; Bajaj and Singhal, 2011; Ozdil and Aydin, 2014). Glutamic acid is an important part of the insulin release/production pathway indicating that polyglutamic acid could potentially play a part in both encapsulating islet cells and stimulating insulin secretion.

In combination with other polymers, γ -PGA hydrogels have been designed for different medical applications like drug and cell delivery (Yang *et al.*, 2002; Sonaje *et al.*, 2010).

1.5.1.4 Agarose

Agarose is another polysaccharide derived from seaweed. Because of its cytotoxicity and non-immunogenicity, it has been applied for use in transplanting islets. After diabetic mice were implanted with agarose cell encapsulated islet cells, they could achieve normoglycaemia for up to 100days. They also showed high degrees of immunoisolation. Another study showed that agarose encapsulated islets transplanted into mice demonstrated normoglycaemia indefinitely (Iwata *et al.*, 1992; Hwang *et al.*, 2016). It has also been shown to protect islets from the immune response via mononuclear infiltration (Kobayashi *et al.*, 2003).

1.5.1.5 Poly(Glycolic Acid)-PGA, Poly(Lactic Acid)-PLA, Poly(L-lactic Acid)- PLLA and Poly(Lactic-co-Glycolic Acid)-PLGA

These are synthetic polymers that have been investigated for their use in different tissue engineering as scaffolds for seeding cells and in making microspheres for encapsulation of cells and drug delivery. They are biodegradable, biocompatible polymers that are good candidates for islet transplantation. Islets encapsulated in PLGA microspheres and transplanted into rats led to decreased glucose levels and greater insulin yields (Abalovich *et al.*, 2001; Anderson and Shive, 2012). Thin PLGA-collagen meshes have also been shown to stimulate insulin release in rat

pancreatic cells (Kawazoe *et al.*, 2009). Islet-like cells derived from stem cells when seeded in PLGA scaffolds could reverse hyperglycaemia (Mao *et al.*, 2009).

Studies have shown that diabetic rats that had been injected with islets co-cultured with PGA had a better morphology of cells, cell viability, lower blood glucose levels and higher insulin content and remained hyperglycaemic up to 3 months post-transplantation (Juang *et al.*, 1996; Chun *et al.*, 2008; Hou *et al.*, 2009). Although these materials pose a good option, their bulk degradation need to be resolved for them to be perfect candidates for islet transplantation.

1.5.1.6 Polycaprolactone (PCL)

PCL is an FDA approved polymer that is used in a wide range of biomedical applications. For islet transplantation, PCL is favourable due to its adjustable degradation rates. It has been more commonly applied in combination with other polymers in islet transplantation. Islets seeded in PCL and alginate scaffolds have been shown to have similar insulin response to free floating islet cells in chicken membrane models. The scaffolds were however able to induce vascularisation (Marchioli, Luca, *et al.*, 2016). MIN6 cells were encapsulated in PCL/PEG nanoporous structures in allogenic mouse models. These systems did not induce an immune response but contributed to rapid vascularisation around the scaffold (Nyitray *et al.*, 2015). PCL/ polyethylene oxide micelles have shown the ability to load and deliver the SP600125 (a c-Jun NH_2-terminal kinase inhibitor) cell signalling modulator that prevents the death of human islets. This is an indication that the addition of these micelles to the scaffolds could improve the chances of islet survival post-transplantation (Savić *et al.*, 2009). Even though PCL scaffolds have

mechanical properties that make them suitable for soft tissue engineering, they have a slow degradation rate of about 2-3 years which is less than ideal for most Tissue Engineering applications (Chen, Liang and Thouas, 2013).

1.5.1.7 Collagen

Collagen is another biopolymer that has been widely explored for tissue engineering purposes. This is largely because it is a protein found in the extracellular matrix so it provides cells with a more native environment than matrices without the ECM proteins (Riopel and Wang, 2014). For islet transplantation, when mice islets were suspended in a collagen gel matrix and transplanted into diabetic C57BL/6 mice, both the viability and insulin release function of these cells was maintained. (Jalili *et al.*, 2011). Although its biocompatibility has been established, due to the availability of a wide variety of collagens, it faces an issue of variability in mechanical and physical properties (Sai K and Babu, 2000; Chen, Liang and Thouas, 2013).

Blended with alginate, collagen has also been shown to improve islet function both *in vitro* and *in vivo* with a reduction in glucose levels to 200mg/dl 60 minutes after transplantation into mice (Lee *et al.*, 2012). Collagen has also been shown to promote the aggregation of different endocrine cells in islets showing it as a potential polymer for bioartificial pancreas (Montesano *et al.*, 1983).

Based on the advantages and drawbacks of materials discussed earlier, alginate was determined to be a material of interest in the creation of bioartificial pancreas.

1.6 ALGINATE

Alginate is an anionic highly hydrophilic polysaccharide with low cost, high biocompatibility, low toxicity and ease of customisation (Kuo and Ma, 2001; Lee and Mooney, 2012). It is a natural occurring polymer produced by brown seaweed species including *Laminaria digitata*, *Laminaria japonica*, *Laminaria hyperborea*. It is also produced by bacteria, especially the *Azotobacter* and *Pseudomonas sp.* (Lee and Mooney, 2012). Bacteria derived alginate is favoured because it has more well defined chemical and physical structures and properties.

1.6.1 Structure of Alginate

Alginate is a family of block copolymers containing β-D-mannuronic (M) and α-L-guluronic (G) acids linked a the (1, 4) positions respectively (Kuo and Ma, 2001; Remminghorst, 2007). The chemical structure is shown in Figure 1.4. The ratios of mannuronic acid to guluronic acid in the structure depends on the source and synthesis of alginate. They can contain consecutive or alternating M and G residues. Due to the different arrangements and combinations possible, a huge variety of alginate polymers exist (Kuo and Ma, 2001; Remminghorst, 2007; Lee and Mooney, 2012).

To form hydrogels, metal salts of alginate (typically sodium or potassium) are crosslinked with ions such as Ca^{2+} derived from $CaCl_2$, $CaCO_3$ and $CaSO_4$. Typically, the Ca^{2+} ions bind to the guluronate residues of each polymer and join up with another polymer chain. Many factors influence the mechanical and physical properties of the hydrogel formed including the M/G ratio, G-block chain and

molecular weight, making it an easily modifiable polymer (Kuo and Ma, 2001; Lee and Mooney, 2012).

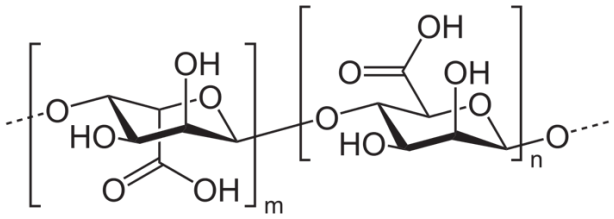

Figure 1.4: Chemical structure of alginate.

1.6.2 Microbial Production of Alginate

Although seaweed are the primary sources of alginate, microbial production of alginate is another area of interest due to its potential environmentally friendly applications.

Microbial production is carried out via fermentation of a range of carbon sources ranging from sugars, glycerol and acetate. Alginate is produced under nitrogen limiting conditions, especially nitrogen and phosphate. Alginate offer protection from adverse conditions like high temperature to bacteria (Mian, Jarman and Righelato, 1978; Clementi, 1997).

Two major species of bacteria have been indicated in the production of alginate, including *Pseudomonas* and *Azotobacter.* Alginate is produced in *Pseudomonads* in microaerophilic conditions and the yield of alginate increases in nutrient limiting conditions (Sabra and Zeng, 2009; Franklin *et al.,* 2011; Hay *et al.,* 2014). The polymer plays a role in cell adhesion and quorum sensing activities of *Pseudomonas*

aeruginosa in opportunistic infections present in conditions like cystic fibrosis. The alginate produced also enhances survival in adverse conditions. *Azotobacter spp.* are Gram-negative bacteria that participate in nitrogen fixation. Alginate is produced extracellularly as part of their life cycle under conditions of nutrient limitation (Clementi, 1997). *Azotobacter vinelandii* is the most widely studied producer of alginate. It produces alginate with more gulucoronic acid residues than alginate produced by *Pseudomonads*. This directly affects the strength of the crosslinking in hydrogel formation as crosslinking efficiency is directly related to proportion of gulucoronic acid residues (Bonartseva *et al.*, 2017). Additionally, due to the safety issues associated with *Pseudomonas aeruginosa,* alginate from *Azotobacter vinelandii* is preferred. The drawback is that the yield of alginate produced from *Azotobacter vinelandii* is very low (Bai *et al.*, 2017).

1.6.3 Biomedical Applications of Alginate

1.6.3.1 Drug Delivery

Alginate has been extensively studied for its use in drug delivery systems. Because of the ease of modification of alginate hydrogel systems, hydrogels with different properties can be developed. These include controlled drug delivery systems, pH and temperature sensitive hydrogels. They can be applied in different forms including capsules, micro and macro spheres and beads (Jain and Bar-Shalom, 2014). Some of these drugs include gentamycin sulphate, pindolol, nitrofurantoin, timolol maleate, diclofenac, lidocaine HCl, sodium salicylate, acebutulol and indomethacin (Filipović-Grćić *et al.*, 1995; Fernández-Hervás *et al.*, 1998; Park *et al.*, 1998; Sezer,

1999; Takka, 1999; Kulkarni *et al.*, 2000; Coppi *et al.*, 2001; Tønnesen and Karlsen, 2002).

1.6.3.2 Wound Dressings

Due to its ability to form hydrogels easily, alginate has been widely investigated for its use in wound healing. One of the areas that have been studied is in diabetic ulcers. Alginate in combination with other materials is mainly used in hydrogel form for wound healing.

Silver alginate dressings have shown long-term anti-microbial effect and efficacy over a 21-day test period (Percival and McCarty, 2015). In combination with DNA, alginate gels have been trialled for their use in diabetic ulcers. These tests showed a high degree of biocompatibility for the hydrogels, proving its potential for use in diabetic ulcers (Tellechea *et al.*, 2015). Chitosan-alginate wound dressings have been proven to promote production of collagen and fibrous tissue, hence speeding up wound healing (Caetano *et al.*, 2015). In combination with curcumin and chitosan nanoparticles, alginate has been shown to accelerate shrinkage, complete epithelialization and formation of collagen (Karri *et al.*, 2016).

1.6.3.3 Islet Cell Encapsulation

Many studies have evaluated alginate hydrogels as materials for cell encapsulation. Most recently, beta cells derived from human embryonic stem cells were encapsulated in alginate derivatives and transplanted into mice. The cells could retain function up to 174 days after transplantation. The alginate derivatives provided support from the IBMIR (Vegas *et al.*, 2016). Sustained function and reversal of

diabetes has been reported after pig islets were encapsulated in alginate and then transplanted into animal models and one human model (Dufrane, Goebbels and Gianello, 2010; Jacobs-Tulleneers-Thevissen *et al.*, 2013). Islets encapsulated in biocompatible capsules formed by crosslinking alginate with barium chloride maintained their levels in non-obese diabetic (NOD) mice up to 350 days post-transplantation (Duvivier-Kali *et al.,* 2001). More frequently, alginate has been used in conjunction with other polymers for encapsulation of islet cells. Combining alginate with other biopolymers like collagen and PEG for encapsulation of islets has helped improve the biocompatibility of the constructs and given the islets a better chance of survival *in vivo* (Montesano *et al.,* no date). Alginate hydrogels embedded in polytetrafluorethylene membranes showed positive graft function in a 60-year-old patient up to 10 months post-transplantation. Sustained insulin response was also observed (Lee *et al.,* 2012). When coated with poly-lysine, implanted alginate hydrogel capsules influenced better insulin response than crude alginate capsules (Vos *et al.,* 1997). Embedding peptides in alginate hydrogels has been shown to increase cell accessibility and adhesion (Vériter *et al.,* 2010; Sun and Tan, 2013). Alginate has been combined with argynyl-glycyl-aspartic acid (RGD peptide) with no immune/ inflammatory reaction up to 60 days after transplantation into rats (Lee *et al.,* 2012).

1.7 POLYHYDROXYALKANOATES (PHAS)

Polyhydroxyalkanoates (PHAs) are polymers of hydroxyalkanoic acids with high molecular weight. The monomer units have hydroxyl groups attached at the 3, 4, 5 or 6-positions (Figure 1.5). Because of this variability in the structures of different

PHAs, they have varying physical properties and hence can be used in many different applications (Lee, 1996a; Khanna and Srivastava, 2005; Keshavarz and Roy, 2010). These fields range from hard tissue engineering like bone to soft tissue applications like cardiac, nerve and skin tissue engineering and delivery systems for drug and cells (Chen and Wu, 2005; Philip, Keshavarz and Roy, 2007; Pooja Basnett, K Y Ching, *et al.*, 2013; Lizarraga-Valderrama *et al.*, 2015). PHAs also exhibit better biocompatibility than other commonly used materials for TE like PLA, PCL and PLGA. This has led to them being applied widely in the biomedical field. Applications that have been investigated include wound patches, cardiac patches, bone tissue engineering, drug delivery, urological stents, artificial oesophagus, nerve tissue engineering and coronary artery stents (Valappil *et al.*, 2007; Akaraonye, Keshavarz and Roy, 2010; Ranjana Rai *et al.*, 2011; Pooja Basnett, K Y Ching, *et al.*, 2013). PHAs have been shown to support the growth of a wide range of cells including murine islet cells, cardiac, nerve, bone and mesenchymal stem cells (Yang *et al.*, 2010; Mouriño *et al.*, 2013; Nigmatullin *et al.*, 2015). They have also been explored for other uses like drug delivery systems, suture materials and cell delivery systems (Ranjana Rai *et al.*, 2011; Garg, Singh and Goyal, 2013)

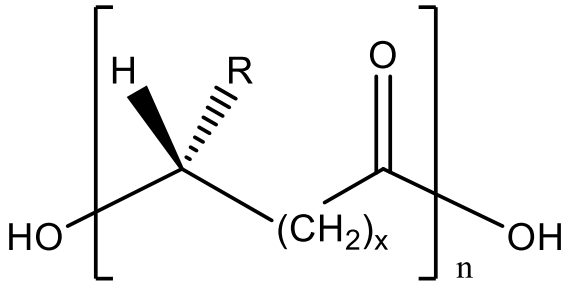

Figure 1.5: The general structure of polyhydroxyalkanoates (x = number of methylene groups in the backbone; n = 1000-10000; R = alkyl groups, C_1-C_{13})

1.7.1 Classes of PHAs

PHAs are classified into two types based on their monomer chain length.

1.1.1.1.Short-Chain Length PHAs (Scl-PHAs)

Short chain length PHAs have 3-5 carbon atoms in their monomers usually accumulated by bacteria of the *Bacillus, Cupriavidus* and *Azotobacter spp*. They are stiff, brittle polymers with high crystallinity, melting temperatures between 160-180^{o}C and glass transition temperatures between -5-+20^{o}C (Basnett and Roy, 2010). They also have high tensile strength, low elongation at break. An example is poly(3-hydroxybutyrate)-P(3HB) (Zinn, Witholt and Egli, 2001; Reddy *et al.*, 2003; Ojumu, Yu and Solomon, 2004; Keshavarz and Roy, 2010).

The brittleness of P(3HB) is a challenge to its processibilty, so blending with mcl-PHAs is preferred for biomedical applications.

1.1.1.2.Medium-Chain Length PHAs (mcl-PHAs)

Mcl-PHAs contain 6-14 carbon atoms in their monomer units. They are accumulated by fluorescent *Pseudomonas spp.* in harsh growth conditions. They exhibit low melting temperatures between 40-60^{o}C, glass transition temperatures between -50-25^{o}C. They also show low tensile strength and high elongation at break, typical of elastic polymers They typically consist of 1,000 monomer units (Sun *et al.*, 2007; Keshavarz and Roy, 2010; R. Rai *et al.*, 2011).

Due to their low thermal characteristics and tensile strength, blending with scl-PHAs is an attractive option for creating blends with optimal properties for biomedical applications (Witholt and Kessler, 1999; P. Basnett *et al.*, 2013).

PHAs can also be classified as homo or heteropolymers. Examples of homopolymers include P(3HO) and P(3HB). Examples of heteropolymers include poly(3-hydroxyhexanoate-co-3-hydroxyoctanoate) P(3HHx-co-3HO) (Keshavarz and Roy, 2010). Blending two classes of PHAs creates polymers with different properties to the individual component polymers. For example, blending P(3HB) and P(3HV) forms a polymer blend that is more malleable than the stiff P(3HB) (R. Rai *et al.*, 2011).

1.7.2 Properties of PHAs

There are a few general properties exhibited by all the classes and types of PHAs. These include:

- Solubility in chlorinated solvents and insolubility in water.
- Wide range of melting temperatures (40-180^{o}C).
- Degradation dependent on the side chains and monomeric units present.
- Biocompatibility.
- Biodegradability.
- Non-toxicity.
- Slow degradation rates.
- Resistant to hydrolytic degradation (Ali Raza, Riaz and Banat, 2017; Basnett *et al.*, 2017; Raza, Abid and Banat, 2018a).

The properties of PHAs can be varied through genetic or physiological strategies. Including a co-monomer or a different hydroxyalkanoic acid monomer into the polymer backbone can alter polymer properties like flexibility, toughness and stiffness (Valappil *et al.*, 2007).

1.7.3 Synthesis of PHAs

PHAs are accumulated in inclusions (granules) in the cytoplasm of cells under nutrient limiting conditions. These inclusions are between 0.25-0.5µm and can be viewed by contrast light microscopes. They are lipid-like molecules and can be stained by Sudan black (Sudesh, Abe and Doi, 2000). Figure 1.6 summarises the pathways involved in the synthesis of PHAs.

1.7.3.1 P(3HB) Synthesis

P(3HB) synthesis takes place on the surface of the granule. It is a three-step process catalysed by important enzymes. 2 Acetyl-CoA molecules from the tricarboxylic acid cycle (TCA) are condensed by β-ketothiolase (PhaA) to form acetoacetyl-CoA. This is then reduced through the NADH-dependent acetoacetyl-CoA reductase (PhaB) at the C_3-position to form 3-hydroxybutyryl-CoA. P(3HB) synthase then esterifies 3-hydroxybutyryl-CoA to P(3HB), releasing the CoA molecules (Zinn, Witholt and Egli, 2001; Verlinden *et al.*, 2007a).

1.7.3.2 Mcl-PHA Synthesis

There are three different metabolic pathways that are involved in supplying mcl-PHA precursors for the final conversion to mcl-PHAs:

- *de novo* fatty acid biosynthesis in which (R)-3-hydroxyacyl-CoA is formed using unrelated carbon sources like sugars.
- Fatty acid degradation by *β-oxidation*, which is the main metabolic route for fatty acids.
- Chain elongation of acyl-CoA to acetyl-CoA.

These pathways all generate mcl-PHA precursors: (R)-3-hydroxyacylacyl-CoA, 3-ketoacyl-CoA and 2-trans-enoyl-CoA. These are then converted to (R)-3-hydroxyacyl-ACP by the actions of 3-hydroxyacyl-CoA epimerase, 3-ketoacyl-ACP-reductase and (R)-specific enoyl-CoA hydratase (PhaJ).

These (R)-3-hydroxyacyl-ACP molecules are then converted to (R)-3-hydroxyacyl-CoA in a reaction catalysed by (R)-3-hydroxyacyl-ACP-CoA transferase (PhaG).

Finally, mcl-PHA synthases (PhaC) modulate the conversion of (R)-3-hydroxyacyl-coA to the respective mcl-PHA with a release of CoA (Witholt and Kessler, 1999; Zinn, Witholt and Egli, 2001; Kim *et al.*, 2007; Chen *et al.*, 2015; Wang, Chung and Chen, 2017).

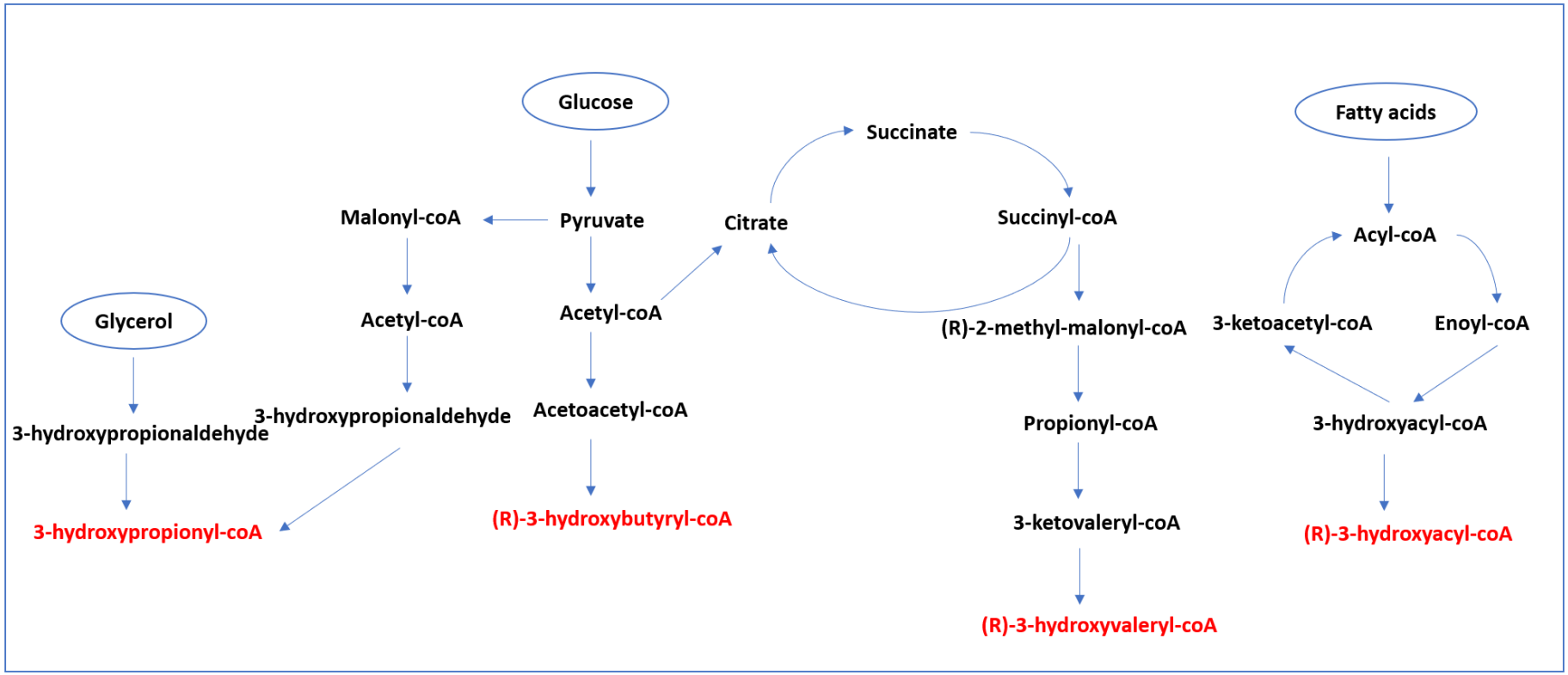

Figure 1.6: Pathways for synthesis of polyhydroxyalkanoates

1.7.4 Microbial Production of PHAs

Ever since granules containing P(3HB) were discovered in cells of *Bacillus megaterium* in 1926, PHAs have been discovered in a wide range of bacteria (Lemoigne, 1926; Lee, 1996b). These bacteria are predominantly of the *Bacillus, Pseudomonas, Azotobacter* and *Cupriavidus sp.* (Anjum *et al.*, 2016; Raza, Abid and Banat, 2018b). Most PHAs are synthesized from structurally similar substrates, so types and quantities of carbon source for fermentation determine the final PHA produced (Lee, 1996a; Ojumu, Yu and Solomon, 2004). Bacteria have PHA synthase enzymes that determine the PHA production pathway undertaken and hence, the particular class of PHAs produced (Anjum *et al.*, 2016).

Bacillus sp. are a class of Gram-positive bacteria in which P(3HB) was first discovered. They have been shown to produce scl-PHAs including P(3HB), P(4HB) and their copolymers using sugars as the carbon source (Aslim, Yüksekdağ and Beyatli, 2002; Valappil *et al.*, 2006; Halami, 2008a). *B. licheniformis, B. megaterium, B. cereus* and *B.subtilis OK2* have all been shown to produce P(3HB) when glucose was used as a carbon source (Chen, König and Lafferty, 1991; Singh, Patel and Kalia, 2009; Sukan, Roy and Keshavarz, 2017; Lukasiewicz *et al.*, 2018).

Organisms belonging to the rRNA class of *Pseudomonas sp.* including *P. putida, P. oleovorans, P.aeruginosa, P.mendocina* have been shown to produce mcl-PHAs through the fatty acid β-oxidation pathway. This occurs when alkanoic acids or fatty acids are used as the carbon source (Suriyamongkol *et al.*, 2007). Some *Pseudomonas sp.* have been shown to use other substrates as carbon sources. These

include sugars (Wang *et al.*, 2016), biodiesel waste (Chanasit *et al.*, 2016) and glycerol (Poblete-Castro *et al.*, 2014).

Cupriavidus necator has been shown to produce P(3HB) from simple sugars (Khanna and Srivastava, 2005) and plant oils (Fukui and Doi, 1998; Kahar *et al.*, 2004).

1.7.5 Biomedical Applications of PHAs

1.7.5.1 Drug Delivery

Because of the high levels of biodegradability and biocompatibility, PHAs are promising candidates for drug delivery. PHA micro and nanospheres have been widely investigated for their use in varying drug delivery applications (Zinn, Witholt and Egli, 2001). P(3HB) is the PHA of choice for drug delivery because of its ready availability, ease of production and application in controlled release of drug. Another advantage of using PHAs as drug delivery systems is that they degrade slower than other commonly investigated biopolymers (Park, Choi and Lee, 2005; Nigmatullin *et al.*, 2015).

PHAs have also been used in drug delivery systems in the form of drug loaded rods and drug eluting scaffolds. Antibiotic loaded PHA rods were transplanted into rabbits with infected tibias. These rods showed both burst and sustained release up to 2 months post-transplantation. Successful antibiotic leaching also resulted in elimination of infection up to six weeks post transplantation (Gursel *et al.*, 2002). Incorporating aspirin into PHA blend films led to uniform distribution and constant aspirin release over 20-30 days (Pooja Basnett, Kuan Yong Ching, *et al.*, 2013)

1.7.5.2 Hard Tissue Engineering

The most prevalent use of PHAs in hard tissue engineering is in bone tissue engineering with P(3HB) as the PHA of choice due to its mechanical strength. Due to its brittleness though, co-polymers or composites of PHAs are commonly used. In comparison to P(3HB), poly(3-hydroxybutyrate-co-3-hydroxyvalerate-co-3-hydroxyhexanoate)- P(3HB-co-HV-co-HHx) has shown higher levels of human marrow mesenchymal stem cell adhesion (Hayati *et al.*, 2012).

Blending PHAs with hydroxyapatite (HA) has been shown to increase their compressive modulus and maximum stress. Additionally, osteoblasts grown on P(3HB)/HA structures showed increased cell growth and alkaline phosphatase activity (Wang *et al.*, 2005). In rats, formation of connective tissue was observed 45 days after P(3HB)/HA composite structures were implanted. These implants also showed complete repair of bone defects in rats post transplantation. By day 30, the bone was completely healed (Shishatskaya *et al.*, 2016).

PHA scaffolds containing Bioglass^{TM} have been shown to have increased bioactivity, protein adsorption and bactericidal effects (Misra *et al.*, 2010). Including zirconium dioxide in PHA scaffolds improved the mechanical properties, making them similar to that of native bone (Meischel *et al.*, 2016).

1.7.5.3 Soft Tissue Engineering

In Cardiac Tissue Engineering, PHAs have been a primary focus. When P(3HO) is blended with P(3HB) in a cardiac stent to provide mechanical support, the structure exhibits significantly high cell viability and protein adsorption (Basnett and Roy,

2010). When mcl-PHA based trileaflet heart valves were incubated with ovine vascular cells, extensive cell attachment and confluence were observed. The structure also exhibits flexibility better than other commonly used polymers (Sodian *et al.*, 2000).

The creation of cardiac patches is another area where PHAs have proven to be important biomaterials. Tepha Inc. have produced a trileaflet scaffold made up of P(4HB) and P(3HOHHx). This scaffold can be used without the need for sutures due to its adhesive properties. (Dubey, 2017). P(3HO) neat patches also showed high cell viabilities, proliferation and adhesion with neonatal ventricular rat myocytes and cardiomyocytes seeded on them (Bagdadi *et al.*, 2018).

Due to their elastomeric properties that can mimic those of the nerves, mcl-PHAs are favoured in nerve tissue engineering. P(3HO) and P(3HB) blend

films seeded with NG 108-15 neuronal cells exhibited appropriate mechanical properties for nerve tissue engineering. They also showed better cell growth and differentiation (Lizarraga-Valderrama *et al.*, 2015). When Schwann cells and neuronal growth factors were included in the P(3HB) scaffolds, the scaffolds showed an increased ability to enhance regeneration (Armstrong *et al.*, 2007). P(3HB) scaffolds with glial growth factor and transplanted into rabbits with 2-4cm gaps in nerves showed nerve regeneration within 63 days post-transplantation (Mohanna *et al.*, 2003).

P(3HB-co-3HHx) nerve conduits implanted in rats exhibited stable mechanical properties, selective permeability and integrity of structure even after >20% loss in molecular weight due to degradation. After 3 months, these factors showed excellent

nerve regeneration, hence confirming their potential as nerve conduits (Bian *et al.*, 2009). P(3HB-co-3HHx) scaffolds exhibited more extensive differentiation of human bone marrow mesenchymal stem cells into nerve cells (Zhang *et al.*, 2018). P(3HB-co-3HHx) nanofibre scaffolds have been shown to promote nerve stem cell differentiation to neurons (Xu *et al.*, 2010).

1.7.5.4 Pancreatic Tissue Engineering

Even though PHAs have been extensively researched for their use in biomedical applications, not a lot of research has been carried out involving PHAs in Islet transplantation. Chaturvedi *et al.* investigated the use of PHA nanoparticles for the oral delivery of insulin and demonstrated that these nanoparticles sustained insulin release (Chaturvedi *et al.*, 2015). Yang *et al.* compared the growth of NIT-1 cells (murine beta cell line) on poly-lactic acid and two different PHAs - poly(3-hydroxybutyrate-co-3-hydroxyhexanoate) and poly(3-hydroxybutyrate-co-4-hydroxybutyrate). Their study showed that the PHAs promoted cell interaction of the NIT-1 cells and increased insulin secretion in comparison to PLA (Yang *et al.*, 2010).

Table 1.2 shows a summary of some of the most popularly used polymers for islet transplantation with their drawbacks.

Table 1.2: Polymers Used in islet transplantation

Polymer	**Natural/ Synthetic**	**Uses**	**Drawbacks**
Poly(ethylene) glycol	Synthetic	• Photo-polymerised hydrogel • Surface coating of microspheres increasing biocompatibility • Surface modification of islets providing immunoprotection.	Non- uniform porosity, non-biodegradability
Polyvinyl alcohol	Synthetic	Hydrogel encapsulating islets	Low mechanical properties
Alginate	Natural	• Encapsulating islets • Increases biocompatibility of other polymers • Reduces IBMIR when modified with peptides	Huge variability in types
PLGA, PGA, PLLA, PGA	Synthetic	• Microspheres stimulating insulin release from islets • Scaffold for cells	Bulk degradation

Polycaprolactone	Synthetic	• Easily tunable • Scaffolds for cells • FDA- approved	Low mechanical strength
Polyhydroxyalkanoates	Natural	• Scaffolds for islets • Wide variety of properties in class of polymers	Expensive to produce

1.8 MULTI-POLYMERIC DEVICES FOR PANCREATIC TISSUE ENGINEERING

To overcome some of the issues associated with islet transplantations, current research has been geared towards the creation of 3D multipolymer scaffolds, otherwise known as bioartificial pancreas. These devices are multifunctional devices created to mimic the native pancreas and give the islets a greater chance of survival. They aim to resolve some of the challenges associated with islet transplantation by targeting multiple issues at the same time. The basic design for most of these devices is to have encapsulated islets and then to surround them with a polymeric scaffold. Several combinations of biopolymers have been exploited for creating this ideal bioartificial pancreas. Table 1.3 summarises some of these devices.

The TRAFFIC device consisting of an alginate hydrogel layer spun around a polymer scaffold was investigated (Figure 1.7). In diabetic mice that received the device, normoglycaemia was observed up to 4 months post-transplantation. When scaled up to beagle dogs, the same effect was observed up to 1 month with the device remaining intact enough to be retrieved (An *et al.*, 2018).

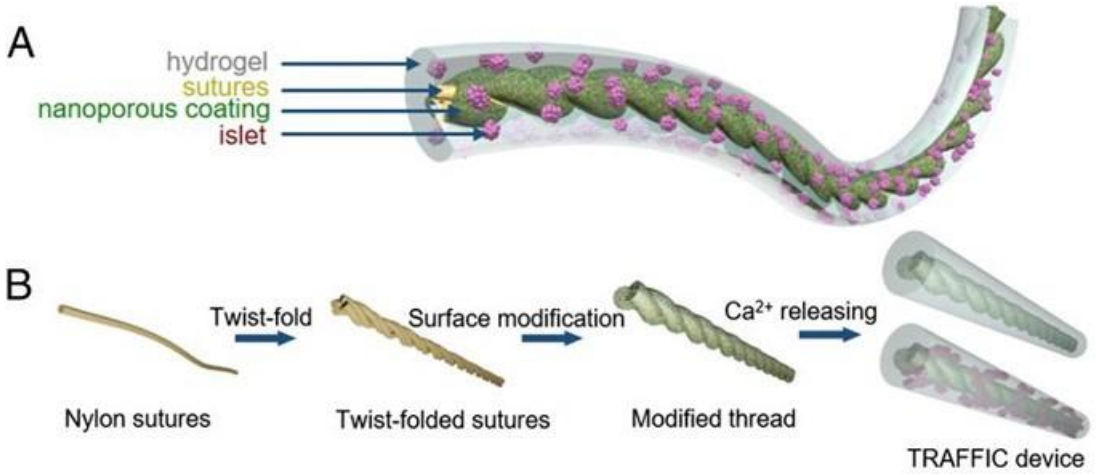

Figure 1.7: Schematic design and fabrication of the TRAFFIC device (An *et al.*, 2018).

Maki and his colleagues at the New England Deaconess Hospital in Boston tested a bioartificial pancreas designed using a porous copolymer membrane in dogs. In dogs given a dose of aspirin after transplantation, 30% did not require exogenous insulin for normoglycaemia (Maki *et al.*, 1991).

Marchioli *et al.* described a 3D device in which a heparin immobilised alginate core functionalised with VEGF is surrounded by a PCL scaffold. This device attempted to provide cytoprotection, immune isolation and vasularisation. Islets encapsulated in this device were shown to be effective in insulin response. The device was also shown to promote vascularisation (Marchioli, Luca, *et al.*, 2016).

Ludwig *et al*. explored the use of alginate and Teflon to create a multifunctional device that provided both immune protection and oxygen supply (Figure 1.8). The device was made of 2 islet modules with polytetrafluorethylene (PTFE) membranes impregnated with alginate. The device contained two islet modules separated by an oxygen module with a port for supplementation (Ludwig *et al.*, 2012, 2013; Neufeld *et al.*, 2013).

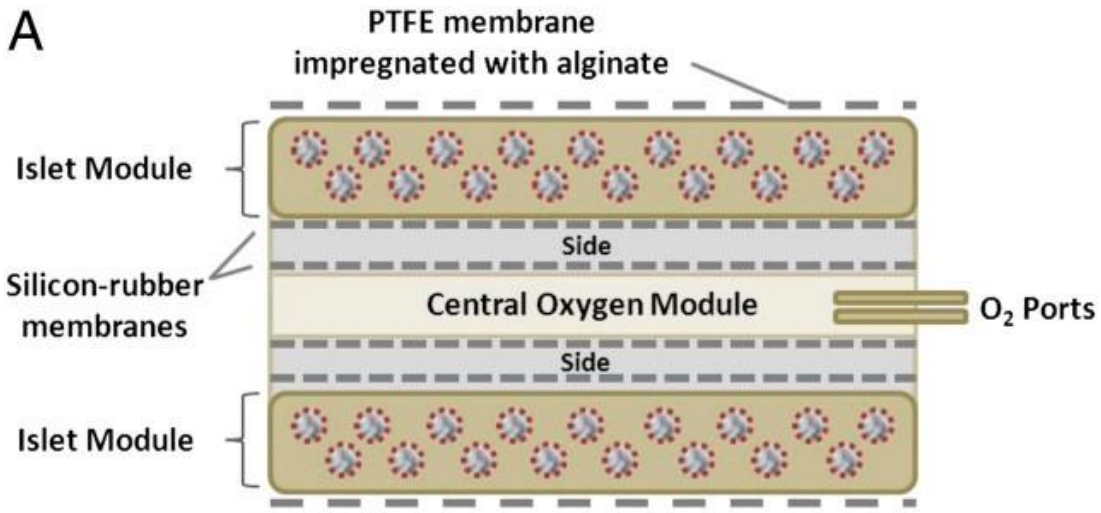

Figure 1.8: Islet transplantation device consisting of PTFE membrane impregnated with alginate and islet modules (Neufeld *et al.*, 2013)

This device was transplanted into a 63-year-old gentleman. The transplanted islets continued to show structural integrity and glucose responsiveness up to 10 months post-transplantation when the device was removed. This technology was scaled up by Beta-O_2 funded by the Juvenile Diabetes Research Foundation (JDRF) who in conjunction with the Uppsala University Hospital have taken it to Phase I clinical trials.

Viacyte, a company that is an offshoot of the Edmonton group have designed the Encaptra drug delivery system which contains embryonic stem cells embedded in a polymeric scaffold. The device contains stem cell precursors of islets. The company received a $16.6-million-dollar grant from the California Institute of Regenerative Medicine and $20 million from a Johnson & Johnson Venture arm. The device is in clinical trials (Dolgin, 2014, 2016; Lou, 2014). Living Cell technologies in New Zealand developed Diabecell, a xenograft of pig islet cells encapsulated in an undisclosed hydrogel. The company received NZ$ 4 million to scale up the technology. Diatranz-Otsuka bought the product licence and have now taken the product to Phase II/III clinical trials (Garkavenko *et al.*, 2011).

Table 1.3: Summary of bioartificial pancreas models available

Source	**Structure**	**Cells**	**Site of Transplant**	**Progress**
New England Deaconess Hospital	Co-polymer membrane	Canine pancreatic cells	Iliac artery	
Marchioli *et al.*	Heparin immobilised alginate core Embedded in PCL scaffold	Human islets	Hepatic portal vein	
Beta-O_2 (β-air)	Alginate hydrogel Polytetrafluorethylene (PTFE) membrane	Human islets	Abdomen	Phase I clinic trials

Viacyte (Encaptra)	Undisclosed polymeric scaffold	Embryonic stem cell precursors of islets (PEC-01)		Phase I/IIa clinical trials
Living Cells Technologies (Diabecell)	Undisclosed hydrogel	Porcine Islets		Phase II/III clinical trials
TRAFFIC device	Alginate hydrogel layer around wettable undisclosed polymer thread	Human islets	Kidney	

AIMS AND OBJECTIVES

The major aim of this project is to create a novel 3D functional bioartificial pancreas for the treatment of insulin deficiency in Type 1 diabetes. This structure will be made up of an outer biodegradable 3D PHA scaffold to provide immuno-protection and structural support. This outer layer will surround an inner hydrogel layer made up of alginate encapsulated pancreatic cells. This inner layer will also provide additional immune-isolation and mimic the morphology of the natural environment of the Islets of Langerhans. Figure 1.9 is a summary of the final outcome 3D printed structure planned from this work.

To achieve this aim, the following objectives were set and achieved:

1. Production and characterisation of polyhydroxyalkanaoates: two kinds of PHAs- P(3HB) and an mcl-PHA, Poly(3-hydroxyoctanoate-co-3-hydroxydecanoate), P(3HO-co-3HD), were produced by fermentation using *Bacillus subtilis*OK2 and *Pseudomonas mendocina* CH50. They were then characterised chemically, mechanically and thermally. Their production was also monitored and profiled with respect to optical density, biomass and usage of nutrients.

2. Fabrication of PHA scaffolds: Both P(3HB) and mcl-PHA, P(3HO-co-3HD), were fabricated into 2D neat films, 2D porous films and 3D porous scaffolds. These structures were characterised mechanically, thermally and physically. Cell viability and insulin release studies were then carried out on pancreatic cells seeded within or on these scaffolds.

3. Mcl-PHA/(P3HB) blends were generated in an attempt to optimise the mechanical and thermal properties of scaffolds to those of the native pancreas. A variety of blends were made and these blends were tested for cell viability and insulin release.

4. Alginate hydrogels were created using two different methods- droplet method for microspheres and 3D- printing. Pancreatic cells were seeded in these and they were then tested for cell viability and insulin release effects.

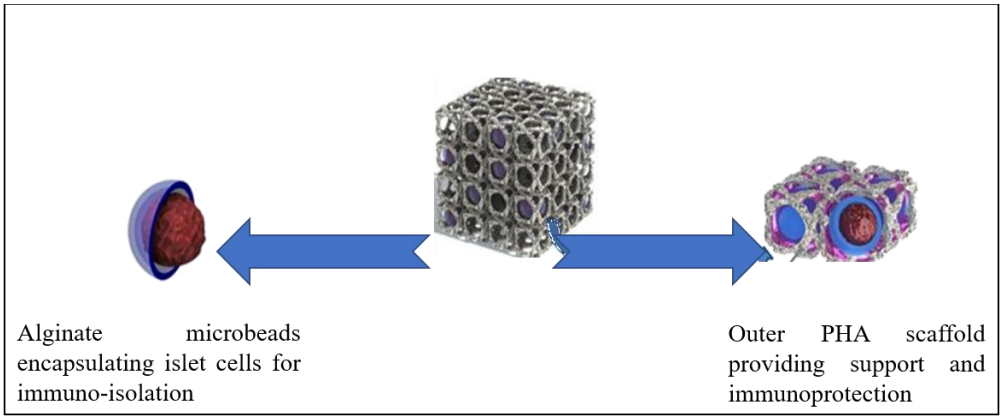

Figure 1.9: The final 3D scaffold planned to be constructed in future using the knowledge developed using the work described in this thesis.

CHAPTER TWO: MATERIALS AND METHODS

2. MATERIALS AND METHODS

2.1. BACTERIAL STRAINS, CELL LINES AND CHEMICALS

All chemicals were purchased from Sigma-Aldrich and VWR except otherwise stated. *Pseudomonas mendocina* CH50 and *Bacillus subtilis* OK2 were derived from the University of Westminster's culture collection with *B. subtilis* OK2 kindly supplied by Professor Fujio Kawamura from the Department of Life Sciences, Rukkyo University, Tokyo Japan. Cell culture studies were carried out using BRIN-BD11, rat pancreatic beta cell line purchased from European Collection of Cell Cultures (ECACC) (Dorset, UK). Cell culture studies were carried out using cell culture grade reagents from Sigma-Aldrich or Gibco. Insulin estimation was carried out using Mouse Insulin ELISA kit from Merck-Millipore.

2.2.PRODUCTION OF THE POLYMERS

2.2.1. Production of P(3HB)

P(3HB) was produced using *Bacillus subtilis* OK2 by fermentation in 10L fermenters (Fermac 310/60, Electrolab, Texas USA) with glucose as carbon source. The production was carried out in two stages and at each stage the inoculum used was 10% of the working volume. Nutrient Broth Number 1 was used to produce the seed culture. The constituents of nutrient broth are shown in Table 2.1.

The production medium was a modified Kannan and Rehacek. Components of the media are as shown in Table 2.2. The media was maintained at pH 6.8.

Table 2.1: Constituents of Nutrient Broth 1 used in P(3HB) Production from B. subtilis OK2

Constituent	**Composition (g/L)**
Glucose	1
Peptone	15
Sodium chloride	6
Yeast extract	3

The growth in nutrient broth was carried out at 30°C with orbital shaking at 140 rpm (C25KC incubator shaker, Edison, NJ, USA). The production stage was inoculated and grown (30°C, pH 6.8 and stirrer speed 200 revs/minute) in 10L glass bench top fermenters (Fermac 310/60, Electrolab, Texas USA). The fermentation was carried out for 48 hours and then harvested.

Table 2.2: Modified Kanan-Rehacek for the production of P(3HB) from B. subtilis OK2

Media Component	**Composition (g/L)**
Yeast extract	2.5
$(NH_4)_2SO_4$	11
Glucose	35

2.2.2. Production of P(3HO-co-3HD):

P(3HO-co-3HD) was produced using *Pseudomonas mendocina* CH50 by fermentation in 20L glass bench top fermenters with e-Z control (Applikon) with glucose as the carbon source. The production process (Figure 2.1) was carried out in three stages and at each stage the inoculum measured 10% of the working volume.

Nutrient Broth Number 2 was used to produce the seed culture. The constituents are shown in Table 2.3.

Table 2.3: Constituents of Nutrient Broth 2 used for P(3HO-co-3HD) Production from P. mendocina CH50

Constituent	**Composition (g/L)**
Meat peptone	4.3
Casein peptone	4.3
Sodium chloride	6.4

Second stage medium and Production Stage medium were slightly modified versions of Mineral Salt Medium (Table 2.4). The media was maintained at pH 7.00. The second stage was inoculated using a 16-hour seed culture and grown at 30°C with orbital shaking at 140 rpm (C25KC incubator shaker, Edison, NJ, USA). Production stage inoculation was carried out when the absorbance of the second stage medium measured 1.6 at 450 nm. Production stage was incubated and grown (30°C, pH 7 and stirrer speed 200 revs/minute) in fermenters 20L glass bench top fermenters with

e-Z control (Applikon). The fermentation was run for 48 hours and then harvested.

Table 2.4: Media Constituents for Second and Production Stages of P(3HO-co-3HD) Production

	Amount (g/L)	
Substance	**Second Stage Medium**	**Production Stage Medium**
$(NH_4)_2SO_4$	0.4	0.5
Na_2HPO_4	3.4	3.8
KH_2PO_4	2.3	2.65
$MgSO_4.7H_2O$	0.4	0.4
Glucose	20	20
Trace elements	1 ml	1 ml

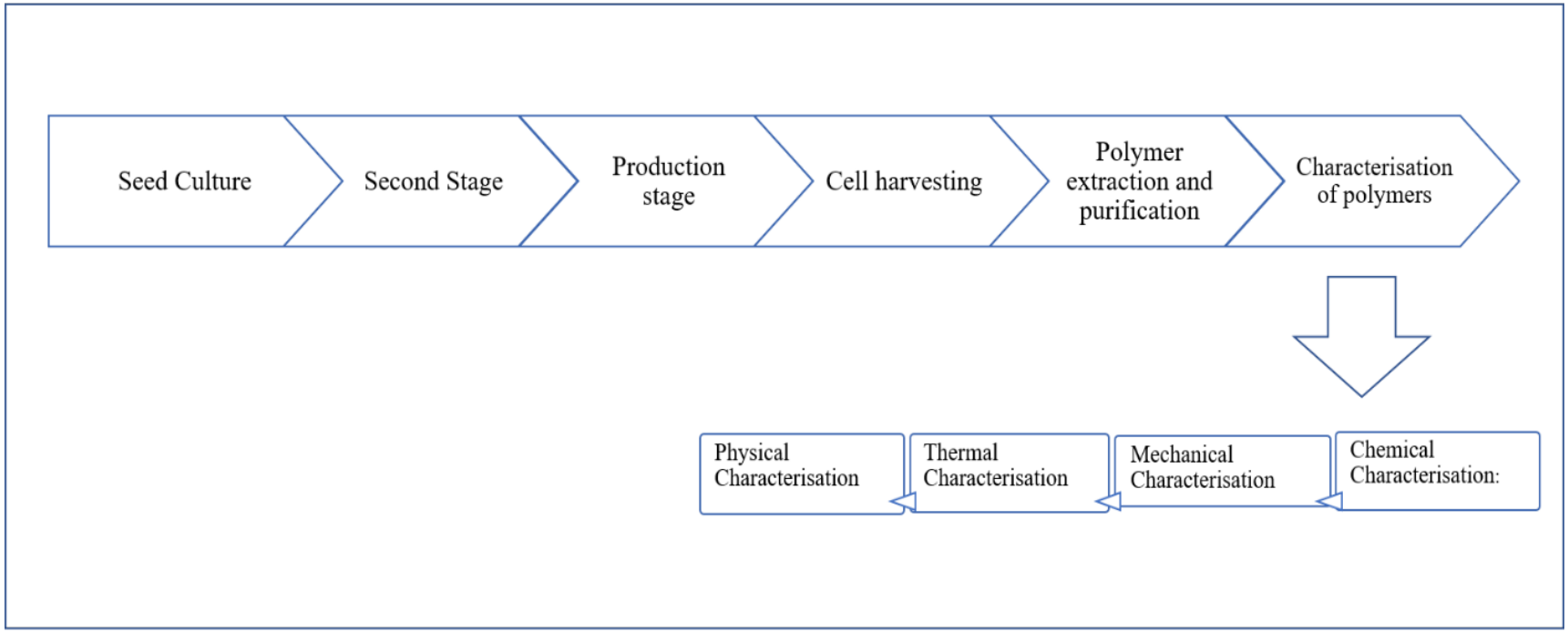

Figure 2.1: P(3HO-co-3HD) Production and Characterisation

2.3. DOWNSTREAM PROCESSING OF POLYMER PRODUCTION

The fermentation broth containing cells and polymer was centrifuged at 4,600 rpm for 30 minutes (Sorvall ST 40R, Thermo Scientific, LED GmbH, Germany). The harvested cells were washed by suspending in 10% ethanol and centrifuged again at 4,600 rpm for 30 minutes to remove extraneous media components and extracellular lipids and proteins from the cells. The cells were then placed in a deep freeze refrigerator at – 20°C for 24 hours and then in a freeze drier for 48 hours.

After drying, cells were lyophilised and the polymer was extracted using a modified Soxhlet extraction method as described by Ramsay *et al.* (Ramsay *et al.*, 1994). Briefly, dried cells were set up in a reflux system containing methanol to remove the impurities in the cells. This process was run at 60^{o}C twice for 24 hours and the methanol was discarded. After obtaining a clear methanol solution, the solvent was then changed to chloroform and then the reflux was run for 24 hours at 45^{o}C.

After this, the chloroform solution was concentrated using a rotary evaporator (R210, Buchi, Postfach, Switzerland). The polymers were then precipitated using ice cold methanol. The precipitated polymers were then purified by re-dissolving in chloroform and re-precipitating. This process was repeated twice to ensure complete elimination of impurities.

2.4.TEMPORAL PROFILING

Temporal profiling of the fermentation was carried out to monitor and control the parameters of fermentation. This was done by taking samples every 3 hours. Optical density, pH, nitrogen concentration, glucose concentration and biomass were measured for every sample. The profile was then drawn using SYSTAT Software Incorporation's SigmaPlot v12.5.

2.4.1. Fermentation Parameters

2.4.1.1. Optical Density

The optical density of the fermentation broth was measured throughout the fermentation to give an indication of the growth of the bacteria during fermentation. The optical densities of samples taken were measured at 450 and 600nm for P(3HO-co-3HD) and P(3HB) production respectively using a UV-spectrophotometer (Jenway 6320D, Bibby Scientific, Essex UK).

2.4.1.2.Biomass

Biomass estimation was carried out to monitor the dry cell weight of bacterial cells throughout the fermentation. 1ml of culture was centrifuged in Eppendorf tubes at 12,000g for 10mins. The supernatant was then discarded. The pellets were freeze dried and weighed. Biomass was calculated as:

$$\text{Biomass (g)} = Weight\ of\ tube\ containing\ dry\ cells - initial\ weight\ of\ tube$$

2.4.1.3.Glucose Estimation

Since glucose was the carbon source for both fermentations, it was important to measure the usage of glucose throughout the fermentation. Hence, glucose estimation was carried out.

Glucose estimation was carried out using the phenol sulphuric acid assay (Rai *et al.,* 2011). The culture was centrifuged at 12,000 g for 10 minutes and the supernatant was diluted 100-fold. 5% phenol in sulphuric acid was then added to the sample. This was then left standing for 10 minutes. It was then vigorously mixed and left standing for a further 30 minutes at room temperature. After this, the absorbance was read at 520nm and values extrapolated from the standard curve.

2.4.1.4.Nitrogen Estimation

Since nitrogen was the limiting nutrient in the fermentations, it was also important to monitor its usage in the process.

Nitrogen estimation (ammonium ion estimation) was carried out using the phenol hypochlorite reaction method. (Rai *et al.,* 2011) Culture samples taken were centrifuged at 12,000g for 10 minutes. The supernatant was diluted 100-fold and the reaction was carried out. Briefly, 1ml of phenol nitroprusside buffer was added in 2.5ml of the sample and mixed. 1.5ml of hypochlorite reagent was then added and the samples were mixed by vortexing with IKA Vortex 3 shaker (IKA, Staufen Germany). After this, the samples were isolated from light and incubated for 45 minutes. The

absorbance at 635nm was then read and values were extrapolated from the standard curve.

Phenol nitroprusside buffer:

The making of the phenol nitroprusside involves two steps

- 3 g each of sodium phosphate tribasic and sodium citrate with 0.3g ethylene tetraacetic acid (EDTA) were dissolved in distilled water. The pH was then adjusted to 12.
- To this solution, 6g of phenol and 20mg of sodium nitroprusside was added. This solution was kept away from light by covering with aluminium foil and keeping in a dark cupboard.

Alkaline hypochlorite solution

40ml of the 1M of sodium hydroxide was mixed with 2.5ml of sodium hypochlorite solution (4% chlorine).

2.5. CHARACTERISATION OF POLYMERS, BLENDS AND SCAFFOLDS

2.5.1. Chemical Characterisation

2.5.1.1. Attenuated Total Reflection Fourier-Transform Infrared Spectroscopy (ATR-FTIR)

ATR-FTIR was carried out in order to identify the polymer by analysing the bonds and functional groups present. Characterisation of the polymer was carried out using the Spectrum Two Spectrometer (PerkinElmer,

Massachusetts USA). 2mg of the polymer was used for these analyses. 10 scans were measured under the following conditions: 4000 - 450 cm^{-1} spectral range, window material CsI, and 4 cm^{-1} spectral resolution, with a temperature stabilised FR-DTGS detector.

2.5.1.2.Gas Chromatography-Mass Spectroscopy (GC-MS)

To identify the monomer content of the polymer GC-MS was carried out. The polymer was made to undergo methanolysis to volatilise it in in the ester form (Huijberts *et al.*, 1994). 30 mg of the polymer were dissolved in 3 ml of chloroform, before adding 20 µl of methyl benzoate and 3 ml of 15% sulphuric acid. Anti-bumping granules, were added and the mixture was placed in reflux and run for 4 or 16 hours for P(3HB) and P(3HO-co-3HD) respectively. This resulted in the separation of phases. The organic phase, which contained the polymer, was collected and mixed with 10 mg of sodium bicarbonate and 10 mg of sodium sulphate. This was then filtered using Whatmann filter paper and placed into the GC vial and frozen at 20°C. GC-MS analysis was carried out using Chrompack CP-3800 (Varian Inc, California, USA) and a Saturn 2000 MS/MS workstation. The CP-3800 gas chromatograph was equipped with Elite-5MS capillary column (PerkinElmer, Massachusetts, USA). The dimensions of the column were 30m length, 0.25mm internal diameter and 0.25µm film thickness. 1 µl of the sample in chloroform was injected along with Helium (1ml/min) as the carrier gas. The column temperature was raised from 40°C to 240°C at 18°C/min and held at the highest temperature for 10 minutes (Akaraonye *et al.*, 2012)

2.5.1.3.Nuclear Magnetic Resonance (NMR)

^{13}C and ^{1}H NMR were carried out to confirm the chemical structure of the polymer.

20 mg of the polymer was dissolved in 1 ml of deuterated chloroform ($CDCl_3$) and transferred into NMR tubes. Prepared samples of PHAs were sent to the Department of Chemistry, University College London (UK) for analysis using Bruker AV400 (400 MHz) (Bruker, Coventry UK). The resulting spectra were analysed using MestRec analytical software suite (Mestrelab, Coruna Spain).

2.5.2. Mechanical Characterisation

Mechanical testing was carried out using Instron 5942 MicroTester (Buckinghamshire, UK) on the PHA structures produced. The films were cut into 23 mm long and 5 mm wide strips. The initial load range was set at 1-6000 mN, at a rate of 200 mN min^{-1}. The set up is shown in Figure 2.2. The results generated were analysed using Bluehill 3 (Instron, Buckinghamshire UK) software to calculate the Young's modulus, tensile strength and elongation at break (%) from the stress-strain curve (Ranjana Rai *et al.*, 2011). The values were calculated as follows:

(a) Young' s Modulus (E) = Stress/Strain

(b) Tensile strength = (load at break) / (original width x original thickness)

(c) Elongation at break = elongation at rupture x 100/initial gauge length

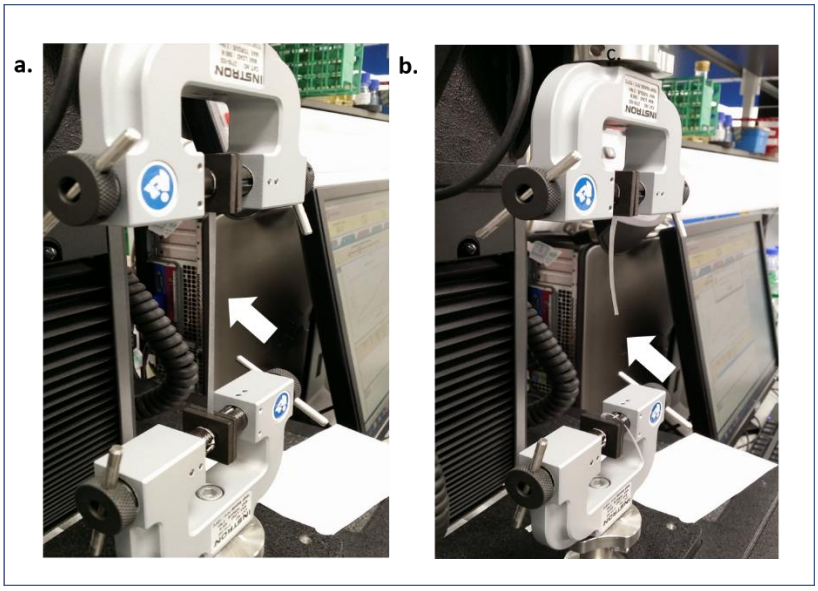

Figure 2.2: Tensile testing showing the PHA film a. during elongation b. at break

2.5.3. Thermal Characterisation

The thermal properties such as glass transition temperature (T_g), melting temperature (T_m) and enthalpy of fusion (ΔH_f) of the polymer were studied by Differential Scanning Calorimetry (DSC). DSC measurements were carried out on samples weighing 3-5 mg using DSC 214 Polyma (Netzsch, Selb, Germany). The samples were placed in pre-weighed aluminium pans and then placed in a nitrogen environment for testing. Heating-cooling-heating cycles were carried out at 20˚Cmin^{-1}, between 50˚C and 200˚C (Misra *et al.*, 2008; Ranjana Rai *et al.*, 2011). Glass transition temperature (T_g), melting temperature (T_m) and enthalpy of fusion (ΔH_m) values were measured from the DSC curve obtained. T_g indicates the temperature at which the amorphous part of the polymer transitions from glass to rubber state and T_m indicates the melting point of the crystalline part of the polymer.

2.5.4. Surface Properties

2.5.4.1.Scanning Electron Microscopy (SEM)

Surface topography of the PHA scaffolds generated was studied using a Jeol JSM- 5410LV SEM (Jeol, Welwyn UK). The samples were placed on 8 mm diameter aluminium stubs and coated with gold-palladium for 2 minutes using gold K 550X sputter coater (Quorum Technologies, Kent UK). Operating pressure of 7 x 10^{-2} bar and deposition current of 20 mA was used (Misra *et al.*, 2008; P. Basnett *et al.*, 2013).

For samples containing cells, the cells were fixed to the samples after cell culture using 3% paraformaldehyde. The samples were then dehydrated using serial dehydration in increasing concentrations of ethanol (50% to absolute). The analysis was carried out at the Department of Biomaterials and Tissue Engineering, Eastman Dental Institute, University College London, UK.

2.5.4.2.Water Contact Angle

Static contact angle testing was performed on the PHA scaffolds to measure the hydrophobicity/hydrophilicity of the samples. This was performed using a KSV Cam 200 goniometer (Biolin Scientific, Vastra Folundra Sweden). About 200 µL- 400 µL of deionized water was dropped onto the surface of the films using a gas-tight micro-syringe. Immediately the water droplet dropped on the sample, 10 images were captured (frame interval= 1s). Images were analysed using the modular KSV Cam 200 software (Biolin

Scientific, Vastra Folundra Sweden). This analysis was carried out in the UCL Eastman Dental Institute of University College London.

2.5.4.3.Protein Adsorption

Protein adsorption was analysed. To do this, samples with areas of $1cm^2$ were incubated in 400uL of foetal bovine serum (FBS). This was incubated at 37^0C for 24 hours. After 24 hours, the samples were washed thrice in PBS. The washed samples are then placed in 1ml of 2% sodium dodecyl sulphate (SDS) in PBS to dissolve the proteins attached to the surface of the samples. These samples were then incubated at a temperature 37^oC and shaking of 150rpm for a further 24 hours. After this, the protein adsorption was measured using the Bicinchonic acid assay (Walker, 2002).

2.6.FABRICATION OF PHA SCAFFOLDS

Polymers were processed into three different structures- 2D non-porous films, 2D porous films, 3D structures and porous 3D- structures.

2.6.1. Non-Porous 2D Films (Neat Films)

Neat films were made by the solvent casting method described by Basnett *et al.* 2013. PHAs were dissolved in chloroform (10%w/v) and left stirring overnight to ensure complete dissolution. After this, the solution was vortexed and cast in glass petri dishes. They were then left to air dry for one week before characterisation tests were carried out.

2.6.2. Porous 2D Films

2.6.2.1.Porous Films with Different Sizes of Porogen (NaCl)

Porous films were prepared using the salt leaching method. Sodium chloride (NaCl) was sieved using sieves with 100 and 300 µm particle size (Endecotts, London UK) to obtain particles of sizes <100 µm and <300 µm respectively. Then, 5% w/v and 15% w/v of each porogen size was mixed with the polymer-chloroform solution and left to dissolve for 24 hours (Marchioli, Hertsig, *et al.*, 2016). After complete stirring, films were cast in glass petri dishes and left to dry. After drying, the samples were thoroughly washed in HPLC grade water three times. The porous samples created are recorded in the Table 2.5.

Table 2.5: Concentrations and sizes of NaCl used to create porous films

Porogen Size- Diameter (µm)	**Porogen Concentration (%w/v)**	
	5	15
100	A	B
300	C	D

2.6.2.2.Comparison of Porous Films with (NaCl & Sucrose)

Porous films were made with two different porogens (NaCl & sucrose). As described earlier, porogens of sizes <100 µm and <300 µm were used to create porous films by salt leaching. Samples were cast in petri dishes and left to dry. After drying, they were washed with 5 times with 20ml HPLC grade water.

2.6.3. 3D-Structures

PHAs were printed using the Inkredible+ bioprinter (Cellink, Goteborg Sweden). Figure 2.3 shows the printer set up. The method of printing was extrusion printing from a solution. For PHAs, 50% PHA solution in chloroform was prepared. The solution was then poured into an aluminium syringe with nozzle size 20G (outer diameter 0.9081mm, inner diameter 0.603mm).

A pre-programmed model from the Slic3r software was used. The tissue culture model was loaded on an SD card and transferred to the printer. The printer settings are shown in Table 2.6. The structure was then printed at pressures between 180-220KPa into 24 well tissue culture plates (Apelgren *et al.*, 2017).

Table 2.6: 3D printer settings

Parameter	**Value**
Model size	13.5x13.5x13.5mm
Layer height	0.30mm
Layer count	45 printed, 94 visited
Extruder speed	10.00mm/s
Move speed	80.00mm/s
Retract speed	40.00mm/s
Print time per layer	20.6 seconds
Total print time	23.44 minutes

Temperature	30ºC

After drying, the structures were washed with ethanol and incubated at 37°C in a 5% CO_2 atmosphere ready for cell culture.

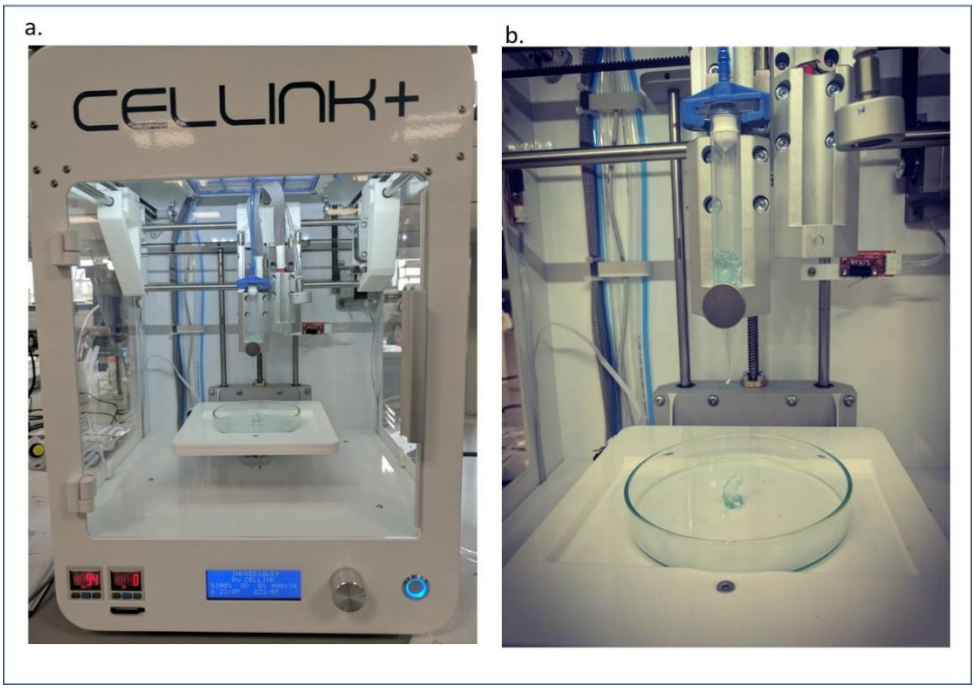

Figure 2.3: a. Cellink Inkredible+ 3D Bioprinter b. Close up of the syringe system.

2.6.4. Porous 3D-Structures

Porous 3D-structures were made by the solvent casting and salt leaching method using NaCl as the porogen (pore size ≤100µm). 5g of porogen and 0.27g of PHA was dissolved in 6ml chloroform. After complete stirring, the solution was poured into Teflon moulds and left to dry. After drying, scaffolds were removed and washed in HPLC water for 48 hours, changing the water every 3 hours.

2.7.FABRICATION OF ALGINATE STRUCTURES

2.7.1. Alginate Microencapsulated Cells.

Alginate encapsulated BRIN BD11 cells were prepared using a modified method described by Fritschy *et al*. and Hamid *et al*. (Fritschy *et al.*, 1991; Hamid *et al.*, 2001). After BRIN BD11 cells reached 70% confluence, they were harvested and suspended in 1.2% sodium alginate solution at a density of 1-5 X 10^5/ml. Microbeads were formed by dropping the cell solution through a 22-gauge needle into 0.12M $CaCl_2$ solution. The beads were left in the solution for 10 minutes for gelation. After 10 minutes, the beads were re-suspended in 0.06M $CaCl_2$ and 0.03M $CaCl_2$ solutions and left to gel for 10 minutes in each solution. The beads were then placed in 1mM egtazic acid (EGTA) solution for 10 minutes. Following complete washing with Kreb's Ringer Bicarbonate Buffer Solution (KRB), the beads were equilibrated in RPMI 1640 media overnight before cell culture and insulin release analyses.

2.7.2. 3D-printed Alginate Hydrogels

2.7.2.1.Preparation of Alginate Solution

2, 4, 5% w/v alginate in water solutions were prepared. This produced viscous solutions that were manually mixed to ensure complete dissolution. The solutions were then transferred into plastic syringes with 25G needles attached (precision conical bioprinting nozzles- Cellink, Gutenberg Sweden).

2.7.2.2.Preparation of Gelatin Slurry

A slurry of gelatin in $CaCl_2$ for the crosslinking of alginate was prepared. 150ml of 4.5% gelatin solution was prepared in 11mM $CaCl_2$. The solution was stored at 4^{o}C overnight to ensure complete gelation. This solution was then mixed with an additional 350ml of 11mM $CaCl_2$ and blended at pulse setting.

This pulsed solution was then centrifuged at 4,200rpm for 5 minutes. The supernatant was discarded and replaced with ice cold 11mM $CaCl_2$. The centrifugation process was repeated until the supernatant contained no more bubbles. The slurry was then transferred into glass petri dishes and stored at 4^{o}C until needed for printing (Hinton *et al.*, 2015; Webb and Doyle, 2017).

2.7.2.3.Printing of Alginate Hydrogels

A 3D model of the hydrogel to be printed including the shape, dimensions, printing temperature and speed was generated using AutoCAD (AutoDesk, London UK). Figure 2.4 is a summary of the 3D printing process for fabricating 3D printed alginate hydrogel.

The model generated in AutoCAD was then loaded in a Repetier-Host software (Hot-World GmbH, Willich Germany) and edited to match the printer's specifications. The edited model was then converted into G-code (Figure 2.5) using Slic3r open source software to generate a G-code that was then loaded on to an SD card. The SD card was then placed into the printer and the code was printed with the Cell Ink Inkredible+.

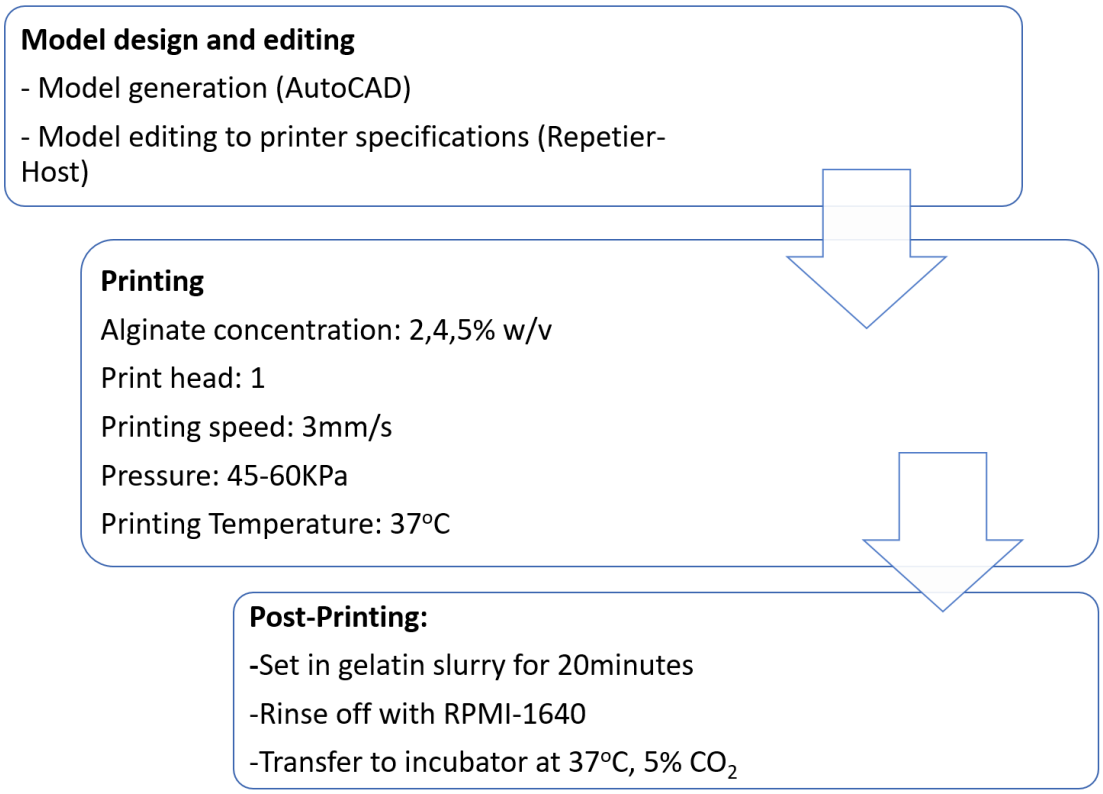

Figure 2.4.: 3D printing of alginate hydrogel.

Before printing, the printer was sterilised with 70% ethanol and a high efficiency particulate air (HEPA) filter-0.3µm was attached to the printer to prevent contamination. The alginate solution was then transferred in a plastic syringe with a plastic nozzle plastic (nozzle size 25G, pressure- 45-60KPa). The hydrogel was printed into a glass dish filled with the gelatin slurry containg $CaCl_2$. After printing, the hydrogel was allowed to set in the gelatin slurry for 20 minutes and then used for cell culture to allow for crosslinking to occur.

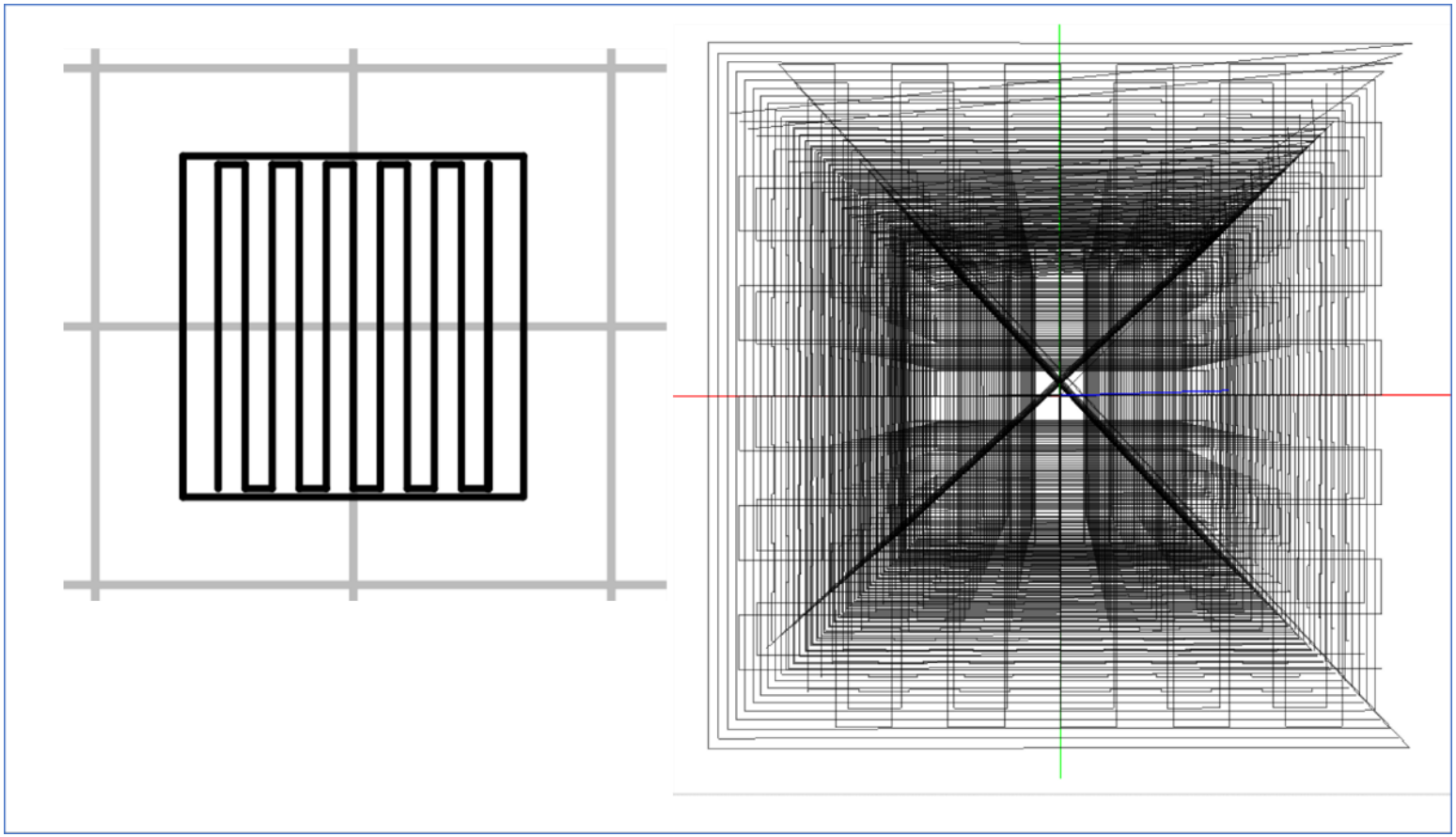

Figure 2.5: G-code generated 2D and 3D models of structures printed showing printer path

2.8.CELL CULTURE

2.8.1. Culturing of Pancreatic Beta Cell (BRIN-BD11)

Clonal pancreatic BRIN-BD11 cells were routinely cultured in Roswell Park Memorial Institute medium (RPMI) 1640 (passage numbers 20–30) containing 11.1 mM glucose, 0.3 g/L L-glutamine supplemented with 10% (v/v) foetal bovine serum, penicillin 100 IU/ml and streptomycin 0.1 g/L in sterile vented 75 cm^2 tissue culture flasks (Thermo Scientific, Hvidovre Denmark) at 37°C with 5% CO_2 and 95% air using a Binder GmbH cell culture incubator (Tuttlingen, Germany), as described previously (McClenaghan, Barnett, Ah-Sing, *et al.*, 1996). BRIN BD11 cells were passaged when cells reached 70 % confluence. Prior to detachment, cells were washed twice with 10 ml Phosphate Buffered Solution (PBS) followed by treatment with 0.025 % trypsin (w/v), 1 mM EDTA in PBS (w/v) at 37^oC. Detachment of cells from flasks was confirmed by viewing the flasks under 100X magnification using an Olympus CX41 phase contrast microscope (Olympus, Southend-on-Sea, UK).

2.8.2. Seeding Cells

After the cells had reached 70% confluence in the 75 cm^2 tissue culture flasks, they were detached using trypsin-EDTA solution as described above. After treatment with trypsin-EDTA, the mixture was centrifuged at 1,000 rev/min for 5minutes. The cell pellets were recovered and resuspended in media. They were then counted using a haemocytometer.

The polymer films were cut into pieces with $1cm^2$ area. The cut samples were dipped in ethanol and placed in 24 well plates. After air-drying, the plates were sterilised using UV at 254nm for 30 minutes. After sterilisation, the cells were added to the samples at a density of 200,000 cells/ml.

The hydrogel samples were cut into 1mm cubes and cells seeded as described as above.

2.8.3. *In vitro* Direct Cell Viability Analysis

Cell viability tests using BRIN BD11 cells were carried out on the PHA structures and alginate microbeads. The seeded scaffolds samples were then incubated with 1ml of complete RPMI media for 3-7 days at 37°C in a 5% CO_2 atmosphere. Samples were fixed on day 1, day 3, day 5 and day 7 to analyse the cell viability. This was done using the MTT assay which determines the metabolic activity of the cells (Mosmann, 1983; Gerlier and Thomasset, 1986). The yellow tetrazolium MTT is reduced to purple formazan within metabolically active cells. The experiment was carried out in triplicate for each test. The assay was carried out using standard tissue culture plates with RPMI-1640 medium as the positive control and dimethyl sulfoxide (DMSO) as the negative control. The results of the MTT assay are represented as percentage of viability in comparison to the positive control.

2.8.4. Indirect Cell Viability Analysis

Indirect cell viability tests were carried out on 3D printed alginate hydrogels. Alginate hydrogels were equilibrated overnight in RPMI 1640

media. At the same time, BRIN BD11 cells were cultured in 24-well plates overnight at a density of 200,000cells/ml. After 24 hours, the media from the BRIN BD11 cells was replaced with the media obtained from surrounding of the alginate hydrogels and cultured for 24 hours. After 24 hours, cell viability studies were carried out using the MTT assay.

2.9.BRIN BD11 FUNCTION TESTS

2.9.1. Static Insulin Secretion Assay

Acute insulin secretion assay was performed as described by McClenaghan *et al.* (McClenaghan, Barnett, Ah-Sing, *et al.*, 1996). BRIN BD11 cells were attached to PHA and alginate structures overnight in RPMI-1640 media as described earlier. After overnight attachment of cells, culture medium was discarded and replenished with 1 ml of Krebs Ringer Bicarbonate (KRB) buffer containing 115 mM NaCl, 4.7 mM KCl, 1.28 mM $CaCl_2$, 1.2 mM $MgSO_4$, 1.2 mM KH_2PO_4, 25 mM HEPES, 8.4% (w/v) $NaHCO_3$, 1% bovine serum albumin (BSA) and 1.1 mM glucose (pH 7.4). The structures seeded with cells were then incubated in KRB buffer for 40 min at 37^oC, 5% CO_2 and 95% air. Following pre-incubation KRB buffer was removed and replaced with KRB solution containing 5.6 mM glucose. This was then incubated at 37^oC, 5% CO_2 and 95% air for 20 min. The supernatant (900 µL) was subsequently removed and stored at -20^oC. Immediately after, the supernatant removed was replaced with KRB solution containing 16.7mM glucose and incubated for 20 minutes. Supernatants from both tests were

stored at -20^{o}C prior to measurement of insulin by immunoassay using the mouse insulin ELISA kit (Flatt and Bailey, 1981).

2.10. *IN VITRO* SWELLING AND DEGRADATION TESTS

in vitro swelling and degradation tests were carried out on the hydrogel and polymer films made to monitor the changes in weight over time.

2.10.1. %Water Uptake and %Weight Loss in PHA Samples

To evaluate the %water uptake and %weight loss of PHA samples over time, PHAs were cut into samples with area of 1cm^2. The samples were then incubated in PBS and RPMI-1640. These media were selected because PBS is isotonic and can be used to stimulate body conditions. RPMI-1640 is the optimum medium for BRIN BD11 cell growth. Table 1.6 is a summary of the nutrient compositions of both media. Samples were incubated in either solution at 37^{o}C at 5% CO_2. Samples were weighed before incubation, after retrieval and after drying post-retrieval.

Table 2.7: Nutrient composition of PBS and RPMI-1640

Constituents	**PBS (g/L)**	**RPMI-1640 (g/L)**
NaCl	8	6
KCl	0.2	0.4
Na_2HPO_4	1.42	1.512
KH_2PO_4	0.24	-

$NaHCO_3$	-	2
$MgSO_4$	-	0.1
$Ca(NO_3)_2$	-	0.1

The %water uptake and weight loss were then measured as:

$$\%\text{Water Uptake} = \frac{Wet\ weight\ after\ incubation\ (Mw) - Weight\ after\ drying\ (Mt)}{Initial\ dry\ weight\ (Md)} \times 100$$

$$\%\ \text{Weight Loss} = \frac{Initial\ dry\ weight\ (Md) - Weight\ after\ drying\ (Mt)}{Initial\ dry\ weight\ (Md)} \times 100$$

Where M_d= initial dry weight of samples

M_w= wet weight of samples after incubation over time

M_t= final dry weight after incubation.

2.10.2. Swelling and Degradation of Hydrogel Samples

For the hydrogel samples, swelling and degradation were calculated as % dry weight. To evaluate these, the hydrogel was cut into 1X1X1mm^3 cubes and placed in PBS. After this, samples were incubated at 37ºC at 5% CO_2 humidity. At appropriate time points, the samples were taken out, patted dry with lab roll and weighed. Samples were weighed before incubation and after retrieval.

The %swelling and degradation were then measured as:

$$\% \text{ Swelling} = \frac{weight\ after\ swelling\ (Ms) - initial\ weight\ (Mi)}{Intial\ weight\ (Mi)} \times 100$$

$$\% \text{ Degradation} = \frac{weight\ after\ degradation\ (Md) - initial\ weight\ (Mi)}{Initial\ weight\ (Mi)} \times 100$$

Where M_s= weight after swelling

M_i= initial weight

M_d= weight after degradation

2.11. STATISTICAL ANALYSIS

All data was expressed as mean ± standard error measurement (SEM). Where required, data was compared using one-way, two-way or three-way analysis of variance (ANOVA) tests. The tests were carried our using GraphPad Prism 7 (GraphPad Software Incorporated). Differences were considered significant when *$p \leq 0.05$, **$p \leq 0.01$, ***$p \leq 0.001$ and ****$p \leq 0.0001$. Where $p>0.05$, differences were considered non-significant.

CHAPTER THREE: POLYMER PRODUCTION AND CHARACTERISATION

3. POLYMER PRODUCTION AND CHARACTERISATION

3.1. INTRODUCTION

The ideal material for bioartificial pancreas should be biocompatible, inert, porous- allowing for exchange of oxygen, nutrients, glucose and insulin but also protective of the islet cells, protecting them from response molecules of the immune system (Lim and Sun, 1980; Weir, 2013; Kepsutlu *et al.*, 2014). These biomaterials also need to promote host integration and restoration of ECM-like interactions (Gibly *et al.*, 2011; Tsuchiya *et al.*, 2015; Llacua *et al.*, 2016; Perez-Basterrechea *et al.*, 2018).

A wide range of polymers have been explored for their use in islet transplantation, these include PLLA, PEG, PVA and collagen. All these polymers possess individual advantages and disadvantages. PLLA undergoes bulk degradation which ultimately leads to uncontrolled degradation in the final stages. It also degrades into lactic acid which is highly acidic and can lead to inflammatory responses. PEG is known to reduce the viability and function of islet cells. PVA has been shown to contain impurities due to its manufacturing process. Collagen hydrogels are crosslinked with toxic materials (Gough, Scotchford and Downes, 2002; Beck *et al.*, 2007; Gajra *et al.*, 2012; Krishnan *et al.*, 2014). There is therefore a need for alternative polymers that can fulfil the requirements for scaffolds involved in islet transplantation. In addition, there is a need for

‘intelligent’ scaffolds that not only promote cell adhesion and differentiation, but can also be modified to improve biocompatibility (Malafaya, Silva and Reis, 2007; Khademhosseini and Langer, 2016). It is also important, when engineering a scaffold, to consider the mechanical, chemical, and physical properties of the native tissue and select materials able to mimic these.

PHAs have been shown to be excellent candidates for Tissue Engineering scaffolds (P. Basnett *et al.*, 2013; Lizarraga-Valderrama *et al.*, 2015; Nigmatullin *et al.*, 2015; Bagdadi *et al.*, 2018; Lukasiewicz *et al.*, 2018). In addition, they are also easily modifiable by attaching factors like VEGF (Nigmatullin *et al.*, 2015) or blending with other polymers to improve mechanical, chemical and biocompatibility properties (Misra *et al.*, 2006; Valappil *et al.*, 2008).

Of the bacteria that demonstrate ability to produce PHAs, *Pseudomonas spp.* and *Bacillus spp.* have been reported more frequently in literature. Examples of each include *P. mendocina, P. oleovorans, B. subtilis and B. cereus.* They produce mcl-PHAs and scl-PHAs respectively. The pathways for production of PHAs depend largely on the carbon source used- simple sugars, alkanes, lipids and alkanoic acids (Anderson and Dawes, 1990).

When glucose is used as the carbon source, in scl-PHAs it undergoes the TCA cycle to produce the 2-acetyl-CoA molecules needed for PHA synthesis. Mcl-PHAs precursors can be produced through *de novo* fatty acid synthesis and other processes. (Philip, Keshavarz and Roy, 2007).

To ensure homogeneity and repeatability of the microbial production process, the fermentation conditions must be strictly monitored and controlled throughout the fermentation process. These factors include pH, temperature, airflow rate and agitator speed. As the fermentation proceeds, additional factors must be monitored to ensure the fermentation is progressing as expected. These factors include optical density (OD), biomass, dissolved oxygen tension (DOT), usage of nutrients. Fermentation products most also be thoroughly characterised to ensure purity and potential for use as medical grade matrials.

This Chapter describes the production of two kinds of PHAs, P(3HB) and P(3HO-co-3HD), using optimal conditions in order to encourage the highest yield. The production process was monitoring and controlled throughout the fermentation. The polymers produced were thoroughly characterised.

3.2.RESULTS

3.2.1. P(3HB) Production by *Bacillus subtilis* OK2 using glucose as the carbon source

Temporal profiling of P(3HB) production using *B. subtilis* OK2 (Figure 3.1) showed increasing optical density and polymer yield with time. From the beginning of the fermentation, there was an exponential rise in optical density (OD). At time zero, the OD observed was 0.875. The values from 12-18 hours represented a brief lag phase with the OD values continuing to

rise later, until the end of the fermentation.

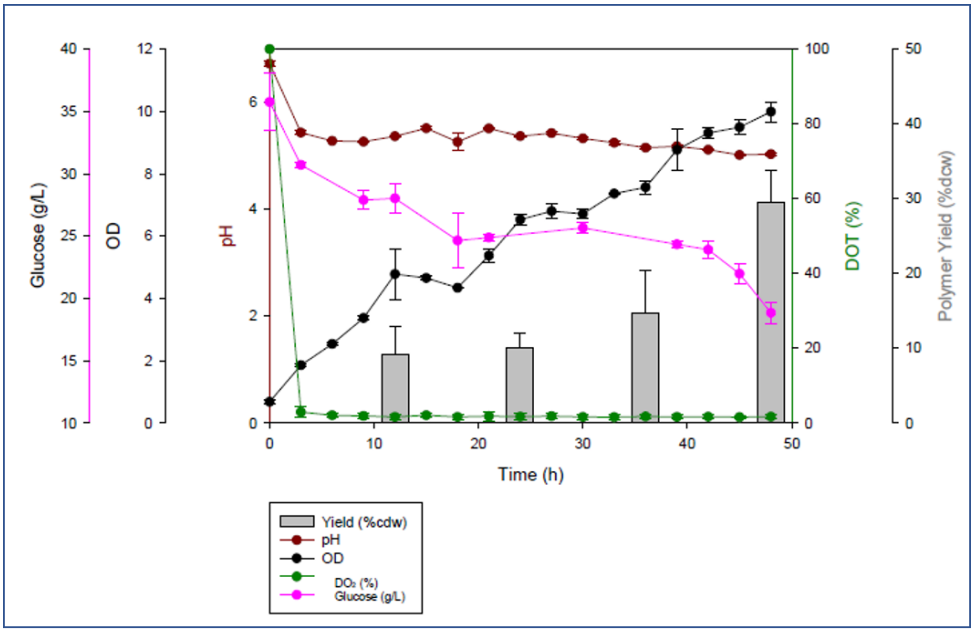

Figure 3.1 Temporal profiling of the production of P(3HB) from B. subtilis OK2 showing variation in OD at 450nm, pH, DOT (%), glucose (g/L) and polymer yield (%dcw).

As the concentration of biomass present in the bioreactor increased, more oxygen was required to support this growth, hence a drastic decrease was observed in the dissolved oxygen tension (%) from 100% to 2.95% after 3 hours. On the other hand, the pH value gradually decreased from 6.80, to 4.89. Glucose values reduced from 35g/L, at the beginning of fermentation, to about 17g/L at the end. This indicated that the glucose was not completely used. The highest OD value was measured at 48 hours and the corresponding polymer yield (% dcw) was found to be about 49% of the dry cell weight at this time point. The yields observed at the 12, 24 and 36 hours were 10, 12.5 and 17.34% dcw respectively. The highest yield observed was 49% dcw at 48 hours, indicating that 48 hours is the best time to harvest the culture and stop the fermentation.

3.2.2. Production of P(3HO-co-3HD) by *Pseudomonas mendocina* CH50 using glucose as the carbon source.

The mcl-PHA, P(3HO-co-3HD) was produced using the method described in section 2.2.2. The production was run in batch mode.

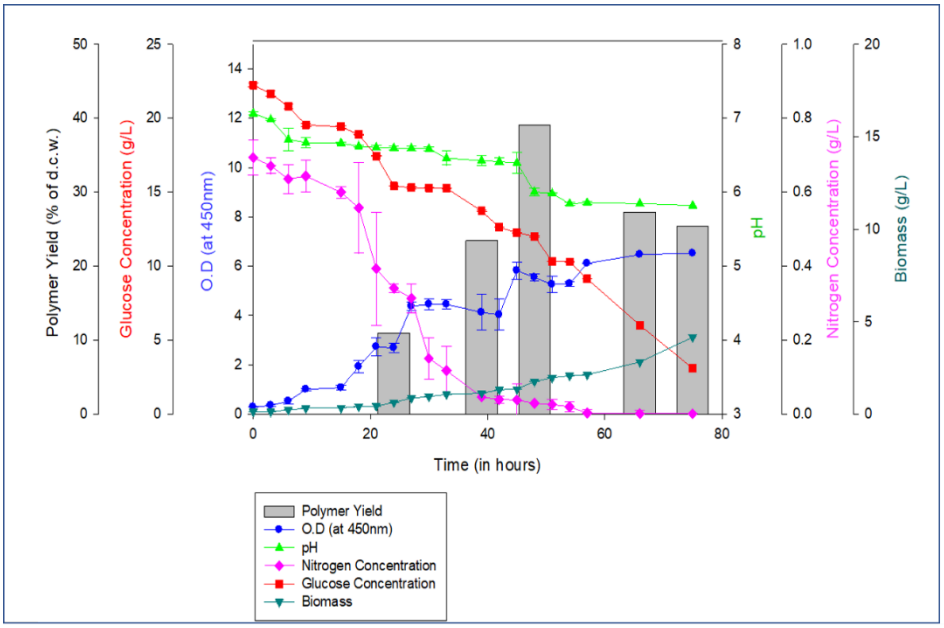

Figure 3.2: Temporal Profiling of P(3HO-co-3HD) production from P. mendocina CH50

Figure 3.2. shows the temporal profile for the production of P(3HO-co-3HD) from *Pseudomonas mendocina* CH50, showing changes in O.D, pH, biomass, nitrogen concentration, glucose concentration and polymer yield. The culture showed an initial lag phase between 0 and 15 hours where the OD value was 1.07. After this, O.D values increased exponentially until 45 hours (5.82) when foaming interfered with the O.D. readings. After

antifoam was added at 57 hours, the readings stabilised at 6.11, indicating a stationary phase. The biomass increased throughout the fermentation from 0.13g/L to 4.17g/L. The pH of the fermentation was not controlled and was seen to drop from 6.98 at the 3rd hour of fermentation to 5.82 at the end of the fermentation. The nitrogen concentration dropped exponentially from the beginning of the fermentation until 39 hours, where it dropped to 0.05 g/L, after which it gradually dropped even further, till the end of the fermentation. The glucose concentration reduced from 20g/L at the beginning of the fermentation to about 3g/L at the end of the fermentation, indicating that the glucose was not used up completely at the end of the fermentation. The yields observed for the production of P(3HO-co-3HD) were 12.3% dcw at 24 hours, 24.9% dcw at 36 hours, 42.1% dcw at 48 hours, 27.8% dcw at 64 hours and 25.6% dcw at 72 hours. The yield at 48 hours was the highest yield observed, indicating that 48 hours is the best time to stop the fermentation and extract the polymer.

3.3. POLYMER CHARACTERISATION

3.3.1. Fourier Transform- Infrared Spectroscopy (FT-IR)

The FT-IR spectrum of P(3HB) obtained from *B. subtilis* OK2 using rapeseed oil as the carbon source is shown in Figure 3.3. The spectrum shows peaks at 1721cm^{-1}, 1278cm^{-1} which are representative of the carbonyl and acyl groups present in P(3HB). The peaks between 400 and 1000cm^{-1}

are indicative of the methyl carbons present in the molecule. These peaks are consistent with peaks expected from P(3HB) (Misra *et al.*, 2010).

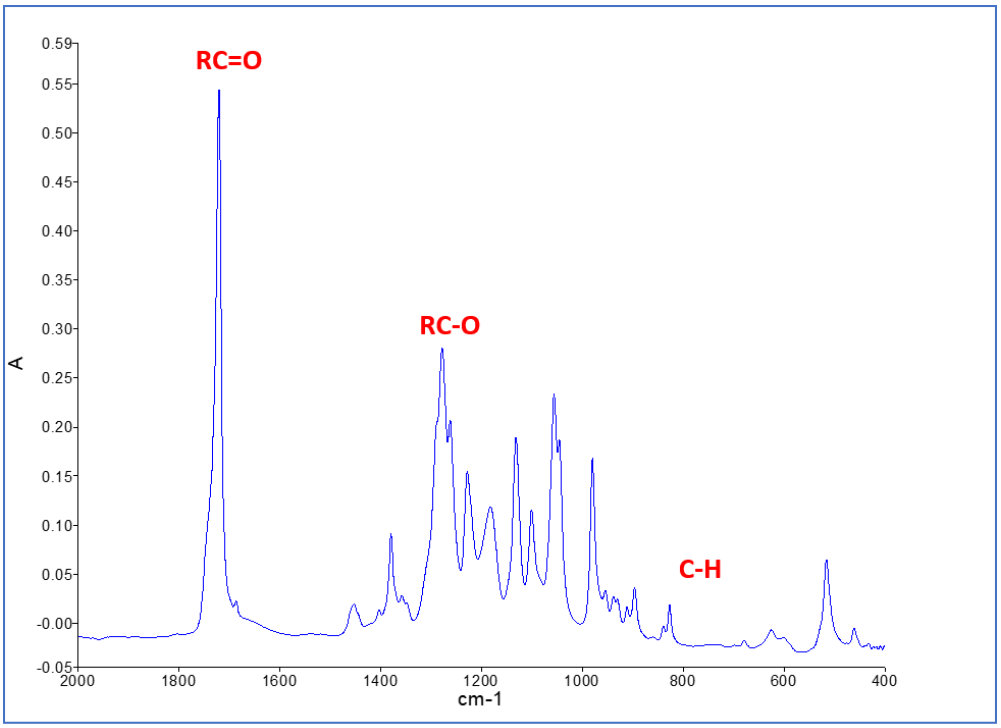

Figure 3.3: The FT-IR Spectrum for P(3HB) derived from B. subtilis OK2

The FT-IR spectrum for P(3HO-co-3HD) derived from *Pseudomonas mendocina* CH50 using glucose as the carbon source is shown in Figure 3.4. The spectrum shows peaks at 1726cm^{-1} and 1161cm^{-1} which are characteristic of the carbonyl and acyl groups present in mcl-PHAs. It also contains a peak at 2924cm^{-1}, indicating a methylene group indicative of mcl-PHAs (R. Rai *et al.*, 2011).

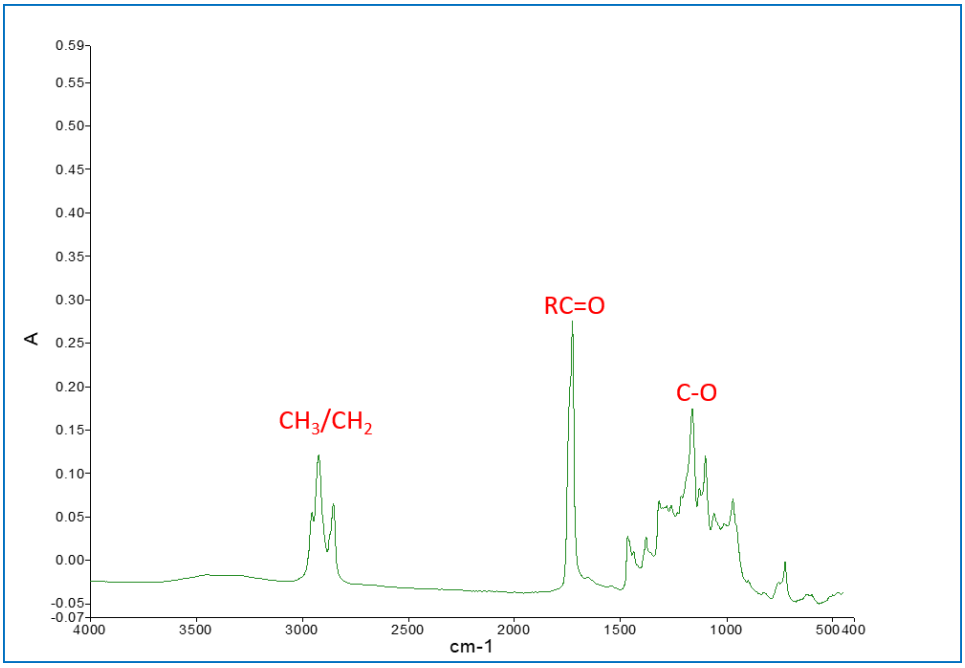

Figure 3.4: FT-IR Spectrum for P(3HO-co-3HD) derived from P. mendocina CH50.

3.3.2. Gas Chromatography Mass Spectroscopy

Figure 3.5 shows the GC spectrum observed for methanolysed P(3HB) from *B.subtilis* OK2. The peak with a retention time (t_R) of 6.4 min was identified to be methyl benzoate, which was the internal standard. The peak observed at t_R of 4.01 min matched that of methyl-3-hydroxybutyrate upon comparison with the NIST spectral library.

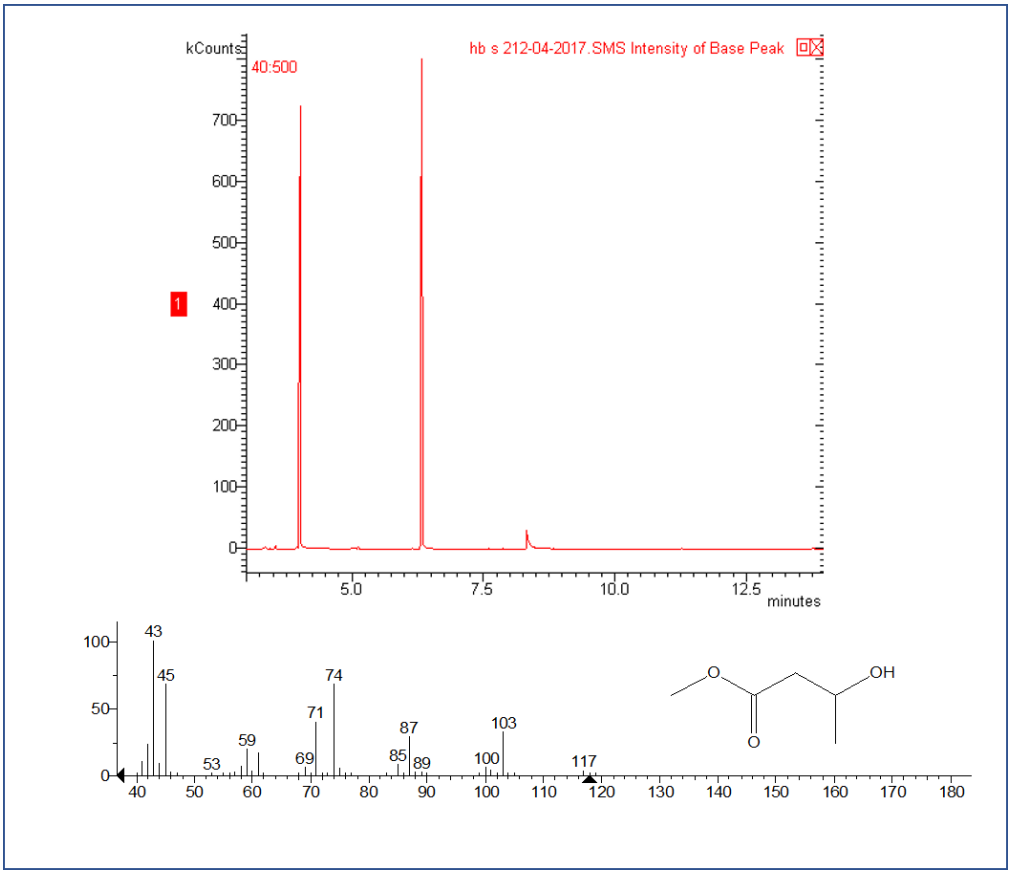

Figure 3.5: Gas chromatogram of P(3HB) produced by B. subtilis OK2 showing the spectrum observed and the relative abundance of the 3-hydroxy methyl ester of butanoic acid

Figure 3.6 is the GC spectrum observed for P(3HO-co-3HD) produced by *P. mendocina* CH50. The peak with a retention time (t_R) of 6.5 min was identified to be methyl benzoate, which was the internal standard. The mass spectra observed at t_R of 7.78 min and 9.40 min were found to match those of methyl-3-hydroxyoctanoate and methyl-3-hydroxydecanoate upon comparison with the NIST spectral library.

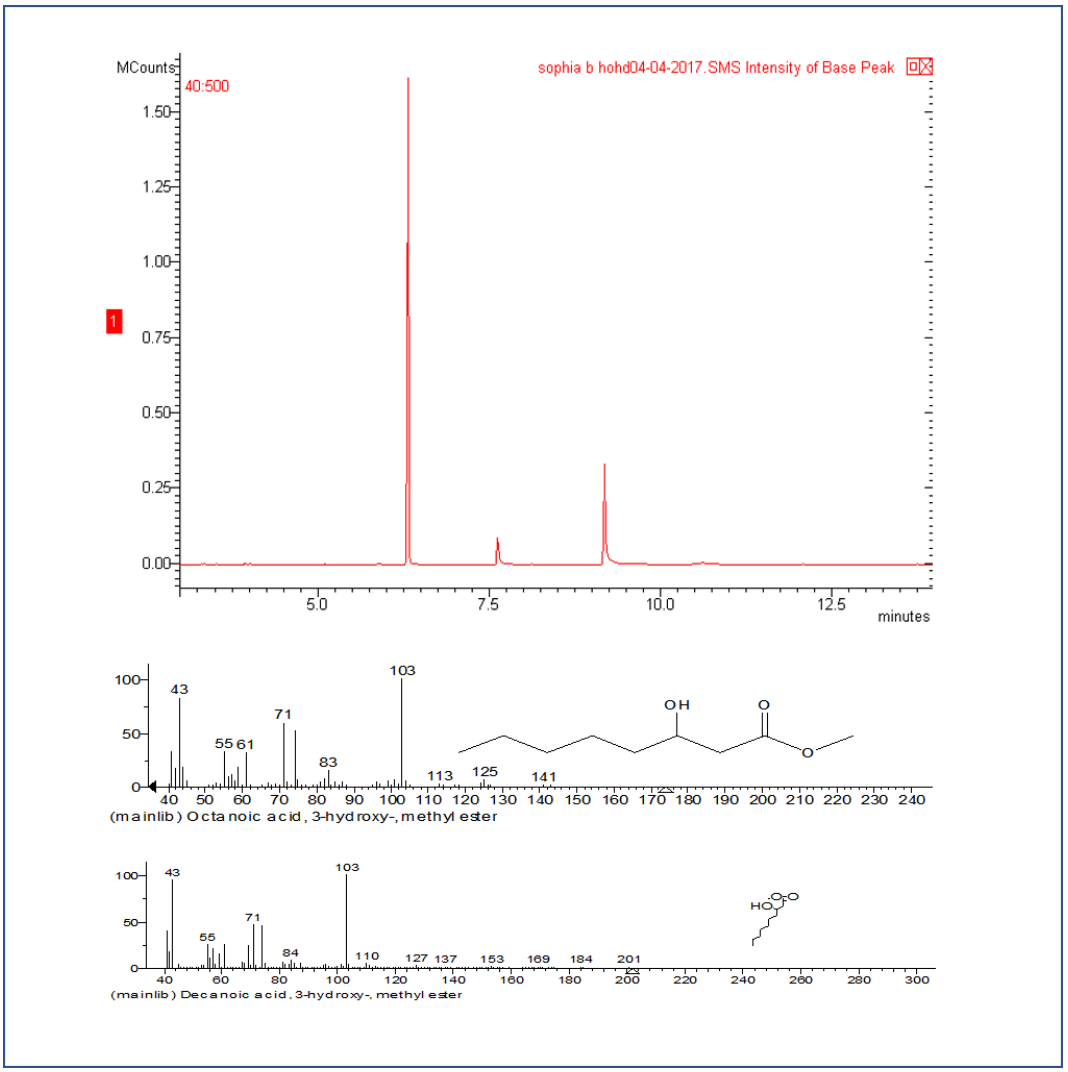

Figure 3.6: Gas chromatogram of P(3HO-co-3HD) produced by P. mendocina CH50 showing the spectrum observed and the relative abundance of the 3-hydroxy methyl esters of octanoic acid and decanoic acid.

The ratio of the monomers present in the co-polymer can be calculated by calculating the area under each peak. The area can be calculated using this formula:

Area of peak $= width\ of\ peak\ at \frac{1}{2}\ height \times height\ of\ peak$

For methyl-3-hydroxyoctanoate, the width= 0.5mm, height= 5mm

So, area= 2.5mm^2

For methyl-3-hydroxydecanoate, the width= 0.5, height= 18mm

So, area= 9mm^2

Based on this, the ratio of methyl-3-hydroxyoctanoate to methyl-3-hydroxydecanoate= 22%:78%. From this data, it can be confirmed that the mcl-PHA produced was P(3HO-co-3HD).

3.3.3. Nuclear Magnetic Resonance

The ^{13}C NMR spectrum from P(3HB) derived from *B. subtilis OK2* is shown in Figure 3.7. The spectrum shows four peaks corresponding to four different carbon environments in the molecule. The chemical shifts are at 169 ppm, 67 ppm, 38 ppm and 19 ppm representative of the carbons in the C=O, CHO, CH_2CO and RCH_3 group of the P(3HB) molecule.

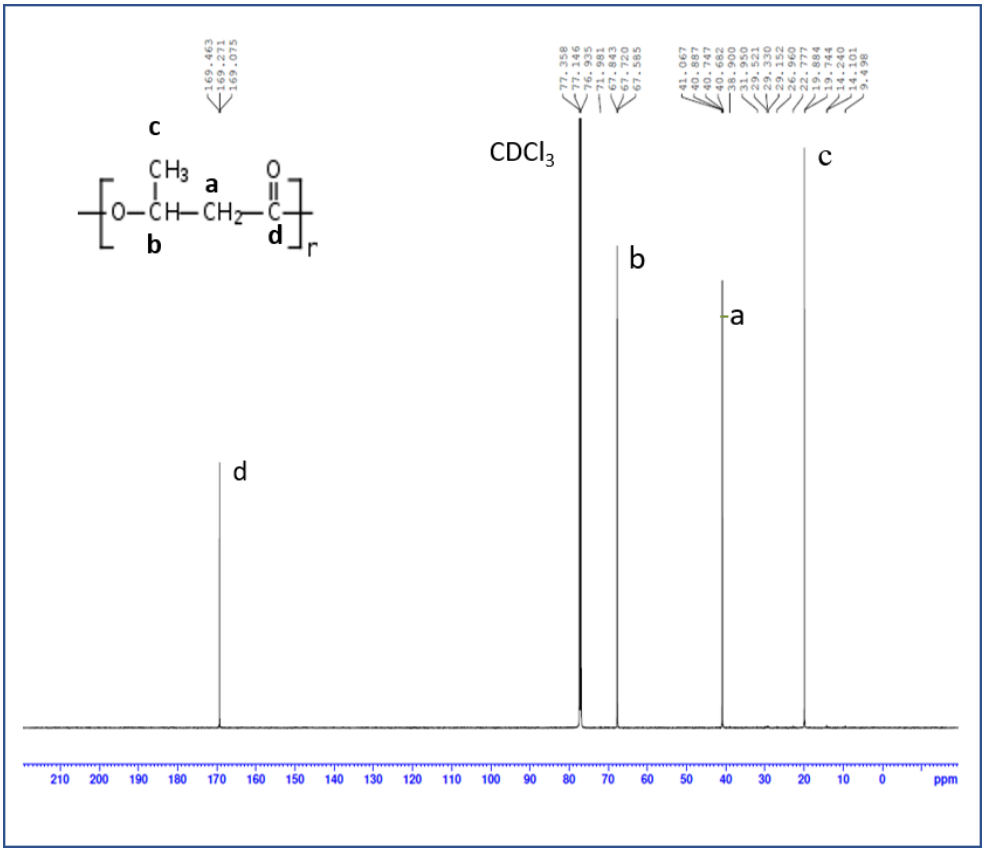

Figure 3.7: ^{13}C NMR Spectrum of P(3HB) derived from B. subtilis OK2

The ^{1}H NMR spectrum of P(3HB) (Figure 3.8) shows four different peaks representing the four different hydrogen environments in the polymer. The first peak at 1.37ppm corresponds to the protons in the (-CH_3-) group. The multiplex peak at 2.4-2.6ppm represents the protons in the (-CH_2-) group. The peak at 5.3ppm represents the protons in the (-CH-) group.

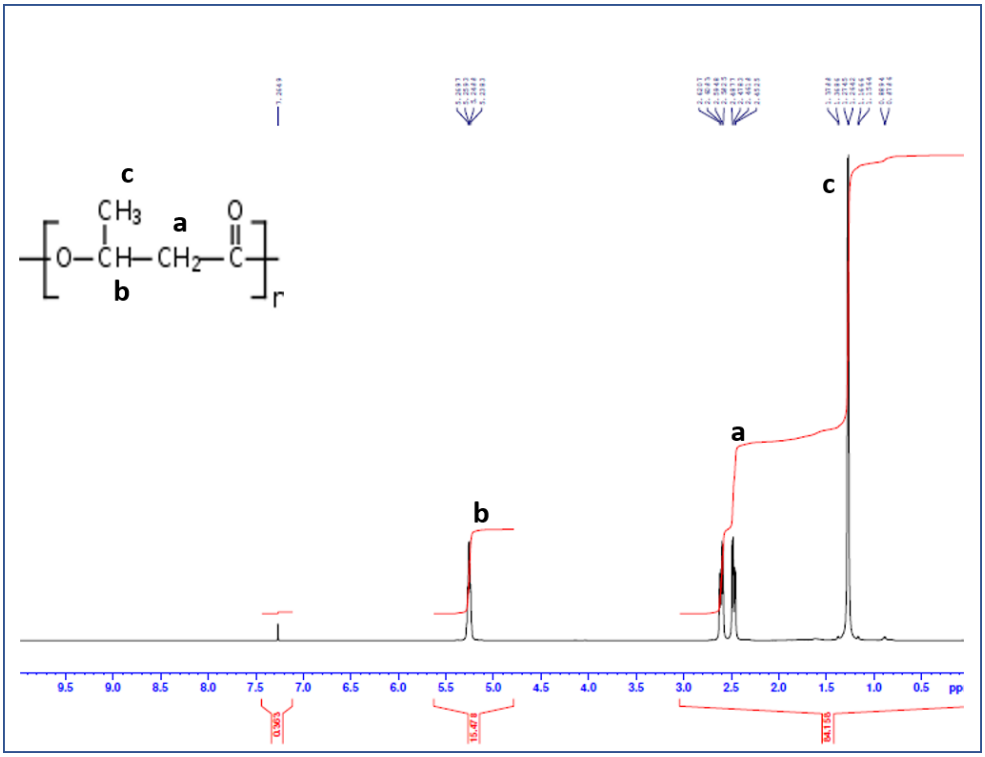

Figure 3.8: ^{1}H NMR Spectrum for P(3HB) derived from B. subtilis OK2

In the ^{13}C NMR of P(3HO-co-3HD) (Figure 3.9), eleven different peaks were observed consistent with different environments for the carbons in the molecule. The chemical shift at 169.40 ppm falls in the range of that expected from C=O group at C_1. The peak at 70.82 ppm represents that of -CHO- group (C_3), 39.20 ppm of -**C**H_2CO group (C_2), 23-34 ppm of -CH_2- group (C_4, C_5, C_6, C_7, C_9), and 13.95 ppm of the -CH_3 group (C_8 C_{10}). These chemical shifts obtained were found to be consistent with the spectrum expected from (3HO) and (3HD) monomers.

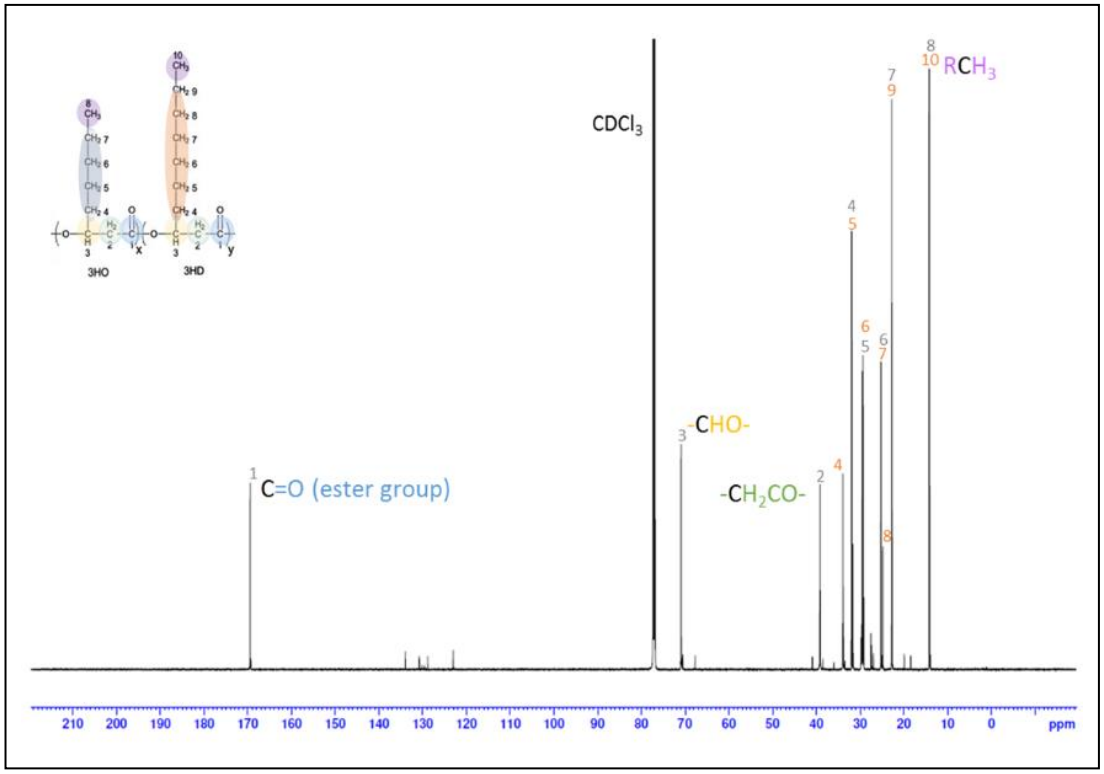

Figure 3.9: ^{13}C NMR Spectrum of P(3HO-co-3HD) derived from P. mendocina CH50

The ^{1}H NMR spectrum (Figure 3.10) shows five different environments for the hydrogen in the polymer. The first peak is shown by the protons bound to C_3 (-CHO-group) that gives a peak at 5.2 ppm. The peaks indicative of protons bound to C_2 (-CH_2CO- group) and C_4 (-CH_2- group) show peaks at 2.5 ppm and 1.6 ppm. The peak at 1.2 ppm is indicative of (-CH_2- group) in C_5, C_6, C_7 of 3-hydroxyoctanoate (3HO) & C_5, C_6, C_7, C_8 and C_9 of 3-hydroxydecanoate (3HD). Finally, the fifth peak at 0.8 ppm belongs to protons found in the (-CH_3) group of C_8 in 3HO and C_{10} (-CH_3) group of 3HD.

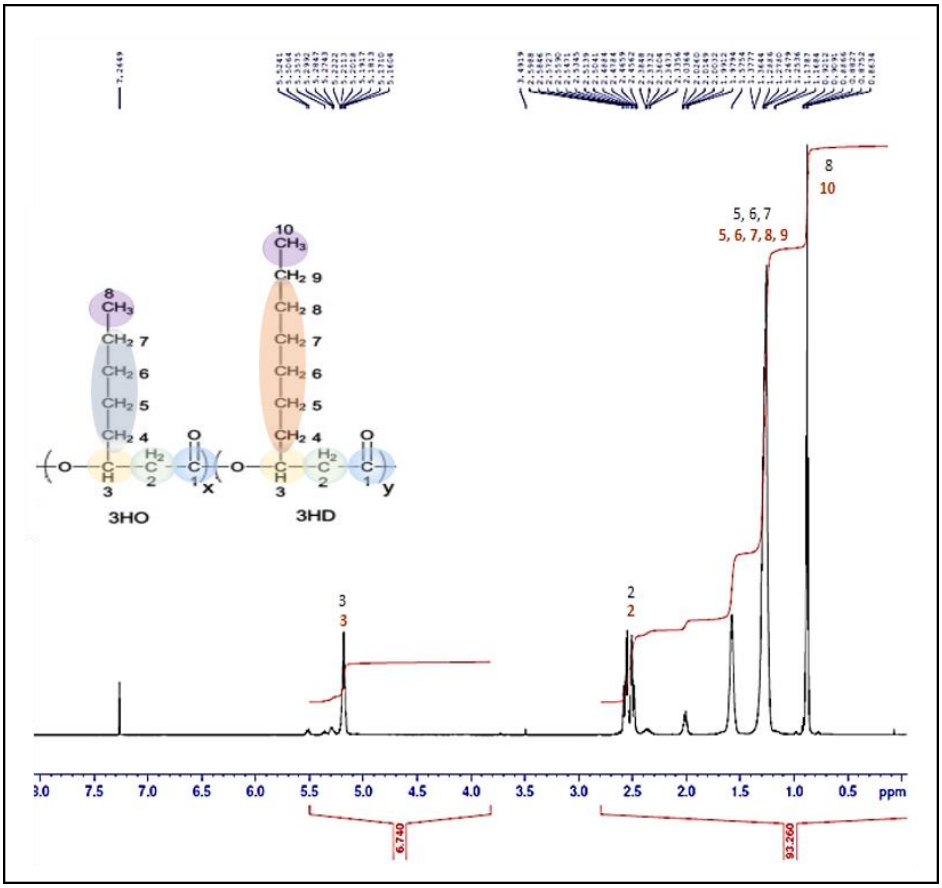

Figure 3.10: ^{1}H NMR spectra of P(3HO-co-3HD) derived from P. mendocina CH50

3.3.4. <u>Differential Scanning Calorimetry</u>

DSC was carried out to determine the thermal properties of the polymers in a bid to further characterise them.

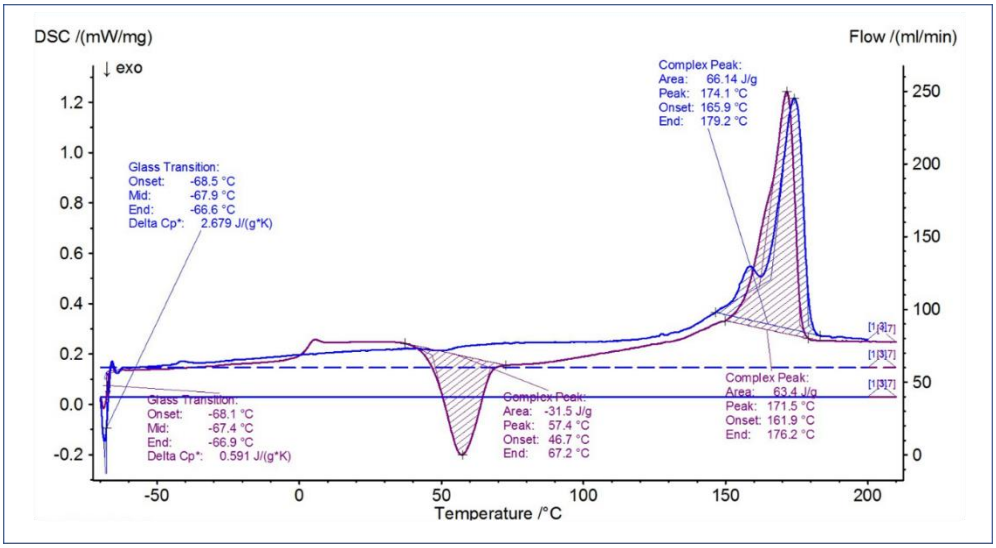

Figure 3.11: DSC Thermogram of P(3HB) derived from B.subtilis OK2

The DSC thermogram of P(3HB) is shown in Figure 3.11. From the graph, glass transition temperature (T_g), melting temperature (T_m) and enthalpy of fusion (ΔH_f) were found to be -67.9ºC, 174.1ºC, 66.14J/g respectively. Crystallisation could also be observed.

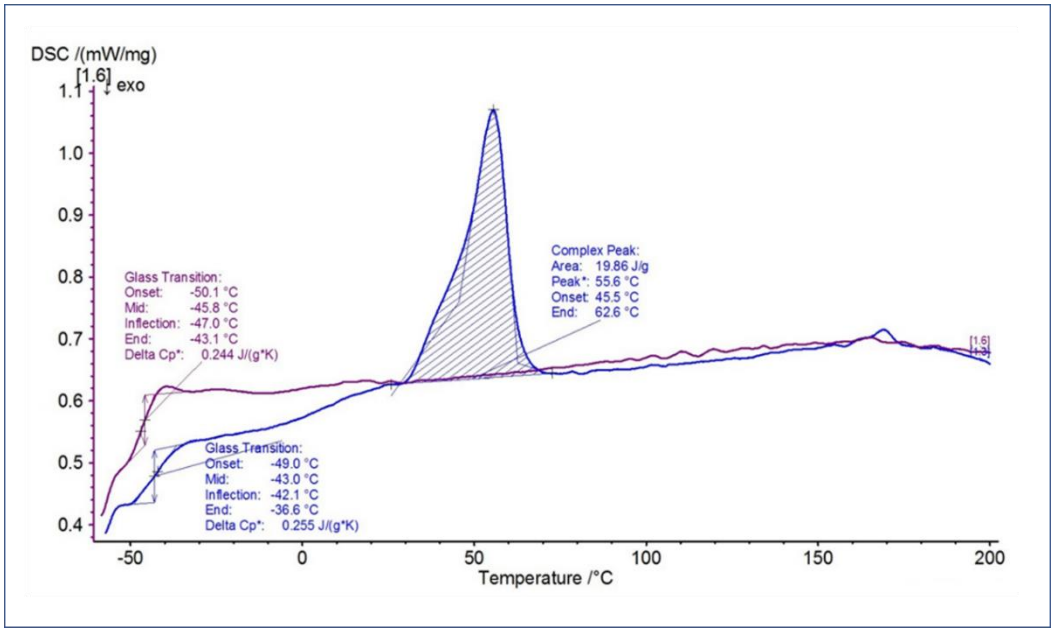

Figure 3.32: DSC Thermogram of P(3HO-co-3HD) derived from P. mendocina CH50

The DSC thermogram of P(3HO-co-3HD) is shown in Figure 1.12. From the graph, glass transition temperature (T_g), melting temperature (T_m) and enthalpy of fusion (ΔH_f) were found to be -42.1°C, 55.6°C and 19.86 J/g respectively. Cold crystallisation was not observed with mcl PHA. Hence, the second heating-cooling-heating cycle did not show a complex peak for the melting transition of the crystalline phase of the polymer.

The thermal properties of both polymers are summarised in Table 3.1.

Table 3.1: Thermal properties of P(3HB) and P(3HO-co-3HD) produced

	Melting Temperature (T_m) °C	**Glass Transition Temperature (T_g) °C**	**Enthalpy of Fusion (ΔH_f) J/g**
P(3HB)	174.1±1.838	-67.9±0.353	60.14
P(3HO-co-3HD)	55.6±3.252	-42.10±0.919	19.86

3.3.5. Tensile Testing

Tensile testing was carried out to measure the mechanical properties of the polymers produced. The slope of the linear region of stress-strain curve obtained was recorded as the Young's modulus (E) and the sharp bend indicated the tensile strength and elongation at break of the polymer.

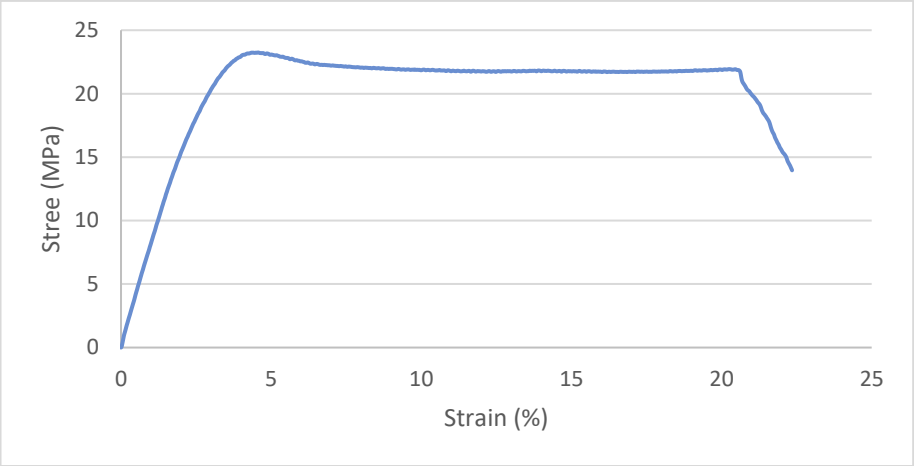

Figure 3.43: Stress-strain curve obtained from P(3HB

Figure 3.13 shows the stress-strain curve obtained from the P(3HB) produced. From the graph, elongation at break was calculated as 22.73%, Tensile Strength as 23.6MPa and the slope is calculated as Young's Modulus of 747.22MPa.

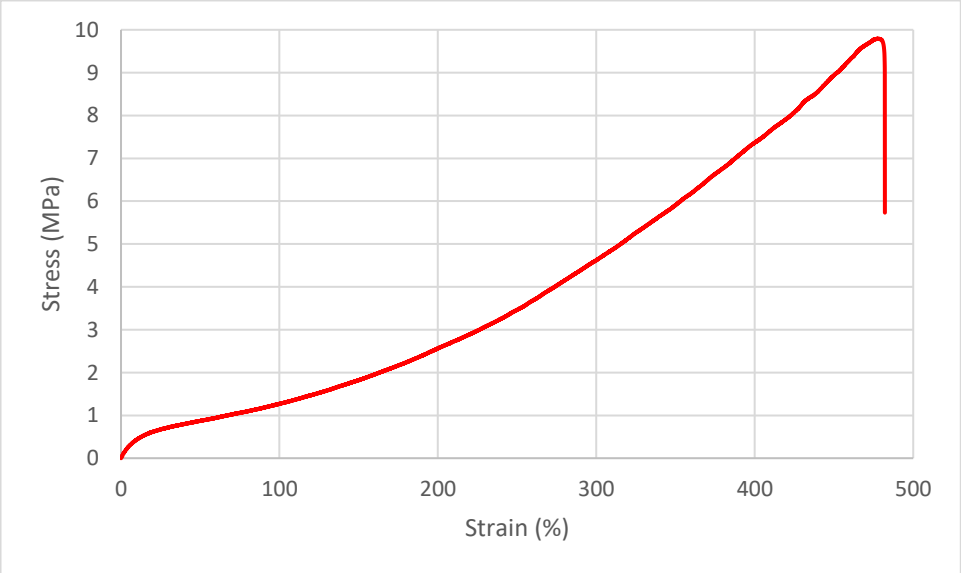

Figure 3.54: Stress-strain curve obtained from P(3HO-co-3HD)

Figure 3.14 shows the stress-strain curve obtained from the P(3HO-co-3HD) produced in the fermentation. From the graph, elongation at break was calculated as 478%, Tensile Strength as 9.78MPa and the slope is

calculated as Young's Modulus of 5.62MPa. These values indicate that P(3HO-co-3HD) is more elastic than P(3HB) but also less stiff and strong than P(3HB).

The mechanical properties of both polymers are summarised in Table 3.2.

Table 3.2: Mechanical properties of polymers produced

Polymer	**Elongation at break (%)**	**Tensile Stress (MPa)**	**Young's Modulus (MPa)**
P(3HB)	27.94±0.021	23.6±0.275	747.22±1.08
P(3HO-co-3HD)	1415±19.16	1.08±0.06	1.39±0.054

3.4. DISCUSSION

In this chapter, the production of two kinds of PHAs- P(3HB) and P(3HO-co-3HD) was carried out. These two PHAs belong to two different classes of PHAs- the stronger, more brittle scl-PHAs and the more elastic, flexible mcl-PHAs. After production, these polymers were then extensively characterised.

Bacillus sp. is the most common species of bacteria used in (P3HB) production. Different carbon sources have been used ranging from purified sugars like fructose, sucrose and glucose to impure sugars like sugarcane molasses and date molasses (Kulpreecha *et al.*, 2009). In this production, glucose was used as the carbon source. Reports of yields of P(3HB) production vary based on the carbon source used. Other factors affecting

yield include the carbon/nitrogen ratio (C/N), the nutrient being limited and the mode of fermentation being used (Khanna and Srivastava, 2005; Verlinden *et al.*, 2007b). *Bacillus* spp. favour the consumption of glucose over other carbon sources in the production of P(3HB) (Silva *et al.*, 2004). The yield of P(3HB) observed in this study was 49% (0.911g/L) in a batch mode. This is similar to the yield of 50% observed when a fermentation was run using glucose as the carbon source with *B. cereus* CFR06 (Halami, 2008b). It is however higher than 34% values observed when *B. megaterium* was run with glucose as the carbon source (Wu *et al.*, 2001). It was also higher than the 24% dcw reported using *Bacillus cereus SPV*, under the same conditions (Valappil *et al.*, 2008).

Pseudomonas mendocina CH50 was used in the production of P(3HO-co-3HD).In mcl-PHA production, the yields can vary depending on the carbon source and the C/N ratio. The yield reported here was 43% dcw at 48 hours during a batch fermentation. The yield is This yield is higher than the 21% observed by Diniz and colleagues using *P. putida* IPT 046. It is however lower than some other yields that have been reported for *Pseudomonas* spp. These values include 52% from *P. stutzeri* 1317. The difference here is that a different carbon/ nitrogen ratio (20) was used in their study in comparison to the 40 that was used in this study.

Complete characterisation was carried out to confirm the polymers produced. The results were as expected confirming the chemical structure intended. FTIR confirmed the presence of PHAs in both polymers as expected. From literature, peaks for PHAs can be observed at 1700-

1760cm^{-1} for the C=O bonds, 1220-1310cm^{-1} for the C-O-C (Wu *et al.*, 2001). P(3HB) has also been reported to have peaks at 400-100cm^{-1} corresponding to the methyl groups (Valappil *et al.*, 2008). Mcl-PHAs have been reported to have a peak around 2924cm^{-1} (Randriamahefa *et al.*, 2003).

GC-MS was used to calculate the monomer ratio in the P(3HO-co-3HD) copolymer. The ratio calculated was 22%: 78% for the methyl-3-hydroxyoctanoate and methyl-3-hydroxydecanoate respectively. This finding was supported as literature as other studies using *Pseudomonas* spp. With glucose as the carbon source have found similar monomer content and ratio. A ratio of 74.3:6.9 for 3HD:3HO was observed when *P. putida* KT2442 was grown with glucose as the carbon source (Huijberts *et al.*, 1992). He *et al.* observed a ratio of 63:21 for 3HD:3HO (He *et al.*, 1998). It was also observed that when *P. guezennei* was grown with glucose as the carbon source, a ratio of 62.8:22 for 3HD:3HO (Simon-Colin *et al.*, 2008) One factor to be noted is that in the other studies, there were a lot of contaminating polymers and peaks. Those were not existent in our study, indicating that our polymer was pure.

As expected, the thermal and mechanical properties of P(3HB) and P(3HO-co-3HD) were different. Reported mechanical properties for P(3HB) are: Tensile Strength: 18-50MPa, Young's Modulus: 1700-3800MPa & Elongation at Break: 1-5% (Avella, Martuscelli and Raimo, 2000; El-Hadi *et al.*, 2002; Godbole *et al.*, 2003; Valappil *et al.*, 2008). For mcl-PHAs, the values are: Tensile Strength: 5-22MPa, Young's Modulus: 4-15MPa and Elongation at break: 250-500% (Sudesh, Abe and Doi, 2000; R. Rai *et al.*,

2011). For thermal properties, in literature values for P(3HB) have ranged from 165-175^{o}C for the T_m. For mcl-PHAs, T_m of 42-75^{o}C have been observed. Simon-Colin *et al*. reported that for P(3HO-co-3HD) polymer, T_m of 49^{o}C, T_g of -44^{o}C and ΔH_f of 19J/g (Simon-Colin *et al.*, 2008).

In conclusion, both P(3HB) and P(3HO-co-3HD) have been produced at yields comparable to those reported in literature. Their production has been closely monitored to ensure that the processes were executed as expected. Finally, the polymers produced from each fermentation batch have been characterised thoroughly in order to confirm their identity and define their properties for use in the production of scaffolds.

CHAPTER FOUR: 2D-POROUS AND NON-POROUS P(3HB) AND P(3HO-co-3HD) SCAFFOLDS

4. 2D-POROUS AND NON-POROUS P(3HB) AND P(3HO-co-3HD) SCAFFOLDS

4.1. INTRODUCTION

One of the most important things to consider in scaffold design is the porosity of the scaffold. This refers to two factors: the concentration of void space (porosity) and pore size. The presence of pores in a material affects the mechanical properties, cell growth, adhesion and proliferation (Karageorgiou and Kaplan, 2005; Loh and Choong, 2013). Porosity is important in Tissue Engineering for the mediation of the exchange of nutrients, products and waste between cells; it also contributes to the formation of barriers, providing protection from immune cells and microorganisms (Stendahl, Kaufman and Stupp, 2009).

Porosity is of interest because it is a factor that can be manipulated to control certain properties that could make the scaffold easily customisable. Since the porosity affects the mechanical properties, depending on the target organ, the pores can be manipulated to create scaffolds similar to those of the target organ. Porosity has also been shown to increase both the surface area and surface roughness of a material which in turn increase the protein adsorption and cell adhesion to the surfaces (Karageorgiou and Kaplan, 2005; Daoud *et al.*, 2011).

One of the major challenges in creating porous scaffolds is finding the right balance of factors. The pore size must be small enough to let nutrients, waste

and products be exchanged but not large enough to prevent aggregation where needed. The degree of porosity must also be just right to allow both cell attachment and aggregation (Loh and Choong, 2013).

The native pancreatic tissue is soft and viscoelastic, with a Young's modulus of 1.4 ± 2.1 kPa (Sugimoto *et al.*, 2014). To achieve values similar to this, porous structures have been used in islet transplantation. Porous structures have also been used since islet survival requires high oxygen demand, access to vascularisation and protection from the body's immunity. Porous structures are highly valued in islet transplantation because they provide structural support and can maintain structural integrity the islets need to function and survive. Due to the roughness that porous scaffolds have, cell attachment is increased. The roughness also encourages the aggregation of β-cells into islet-like clusters. Porous structures have also been shown to trap islets within the interconnected pores, making it more difficult to lose islets and reducing the number of islets needed for transplantation in the long-term. Examples of porous polymer scaffolds that have been used for islet transplantation include: poly-L-lactic acid (PLLA), poly-glycolic acid (PGA), poly(-lactic-co-glycolic acid) PLGA, alginate and polydimethylsiloxane (PDMS) (Elçin *et al.*, 2003; Blomeier *et al.*, 2006; Kawazoe *et al.*, 2009; Pedraza *et al.*, 2013).

Different techniques for fabrication of 2D scaffolds exist. In salt leaching, porogen (sugar, salt) particles of specific sizes are poured in a mould followed by the polymer solution. After drying, the scaffold is thoroughly washed to leach out the porogen leaving pores behind. This technique is

applicable when there are small quantities of polymer and are very easy to make. In gas foaming, gas is used as the porogen and polymer discs are formed by compression moulding. Since high temperature and pressure is required in this technique, it is mainly applicable to polymers with low melting temperatures. (Hutmacher, 2000; Ma, 2004; Li, Thouas and Chen, 2012; Janik and Marzec, 2015).

This chapter aims to evaluate the effect of porosity of 2D PHA scaffolds on the viability and growth of BRIN BD11 cells seeded in them. To achieve this, both porous and non-porous structures were made and characterised. Varying types, concentrations and sizes of porogens were used to determine which scaffolds produced using these conditions is the most viable for islet transplantation.

4.2.RESULTS

4.2.1. Polymers Produced

Two types of PHAs were produced as described in section 2.2 (Figure 4.1). Figure 4.1a shows P(3HO-co-3HD) in its unprocessed form. The polymer itself is translucent in appearance. To the touch, it is flexible and elastic. Since it is elastic and sticky, during precipitation, the polymer sticks to itself and becomes a lump after the solvent is evaporated. Figure 4.1b is the P(3HB) produced in its unprocessed form. It is white in appearance and can be broken or torn apart very easily. It precipitates in clumps and hardens as it dries.

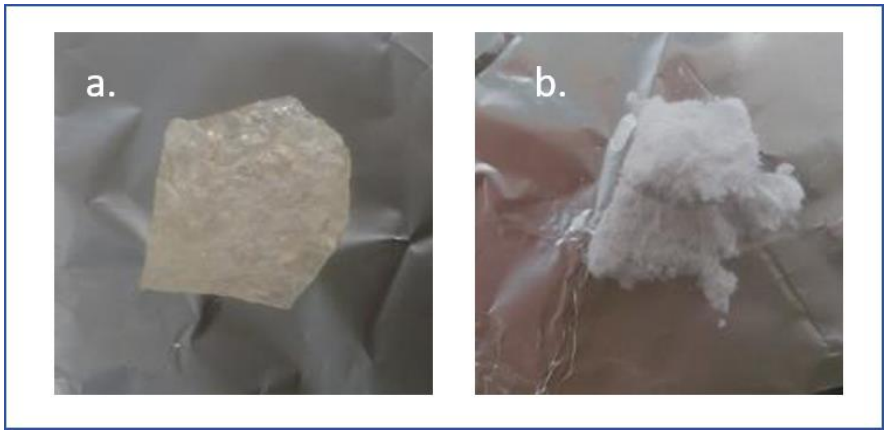

Figure 4.1: Polymers produced a. P(3HO-co-3HD) produced using fermentation of P. mendocina CH50 and glucose as the carbon source b. P(3HB) produced using B. subtilis OK2

2D non-porous scaffolds were made using P(3HB) and P(3HO-co-3HD) (Figure 4.2). These scaffolds were made using the solvent casting method as described in section 2.6.2. After solvent evaporation, P(3HB) scaffolds were easily taken off the glass petri dish diameter 52.4mm. The P(3HB) scaffolds appeared as white, hard and brittle (Figure 4.2a). In contrast, P(3HO-co-3HD) scaffolds appeared completely transparent, elastic and sticky Figure 4.2b. After solvent evaporation, the scaffolds were peeled back from the petri dish Figure 4.2c. Physically, the PLLA scaffolds are transparent and very brittle. The solvent evaporated very rapidly from the surface of the PLLA scaffolds.

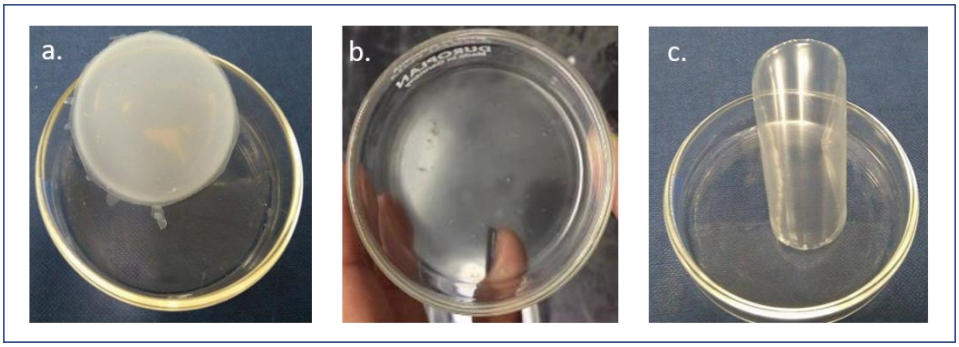

Figure 4.2: 2D Non-porous scaffolds made by the solvent casting method. a. P(3HB) b. P(3HO-co-3HD) after solvent evaporation c. P(3HO-co-3HD) after peeling from petri dish

4.2.2. Comparison of the properties of PHA 2D scaffolds in comparison to PLLA 2D scaffolds

4.2.2.1. Mechanical and Thermal Properties of Polymers

Mechanical and thermal characterisation was carried out on P(3HB) and P(3HO-co-3HD). The results were then compared with those of PLLA, a polymer that has been widely explored commercially for Tissue Engineering applications (Hart *et al.*, 2015). Table 4.1 shows the thermal and mechanical properties of the 3 polymers characterised.

Of the polymers, PLLA was found to be the stiffest and most brittle with Tensile Strength and Young's Modulus up to 50 and 2,500 times greater than that of P(3HO-co-3HD) respectively. P(3HO-co-3HD) was the most elastic of the three with elongation at break approximately 600 times greater than that of PLLA. P(3HB) had mechanical properties more similar to PLLA than P(3HO-co-3HD), although it was found to be less brittle than PLLA.

Thermally, P(3HO-co-3HD) had the lowest melting temperature of the three. P(3HB) had much higher melting temperatures. For glass transition temperature, both PHAs had similar values different to PLLA.

Table 4.1: Mechanical and thermal properties of P(3HB), P(3HO-HD) and PLLA. Values are expressed as mean ± SEM for groups of 6.

	Tensile Strength (MPa)	**Elongation at break (%)**	**Young's Modulus (MPa)**	**Melting temperature (T_m/ºC)**	**Glass transition temperature (T_g/ºC)**
P(3HB)	23.6±0.275	7.94±0.021	747.22±1.08	172.8±1.838	-67.15±0.35
P(3HO-co-3HD)	1.08±0.06	1415±19.16	1.39±0.054	54.7±3.252	-66.95±0.92
PLLA	53.5±3.5	2.4±0.06	3425±12.25	177.3±1.75	-61.73±3.36

4.2.2.2.Direct Cell Viability Tests on P(3HB), P(3HO-co-3HD) and PLLA

Cell viability tests were carried out on three polymers P(3HB), P(3HO-co-3HD) and PLLA using murine BRIN BD11 cells. PLLA was selected because it is an FDA approved biopolymer and has been explored in Tissue Engineering (Hart *et al.*, 2015). The results are shown in Figure 4.3. Compared to the positive control, the polymer that showed the highest BRIN BD11 cell viability was P(3HO-co-3HD), showing viabilities of 84.94%, 97.19% and 98.06% on days 1, 3 and 7 respectively. P(3HB) was the next highest with 66.57%, 84.1% and 88.21%. Cells seeded on PLLA had viabilities of 38.91%, 70.16% and 71.5% on days 1, 3 and 7

respectively. In comparison with the positive control (Tissue Culture Plastic, TCP), by day 3, the cell viability on P(3HO-co-3HD) showed no significant difference. In the case of P(3HB), the difference became less significant with the number of days indicating an increase in cell viability with increase in time. PLLA showed a highly significant difference on all days in comparison to the positive control.

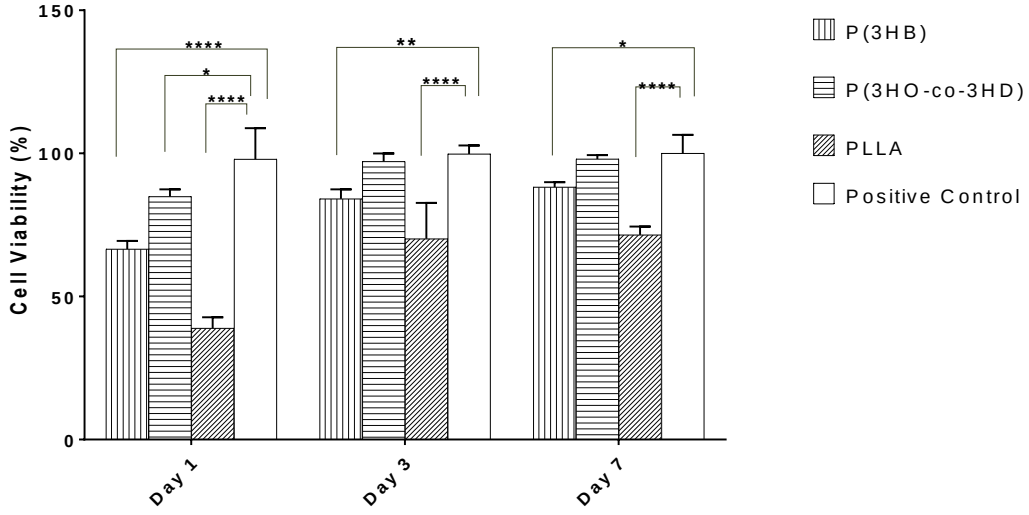

*Figure 4.3: Direct cell viabilities of BRIN BD11 cells seeded on 2D P(3HB) and P(3HO-co-3HD) and PLLA scaffolds. Values are expressed as % positive control (tissue culture plate) mean ± SEM for numbers of 6. p *$p \leq 0.05$, **$p \leq 0.01$, ****$p \leq 0.0001$ when compared with positive control (tissue culture plastic).*

4.2.2.3.Static Insulin Secretion Tests on P(3HB), P(3HO-co-3HD) and PLLA

The average insulin released from BRIN BD11 cells seeded on P(3HO-co-3HD), P(3HB) and PLLA scaffolds are shown in Figures 4.4 and 4.5. Upon addition of 5.6mM glucose (normoglycaemia), the average insulin released for the positive control (tissue culture plastic) was 0.984 ng/10^6 cells/20 min; for P(3HO-co-3HD), 3.742 ng/10^6 cells/20 min; P(3HB), 2.211 ng/10^6 cells/20 min and PLLA, 1.529 ng/10^6 cells/20 min.

Cells seeded on both PHAs had significantly greater insulin release than the positive control with those on P(3HO-co-3HD) released the highest amount of insulin in response to glucose stimulus.

When 16.7mM glucose (hyperglycaemia) was added, the average insulin released for the positive control (tissue culture plastic) was 1.481 ng/10^6 cells/20 min; for P(3HO-co-3HD), 3.967 ng/10^6 cells/20 min; P(3HB), 2.506 ng/10^6 cells/20 min and PLLA, 1.379 ng/10^6 cells/20 min. Again, cells seeded on both PHAs had significantly greater insulin release than the positive control with those on P(3HO-co-3HD) released the highest amount of insulin in response to glucose stimulus.

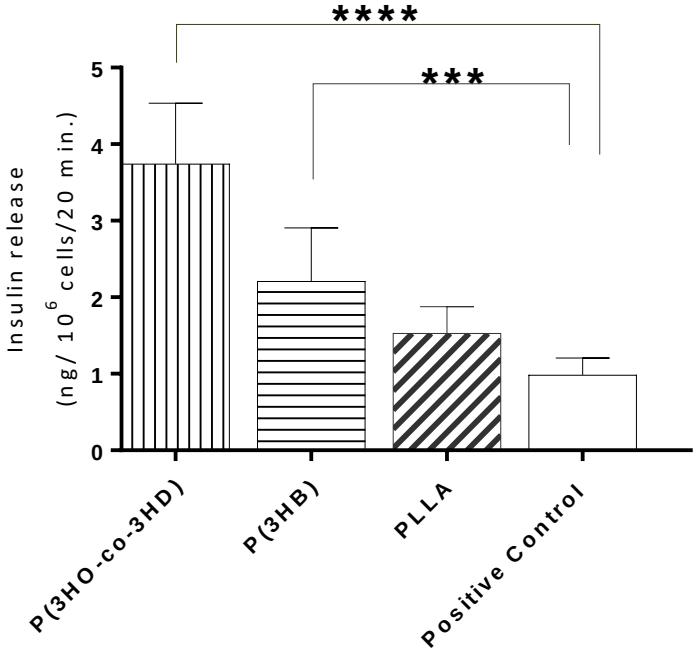

*Figure 4.4: Insulin secretion at normoglycaemia (5.6mM glucose) from BRIN BD11 cells seeded in P(3HO-co-3HD), P(3HB), PLLA scaffolds and positive control (tissue culture plastic) in ng of insulin/10^6 cells/20 minutes. Values are expressed as mean ± SEM for groups of 6. ***$p \leq 0.001$, ****$p \leq 0.0001$ when compared with insulin release from positive control.*

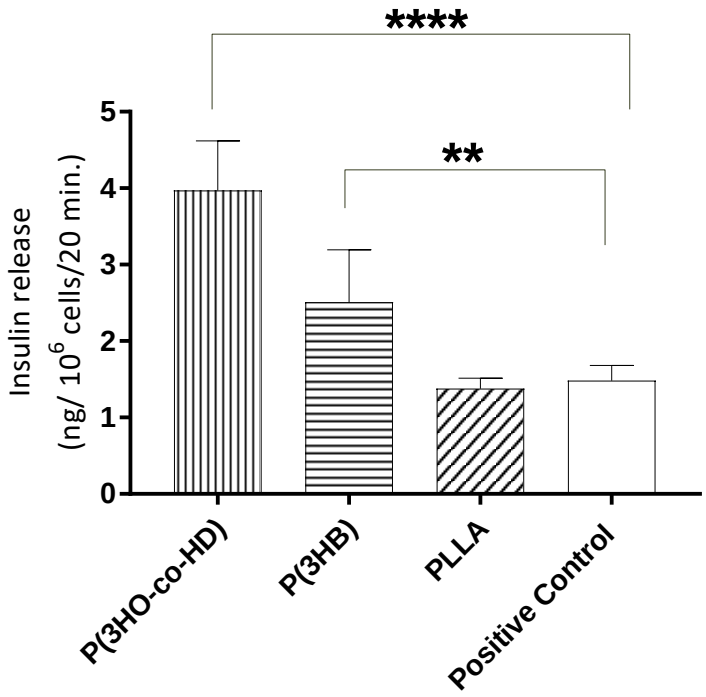

*Figure 4.5: Insulin secretion at hyperglycaemia (16.7mM glucose) from BRIN BD11 cells seeded in P(3HO-co-3HD), P(3HB) PLLA scaffolds and positive control (tissue culture plastic) in ng of insulin/10^6 cells/20 minutes. Values are expressed as mean ± SEM for groups of 6. **$p \leq 0.01$, ****$p \leq 0.0001$ when compared with insulin released from positive control.*

4.2.3. Fabrication of 2D Porous (P3HO-co-3HD) Scaffolds Using NaCl Porogen

4.2.3.1. Physical Properties of Porous P(3HO-co-3HD) Scaffolds

The scaffolds made appeared white with NaCl particles interspersed before leaching (Figure 4.6). After leaching, the scaffolds appeared white with open pores. The scaffolds were physically less elastic and had to be handled carefully. The higher the concentration of porogen used, the more brittle the scaffolds. Similarly, the same thing was observed as the size of the porogen increased.

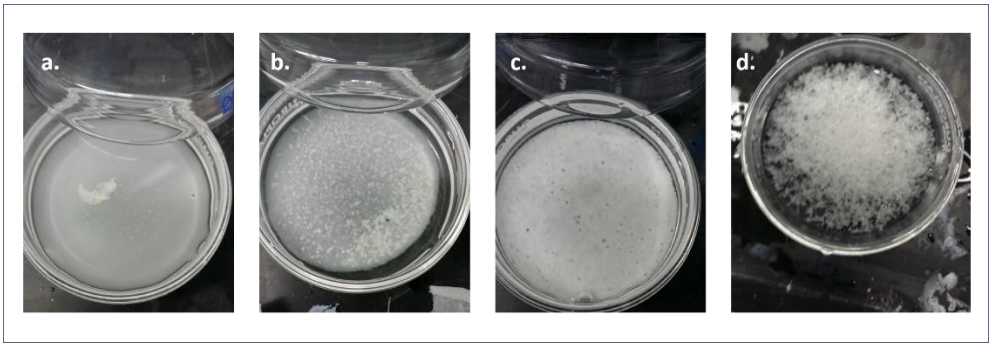

Figure 4.6: Porous P(3HO-co-3HD) scaffolds made before washing.

Figure 4.7 shows SEM images of the porous scaffolds showing their internal structures. When A and B are compared, there is an obvious increase in pores due to the increased concentration of porogen. The diameter of the pores also increases with the size of porogen as expected. This trend is also observed when C and D are compared. The SEM images also show that the salt particles have been completely leached out as there were no salt crystals observed.

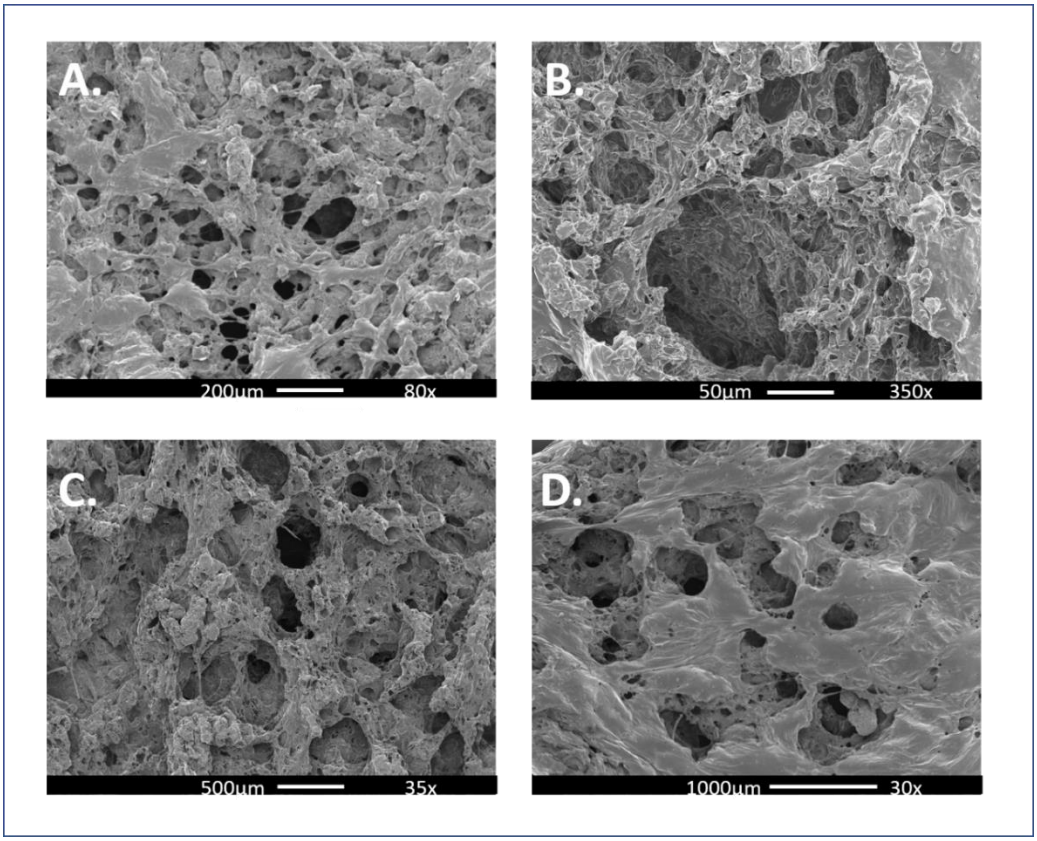

Figure 4.7: Scanning electron microscopy (SEM) images of porous P(3HO-co-3HD) scaffolds made with varying porogen sizes and concentrations of NaCl and sucrose.

4.2.3.2.Mechanical Properties of P(3HO-co-3HD) Porous Scaffolds

The mechanical properties observed are recorded in Table 4.2. The highest value for the Young's modulus (E), a measure of material stiffness, was measured in scaffold A- 3.32±0.78MPa. After A, there is a continuous reduction in the E values as both porosity and pore size increase. The lowest E value was for scaffold D at 2.30±1.47 MPa.

Similarly, tensile strength trend seems to reveal that the higher the porosity and the pore size, the lower the tensile strength, as scaffold A had 3.19 MPa, in comparison to scaffold D which had 0.25 ± 0.17 MPa.

Elongation at break also followed the same trend, indicating that the elasticity reduces gradually from 277.7±29.85% in scaffold A to 49.5±18.2% for scaffold D. Table 4.3 shows a summary of the mechanical properties of the P(3HO-co-3HD) porous scaffolds that were made.

Table 4.2: Summary of mechanical properties of of P(3HO-co-3HD) porous scaffolds produced. Samples are expressed as value±SEM for groups of 6.

Structures	Young Modulus (MPa)	Tensile Strength (MPa)	Elongation break (%)
A	3.32±0.78	3.19±0.84	277.7±29.85
B	3.19±0.86	1.81± 0.47	192.2±27.77
C	2.90 ± 0.97	0.80 ± 0.26	71.6 ± 6.12
D	2.30 ± 0.47	0.25 ± 0.17	49.5 ± 18.2

4.2.3.3. Water Contact Angle (ɵ) of P(3HO-co-3HD) Porous Scaffolds

The static water contact angle is a measure of hydrophobicity or hydrophilicity of a material. Table 4.3 shows the ɵ values for the four different P(3HO-co-3HD) porous scaffolds made. A material is considered hydrophobic if its ɵ >70. Increase in both porosity and pore size led to a decrease in the water contact angle observed. The highest water contact angle was for the neat P(3HO-co-3HD) scaffold while the lowest was for scaffold D.

4.2.3.3.Protein Absorption of P(3HO-co-3HD) Porous Scaffolds

Protein adsorption refers to the attachment of proteins to the surface of a material. It is an indication of the possible cell adhesion and proliferation on a material, the higher the better. Table 4.3 shows the protein adsorption in (μg/cm^2) of the four different P(3HO-co-3HD) porous scaffolds. These values show that as both porosity and pore size increase, the protein adsorption increases. The highest protein adsorption was for the neat scaffold and the lowest was on scaffold A.

Table 4.3: Water Contact Angle (ɵ) and Protein Adsorption (μg/cm^2) for the P(3HO-co-3HD) scaffolds.

Structures	**Water Contact Angle (ɵ)**	**Protein Adsorption (μg/cm^2)**
P(3HO-co-3HD)	104.58±8.63	353.69±19.85
A	120.34±14.79	95.72±11.14
B	104.13±9.65	250.447±17.38
C	116.62±11.59	125.17±7.90
D	94.64±5.69	235.33±25.48

4.2.3.4.Water Uptake (%) of P(3HO-co-3HD) Porous Scaffolds

Water uptake is a measure that is used to measure any potential changes in weight and degradation of a structure *in vivo*. It was measured in samples incubated in both phosphate buffered saline (PBS) and Roswell Park Memorial Institute (RPMI) media, the media for culturing BRIN BD11 cells

at 37^{o}C. The average water absorption value was calculated as a % of the initial weight of the structure. The results are summarised in Figure 4.8. All four structures showed a statisitically significant increase in water absorbed by 30th day in comparison with the P(3HO-co-3HD) neat scaffold. This was observed in samples incubated in both PBS and RPMI.

4.2.3.5.Weight Loss (%) of P(3HO-co-3HD) Porous Scaffolds

Weight loss is another factor that enables the monitoring and calculation of degradation of polymer structures. Figure 4.8 shows that all four scaffolds lost weight after incubation for 30 days. In PBS, all scaffolds had statistically different (increased) weight loss except scaffold A in comparison to the neat P(3HO-co-3HD) scaffold. In RPMI, all four scaffolds had statistically significant (increased) weight loss.

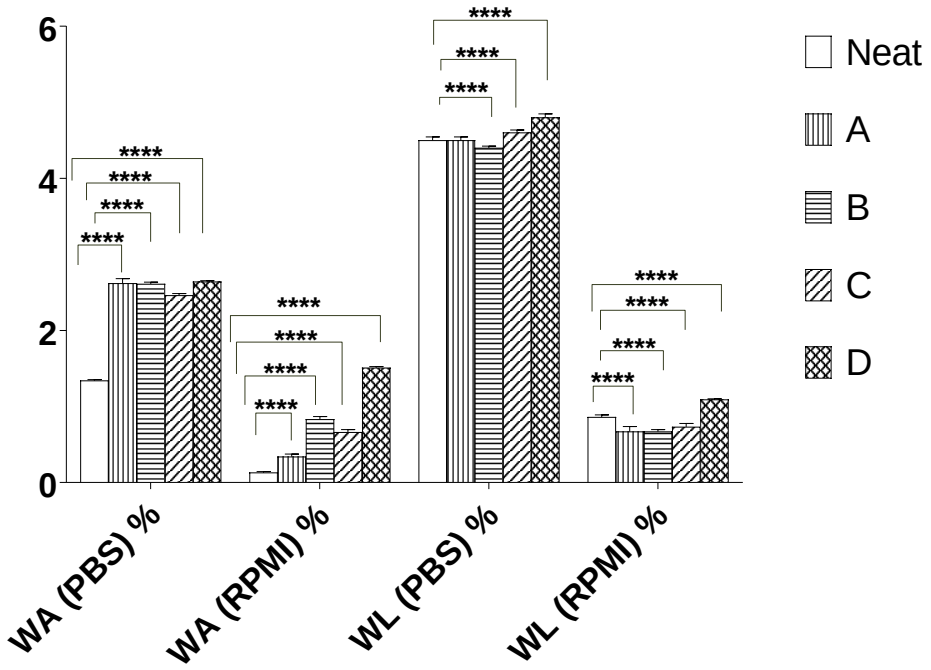

*Figure 4.8: %Water absorption and %weight loss values for porous P(3HO-co-3HD) scaffolds made. Samples are expressed as % of initial weight ± SEM for groups of 6. ****$p \leq 0.0001$ when compared with neat P(3HO-co-3HD) scaffolds.*

4.2.4. Comparison of 2D P(3HO-co-3HD) Porous Structures Made Using NaCl and Sucrose as Porogens

Since porosity was found to be a crucial factor in earlier made scaffolds, an indepth study using two different porogens- sodium chloride (NaCl) and sucrose was carried out.

4.2.4.1. Porogen, Porogen Size and Concentration for P(3HO-co-3HD) Porous Scaffolds with NaCl and Sucrose as Porogens

Table 4.4 is a summary of the porous P(3HO-co-3HD) 2D scaffolds made with both porogens. Both porogens were used at two different particle sizes (100 & 300µm) and two concentrations (5 and 15%).

Table 4.4: Porogen type, concentration and sizes for the production of P(3HO-co-3HD) 2D porous scaffolds.

Porogen	**Porogen Concentration (%w/v)**	**Porogen Size (µm)**	**Identity of the P(3HO-co-3HD) scaffold**
NaCl	5	100	A
NaCl	15	100	B
NaCl	5	300	C
NaCl	15	300	D
$C_6H_{12}O_6$	5	100	E
$C_6H_{12}O_6$	15	100	F
$C_6H_{12}O_6$	5	300	G
$C_6H_{12}O_6$	15	300	H

4.2.4.2. Properties of P(3HO-co-3HD) Porous Scaffolds Made with NaCl and Sucrose

Table 4.5 gives a summary of the mechanical properties of the porous P(3HO-co-3HD) scaffolds made with NaCl and sucrose. From the results obtained, the stiffest of the porous scaffolds is A with the highest Young's modulus. As the porosity increases, the Young's Modulus decreases indicating a reduction in stiffness. Also, as the pore size increases, there is a reduction in the Young's Modulus. The porous scaffolds made with NaCl are stiffer than those made with sucrose.

For tensile strength, the same trend was observed. Although the 2D scaffold C had the highest tensile strength, the general trend observed was that an increase in both porosity and pore size lead to a reduction in the tensile strength of the scaffolds. Also, 2D porous scaffolds made using glucose as the porogen had a reduced value of tensile strength as compared to the ones made using NaCl. The value of elongation at break also followed the same trend with the 2D scaffold A having the highest elongation at break.

Table 4.5: Summary of the mechanical and thermal properties of P(3HO-co-3HD) porous scaffolds produced using NaCl and sucrose. Samples are expressed as value ± SEM for groups of 6.

Scaffolds	**Young's Modulus (MPa)**	**Tensile Strength (MPa)**	**Elongation at break (%)**
A	89.84±14.33	4.20±0.34	83.39±12.56
B	17.60±2.78	1.11±0.052	42.92±9.25
C	57.06±12.27	4.42±0.067	61.12±8.63
D	13.21±1.82	2.84±0.18	29.74±8.93
E	35.63±9.79	3.49±0.071	59.40±4.78
F	8.40±0.123	1.09±0.083	35.10±3.47
G	10.97±0.97	2.45±0.62	36.53±4.41
H	2.75±0.059	1.35±0.071	27.60±5.36

4.2.4.3. *Water Contact Angle (θ) and Protein Adsorption of P(3HO-co-3HD) Porous Scaffolds Made with NaCl and Sucrose*

Water contact angle and protein adsorption tests were carried out to evaluate the effect of porogen on the hydrophobicity and cell adhesion characterisitcs of porous scaffolds.

Table 4.6 is a summary of the water contact angle and protein adsorption values of the 8 porous scaffolds made with two different porogens. Among the scaffolds, the most hydrophobic was A with a water contact angle of 120.34±14.79. For protein adsorption, scaffold D had the greatest adsorption with 253.33±25.48 μg/cm^2.

Table 4.6: Summary of static water contact angle and protein adsorption values of porous P(3HO-co-3HD) scaffolds with different porogens. Samples are expressed ± SEM for groups of 6.

Structures	**Water Contact Angle (θ)**	**Protein Adsorption (μg/cm^2)**
A	120.34±14.79	95.72±11.14
B	104.13±9.65	250.45±17.38
C	116.62±11.59	125.17±7.30
D	94.64±7.23	253.33±25.48
E	107.93±11.96	85.21±15.48
F	106.49±7.44	205.34±27.58
G	123.72±13.56	130.76±32.91
H	95.61±4.21	114.62±20.54

4.2.4.4. *Direct Cell Viability Tests using BRIN BD11 Cells Seeded on P(3HO-co-3HD) Porous Scaffolds with different porogens*

Direct cell viability tests were carried out to measure the cytocompatibility of the eight porous scaffolds. Figure 4.12 shows the cell viabilities of BRIN BD11 cells seeded in the 8 different porous scaffolds produced using NaCl and sucrose as porogens. By day 7, cells in all eight samples had viabilities >80%. 2D Porous scaffold B had the highest cell viability of 99.93±7.5. Increase in porosity led to an increase in cell viability, while increase in pore size led to decreased cell viability. 2D Porous Scaffolds A and B had cell viabilities not significantly different $p > 0.05$ to the neat P(3HO-co-3HD) scaffold.

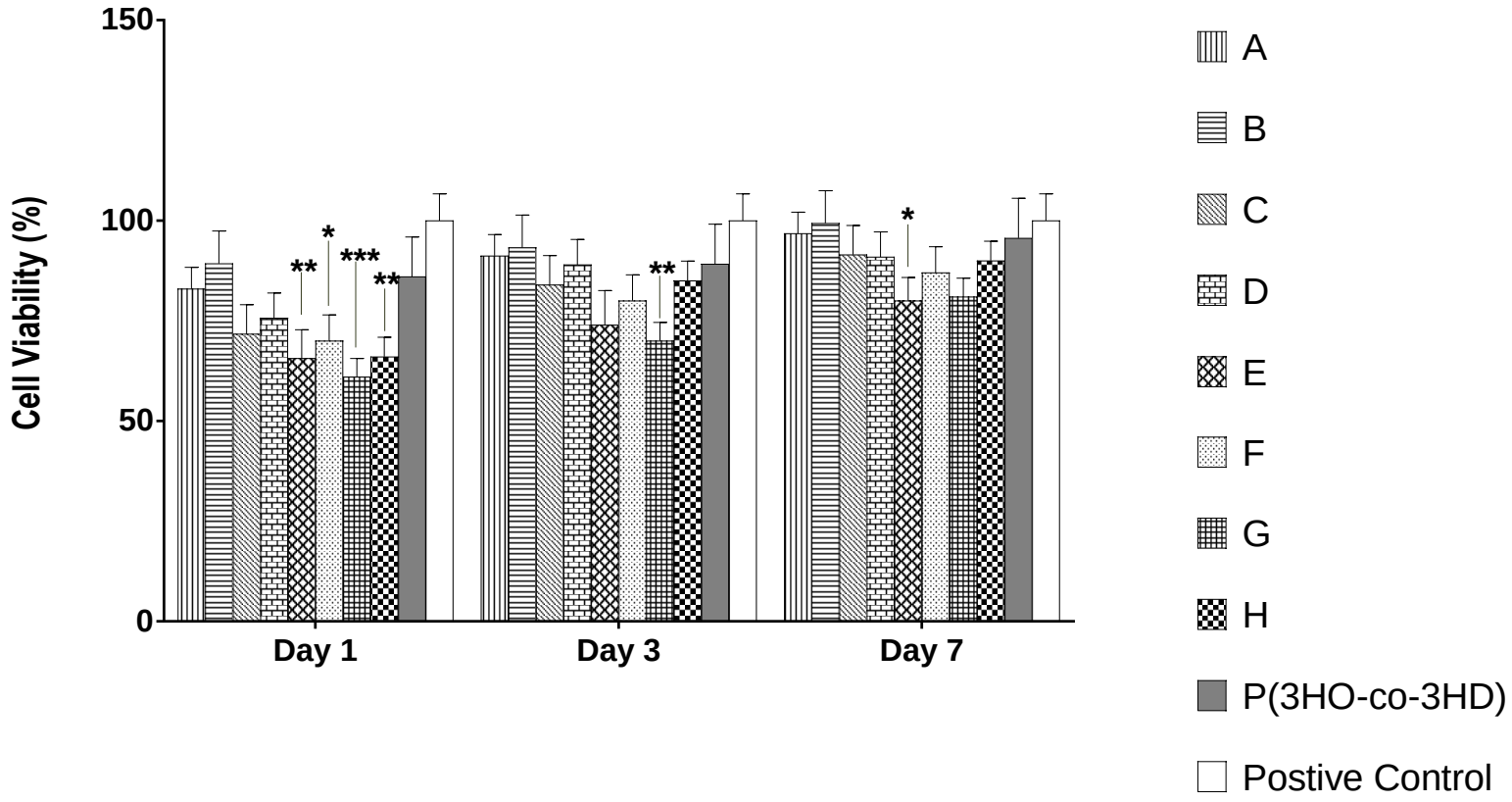

Figure 4.9: Direct cell viability of BRIN BD11 seeded in P(3HO-co-3HD) porous scaffolds with NaCl and sucrose as porogens. Samples are expressed as % of positive control (tissue culture plastic) ± SEM for groups of 6. $^{*}p \leq 0.05$, $^{**}p \leq 0.01$, $^{****}p \leq 0.0001$ when compared with neat P(3HO-co-3HD) scaffolds

4.2.4.5. Static Insulin Secretion from BRIN BD11 Cells Seeded on P(3HO-co-3HD) Porous Scaffolds Using NaCl and Sucrose as Porogens

Insulin release analyses were carried out to evaluate the effect of the porogen on the insulin released from BRIN BD11 cells seeded on the scaffolds, after glucose stimulus, at both normoglycaemia (5.6mM glucose) and hyperglycaemia (16.7mM).

At normoglycaemia- 5.6mM glucose (Figure 4.13), increases in both porosity and pore size led to a decrease in insulin release. At hyperglycaemia- 16.7mM (Figure 4.14), a similar trend was observed. Increasing porosity and pore size led to decreased insulin release. Cells seeded on scaffolds A exhibited insulin release significantly higher than the neat P(3HO-co-3HD) scaffolds.

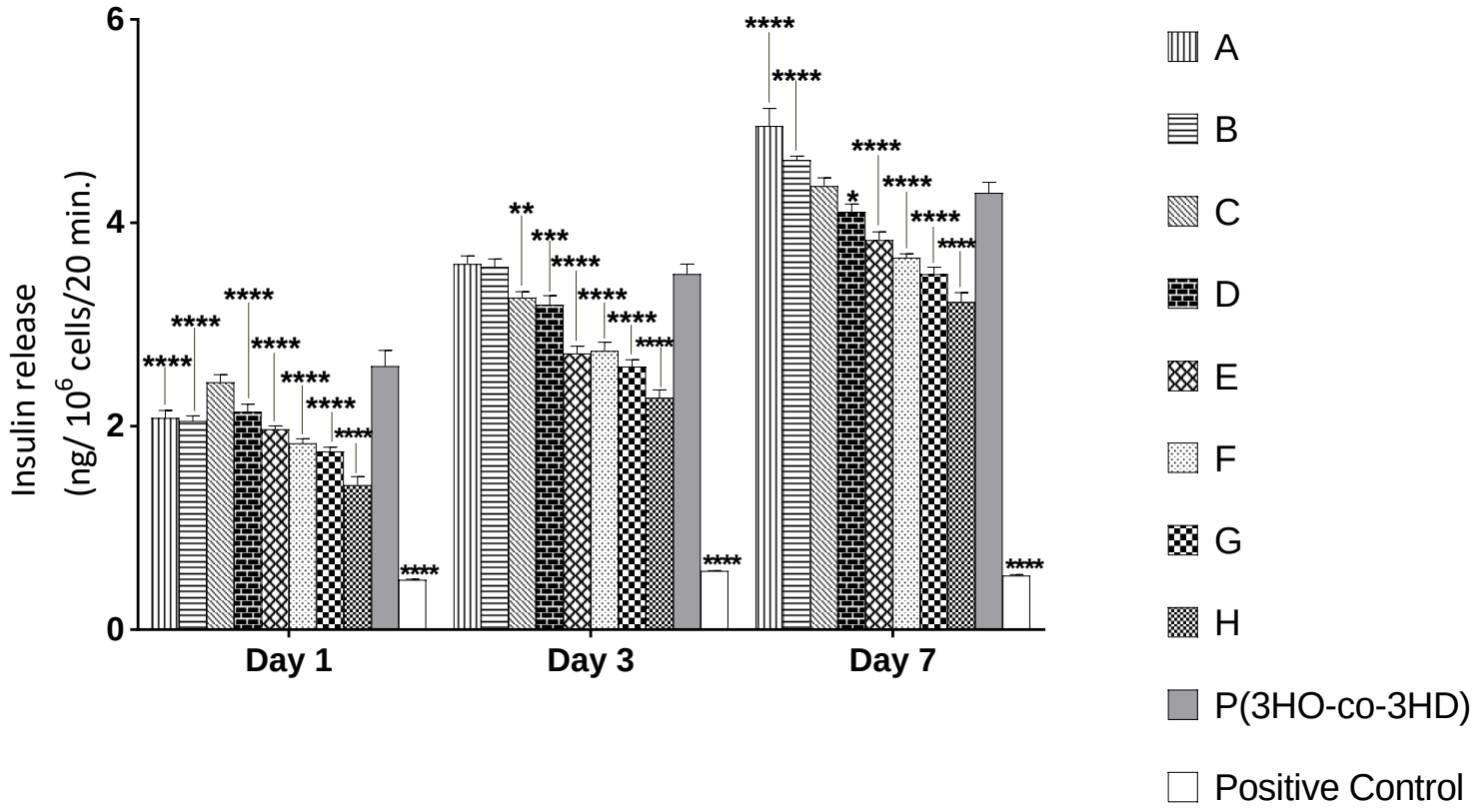

*Figure 4.10: Insulin secretion at normoglycaemia (5.6mM glucose) from BRIN BD11 cells seeded in 2D porous scaffolds made using NaCl and sucrose in ng of insulin/10^6 cells/20 minutes. Values are expressed as mean ± SEM for groups of 6. **p ≤ 0.01, ***p ≤ 0.001, when compared with insulin release from P(3HO-co-3HD) scaffold. ****p ≤ 0.0001 for all other porous scaffolds.*

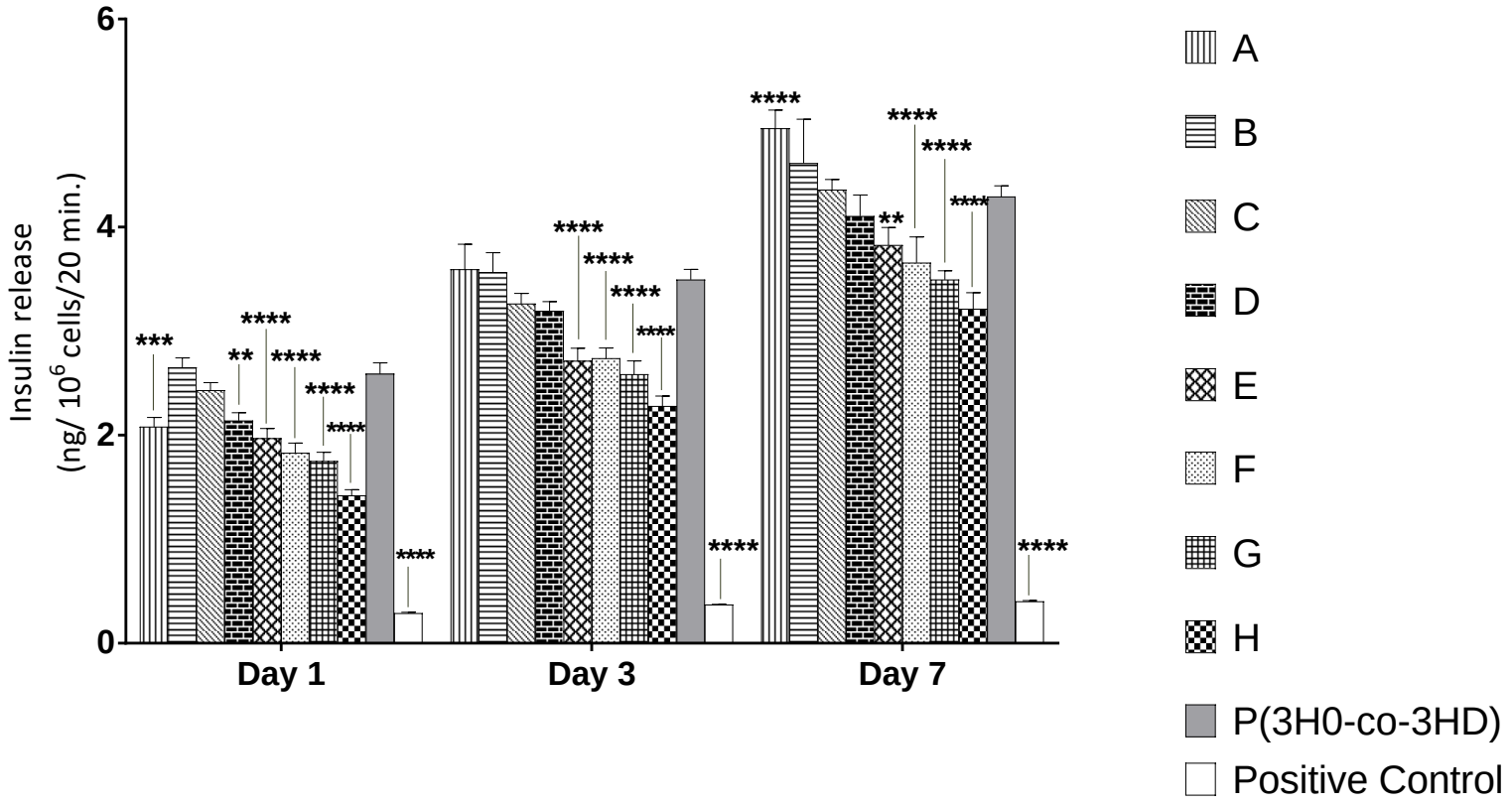

*Figure 4.11: Insulin secretion at hyperglycaemia (16.7mM glucose) from BRIN BD11 cells seeded in 2D porous scaffolds made using NaCl and sucrose in ng of insulin/10^6 cells/20 minutes. Values are expressed as mean ± SEM for groups of 6. **$p \leq 0.01$, ***$p \leq 0.001$, ****$p \leq 0.0001$ when compared with insulin release from P(3HO-co-3HD) scaffold.*

4.3. DISCUSSION

In this chapter, several features were evaluated. First, non-porous 2D scaffolds of P(3HB), P(3HO-co-3HD) and PLLA were evaluated for their thermal and mechanical properties. They were also tested for their effect on the viability of BRIN BD11 cells seeded on them. Next, the effect of porosity and pore size on the properties of porous P(3HO-co-3HD) scaffolds were measured. These properties included mechanical properties, water contact angle, protein adsorption, weight loss and water absorption. BRIN BD11 cells were also seeded in these structures and their viabilities and insulin response was measured.

The mechanical and thermal properties observed for P(3HB), P(3HO-co-3HD) and PLLA all fell within those reported in literature. Previously reported T_m and T_g values for PLLA have been observed to be between -59 ^oC & -61^oC for T_g and 178-181^oC for T_m (Miyata and Masuko, 1998). These values are in line with those observed in this study (T_m: 177.3^oC, T_g: -61.73^oC) confirming PLLA. According to literature, the tensile strength values for PLLA are 55-59MPa, Young's Modulus 3,400-3,700MPa and elongation at break of 2-3% (Perego, Cella and Bastioli, 1996; Miyata and Masuko, 1998; Renouf-Glauser *et al.*, 2005). These are also similar to the values reported in this work (Tensile Strength: 53.5MPa, Young's Modulus: 3,425MPa and elongation at break: 2.4%), further confirming PLLA.

Mechanical and thermal properties for P(3HB) have been widely reported in literature and the values measured in this work fall within the range observed

in literature. These values are Tensile Strength: 18-50MPa, Young's Modulus: 1700-3800MPa & Elongation at Break: 1-5% (Avella, Martuscelli and Raimo, 2000; El-Hadi *et al.*, 2002; Godbole *et al.*, 2003; Valappil *et al.*, 2008) In this work, the Tensile strength observed was 23.6MPa, Young's Modulus: 747.22MPa and elongation at break: 7.94%. Tensile strength observed was within the range reported in literature. However, Young's Modulus and elongation at break are not within the range reported. This could be due to the fact that a different organism was used. *Bacillus subtilis OK2.* was used in this study. In the previously reported studies, *B.cereus, A. eutrophus* and commercially derived P(3HB) were used.

Actual values for P(3HO-co-3HD) have not been reported in literature. This is because this polymer with its monomer content (22% hydroxyoctanoate, 78% hydroxydecanoate) is a novel polymer under patent being reported for the first time. Values for other mcl-PHA monomers have been reported. For hydroxyoctanoate (HO): T_m: 53.7 to 61^oC, T_g: -35 to -42.9^oC (Gross *et al.*, 1989; Liu *et al.*, 2011; Wang, Chung and Chen, 2017). For hydroxydecanoate (HD), T_m: 45.2 to 77.6 ^oC, T_g: -37.2 to -48.1^oC (Gross *et al.*, 1989; Wang, Chung and Chen, 2017). The values observed for T_m and T_g of P(3HO-co-3HD) in this study were 54.7 and -66.95^oC respectively. These values fit into the ranges expected. For Tensile Strength: 1.8-10.1MPa, Young's Modulus: 1.3-11.6MPa and elongation at break of 198-511.3% for hydroxyoctanoate (Marois *et al.*, 1999; Dufresne and Vincendon, 2000; Lee and McCarthy, 2009; Ranjana Rai *et al.*, 2011). For hydroxydecanoate, Tensile Strength: 19.86MPa, Young's Modulus: 11.96MPa and elongation at break: 312.86% (Liu *et al.*, 2011). The values derived in this study for P(3HO-co-3HD) deviate from those reported in

literature. This could be attributed to the mole composition of the polymer. The values reported are for the monomer compositions, so they do not give an accurate picture.

Comparison of the viabilities of BRIN BD11 cells seeded on the P(3HB), P(3HO-co-3HD) and PLLA scaffolds, revealed significant differences between cells seeded in them and the positive control on day 1. By day 7 of cell culture, cells on P(3HO-co-3HD) scaffold had no statistically different cell viabilities to the positive control (tissue culture plastic). This confirms the results from a study conducted by Yang and his colleagues. The study compared two different PHAs- a scl-PHA poly(3-hydroxybutyrate-co-4-butyrate P(3HB-co-4HB) and mcl-PHA poly(3-hydroxybutyrate-co-hexanoate) P(3HB-co-HHX) with PLLA in terms of islet cell growth and function. The results from that study also showed that the islets exhibited higher viability on the mcl-PHA. This could be attributed to surface properties of the polymer. In Yang's study, PLLA and P(3HB) were shown to have very flat, smooth surfaces and hence, the islets were not able to adhere to them. P(3HO-co-3HD) surfaces were not as flat as the others and hence were able to facilitate cell adhesion (Yang *et al.*, 2009). Another factor that could have contributed to the increased cell viability in P(3HO-co-3HD) is the mechanical properties. Of the two polymers investigated, P(3HO-co-3HD) had mechanical properties similar to the native properties of the pancreas; thereby providing similar structure for adhesion and proliferation.

The same pattern was observed in the insulin release studies with cells seeded on P(3HO-co-3HD) scaffolds having higher insulin release on stimuli at both

normoglycaemia (5.6mM) and hyperglycaemia (16.7mM). This was also observed in Yang's study in which NIT-1 pancreatic cell lines seeded in the mcl-PHA had a higher insulin release. Insulin release is exponentially linked to cell growth; hence, increased cell growth will lead to an increase in insulin sensitivity and release. Yang and colleagues found that insulin expression increases where aggregation is present i.e. the mcl-PHA. It is then to be expected that BRIN BD11 cells form more aggregates on the surface of P(3HO-co-3HD) leading to increased insulin expression and release (Sorenson and Brelje, 1997; Yang *et al.*, 2009).

Creation of porous structures for Tissue Engineering has a potential amount of benefits. These include the ability to weaken stiffer materials to produce mechanical properties similar to those of native tissue. Addition of pores would also improve the permeability of the material to allow exchange of nutrients and waste materials (Hollister, 2005). One of the challenges of designing porous scaffolds is achieving just the right balance of strength and stiffness in a porous material to enable it to bear the load while also maintaining structural integrity. The presence of pores in a material increases the interconnectivity but reduces the integrity of the structure and hence the more porous a material is, the lower its load bearing capacity. Pore size is also an important factor as bigger pore sizes leave bigger voids in the structure, thus weakening it even further. As porosity increases, tensile strength, stiffness and elongation at break decrease (Nam and Park, 1999; Chen, Ushida and Tateishi, 2001; Hollister, 2005). This was observed in this study as tensile strength, Young's Modulus and elongation at break decreased as the porogen and pore size increased. The same trend was observed when both NaCl and sucrose were used as porogens.

It was also observed that in comparison to porous scaffolds made with NaCl, porous scaffolds made with sucrose had decreased tensile strength, Young's Modulus and elongation at break. This is corroborated by Dorati's study in which NaCl and sucrose were used to make porous PLGA structures and compared. Their study found that the mechanical properties of sucrose-based structures were lower than those of NaCl based structures. This is due to the fact that NaCl and sucrose provide different polymer matrices when they are used as porogens (Dorati *et al.*, 2010). These differences could also be attributed to the solubilities of NaCl and sucrose.

Both water contact angle and protein adsorption are connected closely with surface roughness. In porous surfaces, roughness depends on the surface microstructure and the size and shape of the pores. The rougher a surface, the higher its wettability and hence, higher the protein adsorption to the surface. As a result, cell adhesion is directly linked to porosity (Boyan *et al.*, 1996; Wei and Ma, 2004; Arima and Iwata, 2007; Förch, Schönherr and Jenkins, 2009). This was observed in this study, where as water contact angle increased, protein adsorption decreased. As the concentration of porogen increased, the cell viability increased. However, as the size of porogen increased, the cell viability decreased. The average islet cell is 80-100µm in size, suggesting that pore sizes ~100µm will be ideal for islet transplantation (Ionescu-Tirgoviste *et al.*, 2015). This validates the data from this study that shows the 2D scaffolds A (pore size 100µm/ porogen concentration 5%) and B (pore size 100µm/ porogen concentration 15%) have the best combination of properties making them ideal porous materials.

Degradation is another important factor to be considered in the design of scaffolds with biomaterials. It is defined by factors like water uptake/ absorption and weight loss (Lu *et al.*, 2000; Wei and Ma, 2004). The % water uptake and % weight loss observed in this study confirm a steady rate of degradation typical of PHAs. Although degradation rates have been shown to affect cell growth negatively, the degradation products of PHAs are not toxic. PHAs are degraded into their water-soluble monomers and oligomers (Numata, Abe and Iwata, 2009; Ong, Chee and Sudesh, 2017). On the other hand, PLLA degrades into lactic acid (Leenslag *et al.*, 1987).

In conclusion, in comparison to PLLA (FDA approved polymer for Tissue Engineering), P(3HB) was found to have similar properties while P(3HO-co-3HD) exhibited mechanical properties similar to soft tissue. In terms of islet viability, cells seeded on P(3HO-co-3HD) scaffolds had the highest viabilities. The mechanical properties of P(3HO-co-3HD) were finetuned to be more similar to those of the pancreas through the integration of pores. The question of optimum pore size and porosity for porous structures in Tissue Engineering has been researched for decades. It is widely accepted that it depends on the cell type and its particular needs. In this work, it was confirmed that the optimum pore size for pancreatic islets is 100µm. Water contact angle, protein adsorption and cell adhesion were shown to be dependent on the porosity of the materials. It was also observed that scaffolds that had NaCl as the porogen exhibited better cell viability results for BRIN BD11 cells. In light of all the findings, scaffolds A&B were selected as the best options for scaffolds.

CHAPTER FIVE: P(3HB) & P(3HO-co-3HD) 2D/3D STRUCTURES

5. P(3HB) & P(3HO-co-3HD) 2D/3D STRUCTURES

5.1. INTRODUCTION

In the early stages of Tissue Engineering, the scaffolds used were 2D constructs used mainly as support for cells. As understanding has matured, the need for these structures to be improved to have appropriate mechanical, physical and biological properties to mimic the *in vivo* environment of the cells *in vitro* became apparent (Santos *et al.*, 2012). This has shifted research to 3D structures to better understand the interactions between cells, scaffolds, molecules and component of the extracellular matrix (Coronel and Stabler, 2013). In islet transplantation, especially, these interactions are important for islet cell growth, proliferation and function (Goh *et al.*, 2013). There are a wide range of methods to create 3D scaffolds for Tissue Engineering. They range from the classic porogen leaching, gas foaming, phase separation to the newer techniques like fibre making and 3D printing (Chen, Ushida and Tateishi, 2002).

In islet transplantation, 3D structures have been widely investigated. Ethisorb (a scaffold made of a composite of polygalactin, poly-p-dioxanone) has been used to transplant islets in large animal models. One of the dogs that received the scaffold containing the highest number of islets achieved normoglycaemia up to 5 months post-transplantation. Those dogs that received an average number of islets, maintained normoglycaemia up to 2 months post-transplantation (Kin *et al.*, 2008). Ethisorb has also been

used for islet transplantation in monkeys, with similar results (Berman *et al.*, 2009).

When PLGA-collagen hybrid meshes were used to culture rat RIN-5F insulin producing cells, the results were positive. The meshes promoted insulin production while also supporting adhesion, proliferation and differentiation of RIN-5F cells (Kawazoe *et al.*, 2009). Different PLGA 3D structures have been used in islet transplantation. Islets transplanted in this structure survived longer while also maintaining their native shape and function in comparison to the control group. PLGA discs were also used to transplant islets into BALB/C mice. Mice that received these seeded discs took 45% less time to attain normoglycaemia than the control group (Dufour *et al.*, 2005).

Islets encapsulated in silk 3D hydrogels remained viable and retained their insulin secretion up to 7 days post-transplantation. In combination with mesenchymal stem cells and ECM proteins, by day 7 the insulin release has increased 3.2 fold than the control group (Davis *et al.*, 2012). Islets cultured in agarose cryogels exhibited 15 fold higher insulin release at 3mM glucose than the control (Bloch *et al.*, 2005).

In 3D printing, a 3D printing device controlled by a computer deposits cells, molecules, and biomaterials into exact structures that mimic native tissue structures. 3D printing biological scaffolds can create replacements for damaged tissues and organs and can also create small models for research purposes quickly and reproducibly (Skardal and Atala, 2015). The major challenge of 3D printing is finding the balance between maintaining the

architecture of the scaffold and the functionality of the scaffolds. The biomaterials for 3D printing can be used in two ways: as curable inks either by melting or solvent dissolution with the cells seeded after formation of the scaffold or as cell supporting hydrogels with the cells printed within the hydrogels (Skardal and Atala, 2015).

Two predominant techniques in 3D printing exist. Inkjet printing involves the use of a cartridge filled with biomaterial ink that is dropped into XYZ plotting devices. The cells and biomaterials can be loaded into multi cartridges and printed at the same or at different times. This technique requires 'bioink' that is quick to polymerise, so each drop stabilises before the next drop. A modification of this technique called thermojet printing can also be used for biomaterials that require melting (Murphy and Atala, 2014; Skardal and Atala, 2015).

In extrusion printing, pneumatic pressure is used to drive an extrudable material out of a syringe in a fixed manner. Materials to be printed using this technique must exhibit fluid-like properties and must hold their shape post-extrusion. Viscosity and pressure are really important factors in this method and can be altered to determine the structure(s) printed (Griffith and Naughton, 2002; Ventola, 2014; Skardal and Atala, 2015).

Since the Edmonton protocol, the field of Islet Transplantation has researched ways to provide the minimum number of islets necessary in a manner that requires the least immunosuppression. This has led to the development of the bioartificial pancreas.

"*A bioartificial pancreas is a 3D biomimetic device that substitutes for the endocrine portion of the pancreas while also avoiding the need for immunosuppression*." - (Kizilel, Garfinkel and Opara, 2005)

The bioartificial pancreas contains cells or cell clusters in a membrane separating foreign tissues from the immune system (Silva *et al.*, 2006). Valdes-Gonzalez and his colleagues designed a bioartificial pancreas containing surgical grade stainless steel and polytetrafluoroethylene (PTFE) rods. This device was transplanted into 12 humans and in half of the group, there was a significant reduction in the exogenous insulin required (Valdés-González *et al.*, 2005). Maki and his colleagues made a device containing islets in a semi-permeable tube-like membrane connected to the vascular system. Of the 13 dogs that received this device, 8 dogs required a reduced amount of insulin supplementation and 4 dogs required no supplementation up to 3 weeks post-transplantation (Maki *et al.*, 1991; Monaco *et al.*, 1991). Ludwig and her colleagues at Beta-O2 designed a device containing a PTFE membrane with alginate encapsulated islets. The device normalised blood glucose levels in diabetic rodents up to 3 months post-transplantation. It also reduced the number of islets required for transplantation and no delay in insulin response to glucose stimulus was observed (Ludwig *et al.*, 2012).

5.2.RESULTS

5.2.1. PHA blend based 2D & 3D Scaffolds

2D and 3D scaffolds were fabricated using P(3HB) and P(3HO-co-3HD) to determine the effect of surface area, geometry, porosity and surface roughness on viability of murine BRIN DB11 cells seeded on them.

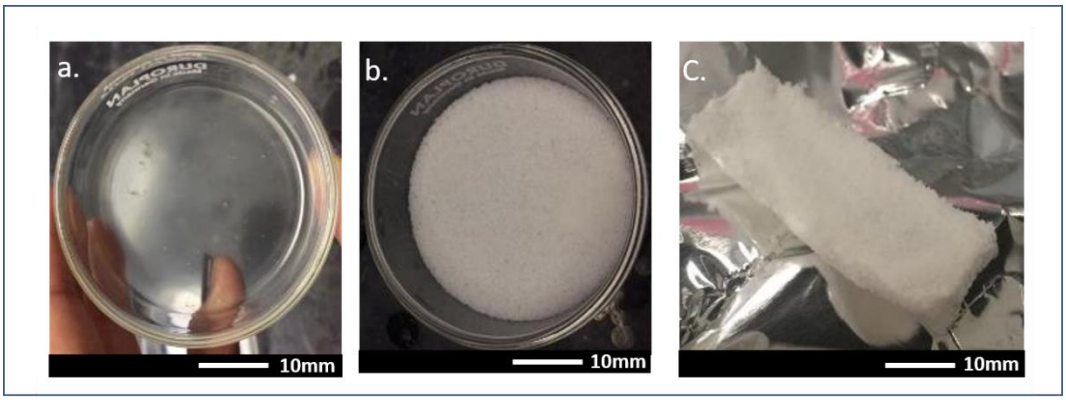

Figure 5.1: P(3HO-co-3HD) fabricated structures. (a.) 2D- Non-Porous Film (b.) 2D-Porous Film (c.) 3D Structure, bars: 10mm.

Figure 5.1 shows the three different P(3HO-co-3HD) structures that were made. 5.1a is a solvent cast P(3HO-co-3HD) film. The film appears transparent and elastomeric fitting with the structural characteristics of mcl-PHAs. 5.1b is a P(3HO-co-3HD) porous film that was solvent cast using NaCl as porogen. The film appears flat, with macroscopic pores. Both neat and porous films have diameters of about 35-45mm. 5.1c is a P(3HO-co-3HD) 3D porous structure made by solvent casting technique with NaCl as a porogen. The 3D structures were cast in Teflon moulds. The final 3D structure created had dimensions of 35 x 10 x 0.5mm.

5.2.2. Mechanical Properties of 2D & 3D Structures

As shown in Table 5.1, for P(3HB) 2D and 3D scaffolds, the 3D scaffold has a higher ($p \leq 0.0001$) Young's Modulus value of 850.24±45.19MPa than 747.59±58.08MPa for the P(3HB) 2D structure. This is an indication that the P(3HB) 3D structure is stiffer than the P(3HB) 2D structure. Tensile Strength for the P(3HB) 3D structure was 37.5±2.28MPa as compared to that of the P(3HB) 2D structure (23.6±0.28MPa). On the other hand, the elongation at break of the P(3HB) 2D structure was measured to be 7.94±0.21% while that of the 3D structure was 6.8±0.79%. No significant difference ($p > 0.05$) was observed between the Tensile Strength, Young's Modulus and elongation at break of both the P(3HB) 2D and 3D structures.

Table 5.1: Summary of mechanical properties of P(3HB) and P(3HO-co-3HD) 3D and 2D structures. Values are expressed as ± SEM for groups of 6.

Structures	Young Modulus (MPa)	Tensile Strength (MPa)	Elongation break (%)
P(3HB)-2D	747.59±58.08	23.6±0.28	7.94±0.21
P(3HB)-3D	850.24±45.19	37.5±2.28	6.8±0.79
P(3HO-co-3HD)-2D	1.37±0.054	1.19±0.06	1415±19.16
P(3HO-co-3HD)-3D	2.20±0.75	2.15±0.93	946.59±30.547
P(3HO-co-3HD)-2D Porous	1.05±0.032	1.08±0.08	192.2±27.77

P(3HO-co-3HD)-3D Porous	1.17±0.37	1.17±0.03	236.23±22.47

Between the P(3HO-co-3HD) 2D and 3D structures, no significant difference ($p > 0.05$) was observed between the two structures for both Tensile Strength and Young's Modulus. For the elongation at break, there was a significant ($p \leq 0.05$) difference between both structures; elongation at break of the P(3HO-co-3HD) 2D structure 1415±19.16% for the 2D and 946.59±30.547% for the 3D structure. This is an indication that the P(3HO-co-3HD) 2D structure is more elastic than the P(3HO-co-3HD) 3D structure.

Comparing both P(3HO-co-3HD) porous 2D and 3D structures, no significant difference ($p > 0.05$) was observed between the Tensile Strength for the P(3HO-co-3HD) porous 2D (1.08±0.08 MPa) and P(3HO-co-3HD) porous 3D (1.17±0.03 MPa) structure. The same trend was observed for the Young's Modulus values of the P(3HO-co-3HD) porous 2D and P(3HO-co-3HD) porous 3D of 1.05±0.032MPa and 1.17±0.37MPa respectively. Similarly, no significant difference was observed between the elongation at break of 192.20±27.77% and 236.23±22.47% for the P(3HO-co-3HD) porous 2D and P(3HO-co-3HD) porous 3D structures.

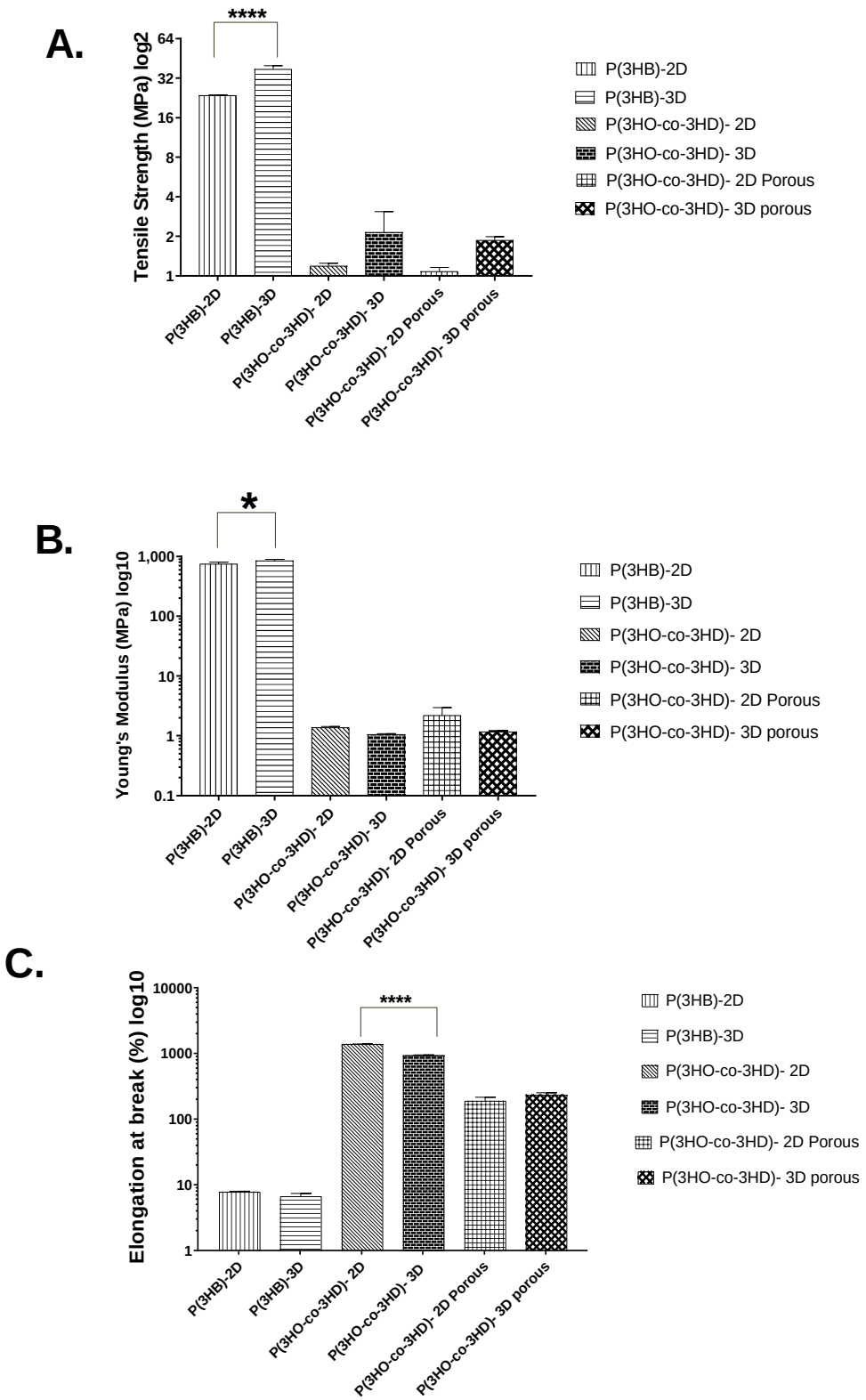

Figure 5.2: Mechanical properties of P(3HB) and P(3HO-co-3HD) 2D and 3D structures a) Tensile Strength (MPa) b) Young's Modulus (MPa) c) Elongation at break (%). Values are expressed as mean ± SEM for

*groups of 6. *p ≤ 0.05, ****p ≤ 0.0001 when 2D and 3D structures were compared.*

5.2.3. Water Contact Angles of 2D & 3D Structures

The water contact angles for all the structures made are shown in Figure 5.3. The water contact angles for the P(3HB) 2D and 3D structures were 72.12°±8.67 and 74.37°±5.92. No significant difference ($p > 0.05$) was observed between both values.

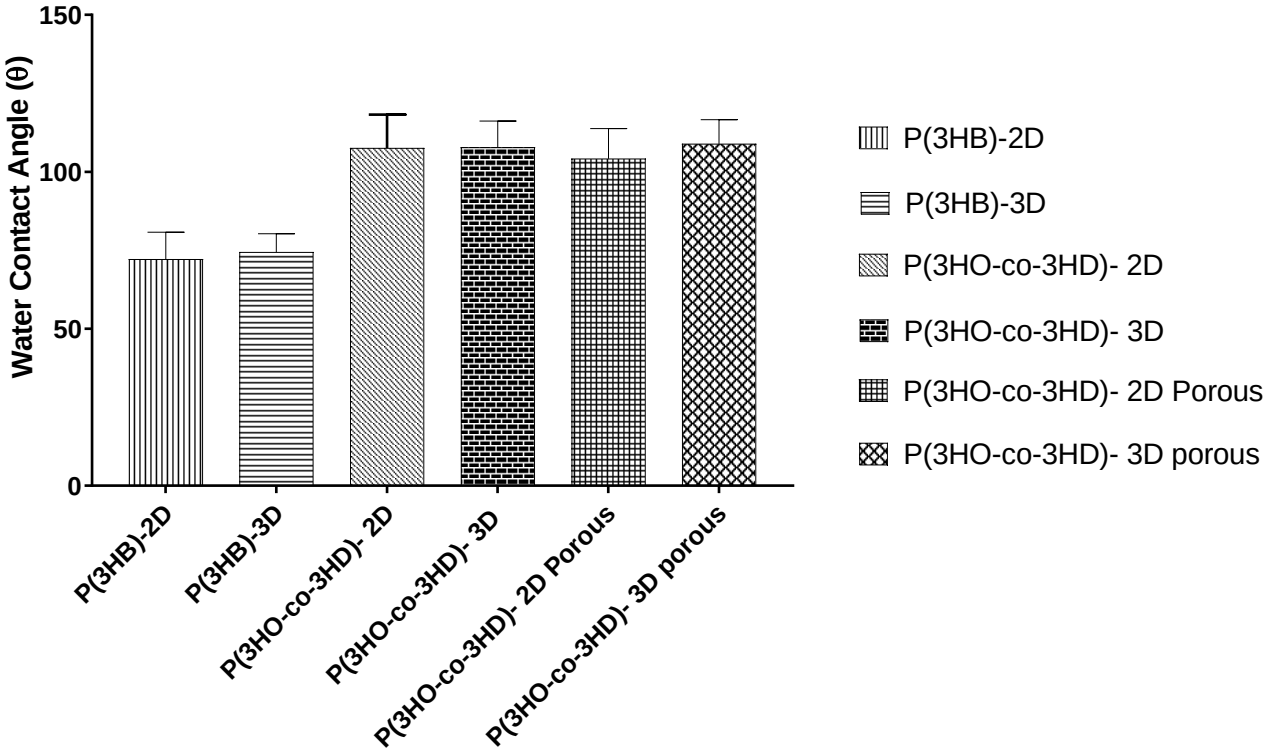

Figure 5.3: Static water contact angle (ɵ) of P(3HB) and P(3HO-co-3HD) 2D and 3D structures. Values are expressed as mean ± SEM for groups of 6. No significant difference ($p > 0.05$) was observed when 2D structures were compared with 3D structures.

For the P(3HO-co-3HD) 2D and 3D structures, the water contact angles were 107.580^{o}±10.63 and 107.78^{o}±8.39 respectively with no significant difference ($p > 0.05$).

For both P(3HO-co-3HD) 2D and 3D porous structures, the water contact angles were 104.13^{o}±9.65 and 108.92^{o}±7.67. Similarly, no significant difference ($p > 0.05$) was observed between the two types of structures.

5.2.4. Protein Adsorption of 2D & 3D Structures

The protein adsorption for the P(3HB) and P(3HO-co-3HD) 2D and 3D structures are shown in both Figure 5.4. For the 2D and 3D P(3HB) scaffolds, the protein adsorption values were 204.19±11.91μg/cm^2 and 247.68±14.76μg/cm^2 respectively. The protein adsorption value for the P(3HB) 3D structure was significantly higher ($p \leq 0.001$) than that of the P(3HB) 2D scaffold.

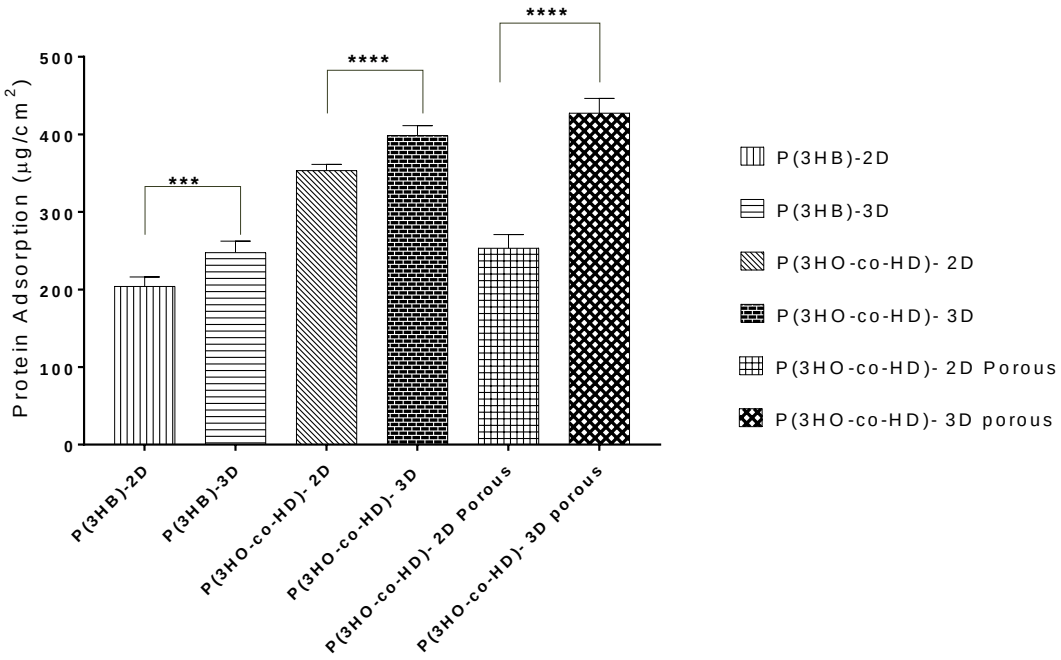

*Figure 5.4: Protein adsorption of P(3HB) and P(3HO-co-3HD) 2D and 3D structures. Values are expressed as mean ± SEM for groups of 6. ***p ≤ 0.001, ****p ≤ 0.0001 when 2D structures were compared with 3D structures.*

For the P(3HO-co-3HD) 2D and 3D structures, the protein adsorption values were 353.65±7.61µg/cm^2 and 398.72±12.55µg/cm^2 respectively. The value observed for the P(3HO-co-3HD) 3D structure was higher ($p \leq 0.0001$) than that of the P(3HO-co-3HD) 2D structure. Finally, the protein adsorption values of both P(3HO-co-3HD) 2D and 3D porous structures were 253.45±17.3861µg/cm^2 and 427.50±18.79µg/cm^2 respectively. The values for the P(3HO-co-3HD) porous 3D structure was higher ($p \leq 0.0001$) than the P(3HO-co-3HD) porous 2D structure.

5.2.5. Cell Viability Tests on BRIN BD11 Cells in 2D & 3D Structures

Figure 5.5 shows the cell viability tests carried out to evaluate the effects of the scaffolds on BRIN BD11. For BRIN BD11 cells seeded in P(3HB) 2D and 3D structures, the indirect cell viabilities were 94.59±5.52% and 95.61±6.57% respectively. No significant difference ($p>0.05$) was observed between the cell viability of the two types of structures.

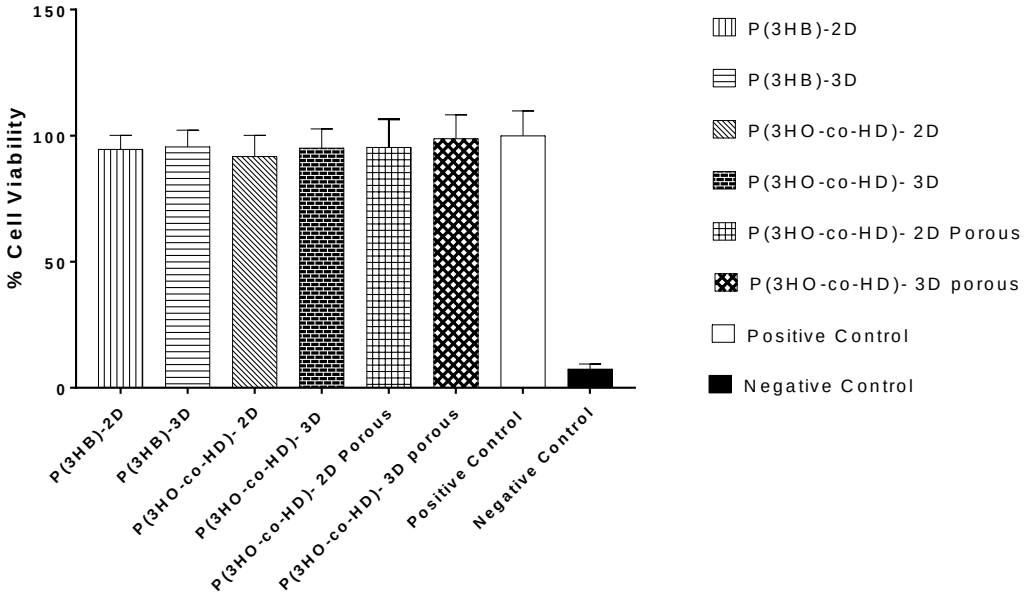

Figure 5.5: Cell viability of BRIN BD11 cells seeded in P(3HB) and P(3HO-co-3HD) 2D and 3D structures. Values are expressed as % of positive control (tissue culture plastic) ± SEM for groups of 6. P > 0.05 when 2D structures were compared with corresponding 3D structures.

Comparing the P(3HO-co-3HD) 2D and 3D structures, the viabilities of the cells seeded in them were 91.78±8.33 and 95.13±7.51 respectively. There was no significant difference ($p>0.05$) observed between both structures. No significant difference ($p>0.05$) was observed between the 2D (95.39±11.19) and 3D (98.55±9.38) porous P(3HO-co-3HD) structures.

5.2.6. Static Insulin Secretion from BRIN BD11 Cells in 2D & 3D Structures

Insulin release tests were carried out in BRIN BD11 cells seeded in media incubated with the P(3HB) and P(3HO-co-3HD) 2D and 3D structures. The results are shown in Figure 5.6. The tests were carried out at two different concentrations of glucose.

At 5.6mM (normoglycaemia), the insulin release values for P(3HB) 2D and 3D structures were 2.978±0.093ng/10^6cells/20 minutes and 3.026±0.159 ng/10^6cells/20 minutes respectively. No significant difference ($p > 0.05$) was observed between the two structures. For the P(3HO-co-3HD) 2D and 3D structures, the insulin release values were 3.373±0.155ng/10^6cells/20 minutes and 3.565±0.079ng/10^6cells/20 minutes. Again, no significant difference ($p > 0.05$) was observed. Finally, comparing the porous P(3HO-co-3HD) porous 2D and 3D structures, the insulin release was 3.923±0.064 ng/10^6cells/20 minutes and 4.278±0.358 ng/10^6cells/20 minutes respectively. In this case, no significant difference ($p > 0.05$) was also observed.

At 16.7mM glucose (hyperglycaemia), the insulin release values for P(3HB) 2D and 3D structures were 3.279±0.095ng/10^6cells/20 minutes and 3.682±0.078 ng/10^6cells/20 minutes respectively. No significant difference ($p > 0.05$) was observed between both. For the P(3HO-co-3HD) 2D and 3D structures, the insulin release values were 4.292±0.106ng/10^6cells/20 minutes and 4.340±0.254ng/10^6cells/20 minutes. Again, no significant difference ($p > 0.05$) was observed between the 2D and 3D structures. Finally, comparing the porous P(3HO-co-3HD) 2D and 3D structures, the

insulin release was 4.995±0.23ng/10^6cells/20 minutes and 5.106±0.32ng/10^6cells/20 minutes respectively. In this case too, no significant difference ($p > 0.05$) was also observed.

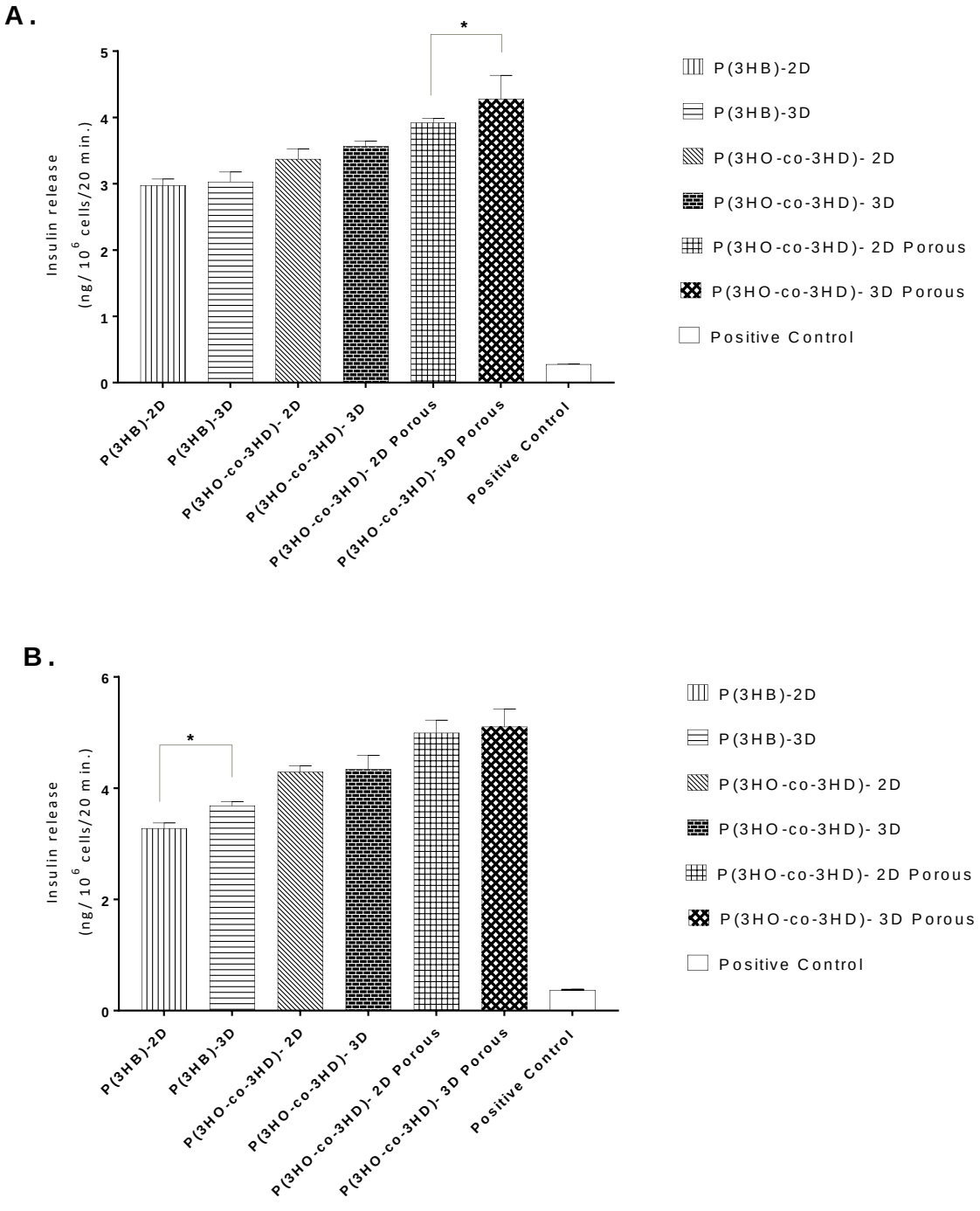

*Figure 5.6: Insulin secretion from BRIN BD11 cells seeded in media from P(3HB) and P(3HO-co-3HD) 2D and 3D structures at a.) normoglycaemia (5.6mM glucose) and b.) hyperglycaemia (16.7mM glucose) in ng/10^6cells/20 minutes. Samples are expressed as % of positive control (tissue culture plastic) ± SEM for groups of 6. *$p \leq 0.05$, $p > 0.05$ when 2D structures were compared with 3D structures.*

5.3.DISCUSSION

In this chapter, P(3HB) and P(3HO-co-3HD) 2D and 3D structures were made and characterised with respect to mechanical properties, water contact angle and protein adsorption. Indirect cell viability and insulin release tests were also carried out on BRIN BD11 cells seeded on them. The same processes were applied to the porous P(3HO-co-3HD) porous 2D and 3D structures. These properties were then compared to evaluate the differences between 2D and 3D structures.

Measuring mechanical properties showed no significant difference between the 2D and 3D structures. This could be attributed to the fact that mechanical properties of 2D and 3D structures are not exactly comparable. 3D structures may not lend themselves to direct comparison with those of 2D structures. In addition, the mechanical properties were all measured in dry conditions so a whole picture could not be drawn (Huang *et al.*, 2005; Hess *et al.*, 2017).

For the water contact angle measurement, no significant difference was observed when the P(3HB) and P(3HO-co-3HD) 2D and 3D porous and non-porous structures were compared. This is because static water contact angle is a surface measurement and will only be affected by surface roughness, not surface area (Cassie and Baxter, 1944).

For protein adsorption, in every 2D/3D pairing, there were significant differences in protein adsorption observed. Increases between 1.2-1.8-fold were observed on the 3D structure as compared to the 2D structure. Protein adsorption is dependent on surface area and the increased surface area in 3D structures provides more room for the protein to be adsorbed (Du, Chandaroy and Hui, 1997; Roach, Farrar and Perry, 2006; Wei and Ma, 2009).

Native β-cells exist in aggregates with α, δ and Pancreatic Polypeptide producing (PP) cells in clusters called islets of Langerhans (Wills, Thomas and Gillham, 2006). These islets contain multiple cells and have an average size of 100μm. When these cells are grown on porous surfaces, the pores must be big enough that multiple aggregates could fit through them.

In this work, murine BRIN BD11 cells were selected. BRIN BD11 cells are created from electrofusion of RINm5f cells with rat pancreatic islets hence they combine the insulin release function of their parent cells with immortality (McClenaghan, Barnett, Ah-Sing, *et al.*, 1996). In comparison with other existing pancreatic cell lines like INS-1, MIN6 and NIT-1, BRIN BD11 cells are relatively more responsive to increasing glucose concentrations (Skelin, Rupnik and Cencič, 2010). BRIN BD11 cells also exhibited pronounced responses to a range of amino acids including leucine, arginine and alanine (McClenaghan, Barnett, O'Harte, *et al.*, 1996; Skelin, Rupnik and Cencič, 2010). BRIN BD11 cells also show a pattern comparable to rat islets when secretory responses were measured (Hamid *et al.*, 2002). BRIN BD11 cells have been studied extensively in terms of

insulin inhibition, amino acid consumption and gene expression (McClenaghan and Flatt, 1999; Ahmad *et al.*, 2000; Dixon *et al.*, 2003).

No significant differences were observed between cell viabilities of the 2D and 3D P(3HB) and P(3HO-co-3HD) structures. On the other hand, there was also no significant difference observed between the cell viabilities of BRIN BD11 cells in 2D and 3D porous P(3HO-co-3HD) structures. Islets have a higher tendency to cluster, rather than migrate (Aloysious and Nair, 2014). This could be because the pores in the 3D scaffold may have already been occupied by these clusters. It is also possible that the cells perceive the 3D structure as a 2D surface with ridges (Biomater *et al.*, 2009). Insulin release is a direct consequence of cell viability, so no significant difference was also observed in that case.

Another factor that could have led to this is the number of cells seeded on the surface. Islet density has been shown to have a direct effect on the viability and survival of islets post-transplant (McCall and Shapiro, 2012). Porous structures and 3D structures have an increased surface area so using the same number of cells for both structures would not give an accurate comparison.

Incidentally, it was also discovered in this study that upon stimulation at both normoglycaemia and hyperglycaemia glucose, cells seeded in both PHA structures release up to 10-fold more insulin than cells seeded in the positive control (tissue culture plastic). This confirms work from Chapter 4 and can be explained by the aggregation that the PHA surfaces and porosity provide.

In conclusion, comparison of the mechanical properties of 2D and 3D porous/non-porous structures revealed no significant difference. The water contact angle measured also showed no significant difference between the 2D and 3D structures. Protein adsorption measurements on the other hand, demonstrated significant differences between 2D and 3D structures owing to the differences in available surface area. Even though differences were observed in protein adsorption, no significant differences were observed in cell viability and insulin release values. Further investigation is needed in order to evaluate the correlation between the surface area and cell density in both 2D and 3D scaffolds.

CHAPTER SIX: P(3HO-co-3HD)/P(3HB) BLENDS

6. P(3HO-co-3HD)/P(3HB) BLEND SCAFFOLDS

6.1. INTRODUCTION

One of the most important factors in scaffold design is the choice of scaffold materials. The Scaffold material should ideally have similar mechanical and thermal properties as the targeted tissue.

Having shown PHAs to be excellent materials for use in islet transplantation, it is important to select the specific PHA fit for this role. Two classes of PHAs have been discussed in Chapters 3 and 4. Even though P(3HB) is the stronger of both PHAs, it is very brittle and lacks the flexibility required from materials for soft tissue engineering. Mcl-PHAs, on the other hand, are more suited to soft tissue engineering due to their flexibility but lack strength and hence are difficult to handle.

Blending of both classes of PHAs is a process of that can lead to the production of new polymers with properties different to their parent polymers. In blending, one has the capability of tuning the physical and mechanical properties of the final polymer by adjusting the amounts of each polymer type present. Blending P(3HB) with mcl-PHAs have been shown to reduce its brittleness and increase its biocompatibility (Li, Yang and Loh, 2016).

When chondrocytes were grown on two different PHA scaffolds: P(3HB), P(3HB)/P(3HHx), almost two-fold cell proliferation was observed on the P(3HB)/P(3HHx) blend scaffold in comparison with the neat P(3HB) scaffold (Deng *et al.*, 2002). Neuronal cells cultured on (P3HO), P(3HB)

and P(3HO)/P(3HB) blend films showed increased viabilities on the blends in comparison to the neat (P3HO) and P(3HB) films (Lizarraga-Valderrama *et al.*, 2015). HMEC-1 cells seeded in P(3HO)/P(3HB) blend films had better viabilities than those of (P3HO) and P(3HB) films (Basnett *et al.*, 2013).

In this chapter, P(3HO-co-HD) dominated P(3HO-co-HD)/ P(3HB) blend scaffolds were made in three different concentrations: 95:5, 90:10 and 80:20. These different scaffolds were then characterised and evaluated for cell viability and insulin release. After this evaluation, the most promising blend concentration was then fabricated into three different structures: non-porous 2D, porous 2D and porous 3D scaffolds. These structures were also characterised and evaluated for cell viability and influence on insulin release of the insulin producing BRIN BD11 cell line.

6.2.RESULTS

6.2.1. DSC Analysis of P(3HO-co-3HD)/P(3HB) Blends

DSC analysis was carried out on the P(3HB), P(3HO-co-HD) and P(3HO-co-3HD)/P(3HB) blends to determine the effects of blending on their thermal behaviour. The results observed are recorded in table 6.1.

During the 1st DSC cycle, the initial peak indicated the melting temperature of the P(3HO-co-HD) in the blend. The second peak corresponded to the melting temperature of the P(3HB) present. After the second heating cycle in the DSC run, only a peak for P(3HB) could be observed. For each blend,

two melting temperatures were recorded. An initial, lower one belonging to the P(3HO-co-HD) component and the second higher one to P(3HB) component.

For the lower melting temperatures observed, as the concentration of P(3HO-co-HD) in the blends decreased, the melting temperature decreased from about 54.7^{o}C for pure P(3HO-co-HD) to 51.2^{o}C for the 80:20 P(3HO-co-3HD)/P(3HB) blend. For the higher melting temperatures, as the P(3HB) concentration increased, the melting temperature increased from 164.5^{o}C for the 95:5 P(3HO-co-3HD)/P(3HB) blend to 172.8^{o}C for P(3HB).

Considering glass transition temperatures observed, there was a marked difference observed in the glass transition temperatures of the 90:10 and 80:20 P(3HO-co-3HD)/P(3HB) blends. T_g of -48.05^{o}C and -44^{o}C were observed in comparison to the -65 to -67^{o}C observed for all the other polymers and blends.

Table 6.1: Thermal properties of P(3HB), P(3HO-co-HD) and P(3HO-co-3HD)/P(3HB) blends.

Polymer	**Melting Point, T_m (°C)**	**Glass transition, T_g (°C)**
P(3HB)	172.8 ± 1.83	-67.15 ± 0.35
80:20	a. 51.2 ± 0.07 b. 170.4 ± 0.78	-44.0 ± 0.64
90:10	a. 51.7 ± 0.71 b. 170.15 ± 1.77	-48.05 ± 1.20

95:5	a. 54.55 ± 2.33 b. 164.5	-65.9 ± 0.85
P(3HO-co-HD)	54.7 ± 3.25	-66.95 ± 0.92

6.2.2. Mechanical Analysis of P(3HO-co-3HD)/P(3HB) Blends

Mechanical analysis was carried out on the P(3HB), P(3HO-co-HD) and P(3HO-co-3HD)/P(3HB) blends to evaluate the effect of blending on their strength, stiffness and flexibility. The results observed are recorded in table 6.2.

For elongation at break, it was observed that as the P(3HB) component was increased in the P(3HO-co-3HD)/P(3HB) blends, the elongation at break decreased, indicating a decrease in flexibility. Tensile strength, on the other hand, increased as the P(3HB) component was increased in the P(3HO-co-3HD)/P(3HB) blend. A similar pattern was observed with the Young's Modulus which also increased as the P(3HB) component was increased in the P(3HO-co-3HD)/P(3HB) blend.

So as the P(3HB) component was increased in the P(3HO-co-3HD)/P(3HB) blends, the strength and stiffness increased while the flexibility redces.

Table 6.2: Mechanical properties of P(3HB), P(3HO-co-HD) and P(3HO-co-3HD)/P(3HB) blends.

Polymer	Elongation at break (%)	Tensile strength (MPa)	Young's Modulus, E (MPa)
P(3HB)	7.94 ± 0.02	23.6± 0.28	747.22 ± 1.08
80:20	621.7 ± 0.54	6.81 ± 0.98	1.77 ± 0.04
90:10	818.8 ± 0.14	5.57 ± 2.67	1.66 ± 0.39
95:5	1318.7 ± 0.02	2.11 ± 0.06	1.64 ± 0.37
P(3HO-co-HD)	1415.1± 0.02	1.08 ± 0.06	1.39 ± 0.05

6.2.3. Cell Viability Studies on P(3HO-co-3HD)/P(3HB) Blends

Cell viability studies were carried out on the P(3HB), P(3HO-co-HD) and P(3HO-co-3HD)/P(3HB) blends to determine their suitability as scaffolds for bioartificial pancreas. These studies were carried out using the murine BRIN BD11 islet cell line. The cell viabilities observed were expressed as % of the positive control (tissue culture plastic) as shown in Figure 5-3.

In all the polymers and blends, the viabilities of BRIN BD11 cells seeded in them increased from day 1 to day 7. In comparison to the P(3HO-co-HD) polymer, on all days both the 95:5 and 90:10 P(3HO-co-3HD)/P(3HB)

blends showed no significant difference in viabilities. By day 7, cells seeded on both blends and P(3HO-co-HD) showed no significant difference when compared to the positive control.

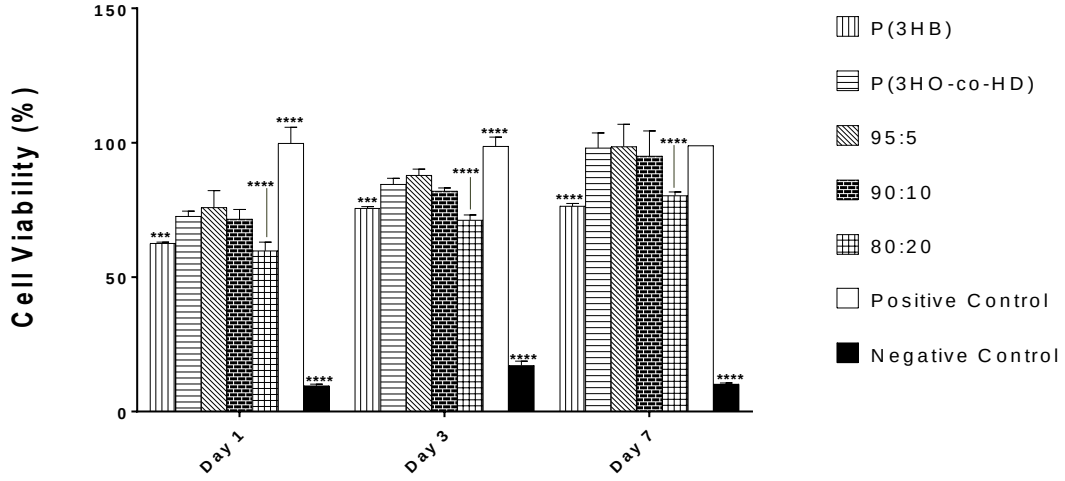

*Figure 6.1: Cell viability of BRIN BD11 cells seeded on P(3HB), P(3HO-co-HD) and P(3HO-co-3HD)/P(3HB) blends. Values are represented as %positive control (tissue culture plastic) mean ± SEM for groups of 6. ***p ≤ 0.001, ****p ≤ 0.0001 when compared with P(3HO-co-HD).*

6.2.4. Static Insulin Secretion on P(3HO-co-3HD)/P(3HB) Blends

Insulin release studies were carried out to evaluate the functionality of the BRIN BD11 cell line seeded on the P(3HB), P(3HO-co-HD) and P(3HO-co-3HD)/P(3HB) blends. The analyses were run at normoglycaemia (5.6mM glucose) and hyperglycaemia (16.7mM glucose).

At normoglycaemia (5.6mM glucose), all cells seeded in all the PHA samples exhibited insulin release. From day 1, cells on all scaffolds responded to the glucose stimulus but as the number of days of incubation increased, the insulin release was stronger as shown in Figure 6.4. in

comparison with the insulin released from cells seeded in the P(3HO-co-HD), insulin released from 95:5 P(3HO-co-3HD)/P(3HB) blend showed no significant difference on all days. By days 3&7, cells seeded on the 90:10 P(3HO-co-3HD)/P(3HB) blend also showed no significant difference in insulin release. Insulin released from cells seeded in the 80:20 blend was significantly lower than the P(3HO-co-HD).

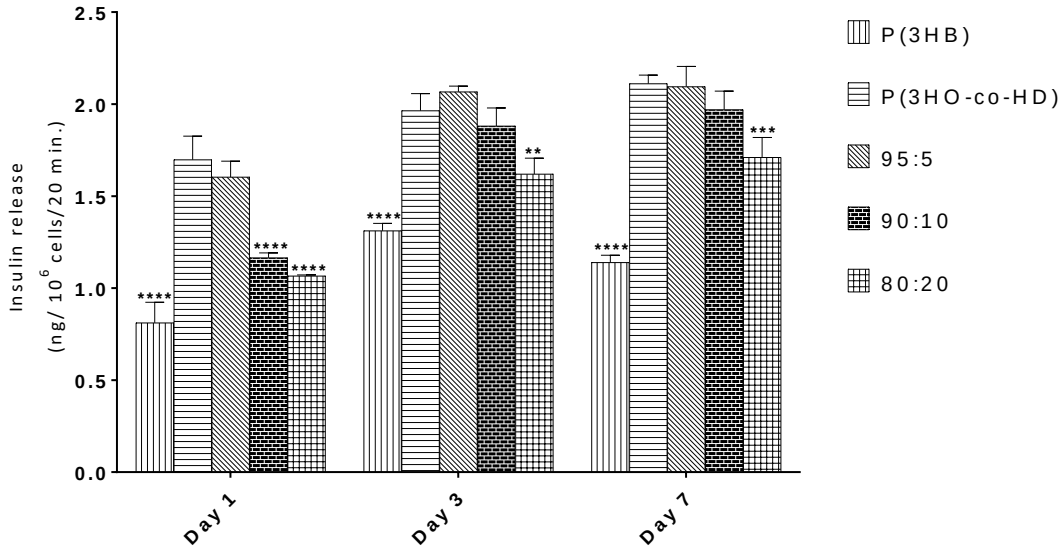

*Figure 6.2: Insulin secretion at normoglycaemia (5.6mM glucose) from BRIN BD11 cells seeded P(3HB), P(3HO-co-HD) and P(3HO-co-3HD)/P(3HB) blends in ng of insulin/10^6 cells/20 minutes. Values are expressed as mean ± SEM for groups of 6. **p ≤ 0.01, ***p ≤ 0.001, ****p ≤ 0.0001 when compared with insulin release from cells seeded in P(3HO-co-HD).*

At hyperglycaemia (16.7mM), a similar pattern was observed where in comparison to the cells seeded in the P(3HO-co-HD), the insulin released from 95:5 P(3HO-co-3HD)/P(3HB) blend showed no significant difference on all days. On the other hand, by day 7, insulin released from cells seeded

in both 90:10 and 80:20 P(3HO-co-3HD)/P(3HB) blends were significantly lower.

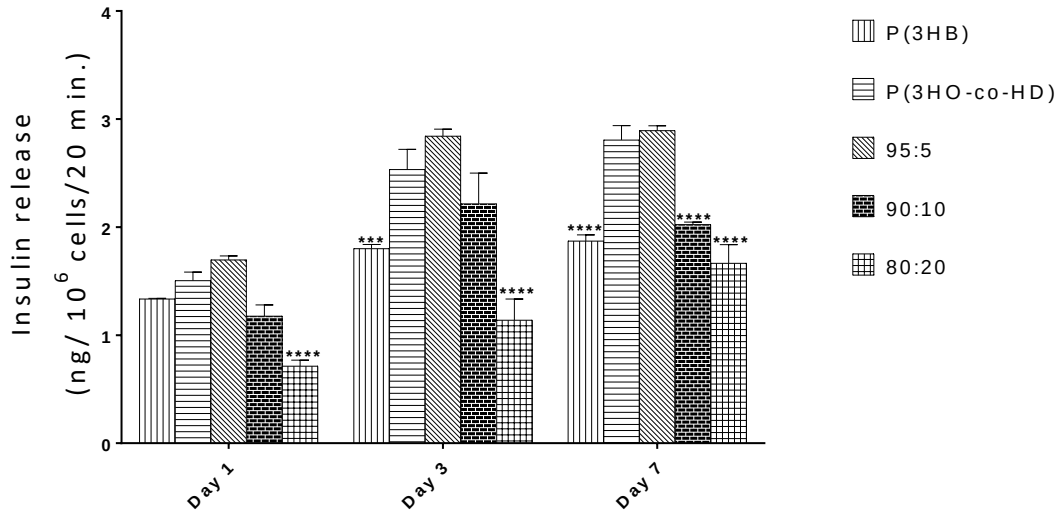

*Figure 6.3: Insulin secretion at hyperglycaemia (16.7mM glucose) from BRIN BD11 cells seeded P(3HB), P(3HO-co-HD) and P(3HO-co-3HD)/P(3HB) blends in ng of insulin/10^6 cells/20 minutes. Values are expressed as mean ± SEM for groups of 6. ***$p \leq 0.001$, ****$p \leq 0.0001$ when compared with insulin release from cells seeded in P(3HO-co-HD).*

6.2.5. Processing 95:5 P(3HO-co-3HD)/P(3HB) Blend into Scaffolds

Since the 95:5 blend showed the best cell viability and insulin release data, this blend was selected to be processed into porous 2D and 3D scaffolds.

6.2.6. Cell Viability Studies on Cells seeded in 95:5 P(3HO-co-3HD)/P(3HB) Blend Scaffolds

Direct cell viability studies were carried out on the P(3HO-co-HD) and 95:5 P(3HO-co-HD)/P(3HB) blend scaffolds to determine their suitability as scaffolds for bioartificial pancreas. These studies were carried out using the

murine BRIN BD11 islet cell lines. The cell viabilities observed were expressed as % positive control (tissue culture plastic) and shown in Figure 6.4. When all 95:5 P(3HO-co-3HD)/P(3HB) blend scaffolds were compared to their corresponding P(3HO-co-HD) scaffolds, no significant difference was observed except in the 3D structures on day 1. By day 7, when all structures were compared to both positive control and their corresponding P(3HO-co-HD) scaffolds, no significant difference was observed.

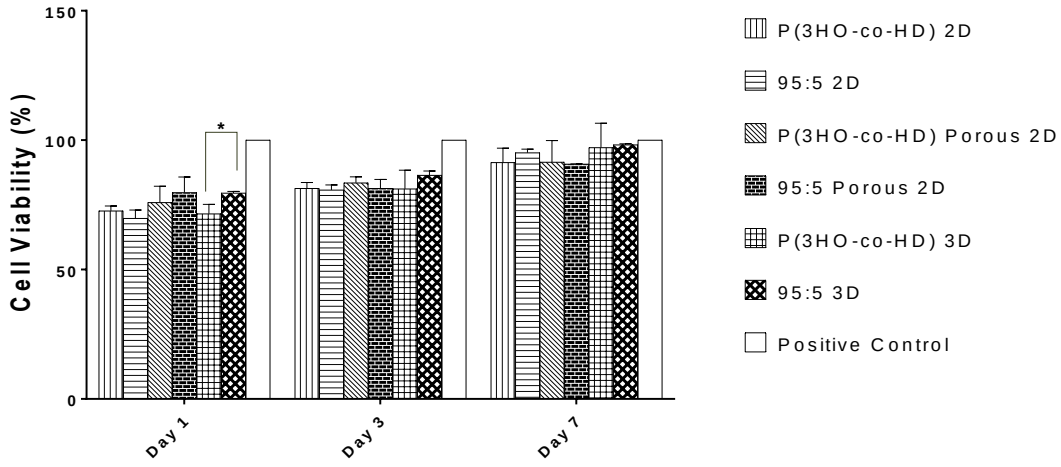

*Figure 6.4: Cell viability of BRIN BD11 cells seeded on 2D and 3D P(3HO-co-HD) and 95:5 P(3HO-co-3HD)/P(3HB) blend scaffolds. Values are represented as %positive control (tissue culture plastic) mean ± SEM for groups of 6. *$p \leq 0.05$, when 95:5 P(3HO-co-3HD)/P(3HB) 3D scaffold was compared with P(3HO-co-HD) 3D scaffold.*

6.2.7. Static Insulin Secretion from 95:5 P(3HO-co-3HD)/P(3HB) Blend Scaffolds

Insulin release studies were carried out to compare the functionality of the BRIN BD11 cell line seeded on the P(3HO-co-HD) and 95:5 P(3HO-co-HD)/P(3HB) blend scaffolds. Figure 6.5 shows insulin release from cells seeded in different P(3HO-co-HD) and 95:5 P(3HO-co-HD)/P(3HB) blend

scaffolds at hyperglycaemia (16.7mM glucose). In comparison with their corresponding P(3HO-co-HD) scaffolds, no significant difference was observed in the insulin release from cells seeded in 95:5 P(3HO-co-HD)/P(3HB) blend scaffolds. It was also observed that the insulin release from the cells seeded in 3D structures was highest.

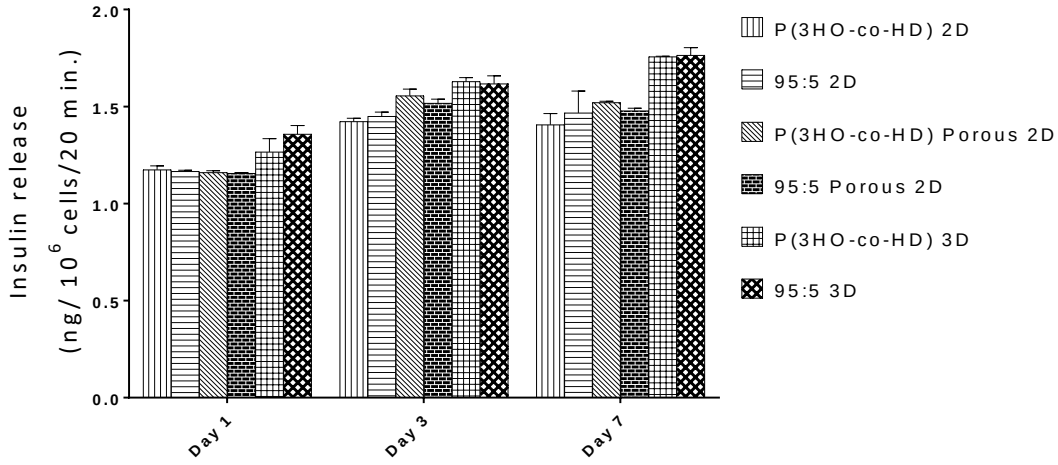

Figure 6.5: Insulin secretion at hyperglycaemia (16.7mM glucose) from BRIN BD11 cells seeded on 2D and 3D P(3HO-co-HD) and 95:5 P(3HO-co-3HD)/P(3HB) blend scaffolds in ng of insulin/10^6 cells/20 minutes. Values are expressed as mean ± SEM for groups of 6. P > 0.05 (not significant) when compared with corresponding with P(3HO-co-HD) scaffold.

6.2.8. Scanning Electron Microscopy of P(3HO-co-3HD) & 95:5 P(3HO-co-3HD)/P(3HB) Blend Scaffolds

Scanning electron microscopy was carried out on BRIN BD11 cells seeded on 2D P(3HO-co-3HD) & 95:5 P(3HO-co-3HD)/P(3HB) blend scaffolds to evaluate their surface topography and morphology of growth of the BRIN BD11 cells.

It was observed that the surfaces were entirely covered by the BRIN BD11 cells growing in clusters as expected for BRIN BD11 cells.

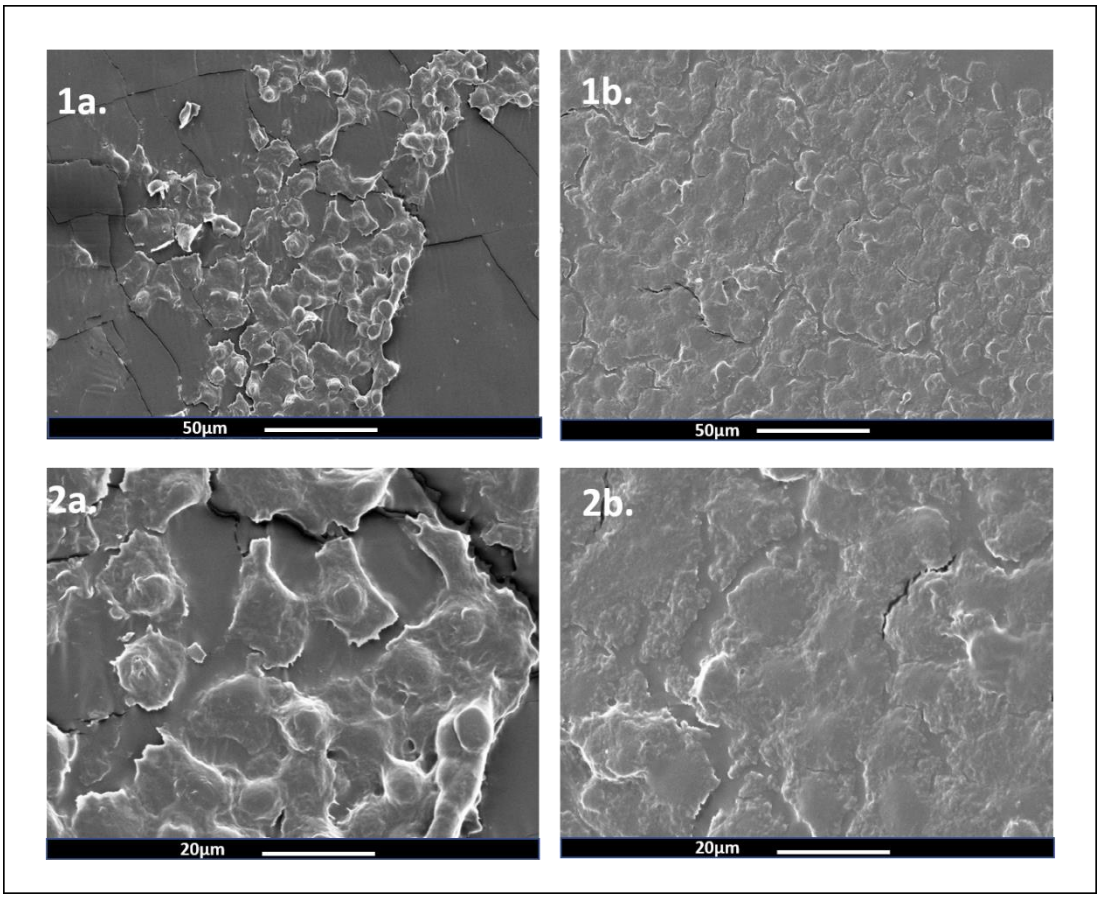

Figure 6.6: Scanning electron microscopy of 1a) P(3HO-co-HD) 2D scaffold (500X), 1b) 95:5 P(3HO-co-3HD)/P(3HB) blend 2D scaffolds (500X), 2a) P(3HO-co-HD) 2D scaffold (1500X) and 2b) 95:5 P(3HO-co-3HD)/P(3HB) blend 2D scaffolds (1500X).

6.3.DISCUSSION

In this chapter, three different P(3HO-co-HD) dominated P(3HO-co-3HD)/P(3HB) blends were made: 95:5, 90:10 and 80:20. These blends were then characterised mechanically and thermally to evaluate the miscibility of the P(3HO-co-3HD)/P(3HB) blends. They were also evaluated for the viability of BRIN BD11 cells seeded in them and for the insulin release upon

glucose stimulus from cells seeded in them. Finally, the most suitable blend was picked, fabricated into 2D & 3D scaffolds and compared to P(3HO-co-HD) based on the viability and insulin release of BRIN BD11 cells seeded in them.

In the thermal analysis of the polymers, the melting and glass transition temperatures observed in this study were within range of those observed in other studies of mcl-PHA/scl-PHA blends (Basnett *et al.*, 2013; Lizarraga-Valderrama *et al.*, 2015). The appearance of two melting events in each blend thermogram is an indication of the incompatibility and immiscibility of the blends; since each component is crystallising separately (Olabisi, 1981; Zhu *et al.*, 1999; Bhatia *et al.*, 2007). Addition of P(3HB) into the P(3HO-co-HD) introduces another independent melting event because the polymers are in different states (Bhatia *et al.,* 2007). Introduction of the crystalline P(3HB) into amorphous P(3HO-co-HD) reduces the mobility of the amorphous region (Basnett *et al.*, 2013).

At the same time, only one glass transition temperature was observed for each blend. This glass transition temperature increased as the amount of P(3HB) in the blend increased, largely owing to the inclusion of crystalline P(3HB) into the amorphous P(3HO-co-HD) (Bhatia *et al.*, 2007). This corresponds with the results observed when Basnett and colleagues incorporated P(3HB) into P(3HO) (Basnett *et al.*, 2013).

Although the values for Young's Modulus (E), Tensile Strength and Elongation at break have never been reported for these novel blends, the patterns observed were similar to those reported in literature for other mcl-

PHA/scl-PHA blends. The addition of P(3HB) into the mcl-PHAs led to an increase in the Young's Modulus and Tensile Strength of the blends. This could be attributed to the increase in crystallinity with addition of P(3HB) which is related to increased stiffness and strength. These trends have been observed in P(3HO)/P(3HB) blends as well as blends of mcl-PHAs with other crystalline polymers like PLA (Qiu *et al.*, 2005; Martelli *et al.*, 2012; Basnett *et al.*, 2013; Lizarraga-Valderrama *et al.*, 2015).

The primary aim of creating these blend structures is to assess their suitability for use as scaffolds for bioartificial pancreas. Hence, it is important to evaluate their biocompatibility with BRIN BD11 murine islet cells. In this study, all P(3HO-co-3HD)/P(3HB) blends made exhibited >80% cell viability with BRIN BD11 cells with the 95:5 P(3HO-co-HD)/P(3HB) blend exhibiting the highest viability of 98.54%. This further confirmed the results obtained in Chapter 4. The P(3HO-co-3HD) and the related blends showed greater cell viability than P(3HB). This could be attributed to their relative mechanical properties. The elasticity and strength of mcl-PHAs are similar to the those of the native pancreas and so they are able to better mimic the natural environment for the cells. In comparison, P(3HB) is not able to provide that and exhibits lower cell viability. In the cases of the blends, with the addition of P(3HB), the mechanical properties were altered favourably, leading to slight increases in strength and stiffness. This resulted in samples better suited for scaffold architecture. This could explain why the 95:5 blend performed better than the neat P(3HO-co-3HD) samples.

These results were confirmed by the insulin release data, which showed that creating the blends not only improved the mechanical properties of these samples, it also increased the viability and functionality of BRIN BD11 cells grown on them.

In the second part of the study, the P(3HO-co-HD) and 95:5 blend samples were fabricated into three different structures: non-porous 2D, porous 2D and porous 3D scaffolds. They were then seeded with cells for viability and insulin release tests. No significant differences were observed, confirming the points already discussed in chapter 5.

In conclusion, in this chapter, three P(3HO-co-HD)/P(3HB) blend compositions were made- 95:5, 90:10 & 80:20. These blends were characterised mechanically and thermally; showing the effect of the addition of P(3HB) to the P(3HO-co-HD). All the trends observed followed those predicted and observed in other studies. Cell viability and insulin release studies were carried out to determine which of the blends better supported BRIN BD11 cell viability and the insulin release function. The P(3HO-co-3HD)/P(3HB) 95:5 blend showed the most promising results. Hence this blend, along with the neat mcl-PHA as a control was processed into three scaffold structures. Of the three scaffold structures, 2D, 2D porous and 3D structures, the 95:5 3D structure showed the best combination of mechanical, thermal, cell viability and insulin release data to make it the best blend composition for a scaffold for the development of bioartificial pancreas.

CHAPTER SEVEN: ALGINATE HYDROGELS

7. ALGINATE HYDROGELS

7.1. INTRODUCTION

Hydrogels refer to a group of hydrophilic polymers that possess linkages that enable them to absorb large volumes of water from 10% of their dry weight up to hundred/ thousand times of their dry weight. Due to their ability to form stable, porous, 3D structures and their ability to mimic the ECM, they have been widely accepted as model materials for Tissue Engineering (Hoffman, 2012; Sivashanmugam *et al.*, 2015). They have found applications in a wide range of fields from drug delivery (Hoare and Kohane, 2008), cell culture (Caliari and Burdick, 2016), wound dressings (Murphy and Evans, 2012), ocular lenses (Lloyd, Faragher and Denyer, 2001), muscle tissue engineering (Christman *et al.*, 2004), bone tissue engineering (Lee and Mooney, 2001) and islet transplantation (Vos *et al.*, 1997).

Hydrogels can be classified in many ways. Based on the materials, they can be classified into natural and synthetic hydrogels. Natural polymers include alginate, agarose, collagen, gelatin and chitosan. Synthetic polymers include poly(acrylic acid), poly(ethylene oxide) and polyvinyl alcohol (Mooney and Drury, 2003; Lee and Mooney, 2012).

Another method of classifying hydrogels is by the manner of synthesis. Based on this, there are gels where the crosslinking is via non-covalent interactions including hydrophobic links, hydrogen and ionic bonds. Due to their reversible nature, they are not widely accepted in Tissue Engineering

(Ullah *et al.*, 2015). Chemical gels with covalent linakges are more useful in Tissue Engineering because of their stability and desirable mechanical properties (Akhtar, Hanif and Ranjha, 2016).

Alginate is a class of natural anionic polysaccharide derived from brown algae and fermentation of *Pseudomonas.* They are made of D-mannuronic acid and L-glucuronic acid. It is widely used in Tissue Engineering due to the ease of cross-linking, its ability to mimic the ECM and the low cost of production and processing (Vlierberghe, Dubruel and Schacht, 2011; Lee and Mooney, 2012). It is biocompatible and non-immunogenic (Bidarra, Barrias and Granja, 2014). It has also been shown to have cell protective qualities; a factor particularly important for islets (Bidarra, Barrias and Granja, 2014). It can be used in the form of microspheres, microcapsules for cell encapsulation and as block hydrogels (Vlierberghe, Dubruel and Schacht, 2011).

Alginate hydrogels have been applied as microspheres, microcapsules and block hydrogels in drug, cell and protein delivery (Lee and Mooney, 2012; Bidarra, Barrias and Granja, 2014), wet and dry patches in wound dressings, 3D model systems in cell culture (Lee and Mooney, 2012), bone marrow and delivery of growth factors in bone tissue engineering (Vlierberghe, Dubruel and Schacht, 2011), macroporous gels for cartilage tissue engineering (Bedian *et al.*, 2017), muscle (Rowley, Madlambayan and Mooney, 1999), liver (Bedian *et al.*, 2017) and islet tissue engineering (Vos *et al.*, 1997; Ludwig *et al.*, 2012).

Diabetic AO-rats that received islet encapsulated in alginate microcapsules became normoglycemic from 5 days up to 20 weeks post-transplantation (Vos *et al.*, 1997). The same trend was observed in Balb/c mice that received alginate islets, (Schneider *et al.*, 2005). Diabetic male nude mice who also received alginate encapsulated islets retained normoglycaemia up to 134 days post-transplantation (Qi *et al.*, 2008). In primate studies, 8 cynomolgus that received porcine neonatal islets experienced a 36% decrease in supplementary insulin dose requirement, which increased up to 43% at 24 weeks. By 36 weeks, one of the monkeys was weaned off supplementary insulin (Elliott *et al.*, 2005).

Not a lot of research exists in the application of 3D printing of alginate hydrogel and islets (Marchioli *et al.*, 2015). 3D printing has been used to print murine alginate-gelatin structures with INS1E insulin producing cells embedded within (Marchioli *et al.*, 2015). 3D printing has also been used to print macroporous alginate structures with pluripotent stem cells that differentiated into β-cells (Song and Millman, 2016).

This chapter aimed to evaluate the difference between alginate microbeads and 3D printed block alginate hydrogel structures with respect to the cell viability and insulin release using encapsulated/incorporated BRIN BD11 cells. Thus, two kinds of alginate hydrogel systems- BRIN BD11 encapsulated alginate microbeads and 3D printed block hydrogel structures with BRIN BD11 cells were produced. They were characterised with respect to their swelling and degradation behaviour. BRIN BD11 cells in them were then tested for cell viability and insulin release. Finally, both hydrogel

systems were compared with respect to cell viability and insulin release of the BRIN BD11 cells seeded within them.

7.2.RESULTS

7.2.1. Alginate Microbeads

The alginate microbeads produced in this work are shown in Figure 7.1 is an image of the dry microbeads made, Figure 7.2 is light microscopy images of wet alginate microbeads made. The dry alginate microbeads appeared as heterogenous white beads with average diameters of 0.87±0.13mm. Light microscopy of wet beads showed spherical beads filled with water. Wet spheres measured 1.26±0.59mm in diameter.

Figure 7.1: Dry alginate microbeads. Beads measure 0.87±0.13µm, bars: 1 µm.

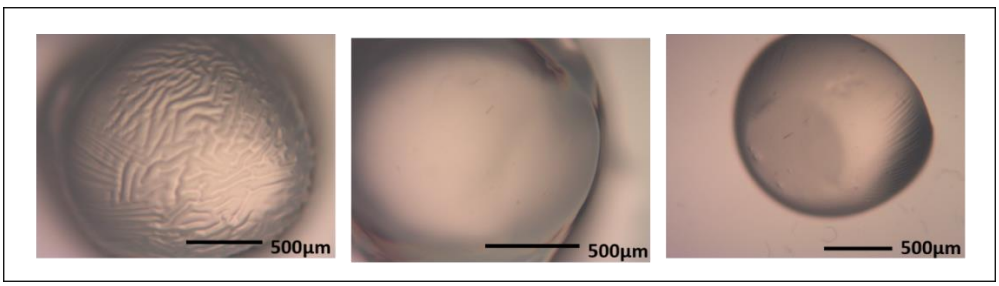

Figure 7.2: Light microscopy of wet alginate microbeads. Magnification 100X, Bars: 500µm.

7.2.2. 3D Printed Alginate Block Hydrogel

The 3D printed alginate block hydrogel was a white cube with a length/width/height of 13.5mm (Figure 7.3). For the cell culture studies, cubes of 1x1x1mm were made.

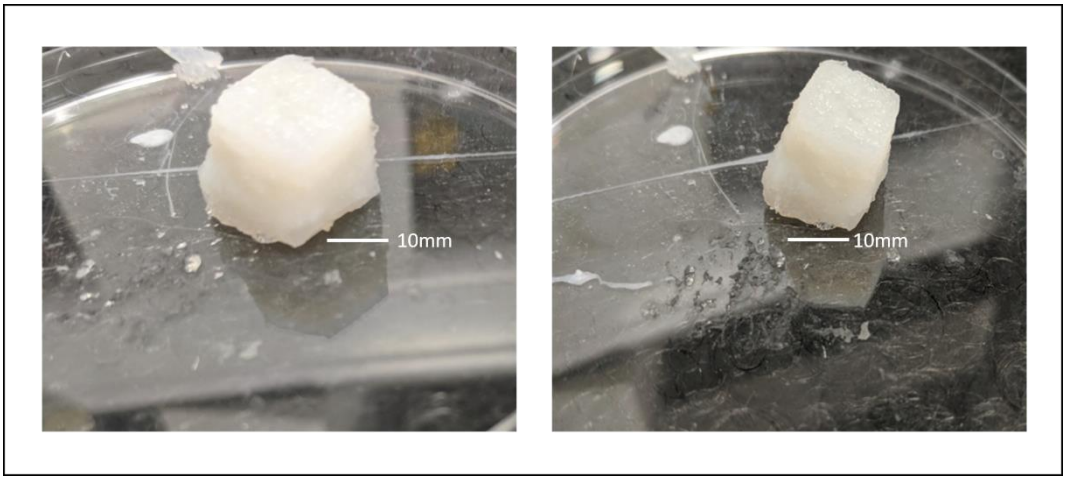

Figure 7.3: 3D Printed Alginate Hydrogel Cube measuring 13.5x13.5x13.5mm, bars:10mm.

7.2.3. Cell Viability of BRIN BD11 Cells in Alginate Microbeads

Cell viability assays were carried out to evaluate the effect of cell density on the viability of cells and to determine the optimum cell density for encapsulation.

Figure 7.4 shows the cell viabilities observed. In comparison with the positive control (tissue culture plastic), microbeads with the lower cell density ($1x10^5$cells/ml) exhibited significantly lower cell viabilities ($p \leq 0.001$). On the other hand, microbeads with the higher cell density ($5X10^5$cells/ml) showed no significant difference ($p > 0.05$) in comparison

to the positive control. The viability for microbeads with cell density $5X10^5$cells/ml was higher ($p \leq 0.05$) than the beads with cell density $1X10^5$cells/ml, indicating an increase in cell viability with increase in cell density.

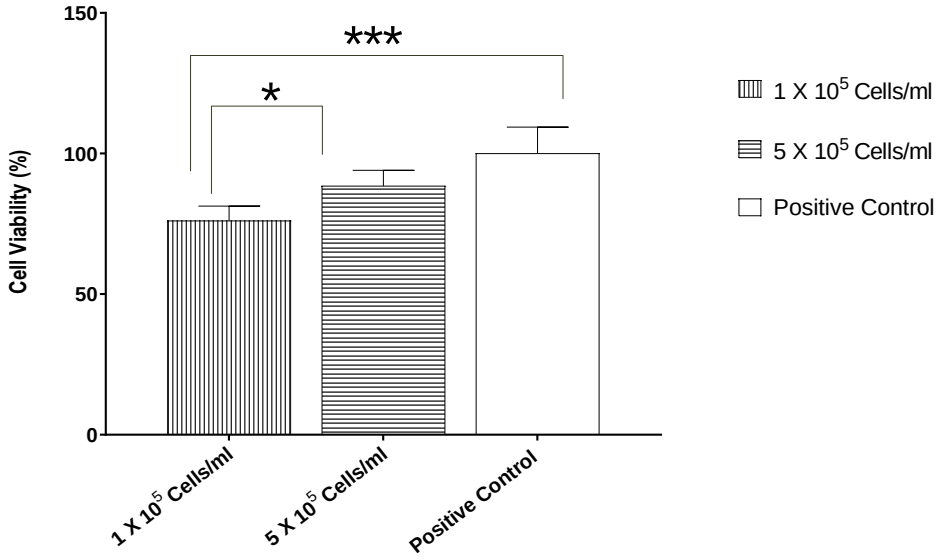

*Figure 7.4: Cell viabilities of BRIN BD11 encapsulated at densities of $1x10^5$ cells/ml and $5x10^5$cells/ml in alginate microbeads. Values are expressed as % of positive control (tissue culture plastic) ± SEM for groups of 6. *$p \leq 0.05$ in comparison with $5x10^5$cells/ml, ***$p \leq 0.001$ when compared with the positive control (tissue culture plastic).*

7.2.4. Static Insulin Secretion from BRIN BD11 Cells Encapsulated in Alginate Microbeads

Insulin release analyses were carried out to evaluate the effect of cell densities on the insulin release from alginate microbeads. The results are shown in Figure 7.5.

At normoglycaemia (5.6mM glucose), the insulin released in response from microbeads with both low and high cell densities were significantly higher ($p \leq 0.0001$) than that of the positive control (Figure 7.5A). In addition, the

insulin released from microbeads with higher cell density ($5X10^5$cells/ml) was significantly higher ($p \leq 0.0001$) than that with low cell density ($1X10^5$ cells/ml). These results indicate that increasing cell density increases insulin released at a rate higher than cell viability.

A similar result was obtained at hyperglycaemia (16.7mM glucose), shown in Figure 7.5B. Insulin released from microbeads at both cell densities was significantly higher ($p \leq 0.0001$) than that of the positive control (tissue culture plastic). Insulin released from microbeads with higher cell density ($5x10^5$cells/ml) was significantly higher ($p \leq 0.001$) than that with low cell density ($1x10^5$ cells/ml).

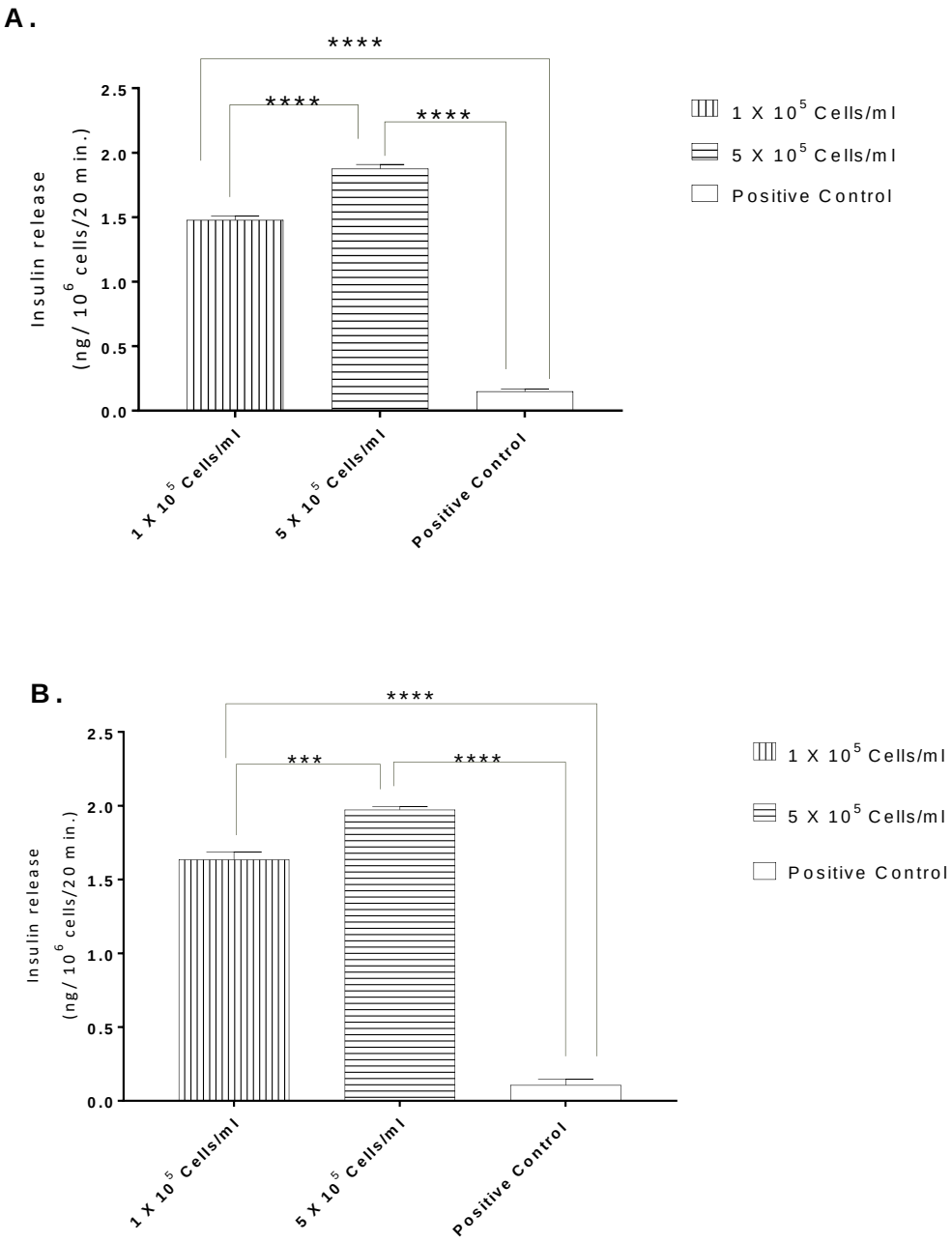

*Figure 7.5: Insulin release from BRIN BD11 cells encapsulated in alginate microbeads at densities of $1x10^5$ cells/ml and $5x10^5$cells/ml at A. normoglycaemia (5.6mM glucose) and B. Hyperglycaemia (16.7mM glucose) in ng/10^6cells/20 minutes. Samples are expressed as values± SEM for groups of 6. ***$p \leq 0.001$ when compared with microbeads with cell density $5x10^5$cells/ml and ****$p \leq 0.0001$ when compared with both the positive control.*

7.2.5. The swelling behaviour of the Alginate Block Hydrogels

The swelling behaviour of the alginate block hydrogel was evaluated at varying w/v% concentrations of alginate (2%, 4%, 5%) to monitor the behaviour of the hydrogel in a buffer (PBS) over 300 minutes and to test the influence of the alginate concentration on the swelling behaviour (Figure 7.6). For all concentrations, there was a steady increase in weight gain (% dry weight) until about 60minutes; after which there was a steady phase until the weight gain started to decrease very slowly. Of the 3 concentrations, 5% w/v absorbed the maximum amount of water.

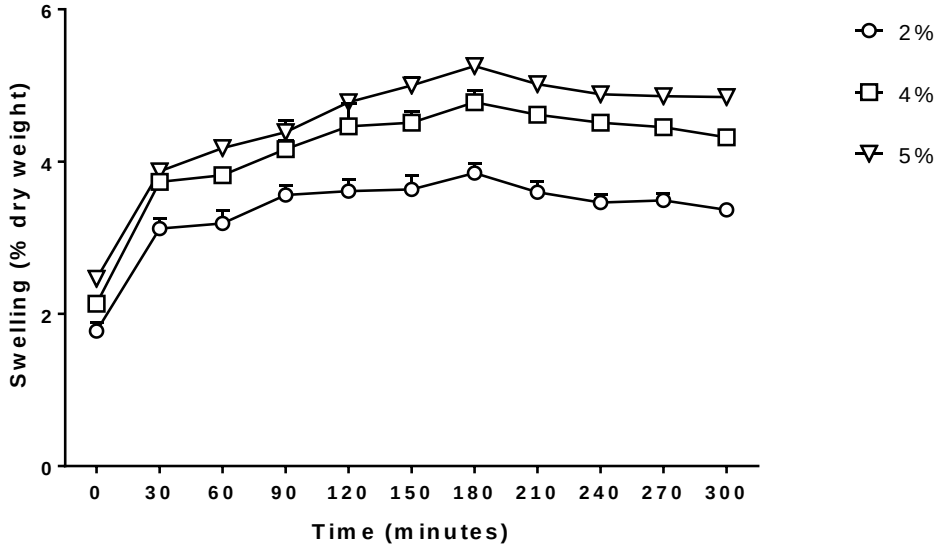

Figure 7.6: Swelling (% dry weight) of 2%, 4% & 5% w/v alginate block hydrogels. Values are expressed ±SEM for groups of 3 over 300 minutes.

7.2.6. Cell Viability of BRIN BD11 Cells in the 3D Alginate Block Hydrogel

Cell viability assays were carried out to evaluate the effect of alginate concentration on the viability of BRIN BD11 cells in hydrogels and to determine the optimum alginate concentration for the hydrogel.

Figure 7.7 shows the cell viabilities observed for BRIN BD11 cells seeded in the hydrogels made using 2%, 4% and 5% alginate concentrations. In comparison with the positive control, only cells seeded in 2% alginate hydrogel showed significantly lower ($p \leq 0.01$) cell viability. No significant difference ($p > 0.05$) was observed between the viabilities observed for all three concentrations indicating that increasing alginate concentrations does not affect cell viabilities.

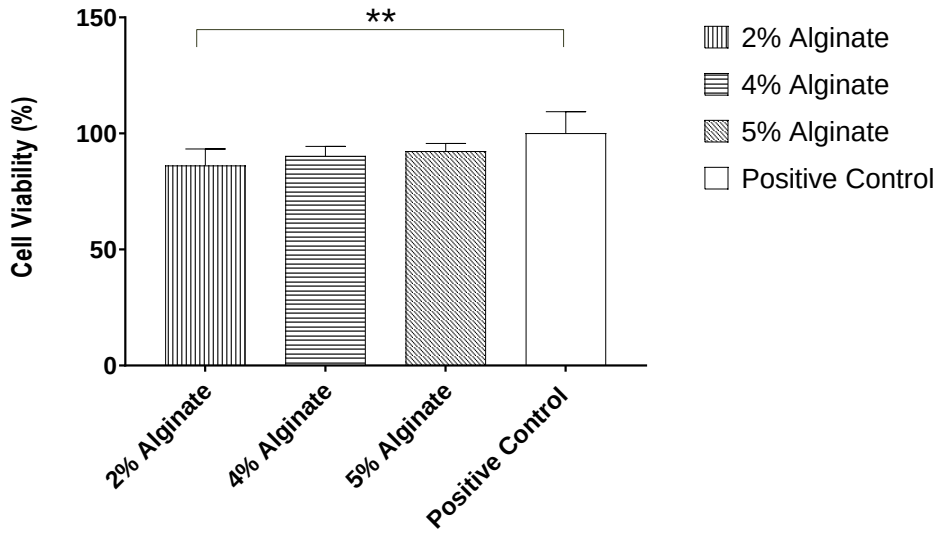

*Figure 7.7: Cell viability of BRIN BD11 cells in 2, 4 & 5% w/v alginate block hydrogels. Values are expressed as % of positive control (tissue culture plastic) ± SEM for groups of 6. **$p \leq 0.01$ in comparison with the positive control, $p > 0.05$ when all other 4% and 5% were compared to the positive control.*

7.2.7. Static Insulin Secretion from BRIN BD11 Cells Seeded in 3D Printed Alginate Hydrogel

Insulin release analyses were carried out to evaluate the effect of alginate concentration on the insulin release from BRIN BD11 cells in the alginate hydrogel. The results are shown in Figure 7.8.

At normoglycaemia (5.6mM glucose), insulin release from all three concentrations of hydrogel were significantly higher ($p \leq 0.0001$) than the positive control. A steady increase in insulin release was observed as the concentration of alginate increased. In comparison with 2% and 4% alginate hydrogels, the insulin release from the 5% alginate hydrogel was significantly higher ($p \leq 0.0001$ & $p \leq 0.001$ respectively).

At hyperglycaemia (16.7mM glucose), a similar pattern was observed. Insulin release increased as alginate concentration increased. In comparison with 2% and 4% alginate hydrogels, the insulin release from the 5% alginate hydrogel was significantly higher ($p \leq 0.001$ & $p \leq 0.01$ respectively).

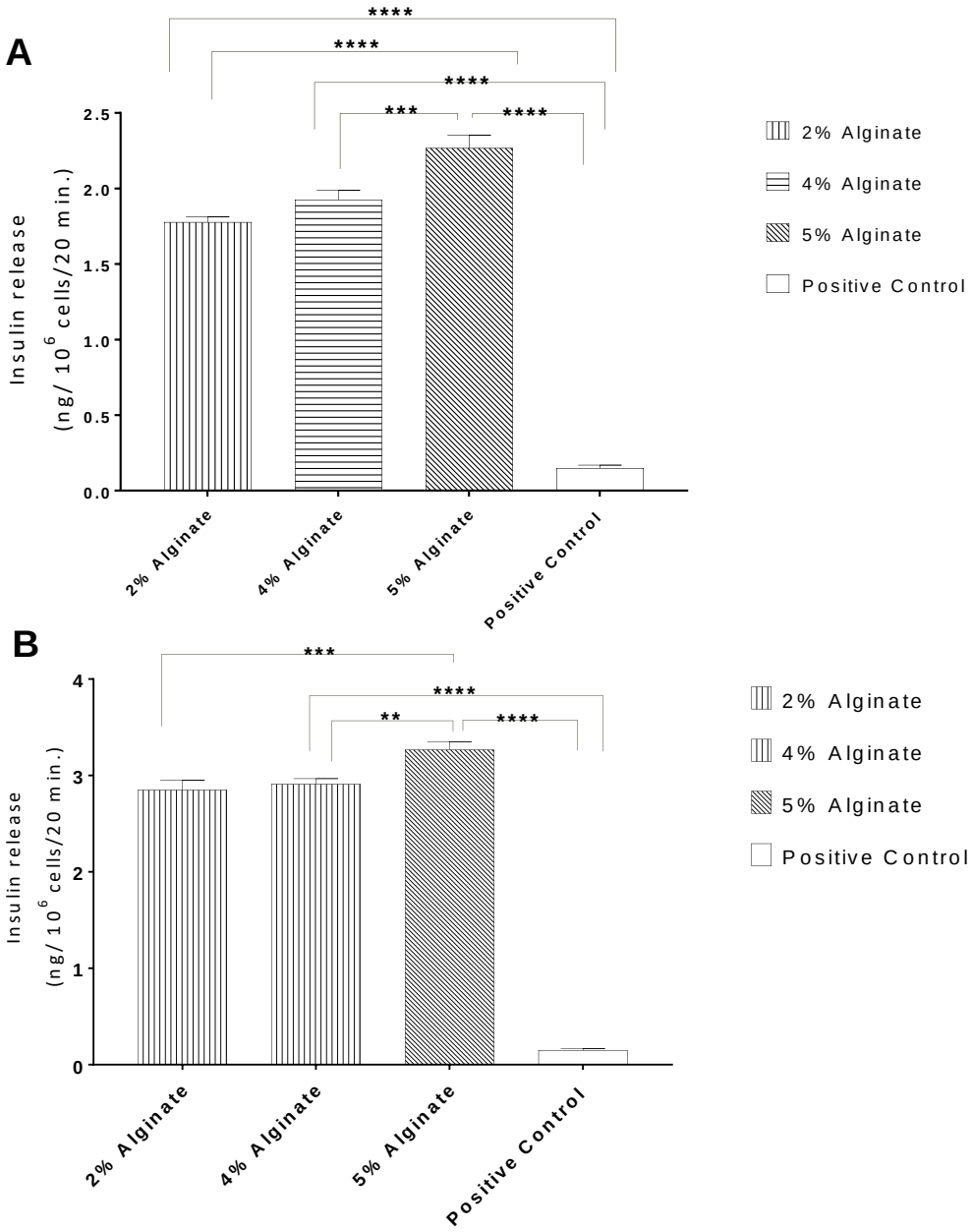

*Figure 7.8: Insulin release from BRIN BD11 cells in 2, 4 & 5% w/v alginate hydrogels at A. Normoglycaemia (5.6mM glucose) and B. Hyperglycaemia (16.7mM glucose) in ng/10^6cells/20 minutes. The insulin release values are expressed as values± SEM for groups of 6. **$p \leq 0.01$, ***$p \leq 0.001$, ****$p \leq 0.0001$ in comparison with the 5% alginate hydrogel and positive control.*

7.2.8. Comparison of Alginate Microbeads & 3D Alginate Block Hydrogels

A comparison of the cell viability and insulin release from BRIN BD11 cells encapsulated in alginate microbeads at a density of $5x10^5$cells/ml and seeded in 3D alginate block hydrogel at a density of $5x10^5$cells/ml was carried out to evaluate the effect of the structure of the alginate hydrogel on the cells.

7.2.8.1. Cell Viability of BRIN BD11 in Alginate Microbeads and 3D Alginate Block Hydrogel

The cell viabilities of BRIN BD11 encapsulated in alginate microbeads and seeded in 3D alginate hydrogel are shown in Figure 7.9. The cell viabilities observed were 79.49±5.54% for the microbeads and 92.27±8.39% for the block hydrogel. There was a significant difference ($p \leq 0.01$) observed between the cell viabilities indicating that block hydrogel is a more suitable environment for the BRIN BD11 cells.

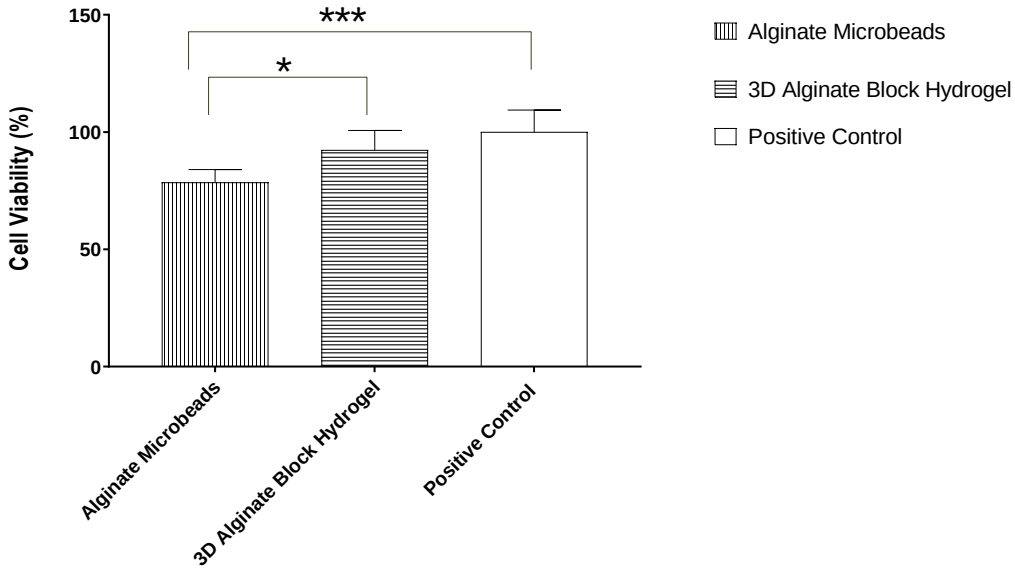

*Figure 7.9: Cell viabilities of BRIN BD11 cells in alginate microbeads and 3D printed block alginate hydrogels. Values are expressed as % of positive control (tissue culture plastic) ± SEM for groups of 6. *p ≤ 0.05 when microbeads and the 3D printed block hydrogel are compared, ***p ≤ 0.001 when compared to the positive control. P > 0.05 when block hydrogel was compared to the positive control.*

7.2.8.2. Static Insulin Secretion from BRIN BD11 Cells in Alginate Microbeads and 3D Block Alginate Hydrogel

The insulin released from BRIN BD11 cells in both alginate microbeads and 3D alginate hydrogel are shown in 7.10. At both normoglycaemia and hyperglycaemia (5.6mM & 16.7mM glucose respectively), insulin released from the microbeads and 3D hydrogel were significantly higher ($p \leq 0.0001$) than the positive control. When the microbeads and 3D block hydrogel were compared, insulin released from cells in 3D block hydrogels at both normoglycaemia and hyperglycaemia were significantly higher ($p \leq 0.0001$) than that from the microbeads.

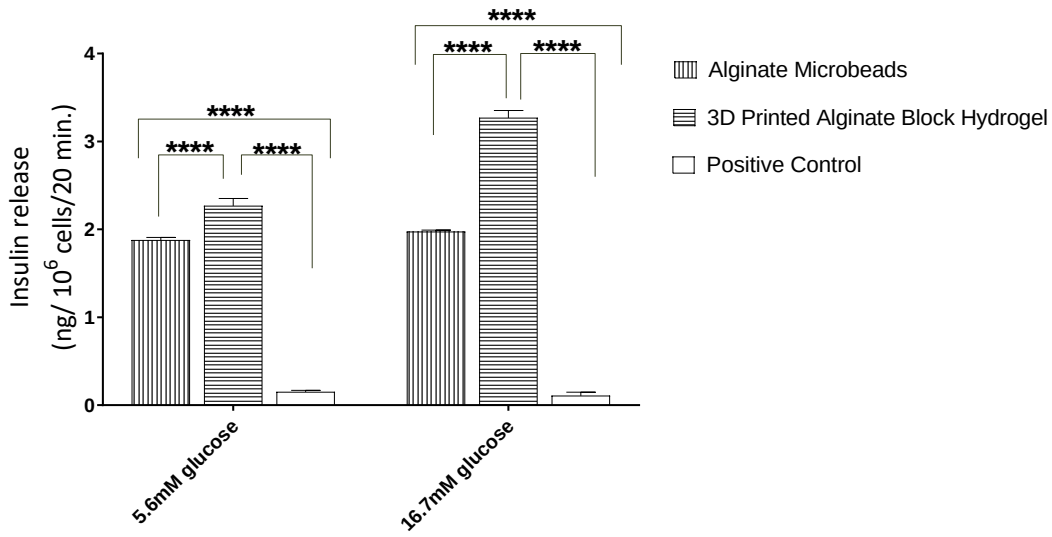

*Figure 7.10: Insulin release from BRIN BD11 cells in alginate microbeads and 3D printed alginate hydrogel at normoglycaemia (5.6mM glucose) and hyoerglycaemia (16.7mM glucose) in ng/10^6cells/20 minutes. Samples are expressed as values± SEM for groups of 3. ****$p \leq 0.0001$ when compared with both block hydrogel and postive control (tissue culture plastic).*

7.3.DISCUSSION

Based on results from this chapter, cell viability increases with increase in cell density in both the cells encapsulated in the alginate hydrogel and in the 3D printed block. This is in accordance with literature; although after a certain threshold, loading the hydrogel with more cells is detrimental to the functioning of all the cells as increasing cell load beyond a certain threshold value leads to loss in stability of the beads (Lin and Anseth, 2011). This phenomenon has not been observed in this study which could be due to the fact that perhaps that critical threshold had not been reached.

Cell morphology affects the functionality of the cells, so for the insulin release function of cells, it is important for the cells to remain as true to

nature as possible. The natural conformation of β-cells is to aggregate into islets. Aggregation is very important in the insulin release process in islets. This is because the cells work through cell-to-cell interactions. Islets will always revert to the aggregation morphology (Lucas-Clerc *et al.*, 1993). At low cell densities, aggregation is limited so cells are not able to respond as well to glucose stimulation (Dvir-Ginzberg *et al.*, 2003). At high densities, more aggregates are found leading to the presence of more insulin positive cells (Segev *et al.*, 2004). β-cells in aggregates are able to release up to 3-fold more insulin in response to glucose than cells in unaggregated islets (Hopcroft, Mason and Scott, 1985). This is also observed in this study as the cells at higher densities have higher insulin release values than those at lower densities.

Swelling behaviour is important to measure as it predicts the behaviour of the hydrogel *in vivo*. It is a result of the hydration of the hydrogel, leading to water entry into the polymer chains of the beads to create swelling (Dai *et al.*, 2008). When swelling occurs in PBS, there is an exchange of Ca^{2+} and Na^{+} ions that encourages swelling (Pasparakis and Bouropoulos, 2006). The initial rapid increase in weight gain is due to the rapid exchange of ions that occurs immediately after introduction into PBS (Bajpai and Sharma, 2004). The difference in %weight gain of the 3 different concentrations is due to binding between alginate and $CaCl_2$ and the ease of ion exchange between the hydrogel and PBS. A similar pattern was observed with degradation where the initial rapid weight loss could be attributed to the quicker release of Ca^{2+} than in swelling. Long term studies have shown alginate block hydrogels to be stable for up to 90 days with constant

hydration (Shapiro and Cohen, 1997). In this work, the 5% hydrogel exhibited the least %weight loss of the three concentrations; possibly due to the fact that with higher alginate concentration, the Ca^{2+} ions were more tightly bound. A similar pattern was observed in Bajpai and Sharma's study. When 2%, 3% & 4% w/v alginate solutions were used to make microbeads, the 4% w/v beads were the most stable during swelling (Bajpai and Sharma, 2004).

The concentration of alginate affects many factors that influence the viability of cells in the hydrogels. These include the viscosity of the hydrogel solutions, strength of the block hydrogels and shear force of the hydrogel. In this study, the 5% hydrogel had the highest cell viability. Kong and colleagues found when they evaluated the cell viabilities of three different concentrations of alginate- 2, 3.5 & 5% w/v, that 3.5% w/v had the highest cell viability (Kong, Smith and Mooney, 2003). This could be due to the difference in molecular weight of the alginate used. In their study, they used low molecular weight alginate (~100g/mol), while the alginate used in this study had molecular weight of 216.12g/mol. As a result, the alginate used in this study had higher viscosity than theirs. Cells are better able to form aggregates in solutions of high viscosity (Bohari, Hukins and Grover, 2011). This then has a trickledown effect on the insulin release. Since insulin release is a function of cellular aggregation, it follows that as increase in concentration leads to an increase in cellular aggregation, which then leads to an increase in insulin release.

Of both structures, the 3D block alginate hydrogel proved better for cells with respect to cell viability and insulin release. This is due to many factors, the average diameter of the microbeads was 0.87±0.13mm, with a surface area of 2.32±0.345mm^2 and volume of 0.33±0.061mm^3. The hydrogel on the other hand, had a length of 1mm and surface area of 6mm^2 and volume of 1mm^3. The microbeads have a smaller capacity for cells due to their size; an average islet measures 100μm and even though the microbeads provide the shape, the number of islets are not as adequate. The other factor is the difference in surface area. The hydrogel blocks also provide an open space for cell-cell contact.

In conclusion, in this chapter, it has been shown that 5x10^{5}cells/ml of BRIN BD11 cells was an optimal cell density for use in microbeads with average diameter 0.8±0.13mm and 3D printed block hydrogels of 1mm sides. It was also shown that the 3D-printed block alginate hydrogels behaved the same way as previously reported for alginate hydrogels with respect to swelling. Finally, upon comparison of 2, 4 and 5 w/v% concentrations of alginate, 5% w/v was the best concentration for optimum cell viability and insulin release using the 3D printed block alginate hydrogels.

CHAPTER EIGHT: CONCLUSIONS AND FUTURE WORK

8. CONCLUSIONS AND FUTURE WORK

8.1. CONCLUSIONS

Type 1 Diabetes mellitus remains one of the major chronic diseases plaguing individuals in the UK and around the world (Diabetes UK, 2017). Amongst the variety of treatment options available, islet transplantation has emerged as the gold-star of treatment. One of the major challenges of islet transplantation is the rapid loss of islets after transplantation (Shapiro *et al.*, 2006; McCall and Shapiro, 2012). This work was planned to investigate a potential solution to this issue. In this project, a multilayer approach was investigated. This involved an outer PHA scaffold surrounding an inner alginate hydrogel environment including cells.

Initially, two different PHAs were produced- a short chain length PHA, P(3HB) and a novel medium chain length PHA, P(3HO-co-HD). P(3HB) was made using fermentation of *Bacillus subtilis* OK2, using glucose as the carbon source. The yield reported for P(3HB) was 49% dcw. This value matches the highest reported values for P(3HB) production in literature. A novel medium chain length polymer P(3HO-co-HD) was produced using *Pseudomonas mendocina* CH50, also using glucose as the carbon source. The yield obtained was 43% dcw, which is again promising as it is among the higher reported yields in literature. Both polymers were characterised and identified using FTIR, GCMS and NMR. The novel polymer produced from *Pseudomonas mendocina* CH50 fermentation was identified as a medium chain length PHA with HO and HD monomers in the ratio 22:78.

It was named P(3HO-co-HD). One requirement of tissue engineering is the ability of potential biomaterials to mimic native tissue. In order to determine the properties of these materials, mechanical and thermal characterisation was undertaken. Values observed indicated the differences in both polymers- P(3HB) a stiff, brittle polymer with high melting temperature and P(3HO-co-HD), an elastomeric polymer with low melting temperature. Based on these characteristics, it was postulated that P(3HO-co-HD) was more suited to soft tissue engineering, especially islet transplantation.

To confirm this hypothesis and evaluate the suitability of these PHAs for islet transplantation, their mechanical and thermal properties were compared to PLLA, a FDA approved polymer that has been investigated extensively in tissue engineering and specifically in islet transplantation. BRIN BD11 murine islet cells were seeded on P(3HB), P(3HO-co-HD) and PLLA and evaluated for cell viability. Of the three polymers, cells seeded on P(3HO-co-HD) had the highest cell viabilities with no significant difference observed in comparison with the positive control (tissue culture plastic). The same pattern was identified when the insulin release function of these cells was measured at both normoglycaemia (5.6mM) and hyperglycaemia (16.7mM) blood. At both levels, cells seeded on P(3HB) and P(3HO-co-HD) released higher insulin than cells seeded in both PLLA and the positive control. Cells seeded in P(3HO-co-HD) released 4 and 3-fold more insulin than those seeded on the positive control at normoglycaemia and hyperglycaemia respectively. This indicated that both PHAs were non-toxic and allowed insulin release from BRIN BD11 cells seeded on them.

Even though the Young's modulus of P(3HO-co-HD) is the most similar to soft tissue, it is still higher than that of the native pancreas. The observed Young's modulus of P(3HO-co-HD) from this study was 5.62±0.054MPa while that of the native pancreas is $2.1x10^{-3}$MPa. One way to reduce the mechanical properties of a scaffold is the introduction of pores. Porosity also allows for the exchange of nutrients and waste in the scaffold. In order to determine the optimum porosity, 2D porous P(3HO-co-HD) scaffolds were fabricated. Two different concentrations of porogen (5% and 15%) and porogen sizes (100µm and 300µm) were used in making the scaffolds. Mechanical characterisation of these scaffolds confirmed that the addition of pores reduced the Young's modulus by 5-fold with an increase in porogen concentration and size leading to a decrease in Young's modulus to 1.11±0.052MPa. Additionally, upon examination of their water contact angles, the scaffolds became less hydrophobic as the porogen concentration and size increased. These scaffolds were then examined to determine the effect of pore size and concentration on the viability and insulin release of BRIN BD11 cells seeded in them. Even though porosity decreased Young's modulus and tensile strength, it did not lead to an improvement in the viabilities and insulin release of the BRIN BD11 cells seeded in them. Further, comparing NaCl and sucrose as porogens, it was found that NaCl was a better porogen because the cell viabilities and insulin release of BRIN BD11 cells seeded in them were higher than those in sucrose made scaffolds. The porous scaffold that was the best performing one was the one with 100µm NaCl at a concentration of 15%. This scaffold was used for further investigation.

To better understand the interactions between cells, scaffolds, molecules and components of the extracellular matrix in an *in vivo* context, research in tissue engineering has shifted from 2D to 3D scaffolds (Coronel and Stabler, 2013). To investigate the effect of these interactions on the islets, P(3HB) and P(3HO-co-HD) 3D structures were fabricated. These 3D structures were then compared to 2D structures. No significant differences were recorded when mechanical properties were compared between 2D and 3D structures. Similarly, no significant difference was observed when the viabilities and insulin release of BRIN BD11 cells seeded in them were compared. These results require further investigation as the number of cells seeded per unit surface area of the structures need to be considered.

One of the drawbacks of introducing porosity in 3D structures is that they become difficult to handle. Blending is a technique that has been employed to tune the physical and mechanical properties of a material. In order to improve the handling of the P(3HO-co-HD) 3D structures, blending with P(3HB) was carried out. Three different P(3HO-co-HD) dominated P(3HO-co-HD)/P(3HB) blends were made: 95:5, 90:10 and 80:20. Upon blending of both polymers, another melting peak in the range of the T_m for P(3HB) was observed in the DSC thermogram, indicating the presence of an immiscible phase of P(3HB). Incorporation of P(3HB) into the blend led to an increase in both the tensile strength and Young's modulus, while also decreasing their flexibility. Cells seeded in 95:5 P(3HO-co-HD)/P(3HB) blend were the best performing of all the blends with respect to cell viability and insulin release studies. Further, in comparison to neat P(3HO-co-HD), cells seeded in 95:5 P(3HO-co-HD)/P(3HB) blend showed no significant

difference in viabilities and insulin release. This was positive because an increase in the stiffness did not affect the viabilities of the cells. Based on this data, the 95:5 P(3HO-co-HD)/P(3HB) blend was fabricated into porous 2D and 3D structures. These were then compared with their corresponding P(3HO-co-HD) structures. No significant difference was observed in cell viabilities and insulin release of BRIN BD11 cells seeded in them when they were compared; indicating that the 95:5 P(3HO-co-HD)/P(3HB) blend is the best candidate for the scaffold of a bioartificial pancreas with a handleable structure and good biological performance.

Finally, alginate hydrogels were made and evaluated for their use in islet transplantation. Two kinds of hydrogel structures were made- microbeads and 3D printed block hydrogels containing BRIN BD11 cells. First, two different cell densities ($1x10^5$ & $5x10^5$ cells/ml) were investigated to evaluate the optimum density for making the microbeads. The cell viability and insulin release of BRIN BD11 cells at higher densities were significantly higher than lower densities. Hence, $5x10^5$ cells/ml cell concentration was chosen for further investigation. Next, alginate hydrogel cube blocks were 3D printed using three different concentrations of alginate solution (2,4 & 5 w/v%). These hydrogels were then evaluated for their swelling behaviour where it was observed that the 5 w/v% hydrogel was the most stable. Evaluating them for cell viability and insulin release indicated that the 5 w/v% hydrogel had the highest cell viability and insulin release. Finally, the alginate microbeads were compared with the 3D printed block hydrogels in terms of viability and insulin release of BRIN BD11 cells. In

this case, the 3D printed hydrogel also had significantly higher viability and insulin release than the microbeads.

In summary, based on this work, the 95:5 P(3HO-co-HD)/P(3HB) blend was selected as the scaffold material while the 3D printed alginate hydrogel containing $5x10^5$ cells/ml was selected for the inner hydrogel environment within the bioartificial pancreas.

8.2. FUTURE WORK

This work represents a preliminary step in the use of PHAs alongside alginate in the creation of the bioartificial pancreas. In order to further expand understanding of this work, the following areas should be investigated.

The yields of PHAs produced in this study are not representative of the current data in literature. Optimum yields can be achieved using techniques like low carbon feeding (Mohd Fadzil *et al.*, 2018). In addition, since the P(3HO-co-HD) produced in this study is a novel polymer, further studies into the fermentation process would be interesting. Optimisation studies with mathematical modelling tools like MATLAB should be used to fine tune the mix of conditions necessary for the optimal production of the PHAs.

One of the challenges faced in this work was the accurate measurement of porosity and the consistency of pores. Finetuning of the process of creation of pores should be carried out to ensure better understanding and consistency. There should also be characterisation and evaluation of surface

properties and porosity of both porous and non-porous scaffolds made would be helpful in better understanding the interactions. According to the American Society for Testing and Materials (ASTM), porous structures should be characterised in terms of pore size, pore volume and mechanical properties. In the future, complete porosimetry would be helpful in maintaining the consistency of the scaffolds and adherence to ASTM guidelines.

Following the complete characterisation of porous structures, a standardised method for the comparison of 2D and 3D structures should be established. Both structures behave differently in terms of mechanical properties and their measurements and viability of cells. The design of a standardised way to compare the viabilities of cells seeded in both 2D and 3D structures while accounting for differences in surface area and volume should be considered. This will lead to more accurate assessments.

In evaluating the suitability of a material for biological purposes, measurement of the behaviour of the cells in relation to the scaffolds is important. Complete evaluation of the biocompatibility, toxicity and biodegradability of the scaffolds is paramount. In this work, basic tests like cell viability and short-term insulin secretion have been carried out. Further tests need to be carried out. Extended insulin release tests should be carried out to show long-term insulin secretion. Insulin staining using dithizone should also be carried out to show intracellular insulin. Further, the investigation of insulin release upon the addition of insulinotropic agents like GLP, GIP and amino acids. Eventually, molecular analysis should be

carried out. The hepatocyte nuclear factor-4α (HNF-4α) is of particular interest (Gupta *et al.*, 2005).

After thorough characterisation of the scaffolds with respect to viability of cells, functionalisation of the scaffolds should be carried out to improve the viability of the cells. Since islet cells have been shown to have highly specific demands, the addition of factors and active molecules will better improve the survival of islets post-transplantation.

These factors include VEGF to stimulate vascularisation, oxygen producing molecules and ECM proteins like collagen. Studying these would lead to the production of more robust scaffolds.

Due to time constraints, the final assembly of the bioartificial pancreas was not achieved. Different methods of assembly should be investigated including printing of both layers, layer-by-layer printing, surface coating and surface spraying. After the final printing method is selected, complete characterisation as described above should be carried out as the interactions may differ from final assembly.

Since this is a bioartificial pancreas intended to be used clinically, actual murine and porcine islets should be used in the evaluation of the biocompatibility of these devices.

REFERENCES

Abalovich, A. *et al.* (2001) 'Pancreatic islets microencapsulation with polylactide-co-glycolide', in *Transplantation proceedings*. Elsevier, pp. 1977–1979.

Ahmad, M. *et al.* (2000) 'Effect of type-selective inhibitors on cyclic nucleotide phosphodiesterase activity and insulin secretion in the clonal insulin secreting cell line BRIN-BD11', *British Journal of Pharmacology*, 129, pp. 1228–1234. Available at: www.nature.com/bjp (Accessed: 14 May 2019).

Ahmed, N. (2011) *Clinical biochemistry*. Second. Edited by N. Ahmed. New York: Oxford University Press.

Akaraonye, E. *et al.* (2012) 'Poly (3-hydroxybutyrate) production by Bacillus cereus SPV using sugarcane molasses as the main carbon source', *Biotechnology journal*. Wiley Online Library, 7(2), pp. 293–303.

Akaraonye, E., Keshavarz, T. and Roy, I. (2010) 'Production of polyhydroxyalkanoates: the future green materials of choice', *Journal of Chemical Technology & Biotechnology*. John Wiley & Sons, Ltd., 85(6), pp. 732–743. doi: 10.1002/jctb.2392.

Akhtar, M. F., Hanif, M. and Ranjha, N. M. (2016) 'Methods of synthesis of hydrogels … A review', *Saudi Pharmaceutical Journal*, 24(5), pp. 554–559. doi: 10.1016/j.jsps.2015.03.022.

Alberti, K. and Zimmet, P. (1998) 'Definition, diagnosis and classification

of diabetes mellitus and its complications. Part 1: diagnosis and classification of diabetes mellitus. Provisional report of a WHO consultation.', *Diabetic Medicine*, 15(7), pp. 539–553.

Ali Raza, Z. : P. and C. M. A. for T. F., Riaz, S. and Banat, I. M. (2017) 'Polyhydroxyalkanoates : Properties and Chemical Modification Approaches for Their Functionalization'. doi: 10.1002/btpr.2565.

Aloysious, N. and Nair, P. D. (2014) 'Enhanced Survival and Function of Islet-Like Clusters Differentiated from Adipose Stem Cells on a Three-Dimensional Natural Polymeric Scaffold: An In Vitro Study', *Tissue Engineering Part A*, 20(9–10), pp. 1508–1522. doi: 10.1089/ten.tea.2012.0615.

American Diabetes Association, A. D. (2012) 'Diagnosis and classification of diabetes mellitus.', *Diabetes care*. American Diabetes Association, 35 Suppl 1(Supplement 1), pp. S64-71. doi: 10.2337/dc12-s064.

An, D. *et al.* (2018) 'Designing a retrievable and scalable cell encapsulation device for potential treatment of type 1 diabetes', *Proceedings of the National Academy of Sciences*, 115(2), pp. E263–E272. doi: 10.1073/pnas.1708806115.

Anderson, A. J. and Dawes, E. A. (1990) 'Occurrence, metabolism, metabolic role, and industrial uses of bacterial polyhydroxyalkanoates.', *Microbiological reviews*. Am Soc Microbiol, 54(4), pp. 450–472.

Anderson, J. M. and Shive, M. S. (2012) 'Biodegradation and biocompatibility of PLA and PLGA microspheres', *Advanced Drug*

Delivery Reviews, 64, pp. 72–82.

Anjum, A. *et al.* (2016) 'Microbial production of polyhydroxyalkanoates (PHAs) and its copolymers: A review of recent advancements', *International Journal of Biological Macromolecules*, 89, pp. 161–174. doi: 10.1016/j.ijbiomac.2016.04.069.

Apelgren, P. *et al.* (2017) 'Chondrocytes and stem cells in 3D-bioprinted structures create human cartilage in vivo', *PLOS ONE*. Edited by J. Doh. Public Library of Science, 12(12), p. e0189428. doi: 10.1371/journal.pone.0189428.

Arima, Y. and Iwata, H. (2007) 'Effect of wettability and surface functional groups on protein adsorption and cell adhesion using well-defined mixed self-assembled monolayers', *Biomaterials*. Elsevier, 28(20), pp. 3074–3082. doi: 10.1016/J.BIOMATERIALS.2007.03.013.

Armstrong, S. J. *et al.* (2007) 'ECM Molecules Mediate Both Schwann Cell Proliferation and Activation to Enhance Neurite Outgrowth', *Tissue Engineering*. Mary Ann Liebert, Inc. 140 Huguenot Street, 3rd Floor New Rochelle, NY 10801 USA , 13(12), pp. 2863–2870. doi: 10.1089/ten.2007.0055.

Aslim, B., Yüksekdağ, Z. N. and Beyatli, Y. (2002) 'DETERMINATION OF PHB GROWTH QUANTITIES OF CERTAIN BACILLUS SPECIES ISOLATED FROM SOIL', *Turkish Electronic Journal of Biotechnology Special Issue*, pp. 24–30. Available at: http://www.biyotekder.hacettepe.edu.tr/dergi.html (Accessed: 1 August

2018).

Atkinson, M. A., Eisenbarth, G. S. and Michels, A. W. (2014) ‘Type 1 diabetes.’, *Lancet (London, England)*. NIH Public Access, 383(9911), pp. 69–82. doi: 10.1016/S0140-6736(13)60591-7.

Avella, M., Martuscelli, E. and Raimo, M. (2000) ‘Review Properties of blends and composites based on poly(3-hydroxy)butyrate (PHB) and poly(3-hydroxybutyrate-hydroxyvalerate) (PHBV) copolymers’, *Journal of Materials Science*. Kluwer Academic Publishers, 35(3), pp. 523–545. doi: 10.1023/A:1004740522751.

Bagdadi, A. V *et al.* (2018) ‘Poly(3-hydroxyoctanoate), a promising new material for cardiac tissue engineering’, *Journal of Tissue Engineering and Regenerative Medicine*, 12(1), pp. e495--e512. doi: 10.1002/term.2318.

Bai, S. *et al.* (2017) ‘Comparative study on the in vitro effects of Pseudomonas aeruginosa and seaweed alginates on human gut microbiota’, *PLOS ONE*. Edited by E. G. Zoetendal. Public Library of Science, 12(2), p. e0171576. doi: 10.1371/journal.pone.0171576.

Bajaj, I. and Singhal, R. (2011) ‘Poly (glutamic acid) – An emerging biopolymer of commercial interest’, *Bioresource technology*, 102(10), pp. 5551–5561. doi: http://dx.doi.org/10.1016/j.biortech.2011.02.047.

Bajpai, S. K. and Sharma, S. (2004) ‘Investigation of swelling/degradation behaviour of alginate beads crosslinked with Ca2+ and Ba2+ ions’, *Reactive and Functional Polymers*. Elsevier, 59(2), pp. 129–140. doi: 10.1016/J.REACTFUNCTPOLYM.2004.01.002.

Barton, F. B. *et al.* (2012) ‘Improvement in outcomes of clinical islet transplantation: 1999-2010’, *Diabetes care*, 35(7), pp. 1436–1445. doi: 10.2337/dc12-0063 [doi].

Basnett, P., Ching, K. Y., *et al.* (2013) ‘Aspirin-loaded P(3HO)/P(3HB) blend films: potential materials for biodegradable drug-eluting stents’, *Bioinspired, Biomimetic and Nanobiomaterials*. Thomas Telford Ltd, 2(3), pp. 141–153. doi: 10.1680/bbn.13.00009.

Basnett, P. *et al.* (2013) ‘Novel Poly(3-hydroxyoctanoate)/Poly(3-hydroxybutyrate) blends for medical applications’, *Reactive and Functional Polymers*, 73(10), pp. 1340–1348. doi: 10.1016/j.reactfunctpolym.2013.03.019.

Basnett, P., Ching, K. Y., *et al.* (2013) ‘Novel Poly (3-hydroxyoctanoate)/Poly (3-hydroxybutyrate) blends for medical applications’, *Reactive and Functional Polymers*, 73(10), pp. 1340–1348.

Basnett, P. *et al.* (2017) ‘Production of a novel medium chain length poly(3-hydroxyalkanoate) using unprocessed biodiesel waste and its evaluation as a tissue engineering scaffold’, *Microbial Biotechnology*, 10(6), pp. 1384–1399. doi: 10.1111/1751-7915.12782.

Basnett, P. and Roy, I. (2010) *Microbial production of biodegradable polymers and their role in cardiac stent development.*, *Current Research, Technology and Education Topics in Applied Microbiology and Microbial Biotechnology*. Edited by A. Mendez-Vilas. Badajoz, Spain: Formatex Research Centre.

Beck, J. *et al.* (2007) 'Islet Encapsulation: Strategies to Enhance Islet Cell Functions', *Tissue Engineering*, 13(3), pp. 589–599. doi: 10.1089/ten.2006.0183.

Bedian, L. *et al.* (2017) 'Bio-based materials with novel characteristics for tissue engineering applications – A review', *International Journal of Biological Macromolecules*. Elsevier, pp. 837–846. doi: 10.1016/j.ijbiomac.2017.02.048.

Bergenstal, R. M. *et al.* (2010) 'Effectiveness of sensor-augmented insulin-pump therapy in type 1 diabetes', *New England Journal of Medicine*, 363(4), pp. 311–320.

Berman, D. M. *et al.* (2009) 'Long-term survival of nonhuman primate islets implanted in an omental pouch on a biodegradable scaffold.', *American journal of transplantation : official journal of the American Society of Transplantation and the American Society of Transplant Surgeons*. NIH Public Access, 9(1), pp. 91–104. doi: 10.1111/j.1600-6143.2008.02489.x.

Bhatia, A. *et al.* (2007) 'Compatibility of Biodegradable Poly (lactic acid) (PLA) and Poly (butylene succinate) (PBS) Blends for Packaging Application "Compatibility of biodegradable poly (lactic acid) (PLA) and poly (butylene succinate) (PBS) blends for packaging application"', *Korea-Australia Rheology Journal*, 19(3), pp. 125–131. Available at: http://researchbank.rmit.edu.au/view/rmit:3381/n2006005712.pdf (Accessed: 10 October 2018).

Bian, Y.-Z. *et al.* (2009) 'Evaluation of poly(3-hydroxybutyrate-co-3-

hydroxyhexanoate) conduits for peripheral nerve regeneration', *Biomaterials*, 30(2), pp. 217–225. doi: https://doi.org/10.1016/j.biomaterials.2008.09.036.

Bidarra, S. J., Barrias, C. C. and Granja, P. L. (2014) 'Injectable alginate hydrogels for cell delivery in tissue engineering', *Acta Biomaterialia*. Elsevier, 10(4), pp. 1646–1662. doi: 10.1016/J.ACTBIO.2013.12.006.

Biomater, J. *et al.* (2009) 'Nanofibers for Tissue Engineering Review Paper: A Review of the Cellular Response on Electrospun', *Journal of Biomaterials Applications*, 24(1), pp. 7–29. doi: 10.1177/0885328208099086.

Bloch, K. *et al.* (2005) 'Functional activity of insulinoma cells (INS-1E) and pancreatic islets cultured in agarose cryogel sponges', *Journal of Biomedical Materials Research Part A*, 75(4), pp. 802–809.

Blomeier, H. *et al.* (2006) 'Polymer scaffolds as synthetic microenvironments for extrahepatic islet transplantation.', *Transplantation*. NIH Public Access, 82(4), pp. 452–9. doi: 10.1097/01.tp.0000231708.19937.21.

Bluestone, J. A., Herold, K. and Eisenbarth, G. (2010) 'Genetics, pathogenesis and clinical interventions in type [thinsp] 1 diabetes', *Nature*, 464(7293), pp. 1293–1300.

Bohari, S. P. M., Hukins, D. W. L. and Grover, L. M. (2011) 'Effect of calcium alginate concentration on viability and proliferation of encapsulated fibroblasts', *Bio - Medical Materials and Engineering*. IOS Press, 21, pp.

159–170. doi: 10.3233/BME-2011-0665.

Bonartseva, G. A. *et al.* (2017) ‘Alginate biosynthesis by Azotobacter bacteria’, *Applied Biochemistry and Microbiology*, 53(1), pp. 52–59. doi: 10.1134/S0003683817010070.

Boyan, B. D. *et al.* (1996) ‘Role of material surfaces in regulating bone and cartilage cell response’, *Biomaterials*. Elsevier, 17(2), pp. 137–146. doi: 10.1016/0142-9612(96)85758-9.

Caetano, G. F. *et al.* (2015) ‘Chitosan-alginate membranes accelerate wound healing’, *Journal of Biomedical Materials Research - Part B Applied Biomaterials*, 103(5), pp. 1013–1022. doi: 10.1002/jbm.b.33277.

Caliari, S. R. and Burdick, J. A. (2016) ‘A practical guide to hydrogels for cell culture’, *Nature Methods*. Nature Publishing Group, 13(5), pp. 405–414. doi: 10.1038/nmeth.3839.

Cassie, A. B. D. and Baxter, S. (1944) ‘Wettability of porous surfaces’, *Transactions of the Faraday Society*, 40, p. 546. doi: 10.1039/tf9444000546.

Chanasit, W. *et al.* (2016) ‘Efficient production of polyhydroxyalkanoates (PHAs) from Pseudomonas mendocina PSU using a biodiesel liquid waste (BLW) as the sole carbon source’, *Bioscience, Biotechnology, and Biochemistry*. Taylor & Francis, 80(7), pp. 1440–1450. doi: 10.1080/09168451.2016.1158628.

Chatterjee, S., Khunti, K. and Davies, M. J. (2017) ‘Type 2 diabetes’, *The Lancet*. Elsevier, 389(10085), pp. 2239–2251. doi: 10.1016/S0140-

6736(17)30058-2.

Chaturvedi, K. *et al.* (2015) ‘Oral insulin delivery using deoxycholic acid conjugated PEGylated polyhydroxybutyrate co-polymeric nanoparticles’, *Nanomedicine*, 10(10), pp. 1569–1583.

Chen, G.-Q. *et al.* (2015) ‘Engineering Biosynthesis Mechanisms for Diversifying Polyhydroxyalkanoates’, *Trends in Biotechnology*, 33(10), pp. 565–574. doi: 10.1016/j.tibtech.2015.07.007.

Chen, G.-Q., König, K.-H. and Lafferty, R. M. (1991) ‘Occurrence of poly-d(−)-3-hydroxyalkanoates in the genus Bacillus’, *Fems Microbiology Letters*. Wiley/Blackwell (10.1111), 84(2), pp. 173–176. doi: 10.1111/j.1574-6968.1991.tb04592.x.

Chen, G.-Q. and Wu, Q. (2005) ‘The application of polyhydroxyalkanoates as tissue engineering materials’, *Biomaterials*, 26(33), pp. 6565–6578.

Chen, G., Ushida, T. and Tateishi, T. (2001) ‘Development of biodegradable porous scaffolds for tissue engineering’, *Materials Science and Engineering: C*. Elsevier, 17(1–2), pp. 63–69. doi: 10.1016/S0928-4931(01)00338-1.

Chen, G., Ushida, T. and Tateishi, T. (2002) ‘Scaffold Design for Tissue Engineering’, *Macromol. Biosci*, 2, pp. 67–77.

Chen, J.-P. *et al.* (1998) ‘Microencapsulation of islets in PEG-amine modified alginate-poly (L-lysine)-alginate microcapsules for constructing bioartificial pancreas’, *Journal of Fermentation and Bioengineering*, 86(2), pp. 185–190.

Chen, Q., Liang, S. and Thouas, G. A. (2013) 'Elastomeric biomaterials for tissue engineering', *Progress in Polymer Science*, 38, pp. 584–671. doi: 10.1016/j.progpolymsci.2012.05.003.

Christman, K. L. *et al.* (2004) 'Fibrin Glue Alone and Skeletal Myoblasts in a Fibrin Scaffold Preserve Cardiac Function after Myocardial Infarction', *Tissue Engineering*. Mary Ann Liebert, Inc. , 10(3–4), pp. 403–409. doi: 10.1089/107632704323061762.

Chun, S. *et al.* (2008) 'Adhesive Growth of Pancreatic Islet Cells on a Polyglycolic Acid Fibrous Scaffold', *Transplantation proceedings*, 40(5), pp. 1658–1663. doi: http://dx.doi.org/10.1016/j.transproceed.2008.02.088.

Clementi, F. (1997) 'Alginate Production by Azotobacter Vinelandii', *Critical Reviews in Biotechnology*, 17(4), pp. 327–361. doi: 10.3109/07388559709146618.

Clery, P. *et al.* (2017) 'Systematic review and meta-analysis of the efficacy of interventions for people with Type 1 diabetes mellitus and disordered eating', *Diabetic Medicine*. Wiley/Blackwell (10.1111), 34(12), pp. 1667–1675. doi: 10.1111/dme.13509.

Coppi, G. *et al.* (2001) 'Chitosan-Alginate Microparticles as a Protein Carrier', *Drug Development and Industrial Pharmacy*, 27(5), pp. 393–400. doi: 10.1081/DDC-100104314.

Coronel, M. M. and Stabler, C. L. (2013) 'Engineering a local microenvironment for pancreatic islet replacement', *Current opinion in biotechnology*, 24(5), pp. 900–908. doi: 10.1016/j.copbio.2013.05.004.

Cruise, G. M. *et al.* (1998) ‘A sensitivity study of the key parameters in the interfacial photopolymerization of poly (ethylene glycol) diacrylate upon porcine islets’, *Biotechnology and bioengineering*, 57(6), pp. 655–665.

Dai, Y. *et al.* (2008) ‘Swelling characteristics and drug delivery properties of nifedipine-loaded pH sensitive alginate–chitosan hydrogel beads’, *Journal of Biomedical Materials Research Part B: Applied Biomaterials*. Wiley-Blackwell, 86B(2), pp. 493–500. doi: 10.1002/jbm.b.31046.

Daneman, D. (2006) ‘Type 1 Diabetes’, *The Lancet*, 367(9513), pp. 847–858.

Daoud, J. T. *et al.* (2011) ‘Long-term in vitro human pancreatic islet culture using three-dimensional microfabricated scaffolds’, *Biomaterials*, 32(6), pp. 1536–1542. doi: http://dx.doi.org/10.1016/j.biomaterials.2010.10.036.

Davis, N. E. *et al.* (2012) ‘Enhanced function of pancreatic islets co-encapsulated with ECM proteins and mesenchymal stromal cells in a silk hydrogel.’, *Biomaterials*. NIH Public Access, 33(28), pp. 6691–7. doi: 10.1016/j.biomaterials.2012.06.015.

Deng, Y. *et al.* (2002) ‘Study on the three - dimensional proliferation of rabbit articular cartilage - derived chondrocytes on polyhydroxyalkanoate scaffolds’, *Biomaterials*, 23, pp. 4049–4056.

Diabetes UK (2017) *Diabetes UK- Facts and Stats*. Available at: https://diabetes-resources-production.s3-eu-west-1.amazonaws.com/diabetes-storage/migration/pdf/DiabetesUK_Facts_Stats_Oct16.pdf (Accessed: 3

February 2018).

Dixon, G. *et al.* (2003) ‘A comparative study of amino acid consumption by rat islet cells and the clonal beta-cell line BRIN-BD11-the functional significance of L-alanine’, *Journal of Endocrinology*, 179, pp. 447–454. Available at: http://www.endocrinology.org (Accessed: 14 May 2019).

Dolenšek, J., Rupnik, M. S. and Stožer, A. (2015) ‘Structural similarities and differences between the human and the mouse pancreas’, *Islets*. Taylor & Francis, 7(1), p. e1024405. doi: 10.1080/19382014.2015.1024405.

Dolgin, E. (2014) ‘Encapsulate this’, *Nature Medicine*, 20(1), pp. 9–11. doi: 10.1038/nm0114-9.

Dolgin, E. (2016) ‘Diabetes: Encapsulating the problem’, *Nature*, 540(7632), pp. S60–S62. doi: 10.1038/540S60a.

Dorati, R. *et al.* (2010) ‘Effect of porogen on the physico-chemical properties and degradation performance of PLGA scaffolds’, *Polymer Degradation and Stability*. Elsevier, 95(4), pp. 694–701.

Du, H., Chandaroy, P. and Hui, S. W. (1997) ‘Grafted poly-(ethylene glycol) on lipid surfaces inhibits protein adsorption and cell adhesion’, *Biochimica et Biophysica Acta (BBA) - Biomembranes*. Elsevier, 1326(2), pp. 236–248. doi: 10.1016/S0005-2736(97)00027-8.

Dubey, P. (2017) *Development of cardiac patches using medium chain length polyhydroxyalkanoates for cardiac tissue engineering*. University of Westminster. Available at: http://www.westminster.ac.uk/westminsterresearch (Accessed: 1 March

2018).

Dufour, J. M. *et al.* (2005) ‘Development of an Ectopic Site for Islet Transplantation Using Biodegradable Scaffolds’, *Tissue Engineering*, 11(9–10), pp. 1323–1331.

Dufrane, D., Goebbels, R. M. and Gianello, P. (2010) ‘Alginate macroencapsulation of pig islets allows correction of streptozotocin-induced diabetes in primates up to 6 months without immunosuppression’, *Transplantation*, 90(10), pp. 1054–1062. doi: 10.1097/TP.0b013e3181f6e267 [doi].

Dufresne, A. and Vincendon, M. (2000) ‘Poly(3-hydroxybutyrate) and poly(3-hydroxyoctanoate) blends: Morphology and mechanical behavior’, *Macromolecules*. American Chemical Society, 33(8), pp. 2998–3008. doi: 10.1021/ma991854a.

Duvivier-Kali, V. F. *et al.* (2001) ‘Complete protection of islets against allorejection and autoimmunity by a simple barium-alginate membrane’, *Diabetes*, 50(8), pp. 1698–1705.

Dvir-Ginzberg, M. *et al.* (2003) ‘Liver Tissue Engineering within Alginate Scaffolds: Effects of Cell-Seeding Density on Hepatocyte Viability, Morphology and Function’, *Tissue Engineering*, 9(4), pp. 757–766.

El-Hadi, A. *et al.* (2002) ‘Correlation between degree of crystallinity, morphology, glass temperature, mechanical properties and biodegradation of poly (3-hydroxyalkanoate) PHAs and their blends’, *Polymer Testing*, 21, pp. 665–674. Available at: www.elsevier.com/locate/polytest (Accessed: 11

April 2018).

Elçin, Y. M. *et al.* (2003) 'Pancreatic Islet Culture and Transplantation Using Chitosan and PLGA Scaffolds', in. Springer, Boston, MA, pp. 255–264. doi: 10.1007/978-1-4615-0063-6_19.

Elliott, R. B. *et al.* (2005) 'Intraperitoneal Alginate-Encapsulated Neonatal Porcine Islets in a Placebo-Controlled Study With 16 Diabetic Cynomolgus Primates', *Transplantation Proceedings*, 37(8), pp. 3505–3508. doi: 10.1016/j.transproceed.2005.09.038.

Fernández-Hervás, M. . *et al.* (1998) 'In vitro evaluation of alginate beads of a diclofenac salt', *International Journal of Pharmaceutics*. Elsevier, 163(1–2), pp. 23–34. doi: 10.1016/S0378-5173(97)00333-5.

Filipović-Grćić, J. *et al.* (1995) 'Macromolecular prodrugs. IV. alginate-chitosan microspheres of PHEA-L-dopa adduct', *International Journal of Pharmaceutics*. Elsevier, 116(1), pp. 39–44. doi: 10.1016/0378-5173(94)00269-B.

Flatt, P. R. and Bailey, C. J. (1981) 'Abnormal plasma glucose and insulin responses in heterozygous lean (ob/) mice', *Diabetologia*, 20(5), pp. 573–577.

Förch, R., Schönherr, H. and Jenkins, A. T. A. (2009) *Surface design : applications in bioscience and nanotechnology*. Wiley-VCH.

Franklin, M. J. *et al.* (2011) 'Biosynthesis of the pseudomonas aeruginosa extracellular polysaccharides, alginate, Pel, and Psl', *Frontiers in Microbiology*. Frontiers, p. 167. doi: 10.3389/fmicb.2011.00167.

Fritschy, W. M. *et al.* (1991) ‘Glucose tolerance and plasma insulin response to intravenous glucose infusion and test meal in rats with microencapsulated islet allografts’, *Diabetologia*, 34(8), pp. 542–547.

Fukui, T. and Doi, Y. (1998) ‘Efficient production of polyhydroxyalkanoates from plant oils by Alcaligenes eutrophus and its recombinant strain’, *Applied Microbiology and Biotechnology*. Springer-Verlag, 49(3), pp. 333–336. doi: 10.1007/s002530051178.

Gajra, B. *et al.* (2012) ‘Poly vinyl alcohol hydrogel and its pharmaceutical and biomedical applications: A review’, *International Journal of Pharmaceutical Research*, 4(2), pp. 20–26.

Garg, T., Singh, S. and Goyal, A. K. (2013) ‘Stimuli-sensitive hydrogels: an excellent carrier for drug and cell delivery’, *Critical Reviews^{TM} in Therapeutic Drug Carrier Systems*, 30(5).

Garkavenko, O. *et al.* (2011) ‘Islets transplantation: New Zealand experience’, *Xenotransplantation*, 18(1), p. 60.

Gerich, J. E. (2002) ‘Is reduced first-phase insulin release the earliest detectable abnormality in individuals destined to develop type 2 diabetes?’, *Diabetes*. American Diabetes Association, 51 Suppl 1(suppl 1), pp. S117-21. doi: 10.2337/DIABETES.51.2007.S117.

Gerlier, D. and Thomasset, N. (1986) ‘Use of MTT colorimetric assay to measure cell activation’, *Journal of immunological methods*, 94(1–2), pp. 57–63.

Gibly, R. F. *et al.* (2011) ‘Advancing islet transplantation: from engraftment

to the immune response', *Diabetologia*. Springer-Verlag, 54(10), pp. 2494–2505. doi: 10.1007/s00125-011-2243-0.

Godbole, S. *et al.* (2003) 'Preparation and characterization of biodegradable poly-3-hydroxybutyrate–starch blend films', *Bioresource Technology*. Elsevier, 86(1), pp. 33–37. doi: 10.1016/S0960-8524(02)00110-4.

Godfrey, K. J. *et al.* (2012) 'Stem cell-based treatments for Type 1 diabetes mellitus: bone marrow, embryonic, hepatic, pancreatic and induced pluripotent stem cells', *Diabetic Medicine*, 29(1), pp. 14–23. doi: 10.1111/j.1464-5491.2011.03433.x.

Goh, S.-K. *et al.* (2013) 'Perfusion-decellularized pancreas as a natural 3D scaffold for pancreatic tissue and whole organ engineering.', *Biomaterials*. NIH Public Access, 34(28), pp. 6760–72. doi: 10.1016/j.biomaterials.2013.05.066.

Gough, J. E., Scotchford, C. A. and Downes, S. (2002) 'Cytotoxicity of glutaraldehyde crosslinked collagen/poly(vinyl alcohol) films is by the mechanism of apoptosis', *Journal of Biomedical Materials Research*, 61(1), pp. 121–130. doi: 10.1002/jbm.10145.

Griffith, L. G. and Naughton, G. (2002) 'Tissue engineering--current challenges and expanding opportunities.', *Science* . American Association for the Advancement of Science, 295(5557), pp. 1009–14. doi: 10.1126/science.1069210.

Gross, R. A. *et al.* (1989) 'The biosynthesis and characterization of poly ($β$-hydroxyalkanoates) produced by Pseudomonas oleovorans',

Macromolecules. ACS Publications, 22(3), pp. 1106–1115.

Gruessner, R. W. G. and Gruessner, A. C. (2014) 'What Defines Success in Pancreas and Islet Transplantation—Insulin Independence or Prevention of Hypoglycemia? A Review', *Transplantation proceedings*, 46(6), pp. 1898–1899. doi: http://dx.doi.org/10.1016/j.transproceed.2014.06.004.

Gunatillake, P. A. and Adhikari, R. (2003) 'Biodegradable synthetic polymers for tissue engineering', *Eur Cell Mater*, 5(1), pp. 1–16.

Gupta, R. K. *et al.* (2005) 'The MODY1 gene HNF-4alpha regulates selected genes involved in insulin secretion.', *The Journal of clinical investigation*. American Society for Clinical Investigation, 115(4), pp. 1006–15. doi: 10.1172/JCI22365.

Gursel, I. *et al.* (2002) 'In vitro antibiotic release from poly(3-hydroxybutyrate-co-3-hydroxyvalerate) rods', *Journal of Microencapsulation*. Taylor & Francis, 19(2), pp. 153–164. doi: 10.1080/02652040110065413.

Halami, P. M. (2008a) 'Production of polyhydroxyalkanoate from starch by the native isolate Bacillus cereus CFR06', *World Journal of Microbiology and Biotechnology*. Springer Netherlands, 24(6), pp. 805–812. doi: 10.1007/s11274-007-9543-z.

Halami, P. M. (2008b) 'Production of polyhydroxyalkanoate from starch by the native isolate Bacillus cereus CFR06', *World Journal of Microbiology and Biotechnology*. Springer Netherlands, 24(6), pp. 805–812. doi: 10.1007/s11274-007-9543-z.

Hamid, M. *et al.* (2001) 'Functional examination of microencapsulated bioengineered insulin-secreting beta-cells', *Cell biology international*, 25(6), pp. 553–556.

Hamid, M. *et al.* (2002) 'COMPARISON OF THE SECRETORY PROPERTIES OF FOUR INSULIN-SECRETING CELL LINES', *Endocrine Research*. Taylor & Francis, 28(1–2), pp. 35–47. doi: 10.1081/ERC-120004536.

Hart, D. R. *et al.* (2015) 'Current Concepts in the Use of PLLA', *Plastic and Reconstructive Surgery*, 136, p. 180S–187S. doi: 10.1097/PRS.0000000000001833.

Hassing, L. B. *et al.* (2004) 'Comorbid type 2 diabetes mellitus and hypertension exacerbates cognitive decline: Evidence from a longitudinal study', *Age and Ageing*, 33(4), pp. 355–361. doi: 10.1093/ageing/afh100.

Hay, I. D. *et al.* (2014) 'Genetics and regulation of bacterial alginate production', *Environmental Microbiology*, 16(10), pp. 2997–3011. doi: 10.1111/1462-2920.12389.

Hayati, A. N. *et al.* (2012) 'Characterization of poly(3-hydroxybutyrate)/nano-hydroxyapatite composite scaffolds fabricated without the use of organic solvents for bone tissue engineering applications', *Materials Science and Engineering C*. Elsevier, 32(3), pp. 416–422. doi: 10.1016/j.msec.2011.11.013.

He, W. *et al.* (1998) 'Production of novel polyhydroxyalkanoates by *Pseudomonas stutzeri* 1317 from glucose and soybean oil', *FEMS*

Microbiology Letters. Oxford University Press, 169(1), pp. 45–49. doi: 10.1111/j.1574-6968.1998.tb13297.x.

Henquin, J.-C. and Nenquin, M. (2016) 'Dynamics and Regulation of Insulin Secretion in Pancreatic Islets from Normal Young Children', *PLOS ONE*. Edited by R. Kulkarni. Public Library of Science, 11(11), p. e0165961. doi: 10.1371/journal.pone.0165961.

Hess, S. C. *et al.* (2017) 'Gene expression in human adipose-derived stem cells: Comparison of 2D films, 3D electrospun meshes or co-cultured scaffolds with two-way paracrine effects', *European Cells and Materials*, 34, pp. 232–248. doi: 10.22203/eCM.v034a15.

Hinton, T. J. *et al.* (2015) 'Three-dimensional printing of complex biological structures by freeform reversible embedding of suspended hydrogels', *Science Advances*. American Association for the Advancement of Science, 1(9), pp. e1500758–e1500758. doi: 10.1126/sciadv.1500758.

Hoare, T. R. and Kohane, D. S. (2008) 'Hydrogels in drug delivery: Progress and challenges', *Polymer*. Elsevier, 49(8), pp. 1993–2007. doi: 10.1016/J.POLYMER.2008.01.027.

Hoffman, A. S. (2012) 'Hydrogels for biomedical applications', *Advanced Drug Delivery Reviews*, 64(SUPPL.), pp. 18–23. doi: 10.1016/j.addr.2012.09.010.

Hollister, S. J. (2005) 'Porous scaffold design for tissue engineering', *Nature materials*. Nature Publishing Group, 4(7), p. 518.

Hopcroft, D. W., Mason, D. R. and Scott, R. S. (1985) 'Structure-function

relationships in pancreatic islets: Support for intraislet modulation of insulin secretion', *Endocrinology*, 117(5), pp. 2073–2080. doi: 10.1210/endo-117-5-2073.

Hou, Y. *et al.* (2009) 'Excellent effect of three-dimensional culture condition on pancreatic islets', *Diabetes research and clinical practice*, 86(1), pp. 11–15. doi: http://dx.doi.org/10.1016/j.diabres.2009.07.010.

Huang, Y. *et al.* (2005) 'In vitro characterization of chitosan–gelatin scaffolds for tissue engineering', *Biomaterials*. Elsevier, 26(36), pp. 7616–7627. doi: 10.1016/J.BIOMATERIALS.2005.05.036.

Huijberts, G. N. *et al.* (1992) 'Pseudomonas putida KT2442 cultivated on glucose accumulates poly(3-hydroxyalkanoates) consisting of saturated and unsaturated monomers.', *Applied and environmental microbiology*. American Society for Microbiology, 58(2), pp. 536–44. Available at: http://www.ncbi.nlm.nih.gov/pubmed/1610179 (Accessed: 11 April 2018).

Huijberts, G. N. *et al.* (1994) '13C nuclear magnetic resonance studies of Pseudomonas putida fatty acid metabolic routes involved in poly (3-hydroxyalkanoate) synthesis.', *Journal of bacteriology*. Am Soc Microbiol, 176(6), pp. 1661–1666.

Humbel, R. E. (1965) 'Biosynthesis of the two chains of insulin', *Proceedings of the National Academy*. Available at: http://www.pnas.org/content/53/4/853.short (Accessed: 2 February 2018).

Hutmacher, D. W. (2000) 'Scaffolds in tissue engineering bone and cartilage', *Biomaterials*, 21(24), pp. 2529–2543. doi: 10.1016/S0142-

9612(00)00121-6.

Hwang, P. T. J. *et al.* (2016) ‘Progress and challenges of the bioartificial pancreas’, *Nano Convergence*, 3(1), p. 28. doi: 10.1186/s40580-016-0088-4.

Iacovacci, V. *et al.* (2016) ‘The bioartificial pancreas (BAP): Biological, chemical and engineering challenges’, *Biochemical Pharmacology*, 100, pp. 12–27. doi: 10.1016/j.bcp.2015.08.107.

Inoue, K. *et al.* (1992) ‘Experimental hybrid islet transplantation: application of polyvinyl alcohol membrane for entrapment of islets.’, *Pancreas*, 7(5), pp. 562–8. Available at: http://www.ncbi.nlm.nih.gov/pubmed/1513803 (Accessed: 9 February 2018).

Ionescu-Tirgoviste, C. *et al.* (2015) ‘A 3D map of the islet routes throughout the healthy human pancreas’, *Scientific Reports*. Nature Publishing Group, 5(1), p. 14634. doi: 10.1038/srep14634.

Iwata, H. *et al.* (1992) ‘Agarose for a bioartificial pancreas’, *Journal of Biomedical Materials Research*, 26(7), pp. 967–977. doi: 10.1002/jbm.820260711.

Jacobs-Tulleneers-Thevissen, D. *et al.* (2013) ‘Sustained function of alginate-encapsulated human islet cell implants in the peritoneal cavity of mice leading to a pilot study in a type 1 diabetic patient’, *Diabetologia*, 56(7), pp. 1605–1614.

Jain, D. and Bar-Shalom, D. (2014) ‘Alginate drug delivery systems:

application in context of pharmaceutical and biomedical research', *Drug Development and Industrial Pharmacy*, 40(12), pp. 1576–1584. doi: 10.3109/03639045.2014.917657.

Jalili, R. B. *et al.* (2011) 'Fibroblast populated collagen matrix promotes islet survival and reduces the number of islets required for diabetes reversal', *Journal of Cellular Physiology*, 226(7), pp. 1813–1819. doi: 10.1002/jcp.22515.

Janik, H. and Marzec, M. (2015) 'A review: Fabrication of porous polyurethane scaffolds', *Materials Science and Engineering: C*, 48, pp. 586–591. doi: 10.1016/j.msec.2014.12.037.

Juang, J.-H. *et al.* (1996) 'OUTCOME OF SUBCUTANEOUS ISLET TRANSPLANTATION IMPROVED BY POLYMER DEVICE1', *Transplantation*, 61(11), pp. 1557–1561.

Kahar, P. *et al.* (2004) 'High yield production of polyhydroxyalkanoates from soybean oil by Ralstonia eutropha and its recombinant strain', *Polymer Degradation and Stability*. Elsevier, 83(1), pp. 79–86. doi: 10.1016/S0141-3910(03)00227-1.

Karageorgiou, V. and Kaplan, D. (2005) 'Porosity of 3D biomaterial scaffolds and osteogenesis', *Biomaterials*. Elsevier, 26(27), pp. 5474–5491. doi: 10.1016/J.BIOMATERIALS.2005.02.002.

Karri, V. V. S. R. *et al.* (2016) 'Curcumin loaded chitosan nanoparticles impregnated into collagen-alginate scaffolds for diabetic wound healing', *International Journal of Biological Macromolecules*, 93, pp. 1519–1529.

doi: 10.1016/j.ijbiomac.2016.05.038.

Kawazoe, N. *et al.* (2009) 'Three-dimensional Cultures of Rat Pancreatic RIN-5F Cells in Porous PLGA-collagen Hybrid Scaffolds', *Journal of Bioactive and Compatible Polymers*, 24(1), pp. 25–42. doi: 10.1177/0883911508099439.

Kepsutlu, B. *et al.* (2014) 'Design of Bioartificial Pancreas with Functional Micro/Nano-Based Encapsulation of Islets', *Current Pharmaceutical Biotechnology*, 15(7), pp. 590–608.

Keshavarz, T. and Roy, I. (2010) 'Polyhydroxyalkanoates: bioplastics with a green agenda', *Current opinion in microbiology*, 13(3), pp. 321–326.

Khademhosseini, A. and Langer, R. (2016) 'A decade of progress in tissue engineering', *Nature protocols*. Nature Publishing Group, 11(10), p. 1775.

Khanna, S. and Srivastava, A. K. (2005) 'Recent advances in microbial polyhydroxyalkanoates', *Process Biochemistry*, 40(2), pp. 607–619.

Kim, D. Y. *et al.* (2007) 'Biosynthesis, Modification, and Biodegradation of Bacterial Medium-Chain-Length Polyhydroxyalkanoates', *The Journal of Microbiology The Microbiological Society of Korea*, 45(2). Available at: https://www.researchgate.net/profile/Young_Rhee2/publication/6347200_Biosynthesis_modification_and_biodegradation_of_bacterial_medium-chain-length_polyhydroxyalkanoates/links/0912f509b08fe5d1da000000.pdf (Accessed: 18 February 2018).

Kim, I.-Y. *et al.* (2008) 'Chitosan and its derivatives for tissue engineering

applications', *Biotechnology Advances*, 26(1), pp. 1–21.

Kin, T. *et al.* (2008) 'The Use of an Approved Biodegradable Polymer Scaffold as a Solid Support System for Improvement of Islet Engraftment', *Artificial Organs*, 32(12), pp. 990–993. doi: 10.1111/j.1525-1594.2008.00688.x.

Kizilel, S. *et al.* (2010) 'Encapsulation of Pancreatic Islets Within Nano-Thin Functional Polyethylene Glycol Coatings for Enhanced Insulin Secretion', *Tissue Engineering Part A*, 16(7), pp. 2217–2228. doi: 10.1089/ten.tea.2009.0640.

Kizilel, S., Garfinkel, M. and Opara, E. (2005) 'The Bioartificial Pancreas: Progress and Challenges', *DIABETES TECHNOLOGY & THERAPEUTICS*, 7(6).

Klein, B. E. and Klein, R. (2015) 'Further insight on the limits of success of glycemic control in type 1 diabetes', *Diabetes*, 64(2), pp. 341–343. doi: 10.2337/db14-1447 [doi].

Kobayashi, T. *et al.* (2003) 'Indefinite islet protection from autoimmune destruction in nonobese diabetic mice by agarose microencapsulation without immunosuppression1', *Transplantation*, 75(5), pp. 619–625. doi: 10.1097/01.TP.0000053749.36365.7E.

Kong, H. J., Smith, M. K. and Mooney, D. J. (2003) 'Designing alginate hydrogels to maintain viability of immobilized cells', *Biomaterials*. Elsevier, 24(22), pp. 4023–4029. doi: 10.1016/S0142-9612(03)00295-3.

Krishnan, R. *et al.* (2014) 'Islet and stem cell encapsulation for clinical

transplantation.', *The review of diabetic studies : RDS*. Society for Biomedical Diabetes Research, 11(1), pp. 84–101. doi: 10.1900/RDS.2014.11.84.

Kulkarni, A. R. *et al.* (2000) 'Preparation of Cross-Linked Sodium Alginate Microparticles Using Glutaraldehyde in Methanol', *Drug Development and Industrial Pharmacy*. Taylor & Francis, 26(10), pp. 1121–1124. doi: 10.1081/DDC-100100278.

Kulkarni, R. N. (2004) 'The islet β-cell', *The International Journal of Biochemistry & Cell Biology*. Pergamon, 36(3), pp. 365–371. doi: 10.1016/J.BIOCEL.2003.08.010.

Kulpreecha, S. *et al.* (2009) 'Inexpensive fed-batch cultivation for high poly(3-hydroxybutyrate) production by a new isolate of Bacillus megaterium', *Journal of Bioscience and Bioengineering*. Elsevier, 107(3), pp. 240–245. doi: 10.1016/J.JBIOSC.2008.10.006.

Kuo, C. K. and Ma, P. X. (2001) 'Ionically crosslinked alginate hydrogels as scaffolds for tissue engineering: Part 1. Structure, gelation rate and mechanical properties', *Biomaterials*, 22(6), pp. 511–521. doi: 10.1016/S0142-9612(00)00201-5.

Lang, V. and Light, P. E. (2010) 'The molecular mechanisms and pharmacotherapy of ATP-sensitive potassium channel gene mutations underlying neonatal diabetes.', *Pharmacogenomics and personalized medicine*. Dove Press, 3, pp. 145–61. doi: 10.2147/PGPM.S6969.

Lee, B. R. *et al.* (2012) 'In situ formation and collagen-alginate composite

encapsulation of pancreatic islet spheroids', *Biomaterials*, 33(3), pp. 837–845. doi: http://dx.doi.org/10.1016/j.biomaterials.2011.10.014.

Lee, J. and McCarthy, S. (2009) 'Biodegradable Poly(lactic acid) Blends with Chemically Modified Polyhydroxyoctanoate Through Chain Extension', *Journal of Polymers and the Environment*. Springer US, 17(4), pp. 240–247. doi: 10.1007/s10924-009-0144-9.

Lee, K. Y. and Mooney, D. J. (2001) 'Hydrogels for Tissue Engineering', *Chemical Reviews*, 101(7), pp. 1869–1880. doi: 10.1021/cr000108x.

Lee, K. Y. and Mooney, D. J. (2012) 'Alginate: properties and biomedical applications', *Progress in Polymer Science*, 37(1), pp. 106–126. doi: 10.1016/j.progpolymsci.2011.06.003.

Lee, S. Y. (1996a) 'Bacterial polyhydroxyalkanoates', *Biotechnology and bioengineering*, 49(1), pp. 1–14.

Lee, S. Y. (1996b) 'Plastic bacteria? Progress and prospects for polyhydroxyalkanoate production in bacteria', *Trends in Biotechnology*. Elsevier, 14(11), pp. 431–438.

Leenslag, J. W. *et al.* (1987) 'Resorbable materials of poly (L-lactide): VII. In vivo and in vitro degradation', *Biomaterials*. Elsevier, 8(4), pp. 311–314.

Lemoigne, M. (1926) 'Products of dehydration and of polymerization of β-hydroxybutyric acid', *Bull Soc Chem Biol*, 8, pp. 770–782.

Li, Y., Thouas, G. A. and Chen, Q.-Z. (2012) 'Biodegradable soft elastomers: synthesis/properties of materials and fabrication of scaffolds',

RSC Advances, 2, pp. 8229–8242. doi: 10.1039/c2ra20736b.

Li, Z., Yang, J. and Loh, X. J. (2016) 'Polyhydroxyalkanoates: opening doors for a sustainable future', *NPG Asia Materials*. Nature Publishing Group, 8(4), pp. e265–e265. doi: 10.1038/am.2016.48.

Liljenquist, J. E. *et al.* (1974) 'Effects of Glucagon on Lipolysis and Ketogenesis in Normal and Diabetic Men', *The Journal of Clinical Investigation*. American Society for Clinical Investigation, 53(1), pp. 190–197. doi: 10.1172/JCI107537.

Lim, F. and Sun, A. M. (1980) 'Microencapsulated islets as bioartificial endocrine pancreas', *Science (New York, N.Y.)*, 210(4472), pp. 908–910.

Lin, C.-C. and Anseth, K. S. (2011) 'Cell-cell communication mimicry with poly(ethylene glycol) hydrogels for enhancing beta-cell function.', *Proceedings of the National Academy of Sciences of the United States of America*. National Academy of Sciences, 108(16), pp. 6380–5. doi: 10.1073/pnas.1014026108.

Liu, Q. *et al.* (2011) 'Biosynthesis of poly(3-hydroxydecanoate) and 3-hydroxydodecanoate dominating polyhydroxyalkanoates by β-oxidation pathway inhibited Pseudomonas putida', *Metabolic Engineering*, 13(1), pp. 11–17. doi: 10.1016/j.ymben.2010.10.004.

Lizarraga-Valderrama, L. R. *et al.* (2015) 'Nerve tissue engineering using blends of poly(3-hydroxyalkanoates) for peripheral nerve regeneration', *Engineering in Life Sciences*, 15(6), pp. 612–621. doi: 10.1002/elsc.201400151.

Lizarraga-Valderrama, L. R. *et al.* (2015) ‘Nerve tissue engineering using blends of poly (3-hydroxyalkanoates) for peripheral nerve regeneration’, *Engineering in Life Sciences*.

Llacua, A. *et al.* (2016) ‘Extracellular matrix components supporting human islet function in alginate-based immunoprotective microcapsules for treatment of diabetes’, *Journal of biomedical materials research Part A*. Wiley Online Library, 104(7), pp. 1788–1796.

Lloyd, A. W., Faragher, R. G. A. and Denyer, S. P. (2001) ‘Ocular biomaterials and implants’, *Biomaterials*. Elsevier, 22(8), pp. 769–785. doi: 10.1016/S0142-9612(00)00237-4.

Loh, Q. L. and Choong, C. (2013) ‘Three-dimensional scaffolds for tissue engineering applications: role of porosity and pore size.’, *Tissue engineering. Part B, Reviews*. Mary Ann Liebert, Inc., 19(6), pp. 485–502. doi: 10.1089/ten.TEB.2012.0437.

Van Loon, L. J. C. *et al.* (2003) ‘Amino Acid Ingestion Strongly Enhances Insulin Secretion in Patients With Long-Term Type 2 Diabetes’, *Diabetes care*, 26(3), pp. 625–630. Available at: http://care.diabetesjournals.org/content/diacare/26/3/625.full.pdf (Accessed: 14 May 2019).

Lorenzo, C. *et al.* (2010) ‘Disposition index, glucose effectiveness, and conversion to type 2 diabetes: the Insulin Resistance Atherosclerosis Study (IRAS).’, *Diabetes care*. American Diabetes Association, 33(9), pp. 2098–103. doi: 10.2337/dc10-0165.

Lou, K.-J. (2014) ‘BetaLogics’ in vitro β cells’, *SciBX: Science-Business eXchange*, 7(39).

Lu, L. *et al.* (2000) ‘In vitro and in vivo degradation of porous poly(dl-lactic-co-glycolic acid) foams’, *Biomaterials*. Elsevier, 21(18), pp. 1837–1845. doi: 10.1016/S0142-9612(00)00047-8.

Lucas-Clerc, C. *et al.* (1993) ‘Long-term culture of human pancreatic islets in an extracellular matrix: morphological and metabolic effects’, *Molecular and Cellular Endocrinology*, 94(1), pp. 9–20. doi: 10.1016/0303-7207(93)90046-M.

Ludwig, B. *et al.* (2012) ‘Improvement of islet function in a bioartificial pancreas by enhanced oxygen supply and growth hormone releasing hormone agonist’, *Proceedings of the National Academy of Sciences of the United States of America*, 109(13), pp. 5022–5027. doi: 10.1073/pnas.1201868109 [doi].

Ludwig, B. *et al.* (2013) ‘Transplantation of human islets without immunosuppression’, *Proceedings of the National Academy of Sciences*, 110(47), pp. 19054–19058. doi: 10.1073/pnas.1317561110.

Lukasiewicz, B. *et al.* (2018) ‘Binary polyhydroxyalkanoate systems for soft tissue engineering’, *Acta Biomaterialia*. Elsevier, 71, pp. 225–234. doi: 10.1016/J.ACTBIO.2018.02.027.

Lukic, M. L., Pejnovic, N. and Lukic, A. (2014) ‘New insight into early events in type 1 diabetes: role for islet stem cell exosomes’, *Diabetes*, 63(3), pp. 835–837. doi: 10.2337/db13-1786 [doi].

Ma, P. X. (2004) ‘Scaffolds for tissue fabrication’, *Materials Today*. Elsevier, 7(5), pp. 30–40. doi: 10.1016/S1369-7021(04)00233-0.

Macdonald, P. E. *et al.* (2002) ‘The Multiple Actions of GLP-1 on the Process of Glucose-Stimulated Insulin Secretion’, *Diabetes*, 51(3), pp. S434–S442. Available at: http://diabetes.diabetesjournals.org/content/diabetes/51/suppl_3/S434.full.pdf (Accessed: 14 May 2019).

Maki, T. *et al.* (1991) ‘Successful treatment of diabetes with the biohybrid artificial pancreas in dogs.’, *Transplantation*, 51(1), pp. 43–50.

Malafaya, P. B., Silva, G. A. and Reis, R. L. (2007) ‘Natural–origin polymers as carriers and scaffolds for biomolecules and cell delivery in tissue engineering applications’, *Advanced Drug Delivery Reviews*, 59(4–5), pp. 207–233. doi: 10.1016/j.addr.2007.03.012.

Mao, G. *et al.* (2009) ‘The reversal of hyperglycaemia in diabetic mice using PLGA scaffolds seeded with islet-like cells derived from human embryonic stem cells’, *Biomaterials*, 30(9), pp. 1706–1714. doi: http://dx.doi.org/10.1016/j.biomaterials.2008.12.030.

Marchioli, G. *et al.* (2015) ‘Fabrication of three-dimensional bioplotted hydrogel scaffolds for islets of Langerhans transplantation’, *Biofabrication*, 7(2), p. 025009. doi: 10.1088/1758-5090/7/2/025009.

Marchioli, G., Luca, A. Di, *et al.* (2016) ‘Hybrid Polycaprolactone/Alginate Scaffolds Functionalized with VEGF to Promote de Novo Vessel Formation for the Transplantation of Islets of Langerhans’, *Advanced healthcare*

materials.

Marchioli, G., Hertsig, D., *et al.* (2016) 'Salt-Leached Porous Scaffolds functionalized with VEGF for Islets of Langerhans Transplantation', *A journey towards an extrahepatic islet delivery device with a tissue engineering toolbox in hand*, p. 103.

Marois, Y. *et al.* (1999) 'Hydrolytic and enzymatic incubation of polyhydroxyoctanoate (PHO): A short-term in vitro study of a degradable bacterial polyester', *Journal of Biomaterials Science, Polymer Edition*, 10(4), pp. 483–499. doi: 10.1163/156856299X00225.

Martelli, S. M. *et al.* (2012) 'Obtention and characterization of poly(3-hydroxybutyricacid-co-hydroxyvaleric acid)/mcl-PHA based blends', *LWT - Food Science and Technology*, 47(2), pp. 386–392. doi: 10.1016/j.lwt.2012.01.036.

Matsumoto, I. *et al.* (2004) 'Improvement in islet yield from obese donors for human islet transplants', *Transplantation*, 78(6), pp. 880–885.

McCall, M. and Shapiro, A. M. (2012) 'Update on islet transplantation', *Cold Spring Harbor perspectives in medicine*, 2(7), p. a007823. doi: 10.1101/cshperspect.a007823 [doi].

McClenaghan, N. H., Barnett, C. R., Ah-Sing, E., *et al.* (1996) 'Characterization of a novel glucose-responsive insulin-secreting cell line, BRIN-BD11, produced by electrofusion', *Diabetes*, 45(8), pp. 1132–1140.

McClenaghan, N. H., Barnett, C. R., O'Harte, F. P., *et al.* (1996) 'Mechanisms of amino acid-induced insulin secretion from the glucose-

responsive BRIN-BD11 pancreatic B-cell line.', *The Journal of endocrinology*. BioScientifica, 151(3), pp. 349–57. doi: 10.1677/JOE.0.1510349.

McClenaghan, N. H. and Flatt, P. R. (1999) 'Engineering cultured insulin-secreting pancreatic B-cell lines', *Journal of Molecular Medicine*. Springer-Verlag, 77(1), pp. 235–243. doi: 10.1007/s001090050344.

Meischel, M. *et al.* (2016) 'Adhesive strength of bone-implant interfaces and in-vivo degradation of PHB composites for load-bearing applications', *Journal of the Mechanical Behavior of Biomedical Materials*. Elsevier, 53, pp. 104–118. doi: 10.1016/J.JMBBM.2015.08.004.

Mian, F. A., Jarman, T. R. and Righelato, R. C. (1978) 'Biosynthesis of Exopolysaccharide by Pseudomonas aeruginosa', 134(2), pp. 418–422. Available at: http://jb.asm.org/content/134/2/418.full.pdf (Accessed: 28 February 2018).

Misra, S. *et al.* (2006) 'Polyhydroxyalkanoate (PHA)/inorganic phase composites for tissue engineering applications', *Biomacromolecules*, pp. 2249–2258. doi: 10.1021/bm060317c.

Misra, S. K. *et al.* (2008) 'Comparison of nanoscale and microscale bioactive glass on the properties of P (3HB)/Bioglass< sup>®</sup> composites', *Biomaterials*, 29(12), pp. 1750–1761.

Misra, S. K. *et al.* (2010) 'Poly (3-hydroxybutyrate) multifunctional composite scaffolds for tissue engineering applications', *Biomaterials*, 31(10), pp. 2806–2815.

Misso, M. L. *et al.* (2010) ‘Continuous subcutaneous insulin infusion (CSII) versus multiple insulin injections for type 1 diabetes mellitus’, *The Cochrane Library*.

Miyata, T. and Masuko, T. (1998) ‘Crystallization behaviour of poly(l-lactide)’, *Polymer*. Elsevier, 39(22), pp. 5515–5521. doi: 10.1016/S0032-3861(97)10203-8.

Mohanna, P.-N. *et al.* (2003) ‘A composite poly-hydroxybutyrate-glial growth factor conduit for long nerve gap repairs’, *Journal of Anatomy*. Blackwell Science Ltd, 203(6), pp. 553–565. doi: 10.1046/j.1469-7580.2003.00243.x.

Mohd Fadzil, F. I. *et al.* (2018) ‘Low Carbon Concentration Feeding Improves Medium-Chain-Length Polyhydroxyalkanoate Production in Escherichia coli Strains With Defective β-Oxidation’, *Frontiers in Bioengineering and Biotechnology*. Frontiers, 6, p. 178. doi: 10.3389/fbioe.2018.00178.

Monaco, A. P. *et al.* (1991) ‘Transplantation of Islet Allografts and Xenografts in Totally Pancreatectomized Diabetic Dogs Using the Hybrd Artificial Pancreas’, *Annals of Surgery*, 24(3), pp. 339–360. Available at: https://www.ncbi.nlm.nih.gov/pmc/articles/PMC1358659/pdf/annsurg00151-0165.pdf (Accessed: 2 April 2018).

Montesano, R. *et al.* (1983) ‘Collagen Matrix Promotes Pancreatic Endocrine Cell Reorganization of Monolayers into Islet-like Organoids’, *Journal of Cell Biology*, 97(3), pp. 935–939.

Montesano, R. *et al.* (no date) ‘Collagen Matrix Promotes Pancreatic Endocrine Cell Reorganization of Monolayers into Islet-like Organoids’.

Mooney, D. J. and Drury, J. L. (2003) ‘Hydrogels for tissue engineering: scaffold design variables and applications’, *Biomaterials*, 24(24), pp. 4337–4351. doi: 10.1016/S0142-9612(03)00340-5.

Mosmann, T. (1983) ‘Rapid Colorimetric Assay for Cellular Growth and Survival: Application to Proliferation and Cytotoxicity Assays’, *Journal oflmmunologicalMethods*, 65, pp. 55–63. Available at: http://citeseerx.ist.psu.edu/viewdoc/download?doi=10.1.1.458.9709&rep=rep1&type=pdf (Accessed: 6 March 2018).

Mouriño, V. *et al.* (2013) ‘Composite polymer-bioceramic scaffolds with drug delivery capability for bone tissue engineering’, *Expert opinion on drug delivery*, 10(10), pp. 1353–1365.

Murphy, P. S. and Evans, G. R. D. (2012) ‘Advances in Wound Healing: A Review of Current Wound Healing Products’, *Plastic Surgery International*. Hindawi, 2012, pp. 1–8. doi: 10.1155/2012/190436.

Murphy, S. V and Atala, A. (2014) ‘3D bioprinting of tissues and organs’, *Nature Biotechnology*. Nature Publishing Group, 32(8), pp. 773–785. doi: 10.1038/nbt.2958.

Naish, J. *et al.* (2009) *Medical Sciences.* London: Elsevier Health Sciences.

Nam, Y. S. and Park, T. G. (1999) ‘Porous biodegradable polymeric scaffolds prepared by thermally induced phase separation’, *Journal of Biomedical Materials Research: An Official Journal of The Society for*

Biomaterials, The Japanese Society for Biomaterials, and The Australian Society for Biomaterials and the Korean Society for Biomaterials. Wiley Online Library, 47(1), pp. 8–17.

Nano, R. *et al.* (2005) 'Islet isolation for allotransplantation: variables associated with successful islet yield and graft function', *Diabetologia*, 48(5), pp. 906–912.

Nathan, D. M. (1993) 'Long-term complications of diabetes mellitus', *New England Journal of Medicine*, 328(23), pp. 1676–1685.

Neufeld, T. *et al.* (2013) 'The efficacy of an immunoisolating membrane system for islet xenotransplantation in minipigs', *PLoS One*, 8(8), p. e70150.

Newsholme, P. *et al.* (2007) 'Amino acid metabolism, insulin secretion and diabetes', *Biochemical Society Transactions*, 35(5), p. 1180 LP-1186. doi: 10.1042/BST0351180.

Nigmatullin, R. *et al.* (2015) 'Polyhydroxyalkanoates, a family of natural polymers, and their applications in drug delivery', *Journal of Chemical Technology and Biotechnology*.

Numata, K., Abe, H. and Iwata, T. (2009) 'Biodegradability of poly (hydroxyalkanoate) materials', *Materials*. Molecular Diversity Preservation International, 2(3), pp. 1104–1126.

Nyitray, C. E. *et al.* (2015) 'Polycaprolactone Thin-Film Micro-and Nanoporous Cell-Encapsulation Devices', *ACS nano*, 9(6), pp. 5675–5682.

Ogurtsova, K. *et al.* (2017) 'IDF Diabetes Atlas: Global estimates for the prevalence of diabetes for 2015 and 2040.', *Diabetes research and clinical practice*. Elsevier, 128, pp. 40–50. doi: 10.1016/j.diabres.2017.03.024.

Ojumu, T. V., Yu, J. and Solomon, B. O. (2004) 'Production of polyhydroxyalkanoates, a bacterial biodegradable polymers', *African journal of Biotechnology*, 3(1), pp. 18–24.

Olabisi, O. (1981) 'Interpretations of polymer-polymer miscibility'. ACS Publications, 58(11), pp. 944–950.

Ong, S. Y., Chee, J. Y. and Sudesh, K. (2017) 'Degradation of Polyhydroxyalkanoate (PHA): a review'. Сибирский федеральный университет. Siberian Federal University.

Ozdil, D. and Aydin, H. M. (2014) 'Polymers for medical and tissue engineering applications', *Journal of Chemical Technology & Biotechnology*, 89(12), pp. 1793–1810. doi: 10.1002/jctb.4505.

Panza, J. L. *et al.* (2000) 'Treatment of rat pancreatic islets with reactive PEG', *Biomaterials*, 21(11), pp. 1155–1164.

Park, H.-Y. *et al.* (1998) 'Effect of pH on Drug Release from Polysaccharide Tablets', *Drug Delivery*. Taylor & Francis, 5(1), pp. 13–18. doi: 10.3109/10717549809052022.

Park, S. J., Choi, J. Il and Lee, S. Y. (2005) 'Short-chain-length polyhydroxyalkanoates: Synthesis in metabolically engineered Escherichia coli and medical applications', *Journal of Microbiology and Biotechnology*, pp. 206–215.

Pasparakis, G. and Bouropoulos, N. (2006) ‘Swelling studies and in vitro release of verapamil from calcium alginate and calcium alginate–chitosan beads’, *International Journal of Pharmaceutics*. Elsevier, 323(1–2), pp. 34–42. doi: 10.1016/J.IJPHARM.2006.05.054.

Pederson, R. A. and McIntosh, C. H. (2016) ‘Discovery of gastric inhibitory polypeptide and its subsequent fate: Personal reflections’, *Journal of Diabetes Investigation*. John Wiley & Sons, Ltd (10.1111), 7, pp. 4–7. doi: 10.1111/jdi.12480.

Pedraza, E. *et al.* (2013) ‘Macroporous Three-Dimensional PDMS Scaffolds for Extrahepatic Islet Transplantation’, *Cell Transplantation*. SAGE PublicationsSage CA: Los Angeles, CA, 22(7), pp. 1123–1135. doi: 10.3727/096368912X657440.

Percival, S. L. and McCarty, S. M. (2015) ‘Silver and Alginates: Role in Wound Healing and Biofilm Control.’, *Advances in wound care*. Mary Ann Liebert, Inc., 4(7), pp. 407–414. doi: 10.1089/wound.2014.0541.

Perego, G., Cella, G. D. and Bastioli, C. (1996) ‘Effect of molecular weight and crystallinity on poly(lactic acid) mechanical properties’, *Journal of Applied Polymer Science*, 59(1), pp. 37–43. doi: 10.1002/(SICI)1097-4628(19960103)59:1<37::AID-APP6>3.0.CO;2-N.

Perez-Basterrechea, M. *et al.* (2018) ‘Tissue-engineering approaches in pancreatic islet transplantation’, *Biotechnology and Bioengineering*. Wiley-Blackwell. doi: 10.1002/bit.26821.

Phelps, E. A. *et al.* (2013) ‘Engineered VEGF-releasing PEG–MAL

hydrogel for pancreatic islet vascularization', *Drug Delivery and Translational Research*, pp. 1–12.

Philip, S., Keshavarz, T. and Roy, I. (2007) 'Polyhydroxyalkanoates: biodegradable polymers with a range of applications', *Journal of Chemical Technology and Biotechnology*, 82(3), pp. 233–247.

Poblete-Castro, I. *et al.* (2014) 'Comparison of mcl-Poly(3-hydroxyalkanoates) synthesis by different Pseudomonas putida strains from crude glycerol: citrate accumulates at high titer under PHA-producing conditions', *BMC Biotechnology*. BioMed Central, 14(1), p. 962. doi: 10.1186/s12896-014-0110-z.

Qi, M. *et al.* (2004) 'PVA hydrogel sheet macroencapsulation for the bioartificial pancreas', *Biomaterials*, 25(27), pp. 5885–5892.

Qi, M. *et al.* (2008) 'Encapsulation of human islets in novel inhomogeneous alginate-ca2+/ba2+ microbeads: in vitro and in vivo function.', *Artificial cells, blood substitutes, and immobilization biotechnology*. NIH Public Access, 36(5), pp. 403–20. doi: 10.1080/10731190802369755.

Qi, Z. *et al.* (2012) 'Immunoisolation effect of polyvinyl alcohol (PVA) macroencapsulated islets in type 1 diabetes therapy', *Cell transplantation*, 21(2–3), pp. 525–534.

Qiu, Z. *et al.* (2005) 'Miscibility and crystallization behavior of biodegradable blends of two aliphatic polyesters. Poly(3-hydroxybutyrate-co-hydroxyvalerate) and poly(ε-caprolactone)', *Polymer*. Elsevier, 46(25), pp. 11814–11819. doi: 10.1016/J.POLYMER.2005.10.058.

Rai, R. *et al.* (2011) 'Medium chain length polyhydroxyalkanoates, promising new biomedical materials for the future', *Materials Science and Engineering R: Reports*, 72(3), pp. 29–47. doi: 10.1016/j.mser.2010.11.002.

Rai, R. *et al.* (2011) 'Poly-3-hydroxyoctanoate P (3HO), a medium chain length polyhydroxyalkanoate homopolymer from Pseudomonas mendocina', *Biomacromolecules*, 12(6), pp. 2126–2136.

Ramesh, A., Chhabra, P. and Brayman, K. L. (2013) 'Pancreatic islet transplantation in type 1 diabetes mellitus: an update on recent developments', *Current diabetes reviews*, 9(4), pp. 294–311.

Ramsay, J. A. *et al.* (1994) 'Extraction of poly-3-hydroxybutyrate using chlorinated solvents', *Biotechnology Techniques*, 8(8), pp. 589–594.

Randriamahefa, S. *et al.* (2003) 'Fourier transform infrared spectroscopy for screening and quantifying production of PHAs by Pseudomonas grown on sodium octanoate', *Biomacromolecules*, 4(4), pp. 1092–1097.

Raza, Z. A., Abid, S. and Banat, I. M. (2018a) 'Polyhydroxyalkanoates: Characteristics, production, recent developments and applications', *International Biodeterioration & Biodegradation*, 126, pp. 45–56. doi: 10.1016/j.ibiod.2017.10.001.

Raza, Z. A., Abid, S. and Banat, I. M. (2018b) 'Polyhydroxyalkanoates: Characteristics, production, recent developments and applications', *International Biodeterioration & Biodegradation*. Elsevier, 126, pp. 45–56. doi: 10.1016/J.IBIOD.2017.10.001.

Reddy, C. S. K. *et al.* (2003) 'Polyhydroxyalkanoates: An overview',

Bioresource Technology, pp. 137–146. doi: 10.1016/S0960-8524(02)00212-2.

Remminghorst, U. (2007) *Polymerisation and export of alginate in Pseudomonas aeruginosa: Functional assignment and catalytic mechanism of Alg8/44*. Massey University.

Renouf-Glauser, A. C. *et al.* (2005) 'The effect of crystallinity on the deformation mechanism and bulk mechanical properties of PLLA', *Biomaterials*. Elsevier, 26(29), pp. 5771–5782. doi: 10.1016/J.BIOMATERIALS.2005.03.002.

Riopel, M. and Wang, R. (2014) 'Collagen matrix support of pancreatic islet survival and function', *Frontiers in bioscience (Landmark edition)*, 19, p. 77.

Roach, P., Farrar, D. and Perry, C. C. (2006) 'Surface tailoring for controlled protein adsorption: Effect of topography at the nanometer scale and chemistry', *Journal of the American Chemical Society*. American Chemical Society, 128(12), pp. 3939–3945. doi: 10.1021/ja056278e.

Robertson, R. P. (2000) 'Successful islet transplantation for patients with diabetes--fact or fantasy?', *The New England journal of medicine*, 343(4), pp. 289–290. doi: 10.1056/NEJM200007273430409 [doi].

Rowley, J. A., Madlambayan, G. and Mooney, D. J. (1999) 'Alginate hydrogels as synthetic extracellular matrix materials', *Biomaterials*, 20(1), pp. 45–53. doi: http://dx.doi.org/10.1016/S0142-9612(98)00107-0.

Sabra, W. and Zeng, A. P. Z. (2009) *Microbial production of alginates:*

physiology and process aspects., *Alginates: Biology and Applications*. Berlin: Springer.

Sai K, P. and Babu, M. (2000) 'Collagen based dressings — a review', *Burns*, 26(1), pp. 54–62. doi: 10.1016/S0305-4179(99)00103-5.

Santos, E. *et al.* (2012) 'Novel advances in the design of three-dimensional bio-scaffolds to control cell fate: translation from 2D to 3D', *Trends in Biotechnology*, 30, pp. 331–341. doi: 10.1016/j.tibtech.2012.03.005.

Santulli, G. *et al.* (2015) 'Calcium release channel RyR2 regulates insulin release and glucose homeostasis', *The Journal of Clinical Investigation*. American Society for Clinical Investigation, 125(5), pp. 1968–1978. doi: 10.1172/JCI79273.

Savić, R. *et al.* (2009) 'Block-copolymer micelles as carriers of cell signaling modulators for the inhibition of JNK in human islets of Langerhans', *Biomaterials*, 30(21), pp. 3597–3604.

Schneider, S. *et al.* (2005) 'Long-term graft function of adult rat and human islets encapsulated in novel alginate-based microcapsules after transplantation in immunocompetent diabetic mice.', *Diabetes*. American Diabetes Association, 54(3), pp. 687–93. doi: 10.2337/DIABETES.54.3.687.

Schuit, F. *et al.* (1997) 'Metabolic fate of glucose in purified islet cells. Glucose-regulated anaplerosis in beta cells.', *The Journal of biological chemistry*. American Society for Biochemistry and Molecular Biology, 272(30), pp. 18572–9. doi: 10.1074/JBC.272.30.18572.

Schuit, F. *et al.* (1999) ‘Cellular origin of hexokinase in pancreatic islets.’, *The Journal of biological chemistry*, 274(46), pp. 32803–9. Available at: http://www.ncbi.nlm.nih.gov/pubmed/10551841 (Accessed: 2 February 2018).

Segev, H. *et al.* (2004) ‘Differentiation of Human Embryonic Stem Cells into Insulin-Producing Clusters’, *Stem Cells*, 22(3), pp. 265–274. doi: 10.1634/stemcells.22-3-265.

Sezer, A. D. (1999) ‘Release characteristics of chitosan treated alginate beads: I. Sustained release of a macromolecular drug from chitosan treated alginate beads’, *Journal of Microencapsulation*. Taylor & Francis, 16(2), pp. 195–203. doi: 10.1080/026520499289176.

Shapiro, A. M. J. *et al.* (2000) ‘Islet transplantation in seven patients with type 1 diabetes mellitus using a glucocorticoid-free immunosuppressive regimen’, *New England Journal of Medicine*, 343(4), pp. 230–238.

Shapiro, A. M. J. *et al.* (2006) ‘International trial of the Edmonton protocol for islet transplantation’, *New England Journal of Medicine*, 355(13), pp. 1318–1330.

Shapiro, L. and Cohen, S. (1997) ‘Novel alginate sponges for cell culture and transplantation’, *Biomaterials*, 18(8), pp. 583–590. doi: http://dx.doi.org/10.1016/S0142-9612(96)00181-0.

Shih, L. and Van, Y.-T. (2001) ‘The production of poly-(γ-glutamic acid) from microorganisms and its various applications’, *Bioresource technology*, 79(3), pp. 207–225.

Shishatskaya, E. I. *et al.* (2016) ‘Biomedical Studies of Polyhydroxyalkanoates’, *Journal of Siberian Federal University. Biology*, 1, pp. 6–20. doi: 10.17516/1997-1389-2015-9-1-6-20.

Silva, A. I. *et al.* (2006) ‘An overview on the development of a bio-artificial pancreas as a treatment of insulin-dependent diabetes mellitus’, *Medicinal research reviews*, 26(2), pp. 181–222.

Silva, L. F. *et al.* (2004) ‘Poly-3-hydroxybutyrate (P3HB) production by bacteria from xylose, glucose and sugarcane bagasse hydrolysate’, *Journal of Industrial Microbiology & Biotechnology*. Springer-Verlag, 31(6), pp. 245–254. doi: 10.1007/s10295-004-0136-7.

Simon-Colin, C. *et al.* (2008) ‘Biosynthesis of medium chain length poly-3-hydroxyalkanoates by Pseudomonas guezennei from various carbon sources’, *Reactive and Functional Polymers*. Elsevier, 68(11), pp. 1534–1541. doi: 10.1016/J.REACTFUNCTPOLYM.2008.08.005.

Singh, M., Patel, S. K. and Kalia, V. C. (2009) ‘Bacillus subtilis as potential producer for polyhydroxyalkanoates’, *Microbial Cell Factories*. BioMed Central, 8(1), p. 38. doi: 10.1186/1475-2859-8-38.

Sivashanmugam, A. *et al.* (2015) ‘An overview of injectable polymeric hydrogels for tissue engineering.’, *European Polymer Journal*, 72, pp. 543–565. Available at: https://ac.els-cdn.com/S0014305715002785/1-s2.0-S0014305715002785-main.pdf?_tid=ffb525d0-e7a5-46ce-a2a8-32ebde519199&acdnat=1522799636_157efd6aee37b002a9d07cc76b813610 (Accessed: 4 April 2018).

Skardal, A. and Atala, A. (2015) ‘Biomaterials for Integration with 3-D Bioprinting’, *Annals of Biomedical Engineering*. Springer US, 43(3), pp. 730–746. doi: 10.1007/s10439-014-1207-1.

Skelin, M., Rupnik, M. and Cencič, A. (2010) ‘Pancreatic beta cell lines and their applications in diabetes mellitus research’, *ALTEX*, 27(2), pp. 105–113. doi: 10.14573/altex.2010.2.105.

Slack, J. M. (1995) ‘Developmental biology of the pancreas’, *Development (Cambridge, England)*, 121(6), pp. 1569–1580.

Sodian, R. *et al.* (2000) ‘Technical report: fabrication of a trileaflet heart valve scaffold from a polyhydroxyalkanoate biopolyester for use in tissue engineering’, *Tissue engineering*. Mary Ann Liebert, Inc., 6(2), pp. 183–188.

Sonaje, K. *et al.* (2010) ‘Enteric-coated capsules filled with freeze-dried chitosan/poly (γ-glutamic acid) nanoparticles for oral insulin delivery’, *Biomaterials*, 31(12), pp. 3384–3394.

Song, J. and Millman, J. R. (2016) ‘Economic 3D-printing approach for transplantation of human stem cell-derived β-like cells.’, *Biofabrication*. NIH Public Access, 9(1), p. 015002. doi: 10.1088/1758-5090/9/1/015002.

Sorenson, R. L. and Brelje, T. C. (1997) ‘Adaptation of islets of Langerhans to pregnancy: Beta cell growth’, *Experimental and Clinical Endocrinology and Diabetes*, 105(4), pp. 301–307. Available at: https://www.researchgate.net/profile/Robert_Sorenson/publication/13990023_Adaptation_of_Islets_of_Langerhans_to_Pregnancy_b-

Cell_Growth_Enhanced_Insulin_Secretion_and_the_Role_of_Lactogenic_Hormones/links/0fcfd5148d5caa3647000000.pdf (Accessed: 29 March 2018).

Steiner, D. F. and Oyer, P. E. (1967) 'The biosynthesis of insulin and a probable precursor of insulin by a human islet cell adenoma.', *Proceedings of the National Academy of Sciences of the United States of America*. National Academy of Sciences, 57(2), pp. 473–80. Available at: http://www.ncbi.nlm.nih.gov/pubmed/16591494 (Accessed: 2 February 2018).

Stendahl, J. C., Kaufman, D. B. and Stupp, S. I. (2009) 'Extracellular Matrix in Pancreatic Islets: Relevance to Scaffold Design and Transplantation', *Cell Transplantation*. SAGE PublicationsSage CA: Los Angeles, CA, 18(1), pp. 1–12. doi: 10.3727/096368909788237195.

Sudesh, K., Abe, H. and Doi, Y. (2000) 'Synthesis, structure and properties of polyhydroxyalkanoates: biological polyesters', *Progress in Polymer Science*, 25(10), pp. 1503–1555. doi: 10.1016/S0079-6700(00)00035-6.

Sugimoto, M. *et al.* (2014) 'What is the nature of pancreatic consistency? Assessment of the elastic modulus of the pancreas and comparison with tactile sensation, histology, and occurrence of postoperative pancreatic fistula after pancreaticoduodenectomy', *Surgery*, 156(5), pp. 1204–1211.

Sukan, A., Roy, I. and Keshavarz, T. (2017) 'A strategy for dual biopolymer production of P(3HB) and γ-PGA', *Journal of Chemical Technology & Biotechnology*. Wiley-Blackwell, 92(7), pp. 1548–1557. doi:

10.1002/jctb.5259.

Sun, J. and Tan, H. (2013) ‘Alginate-based biomaterials for regenerative medicine applications’, *Materials*, 6(4), pp. 1285–1309.

Sun, Z. *et al.* (2007) ‘Carbon-limited fed-batch production of medium-chain-length polyhydroxyalkanoates from nonanoic acid by Pseudomonas putida KT2440’, *Biotechnological Products and Process Engineering*, 74, pp. 69–77. doi: 10.1007/s00253-006-0655-4.

Suriyamongkol, P. *et al.* (2007) ‘Biotechnological approaches for the production of polyhydroxyalkanoates in microorganisms and plants — A review’, *Biotechnology Advances*. Elsevier, 25(2), pp. 148–175. doi: 10.1016/J.BIOTECHADV.2006.11.007.

Takka, S. and F. A. (1999) ‘Calcium alginate microparticles for oral adminis tration: I: Effect of sodium alginate type on drug release and drug entrapment efficiency’, *Journal Microencapsulation*. Taylor & Francis, 16(3), pp. 275–290. doi: 10.1080/026520499289013.

Tellechea, A. *et al.* (2015) ‘Alginate and DNA gels are suitable delivery systems for diabetic wound healing’, *International Journal of Lower Extremity Wounds*, 14(2), pp. 146–153. doi: 10.1177/1534734615580018.

Teramura, Y. *et al.* (2013) ‘Microencapsulation of cells, including islets, within stable ultra-thin membranes of maleimide-conjugated PEG-lipid with multifunctional crosslinkers’, *Biomaterials*, 34(11), pp. 2683–2693. doi: 10.1016/j.biomaterials.2013.01.015.

Teramura, Y. and Iwata, H. (2011) ‘Improvement of graft survival by

surface modification with poly (ethylene glycol)-lipid and urokinase in intraportal islet transplantation', *Transplantation*, 91(3), pp. 271–278.

Tønnesen, H. H. and Karlsen, J. (2002) 'Alginate in Drug Delivery Systems', *Drug Development and Industrial Pharmacy*. Taylor & Francis, 28(6), pp. 621–630. doi: 10.1081/DDC-120003853.

Tortora, G. J. and Derrickson, B. (2017) *Principles of anatomy and physiology*. 15th edn. New York: John Wiley & Sons.

Tsuchiya, H. *et al.* (2015) 'Extracellular Matrix and Growth Factors Improve the Efficacy of Intramuscular Islet Transplantation', *PLOS ONE*. Edited by M. Matsusaki. Public Library of Science, 10(10), p. e0140910. doi: 10.1371/journal.pone.0140910.

Ullah, F. *et al.* (2015) 'Classification, processing and application of hydrogels: A review', *Materials Science and Engineering: C*. Elsevier, 57, pp. 414–433. doi: 10.1016/J.MSEC.2015.07.053.

Valappil, S. P. *et al.* (2006) 'Polyhydroxyalkanoates in Gram-positive bacteria: insights from the genera Bacillus and Streptomyces', *Antonie van Leeuwenhoek*. Kluwer Academic Publishers, 91(1), pp. 1–17. doi: 10.1007/s10482-006-9095-5.

Valappil, S. P. *et al.* (2007) 'Large-scale production and efficient recovery of PHB with desirable material properties, from the newly characterised< i> Bacillus cereus</i> SPV', *Journal of Biotechnology*, 132(3), pp. 251–258.

Valappil, S. P. *et al.* (2008) 'Polyhydroxyalkanoate biosynthesis in Bacillus

cereus SPV under varied limiting conditions and an insight into the biosynthetic genes involved', *Journal of applied microbiology*, 104(6), pp. 1624–1635.

Valdés-González, R. A. *et al.* (2005) 'Xenotransplantation of porcine neonatal islets of Langerhans and Sertoli cells: a 4-year study.', *European journal of endocrinology*. European Society of Endocrinology, 153(3), pp. 419–27. doi: 10.1530/eje.1.01982.

Varanasi, A. *et al.* (2011) 'Liraglutide as additional treatment for type 1 diabetes', *European journal of endocrinology / European Federation of Endocrine Societies*, 165(1), pp. 77–84. doi: 10.1530/EJE-11-0330 [doi].

Vegas, A. J. *et al.* (2016) 'Long-term glycemic control using polymer-encapsulated human stem cell-derived beta cells in immune-competent mice', *Nature medicine*.

Ventola, C. L. (2014) 'Medical Applications for 3D Printing: Current and Projected Uses.', *P & T : a peer-reviewed journal for formulary management*. MediMedia, USA, 39(10), pp. 704–11. Available at: http://www.ncbi.nlm.nih.gov/pubmed/25336867 (Accessed: 2 April 2018).

Vériter, S. *et al.* (2010) 'In vivo selection of biocompatible alginates for islet encapsulation and subcutaneous transplantation', *Tissue Engineering Part A*, 16(5), pp. 1503–1513.

Verlinden, R. A. J. *et al.* (2007a) 'Bacterial synthesis of biodegradable polyhydroxyalkanoates', *Journal of Applied Microbiology*. Blackwell Publishing Ltd, 102(6), pp. 1437–1449. doi: 10.1111/j.1365-

2672.2007.03335.x.

Verlinden, R. A. J. *et al.* (2007b) 'Bacterial synthesis of biodegradable polyhydroxyalkanoates', *Journal of Applied Microbiology*. Blackwell Publishing Ltd, 102(6), pp. 1437–1449. doi: 10.1111/j.1365-2672.2007.03335.x.

Vijan, S. (2010) 'Type 2 Diabetes', *Annals of Internal Medicine*. American College of Physicians, 152(5), pp. ITC3-1. doi: 10.7326/0003-4819-152-5-201003020-01003.

Vlierberghe, S. Van, Dubruel, P. and Schacht, E. (2011) 'Biopolymer-Based Hydrogels As Scaffolds for Tissue Engineering Applications: A Review', *Biomacromolecules*, 12, pp. 1387–1408. doi: 10.1021/bm200083n.

Vos, P. De *et al.* (1997) 'Improved biocompatibility but limited graft survival after purification of alginate for microencapsulation of pancreatic islets', *Diabetologia*, 40(3), pp. 262–270.

Walker, J. M. (2002) 'The Bicinchoninic Acid (BCA) Assay for Protein Quantitation', in *Basic Protein and Peptide Protocols*. New Jersey: Humana Press, pp. 5–8. doi: 10.1385/0-89603-268-X:5.

Wang, Y.-W. *et al.* (2005) 'Evaluation of three-dimensional scaffolds made of blends of hydroxyapatite and poly(3-hydroxybutyrate-co-3-hydroxyhexanoate) for bone reconstruction', *Biomaterials*. Elsevier, 26(8), pp. 899–904. doi: 10.1016/J.BIOMATERIALS.2004.03.035.

Wang, Y. *et al.* (2016) 'Enhancement of medium-chain-length polyhydroxyalkanoates biosynthesis from glucose by metabolic engineering

in Pseudomonas mendocina', *Biotechnology Letters*. Springer Netherlands, 38(2), pp. 313–320. doi: 10.1007/s10529-015-1980-4.

Wang, Y., Chung, A. and Chen, G.-Q. (2017) 'Synthesis of Medium-Chain-Length Polyhydroxyalkanoate Homopolymers, Random Copolymers, and Block Copolymers by an Engineered Strain of Pseudomonas entomophila', *Advanced Healthcare Materials*, 6(7), p. 1601017. doi: 10.1002/adhm.201601017.

Webb, B. and Doyle, B. J. (2017) 'Parameter optimization for 3D bioprinting of hydrogels', *Bioprinting*. Elsevier, 8, pp. 8–12.

Wei, G. and Ma, P. X. (2004) 'Structure and properties of nano-hydroxyapatite/polymer composite scaffolds for bone tissue engineering', *Biomaterials*. Elsevier, 25(19), pp. 4749–4757. doi: 10.1016/J.BIOMATERIALS.2003.12.005.

Wei, G. and Ma, P. X. (2009) 'Partially nanofibrous architecture of 3D tissue engineering scaffolds.', *Biomaterials*. NIH Public Access, 30(32), pp. 6426–34. doi: 10.1016/j.biomaterials.2009.08.012.

Weir, G. C. (2013) 'Islet encapsulation: advances and obstacles', *Diabetologia*, 56(7), pp. 1458–1461.

White, S. A., Shaw, J. A. and Sutherland, D. E. R. (2009) 'Pancreas transplantation', *The Lancet*, 373(9677), pp. 1808–1817. doi: http://dx.doi.org/10.1016/S0140-6736(09)60609-7.

Wills, E. D., Thomas, J. H. and Gillham, B. (2006) *Wills' biochemical basis of medicine.* Third. Edward Arnold.

Witholt, B. and Kessler, B. (1999) ‘Perspectives of medium chain length poly(hydroxyalkanoates), a versatile set of bacterial bioplastics’, *Current Opinion in Biotechnology*, 10(3), pp. 279–285. doi: 10.1016/S0958-1669(99)80049-4.

World Health Organisation (2016) *GLOBAL REPORT ON DIABETES*, *WHO Library Cataloguing-in-Publication Data*. Available at: http://www.who.int/about/licensing/ (Accessed: 3 February 2018).

Wu, Q. *et al.* (2001) ‘Production of poly-3-hydroxybutyrate by Bacillus sp. JMa5 cultivated in molasses media’, *Antonie van Leeuwenhoek*. Kluwer Academic Publishers, 80(2), pp. 111–118. doi: 10.1023/A:1012222625201.

Xie, D. *et al.* (2005) ‘Cytoprotection of PEG-modified adult porcine pancreatic islets for improved xenotransplantation’, *Biomaterials*, 26(4), pp. 403–412.

Xu, X.-Y. *et al.* (2010) ‘The behaviour of neural stem cells on polyhydroxyalkanoate nanofiber scaffolds’, *Biomaterials*, 31(14), pp. 3967–3975. doi: https://doi.org/10.1016/j.biomaterials.2010.01.132.

Yang, X.-D. *et al.* (2009) ‘Enhanced insulin production from murine islet beta cells incubated on poly(3-hydroxybutyrate- *co* -3-hydroxyhexanoate)’, *Journal of Biomedical Materials Research Part A*, 9999A, p. NA-NA. doi: 10.1002/jbm.a.32379.

Yang, X. *et al.* (2010) ‘Enhanced insulin production from murine islet beta cells incubated on poly (3-hydroxybutyrate-co-3-hydroxyhexanoate)’, *Journal of Biomedical Materials Research Part A*, 92(2), pp. 548–555.

Yang, Z. *et al.* (2002) ‘Poly (glutamic acid) poly (ethylene glycol) hydrogels prepared by photoinduced polymerization: synthesis, characterization, and preliminary release studies of protein drugs’, *Journal of Biomedical Materials Research*, 62(1), pp. 14–21.

Young, T.-H. *et al.* (2002) ‘Assessment and modeling of poly(vinyl alcohol) bioartificial pancreas in vivo’, *Biomaterials*, 23(16), pp. 3495–3501. doi: http://dx.doi.org/10.1016/S0142-9612(02)00075-3.

Zeng, Y. *et al.* (1994) ‘The Correlation Between Donor Characteristics and The Success of Human Islet Isolation 1,2.’, *Transplantation*, 57(6), pp. 954–958.

Zhang, J. *et al.* (2018) ‘Polyhydroxyalkanoates (PHA) for therapeutic applications’, *Materials Science and Engineering: C*. doi: https://doi.org/10.1016/j.msec.2017.12.035.

Zhu, S. *et al.* (1999) ‘Confinement-induced miscibility in polymer blends’, *Nature*. Nature Publishing Group, 400(6739), p. 49.

Zimmet, P., Alberti, K. and Shaw, J. (2001) ‘Global and societal implications of the diabetes epidemic’, *Nature*, 414(6865), pp. 782–787.

Zinn, M., Witholt, B. and Egli, T. (2001) ‘Occurrence, synthesis and medical application of bacterial polyhydroxyalkanoate’, *Advanced Drug Delivery Reviews*, 53, pp. 5–21.